

# **The Effects of Food Quality and Temperature on Mesozooplankton Physiology**

Submitted to the School of Environmental Sciences of the University of East Anglia

Thesis of the Degree of Doctor of Philosophy

By

**Raffaella Nobili**

[June 2013]

© This copy of the thesis has been supplied on condition that anyone who consults it is understood to recognise that its copyright rests with the author and that no quotation from the thesis, nor any information derived therefrom, may be published without the author's prior, written consent.



This work was made possible through financial support from NERC (studentship NE/H524506/1), the School of Environmental Sciences, UEA and SAHFOS.

The project was carried out in collaboration with the Sir Alister Hardy Foundation for Ocean Science (SAHFOS) in Plymouth, C.A.S.E. partner to the studentship. SAHFOS is an international charity that operates the world wide renowned Continuous Plankton Recorder (CPR) survey. The Foundation has been collecting data from the North Atlantic and the North Sea on biogeography and ecology of plankton since 1931 ([www.sahfos.ac.uk](http://www.sahfos.ac.uk)).



# THE EFFECTS OF FOOD QUALITY AND TEMPERATURE ON MESOZOOPLANKTON PHYSIOLOGY

DOCTOR OF PHILOSOPHY

University of East Anglia, School of Environmental Sciences

Raffaella Nobili, 2013

## ABSTRACT

This study assesses the physiological responses of copepods to variations in the quality of their diet and temperature and explores the variability of food quality in the field. Laboratory experiments were used to constrain the effects of food quality in terms of phytoplankton organic ratios N:P, C:N and C:P and fatty acid content, on *Temora longicornis* feeding, respiration, and egg production rates (EPR). Maximum metabolic rates, assimilation efficiency and gross growth efficiency coincided with an optimum diet of ~16N:1P defining it as the copepod threshold nutrient ratio. In the field, a response of zooplankton biomass to temporal variations in seston N:P ratio was found in the North Sea and in the North Pacific Subtropical Gyre.

Field measurements revealed latitudinal and temporal changes in food quality at the chlorophyll maximum along an Atlantic Meridional Transect (AMT). Better quality food was found in the Temperate and Upwelling domains and included seston with lower C:N ratios, N:P ratios closer to Redfield values and a higher proportion of polyunsaturated fatty acids (PUFA), essential fatty acids such as 20:5(n-3) and 22:6(n-3), high (n-3):(n-6) ratios and lower proportion of saturated fatty acids (SAFA). Time-series data showed that food quantity and quality declined over time in the temperate North region of the Atlantic Ocean.

Ship-board experiments were undertaken to determine the effects of temperature on respiration and EPR of some mesopelagic copepod species along an AMT. 75-85% of the variation in routine metabolic rates was explained by allometric and thermodynamic relationships. Within the range of temperatures measured, estimates of  $E_a$  (activation energy) and  $Q_{10}$  suggested high sensitivity to temperature variation.

Our results highlight the importance of quantifying the effects of a variety of ecological parameters on the physiological responses of copepods to understand the processes that regulate zooplankton dynamics and their effects on biogeochemical cycles and trophic transfer of energy.



## CONTENTS

<b>ABSTRACT</b> .....	<b>V</b>
<b>LIST OF NOTATIONS</b> .....	<b>XIX</b>
<b>ACKNOWLEDGMENTS</b> .....	<b>XXI</b>
<b>1. Introduction</b> .....	<b>2</b>
1.1 Copepods and their role in the marine environment.....	2
1.2 Copepod physiology and environmental variables .....	3
1.2.1 Copepod metabolic activity and respiration.....	4
1.2.2 Copepod basal respiratory cost .....	6
1.2.3 Copepod production and egg production rates (EPR).....	9
1.2.4 Copepod feeding .....	11
1.3 Copepod nutritional requirements.....	14
1.4 Food quality.....	16
1.4.1 Phytoplankton nutritional value .....	16
1.4.2 Fatty acids .....	18
1.4.3 Stoichiometry.....	20
1.5 Variable N:P ratio .....	22
1.6 Thesis objectives .....	24
<b>2. Experimental and analytical methods</b> .....	<b>28</b>
2.1 Field and experimental work overview .....	28
2.2 Algal cultures and food quality experiments.....	28
2.2.1 Continuous cultures.....	28
2.2.2 Zooplankton collection.....	34
2.2.3 Experimental protocol.....	35
2.2.4 Respiration rates .....	35
2.2.5 Egg production .....	37
2.2.6 Feeding rates .....	38
2.2.7 Biochemical Analysis.....	39
2.2.8 Zooplankton size and dry weight .....	41
2.3 The Atlantic Meridional Transect (AMT).....	41
2.3.1 AMT20.....	42
2.3.2 The Atlantic Ocean and oceanic biogeochemical provinces .....	43
2.3.3 Sample collection .....	44
2.3.4 Experimental protocols .....	45
2.3.5 Metabolic rates .....	45
2.3.6 Taxonomic determination and dry weight.....	46
2.3.7 Chemical and biochemical analysis .....	46
2.4 Planar Optode .....	49
2.4.1 Zooplankton respiration .....	49
2.4.2 Instrument inter-comparison .....	52
2.5 Data processing and error propagation.....	54
2.6 Statistical analysis .....	55

<b>3. Food quality regulates the metabolism and reproduction of <i>Temora longicornis</i> (Copepoda: Calanoida)</b> .....	<b>57</b>
3.1 Introduction .....	57
3.2 Methods .....	58
3.2.1 Algal Cultures.....	58
3.2.2 Elemental Composition of the Diet .....	59
3.2.3 <i>T. longicornis</i> sampling and maintenance.....	59
3.2.4 Physiological rates .....	60
3.2.5 Feeding rates .....	60
3.2.6 Respiration rates.....	60
3.2.7 Egg production rates (EPR).....	61
3.2.8 Experimental protocol.....	61
3.2.9 Carbon Budget.....	61
3.2.10 Time Series Data .....	62
3.3 Results.....	63
3.3.1 <i>R. salina</i> quantity and quality.....	63
3.3.2 <i>T. longicornis</i> size and physiological rates.....	65
3.3.3 <i>T. longicornis</i> carbon budget .....	70
3.3.4 Time series data.....	72
3.4 Discussion.....	74
3.4.1 Effects of the diet on physiological rates.....	74
3.4.2 Effects of food quality on copepod carbon budgets .....	76
3.4.3 Ecological implications .....	77
3.4.4 Summary and conclusions .....	80
3.5 Supplementary Material Nobili et al. BG-2013-79.....	82
3.5.1 Supplementary results on fatty acids (FA).....	86
<b>4. Seston quantity and quality in the chlorophyll maximum along an Atlantic Meridional Transect</b> .....	<b>91</b>
4.1 Introduction .....	91
4.2 Methods .....	94
4.2.1 Ecological Domains.....	94
4.2.2 Chemistry and hydrography .....	95
4.2.3 Data analysis.....	96
4.3 Results.....	98
4.3.1 Dissolved inorganic nutrients.....	99
4.3.2 Chl-a .....	101
4.3.3 Particulate organic matter.....	102
4.3.4 Validation of the prediction of particulate organic nutrients.....	103
4.3.5 Equations applicability.....	105
4.3.6 Nutrient ratios.....	111
4.3.7 POC:Chl-a ratio.....	115
4.3.8 Fatty acids.....	116
4.4 Discussion.....	121
4.4.1 Ecological Domains.....	121
4.4.2 Food Quality AMT20 .....	123

4.4.3	Food Quantity and Quality Predictability on AMT20.....	125
4.4.4	Food Quantity and Quality Variation Over Time.....	126
4.4.5	Summary and Conclusions.....	128
<b>5.</b>	<b>The respiration and egg production of some copepod species along an Atlantic Meridional Transect.....</b>	<b>131</b>
5.1	Introduction.....	131
5.2	Methods.....	133
5.2.1	Experimental conditions.....	134
5.2.2	Temperature and allometric-dependent metabolic rates .....	135
5.3	Results .....	136
5.3.1	Temperature and allometric-dependent respiration rates.....	137
5.3.2	Species-specific metabolic responses .....	140
5.3.3	Q <sub>10</sub> Estimates .....	150
5.3.4	Egg production rates (EPR).....	151
5.4	Discussion.....	155
5.4.1	Species distribution .....	155
5.4.2	Egg production rates (EPR).....	157
5.4.3	Species-specific carbon demand and respiration rates.....	158
5.4.4	Allometric exponent.....	161
5.4.5	Temperature dependent metabolic rates, E <sub>a</sub> and Q <sub>10</sub> coefficients .....	162
5.4.6	Summary and Conclusions.....	164
5.5	Supplementary material.....	166
<b>6.</b>	<b>Summary, general discussion and conclusions .....</b>	<b>175</b>
6.1	Thesis summary .....	175
6.2	Discussion.....	178
6.2.1	Food Quality.....	179
6.2.2	Temperature.....	182
6.2.3	Respiration .....	183
6.3	Conclusions.....	184
6.4	Future work .....	186
<b>7.</b>	<b>Methodological appendices A and B.....</b>	<b>190</b>
7.1	Appendix A O <sub>2</sub> analysis and determination – Winkler technique .....	190
7.1.1	Chemicals.....	190
7.1.2	Calibrating thiosulphate with iodate standard.....	191
7.1.3	Procedure for collection and fixing of oxygen samples.....	191
7.1.4	Analysing oxygen samples .....	192
7.1.5	Dissolved oxygen calculation.....	192
7.2	Appendix B Particulate Organic Phosphorus method (POP).....	194
7.2.1	Digestion protocol from Suzumura (2008).....	194
7.2.2	Colorimetric method (Strickland and Parson 1972).....	194

<b>8. Appendix C: O<sub>2</sub> evolution in <i>Emiliana huxleyi</i> cultures measured by electrodes and optode.....</b>	<b>198</b>
8.1 Abstract.....	198
8.2 Introduction .....	198
8.3 Material and methods.....	200
8.3.1 System set up and sensor calibrations .....	200
8.3.2 Precision test.....	202
8.3.3 Comparison test.....	203
8.3.4 Data processing .....	203
8.4 Results .....	203
8.4.1 Precision test.....	203
8.4.2 Respiration/Production experiments.....	204
8.5 Discussion.....	209
8.5.1 Conclusion and recommendations .....	210
8.6 References.....	212
<b>9. References.....</b>	<b>216</b>

## LIST OF FIGURES

### CHAPTER 1

**Figure 1.1.** Biological carbon pump and the role of zooplankton. ....2

### CHAPTER 2

**Figure 2.1.** Chemostats.....31

**Figure 2.2.** Continuous culture apparatus and principles of the system.....32

**Figure 2.3.** AMT cruises from 1995 to 2010. ....42

**Figure 2.4.** AMT20 stations sampled and biogeochemical provinces crossed. ....43

**Figure 2.5.** Manufacturer's calibration curve.....50

**Figure 2.6.** Precision test results. ....53

**Figure 2.7.** Variations in O<sub>2</sub> concentration for *Emiliana huxleyi* (strain RCC1229) culture under increasing light intensities. ....54

### CHAPTER 3

**Figure 3.1.** (A) Relationship between the molar N:P ratio of *R. salina* and clearance and ingestion rates of *T. longicornis*. (B) Relationship between the molar N:P ratio of *R. salina* and respiration rate of *T. longicornis* (normalised by dry weight). (C) Relationship between the molar N:P ratio of *R. salina* and EPR of *T. longicornis*. ....66

**Figure 3.2.** (A) Relationship between the molar C:N ratio of *R. salina* and clearance and ingestion rates of *T. longicornis*. (B) Relationship between the molar C:N ratio of *R. salina* and respiration rate of *T. longicornis* (normalised by dry weight). (C) Relationship between the molar N:P ratio of *R. salina* and EPR of *T. longicornis*. ....67

**Figure 3.3.** (A) Relationship between the molar C:P ratio of *R. salina* and clearance and ingestion rates of *T. longicornis*. (B) Relationship between the molar C:P ratio of *R. salina* and respiration rate of *T. longicornis* (normalised by dry weight). (C) Relationship between the molar N:P ratio of *R. salina* and EPR of *T. longicornis*. ....68

<b>Figure 3.4.</b> (A) Relationship between monthly <i>T. longicornis</i> abundance (ind m <sup>-3</sup> ), monthly average seston N:P ratio (molar) and chlorophyll a concentration (µg L <sup>-1</sup> ) in the North Sea (Arendal station 58° 23'N, 08° 48'E) between 1991 and 2010. (B) Relationship between the N:P ratio of size fractionated zooplankton (Hannides et al., 2009) and the corresponding food N:P ratio .....	73
<b>Figure 3.5.</b> Ingestion and clearance rates as a function of A) cell volume and B) food concentration.....	82
<b>Figure 3.6.</b> Respiration and EPR as a function of carbon ingestion.....	83
<b>Figure 3.7.</b> Respiration and EPR as a function of A) carbon ingestion, B) nitrogen ingestion, and C) phosphorus ingestion.....	84
<b>Figure 3.8.</b> N and P ingestion rates as a function of <i>R. salina</i> N:P ratio. ....	85
<b>Figure 3.9.</b> Gross Growth Efficiency in terms of carbon (GGEC) and nitrogen (GGEN) as a function of <i>R. salina</i> N:P ratio. ....	85
<b>CHAPTER 4</b>	
<b>Figure 4.1.</b> Stations sampled during AMT20, divided into six ecological domains .....	94
<b>Figure 4.2.</b> AMT20 Latitudinal distribution of temperature (°C) in the six ecological domains. The triangles represent the sampling locations at the CM. ....	98
<b>Figure 4.3.</b> AMT20 Latitudinal distribution of chlorophyll a (µg L <sup>-1</sup> ) and CM partitioned by ecological domains.....	101
<b>Figure 4.4.</b> Linear regression (black line) and 1:1 relationship (red dashed line) between measured data from the Bigelow dataset 1 and 2 and predicted (from equations 4.2 and 4.3).....	105
<b>Figure 4.5.</b> Linear regression (black line) and 1:1 relationship (red dashed line) between predicted and measured nutrient data from AMT12 to AMT18 according to equations 4.4 and 4.5. ....	106
<b>Figure 4.6.</b> Chl-a µg L <sup>-1</sup> during six AMT transects between 2003 and 2010. The markers represent the chl-a concentration at the CM depth of the sampling locations which included N+N, POC and PON data for each AMT transect. ....	107

<b>Figure 4.7.</b> Linear regression (black line) and 1:1 relationship (red dashed line) between predicted and measured nutrient data from AMT12 to AMT18 according to equations 4.6 and 4.7. ....	108
<b>Figure 4.8.</b> POC ( $\mu\text{g L}^{-1}$ ) from AMT12 to AMT20 at five locations along the Atlantic transect. The bars highlighted in red indicate predicted values (calculated as stated in section 4.3.4).....	109
<b>Figure 4.9.</b> PON ( $\mu\text{g L}^{-1}$ ) from AMT12 to AMT20 at five locations along the Atlantic transect. The bars highlighted in red indicate predicted values (calculated as stated in section 4.3.4).....	110
<b>Figure 4.10.</b> Organic (PON:POP) and inorganic (N+N:SRP) N:P ratios (mole:mole) at the depth of the chlorophyll maximum in the six ecological domains.....	112
<b>Figure 4.11.</b> Organic C:N ratios (mole:mole) at the depth of the chlorophyll maximum in the six ecological domains. ....	113
<b>Figure 4.12.</b> Organic C:P ratios (mole:mole) at the depth of the chlorophyll maximum in the six ecological domains. ....	114
<b>Figure 4.13.</b> Organic C:N ratios (mole:mole) at the depth of the chlorophyll maximum from AMT12 to AMT20 at five locations along the Atlantic transect.....	115
 <b>CHAPTER 5</b>	
<b>Figure 5.1.</b> AMT20 relationship between temperature ( $^{\circ}\text{C}$ ) and copepod dry weight adjusted respiration rates ( $\mu\text{l O}_2 \text{ mg dw}^{-1} \text{ d}^{-1}$ ). ....	137
<b>Figure 5.2.</b> Arrhenius plot of copepod respiration during AMT20.....	138
<b>Figure 5.3.</b> Relationship between temperature-corrected respiration rates.....	139
<b>Figure 5.4.</b> Comparison between measured and MTE assumed respiration rates.....	140
<b>Figure 5.5.</b> Responses of <i>Undinula vulgaris</i> respiration to temperature and body size ..	143
<b>Figure 5.6.</b> Responses of <i>Pleuromamma gracilis</i> respiration to temperature and body size .....	144

<b>Figure 5.7.</b> Responses of <i>Pleuromamma abdominalis</i> respiration to temperature and body size.....	146
<b>Figure 5.8.</b> Responses of <i>Nannocalanus minor</i> respiration to temperature and body size .....	147
<b>Figure 5.9.</b> Responses of <i>Euchirella sp.</i> respiration to temperature and body size .....	148
<b>Figure 5.10.</b> Q <sub>10</sub> estimations using the whole dataset and 5 individual species of copepod. Different coloured bars represent the comparison between equations 5.2, 5.3, 5.4 and 5.5.....	150
<b>Figure 5.11.</b> Egg production rates of larger copepod species on AMT20. ....	152
<b>Figure 5.12.</b> <i>Undinula vulgaris</i> egg production rates on AMT20.....	154
 <b>CHAPTER 6</b>	
<b>Figure 6.1.</b> General mechanistic model of copepod physiological pathways in a decreased food quality scenario. ....	181
 <b>CHAPTER 8</b>	
<b>Figure 8.1.</b> Schematic of the experimental setup with the three sensors: Unisense microelectrode, NeoFox optode and two Oxygraph Hansatech electrodes.....	201
<b>Figure 8.2.</b> Oxygen concentration ( $\mu\text{mol O}_2 \text{ L}^{-1}$ ) in deionised water at 16.99 °C as a function of time (min) measured by the different sensors in the two chambers. A) chamber 1 with an Oxygraph electrode disc and the Neofox optode, and B) chamber 2 with an Oxygraph electrode disc and the Unisense microrespirometer. ....	204
<b>Figure 8.3.</b> Oxygen concentration changes in the thirteen experiments carried out with the three different devices in the two chambers (numbers 1-13).....	206

## LIST OF TABLES

### CHAPTER 1

**Table 1.1.** Fatty acids in phytoplankton and detritus. ....19

**Table 1.2.** Distribution of N:P and C:N ratios (molar) throughout the world's oceans. ....23

### CHAPTER 2

**Table 2.1.** N and P added in ESAW medium per chemostat.....31

**Table 2.2.** 18 vs 24 hour respiration experiment. ....36

**Table 2.3.** Fluorometer calibration on AMT20.....48

### CHAPTER 3

**Table 3.1.** Stoichiometric ratios (N:P, C:N and C:P mol mol<sup>-1</sup>), carbon, nitrogen and phosphorus content (pg cell<sup>-1</sup>), cell volume (µm<sup>3</sup>) and concentration (cell mL<sup>-1</sup>) of *R. salina* and number of replicates for each respiration (R), egg production (EPR) and feeding experiment (F).....64

**Table 3.2.** Significant regression analyses of fed (R<sub>f</sub>) and unfed (R<sub>u</sub>) respiration rates (nL O<sub>2</sub> dw<sup>-1</sup> h<sup>-1</sup>) and egg production rates (EPR; eggs female<sup>-1</sup> day<sup>-1</sup>) versus food quality (separated into N:P < 16:1 and N:P > 16:1). ....69

**Table 3.3.** Average carbon budget of *T. longicornis* fed on *R. salina* at different N:P ratios. ....71

**Table 3.4.** Regression analyses of significant relationships between *T. longicornis* AE (%), GGE<sub>c</sub> (%), MI (%) and CoE (%) and *R. salina* N:P (separated into > 16:1 and < 16:1) and C:N ratios.....72

**Table 3.5.** Regression analyses of fed (R<sub>f</sub>) respiration rates (nL O<sub>2</sub> dw<sup>-1</sup> h<sup>-1</sup>) and egg production rates (EPR; eggs female<sup>-1</sup> day<sup>-1</sup>) versus the content (%) of major fatty acid classes in *R. salina*. ....86

**Table 3.6.** Significant regression analyses of C:N ratio versus the content (%) of major fatty acid (FA) classes in *R. salina*. ....87

<b>Table 3.7.</b> Major fatty acids (FA) as a proportion of total FA, ratios and nutrients by concentration at different N:P (molar) ratios of <i>R. salina</i> .....	88
---	----

#### CHAPTER 4

<b>Table 4.1.</b> AMT20 Ecological domains, defined according to .....	95
--	----

<b>Table 4.2.</b> List of variables considered in the forward stepwise and multiple linear regression analyses. ....	96
--	----

<b>Table 4.3.</b> List of AMT cruises with respective dates and routes. ....	97
--	----

<b>Table 4.4.</b> Chemical characteristics of water collected at the chlorophyll maximum. ....	99
--	----

<b>Table 4.5.</b> Forward stepwise and multiple regression analysis of nutrients to significant predictor variables. A) Includes data from all the domains.....	100
---	-----

<b>Table 4.6.</b> Validation of POC and PON predictive equations for AMT20.....	104
---	-----

<b>Table 4.7.</b> Validation of POC and PON predictive equations for AMT12 to AMT18. ....	107
---	-----

<b>Table 4.8.</b> Major fatty acids (FA) as a proportion of total FA and ratios by concentration for the seston at the chlorophyll maximum (CM) in different ecological domains. ....	117
---	-----

<b>Table 4.9.</b> Simple regressions and correlations of fatty acids (FA) to individual variables. ....	119
---	-----

<b>Table 4.10.</b> Forward stepwise and multiple regression analysis of FA to significant predictor variables. A) Includes data from all the domains.....	120
---	-----

#### CHAPTER 5

<b>Table 5.1.</b> <i>In situ</i> temperature at the surface, chlorophyll maximum (CM) and 200 m at the stations sampled during AMT20 for determination of copepod physiological rates. ....	134
---	-----

<b>Table 5.2.</b> Estimates of the parameters describing the metabolic scaling of copepod respiration derived from measurements made during AMT20.....	139
--	-----

<b>Table 5.3.</b> Exponential equations relating species- respiration rates ( $\mu\text{l O}_2 \text{ mg dw d}^{-1}$ ) to incubation temperature ( $^{\circ}\text{C}$ ). ....	141
---	-----

<b>Table 5.4.</b> Summary of estimates of the parameters describing the metabolic scaling of the respiration of the 5 copepod species measured during AMT20.....	149
<b>Table 5.5.</b> Difference between $Q_{10}$ coefficients (average between whole dataset and species) from equation 5.2, 5.3, 5.4 and 5.5 in percentage of absolute change between estimates.....	151
<b>Table 5.6.</b> Copepod respiration measured during AMT20.....	166
<b>Table 5.7.</b> Egg Production Rates measured on AMT20.....	169
<b>Table 5.8.</b> Copepod respiration from Ikeda et al. (2007).....	172
<b>CHAPTER 7</b>	
<b>Table 7.1.</b> Pipettes calibration and accuracy. ....	192
<b>Table 7.2.</b> Benson and Krause (1984) solubility constants. ....	194
<b>CHAPTER 8</b>	
<b>Table 8.1.</b> Mean oxygen concentration and standard deviation measured by the four sensors at 4 sample intervals in the precision test. ....	207
<b>Table 8.2.</b> Regression parameters of the two sensors from the same chamber.....	207
<b>Table 8.3.</b> Mean of the ratios of the oxygen concentrations measured by the two sensors inside the same chamber at the different light intensities: A) optode/ Oxygraph ratio, B) Unisense/ Oxygraph ratio.....	208
<b>Table 8.4.</b> Advantages and disadvantages of the sensors used in the present article. ..	211



## LIST OF NOTATIONS

AA	Arachidonic acid	PIC	Particulate inorganic carbon
AE	Assimilation efficiency	PL	Prosome length
ALA	$\alpha$ -linoleic acid	PML	Plymouth Marine Laboratory
AMT	Atlantic Meridional Transect	POC	Particulate organic carbon
BAS	British Antarctic Survey	PON	Particulate organic nitrogen
BODC	British oceanographic data centre	POP	Particulate organic phosphorus
BS	Backscatter	PUFA	Polyunsaturated fatty acids
<i>chl-a</i>	Chlorophyll a	$R_f$	Respiration fed
CM	Chlorophyll maximum	RQ	Respiratory quotient
CMT	Chlorophyll maximum temperature	$R_u$	Respiration unfed
CoE	Cost of Egg Production	S	Salinity
DHA	22:6(n-3)	SAFA	Saturated fatty acids
<i>dMLCM</i>	distance between the mixed layer and chlorophyll maximum	SAHFOS	Sir Alister Hardy foundation for ocean sciences
<i>dw</i>	dry weight	SDA	Specific dynamic action
$E_a$	Activation energy	SRP	Soluble reactive phosphorus
ENSO	El Niño–southern oscillation	SST	Sea surface temperature
EPA	20:5(n-3)	TLC	Thin layer chromatography
<i>EPR</i>	Egg production rates	$T_x$	Length of time of incubation, x= number of hours
ESAW	Enriched seawater, artificial water	VIF	Variance inflation factor
ETO	Evolutionary trade-off	WP2	Standard zooplankton net
FA	Fatty acids	$R$	metabolism/respiration
FID	Flame ionisation detector	$k$	constant
FSW	Filtered seawater	$T$	temperature degree Kelvin
G	Growth	$t$	temperature degree Celsius
GC	Gas chromatogram	$M$	Body size
GF/F	Glassfiber filter "F" type (0.7 $\mu$ m pore size)	$b$	Allometric exponent
GGE	Gross growth efficiency	$Q_{10}$	$Q_{10}$ coefficient
HOT	Hawaii ocean time series	$V$	Volume
$I$	Ingestion	$N$	Number of copepods
Ln	Natural logarithm	$n$	Cell concentration
MEI	Multivariate ENSO index	$g$	Grazing coefficient
MI	Metabolic increment	$S$	Fatty acid
MLD	Mix layer depth	$X_M$	molar concentration
MTE	Metabolic theory of ecology	$A$	Area
MUFA	Monounsaturated fatty acids	$F$	Fluorescence
$N+N$	Nitrate + nitrite	$f$	Flow rate
n-3	Omega 3	$\mu$	Growth rate
n-6	Omega 6	$D$	Dilution rate
NA	Not available	UL	Urosome Length
ND	Below the limit of detection	UW	Urosome Width
NERC	National Environmental Research Council	PW	Prosome Width
NOCS	National Oceanographic Centre Southampton	$[O_2]$	Oxygen concentration
NPSG	North-Pacific subtropical gyre	$\tau$	Tau
OLS	Ordinary least square	$a$	Cycle time
PCC	Pearson product-moment correlation coefficient	$\sigma$	Standard deviation



## ACKNOWLEDGMENTS

I wish to take this opportunity to sincerely thank all the people that supported me in these past few years. My journey begun back in 2009, when spirits were high and the desire to achieve stood tall. Over time these feelings may have occasionally wavered but they were never broken.

I want to thank Carol Robinson for her constant support, not just in work related matters. Her words of encouragement and her constructive criticism helped me to look at things from a different perspective which made all the difference in the quality of my work. Also, my utmost thanks to Claudia Castellani, her comments have always been straight to the point and have always added greatly to my efforts, I often wished you weren't so far away as I thought I had a lot more to learn from you. Thanks to Erik Buitenhuis and his mathematical brain.

I am grateful to David Pond for his support at BAS and Rob Utting for his support in the lab at UEA. To all of my cheery (and not so cheery at times) office mates thank you all, sharing this with you made all more pleasant. Thanks to the people in PML, the MBA and SAHFOS in Plymouth involved with L4, the RV Quest and the taxonomy labs and a particularly big applause to the jolly bunch in the workshop at SAHFOS! I also thank all the crew and fellow scientists that I sailed with on board the RRS James Cook back in 2010.

I thank all the time-series programmes I have taken data from: The Hawaii Ocean Time-series (HOT), the Atlantic Meridional Transect (AMT), which data is stored at the British Oceanographic Data Centre (BODC), the Continuous Plankton Recorder (CPR), which data is collected from SAHFOS and the Norwegian Coastal Surveillance Program (NCSP), which data is supplied by the Norwegian Institute of Marine Research.

Particular thanks go to Gardline Environmental Ltd for the collection of fresh zooplankton in the North Sea and, on a more personal note, my dear friends Lucinda McCombe, Farah Chaudry and Cansu for making it possible and being close to me throughout this experience.

Many, many... many thanks to my lovely family back in Italy for their encouragement and love, grazie mamma Fernanda, papa' Giuseppe, sorellina Valentina (Wile) e fratellino Cesare (Cesurre). Last but not least I would like to thank Richard Godsall, my constant companion. Thank you so much for your patience and for always being there, providing entertainment. Sorry for leaving you to do things on your own these past few months.



# **CHAPTER 1**

## 1. Introduction

### 1.1 Copepods and their role in the marine environment

Meso-zooplankton are defined as zooplankters between 200  $\mu\text{m}$  to 2 mm in size. They are ubiquitously distributed heterotrophic metazoans with an estimated biomass of  $21.5 \times 10^9$  tons, 2.15-fold and 20-fold greater than that of zoobenthos and nekton in the ocean respectively (Hernandez-Leon and Ikeda 2005a).

In marine ecosystems, copepods account for 55 to 95% of total zooplankton biomass (Longhurst 1985). However, what makes copepods so significant is not just the sheer scale of their dominance of the world's oceans but also their effect on all nutrient biogeochemical cycles, marine carbon flux (biological pump) and their role as a link (primary consumers - secondary producers) between the microbial loop and larger consumers (such as fish) in aquatic food webs (Figure 1).

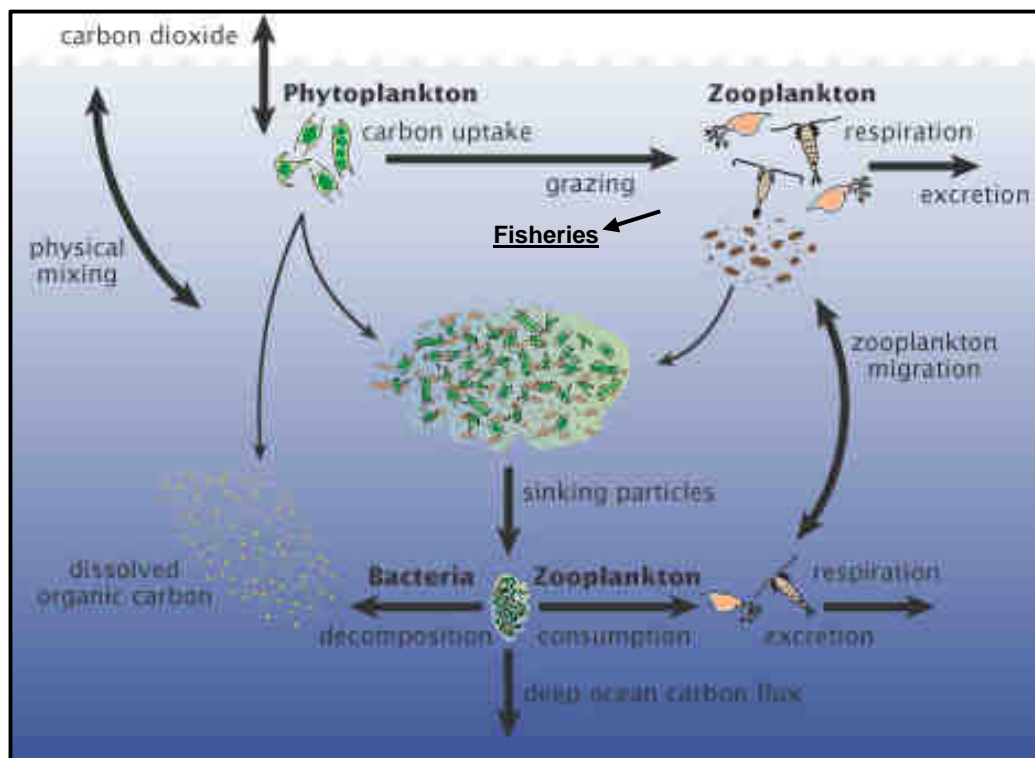


**Figure 1.1.** Biological carbon pump and the role of zooplankton. Picture taken from <http://earthobservatory.nasa.gov>.

Copepod physiology, through the processes of organic matter consumption, assimilation metabolism and growth, shapes ocean ecology and chemistry by means of remineralisation and regeneration of elemental compounds (Redfield 1934; Falkowski and Davis 2004). One of the key roles of copepods, through uptake, production and export, is to support the oceanic biogeochemical cycles of nutrients (such as carbon, nitrogen and phosphorus), contributing to the regeneration of the nutrient pool available for phytoplankton above the pycnocline (Sterner 1990). Additionally, copepods play a fundamental role via input of organic material from the upper water column to the aphotic zone and the seafloor via active and passive fluxes of organic matter, a process also known as carbon export (Longhurst and Harrison 1989).

According to the concept of the trophic food web, in their role as secondary producers, they are responsible for transferring autotroph-derived energy and nutrients to higher trophic levels (Sterner and Elser 2002; Kiorboe 2008). Copepods constitute the main food source for all planktivorous fish; through their physiological processes, copepods assimilate and convert organic matter into carbohydrate, protein and lipid, in turn to be consumed and assimilated higher up the oceanic food web. Through their population dynamics and biomass variability, caused by productivity and mortality, they also affect fisheries management. This is because fluctuations in the abundance of key copepod species leads to bottom-up control of commercially exploited fish stocks (Beaugrand et al. 2003; Beaugrand and Reid 2003).

Copepod physiological responses are dynamic and can actively vary depending on the state of the ecosystem (Moloney et al. 2011). Therefore, to understand the constraints of their ecological and biogeochemical interactions, their overall effect on ecosystems and assess potential climatic feedbacks it is necessary to study copepod physiology and quantify their impact on the ecology of the world's oceans.

## **1.2 Copepod physiology and environmental variables**

Copepods are poikilotherms, therefore they can only regulate their bodily processes in the face of moderate environmental change and within the boundaries dictated by a species' tolerance limits and adaptation potential. Generally these responses to environmental change are controlled through physiological adjustment (acclimatisation) allowing them to sustain their metabolic performance and/or survive (Withers 1992). If those changes become too great and/or too quick, these organisms stop tolerating and die (Withers 1992). Therefore, understanding how a copepod's performance and activities are affected under a variety of environmental conditions can provide important information on the short and long term consequences of environmental change on these organisms. Thus we can

assess how changes in their performance can impact their feedback on biogeochemical cycles, food web interactions and therefore the entire ecosystem.

Physiological rates such as respiration, excretion, faecal pellet production, egg production and feeding have been shown to be affected by a number of biotic and abiotic factors such as gender, body mass, physical condition, activity, geographical region, season, temperature, light and food availability (Mauchline 1998). In terms of environmental variables, the study of the responses of copepods to variation in food availability, quality and temperature are of primary interest since they are the most significant environmental variables affecting physiological rates in heterotrophs (Moloney et al. 2011; Glibert et al. 2012).

### 1.2.1 Copepod metabolic activity and respiration

Metabolism is the process that sustains life in an organism. This is because metabolism is the combination of chemical processes converting materials into energy in the organism (through oxidation). Metabolism breaks down organic matter obtained through feeding (catabolism), to release energy in the form of ATP and waste products (in the form of CO<sub>2</sub> through respiration) and synthesize new compounds (anabolism) allocating them to survival, growth and reproduction and excrete altered forms back into the environment (Withers 1992). The metabolic rates therefore, represent the resource demands of that organism, as well as the level of adaptation to their habitat, closely linked to their evolutionary history. This is because the mechanisms behind the organism's physiological responses represent the species' evolutionary solution to environmental constraints.

Metabolism is of primary importance since it accounts for 42-72% of an organism's energy budget in the ocean (Ikeda 1985). Copepod metabolism can be quantified experimentally by examining the animal's physiological responses, in the form of oxygen consumption rates and inorganic nutrient excretion, which vary with changes in habitat and environmental stimuli. Differing from the concepts of production and feeding (energy gain), metabolic demand is accountable in terms of energy loss (Withers 1992).

Since there is a quantitative relationship between metabolic rates and material oxidised to produce energy (Clarke 1987), oxygen consumption rates are indicative of their food and energy requirements. Consequently the assessment of respiration rates in planktonic communities is a prerequisite to estimating energy demand and energy fluxes in marine ecosystems (Hernandez-Leon and Ikeda 2005b).

Oxygen consumption (or metabolism) is strongly affected by the level of motor activity of the organism itself, where little or no activity results in a reduced amount of oxygen respired compared to respiration rates during higher levels of movement.

Metabolic rate therefore, is defined in terms of activity:

- Basal metabolic rate: no motor activity, also known as minimal energy expenditure or basal metabolic cost required for survival (maintenance).
- Routine metabolic rate: at minimum uncontrolled motor activity.
- Active metabolic rate: during stimulated and enforced motor activity, also known as maximum energy expenditure.
- Specific Dynamic Action or SDA: respiration during feeding.

The average daily minimal metabolic expenditure is typically a number in between routine and active metabolic rate; this has been suggested to be generally two to three times the basal metabolic rate (Whiteley et al. 2001; Brown et al. 2004 and references therein).

The fluctuation in habitat conditions over the seasonal cycle, such as temperature and salinity, has a significant effect on copepod metabolic rates (Conover 1959; Marshall and Orr 1958); feeding activity in particular has a pronounced impact. For instance, Schmoker and Hernandez-Leon (2003) found a positive correlation between respiration rates and ingestion rates of *Daphnia magna*, which increased rapidly after the addition of food to the respiration chambers. In the field, *T. longicornis* respiration rates followed an asymptotic trend with chl-a concentration reaching their maximum values during the spring bloom (Castellani and Altunbaş 2013). The respiration rates of *Temora stylifera* were also found to increase with ingestion up to a critical level and then reach a plateau at certain food concentrations (Abou Debs 1984).

SDA is considered the energetic cost of protein biosynthesis and therefore growth (Kiorboe 1985; Hernandez-Leon and Ikeda 2005b; Thor 2002). Kiorboe et al. (1985) found that the magnitude of SDA as well as clearance, ingestion and egg production in *Acartia tonsa*, changed in relation to food concentration. Respiration at saturating food concentrations was up to four times higher than rates measured in starved copepods. These findings were supported by Thor (2002) working on *Acartia tonsa* and *Calanus finmarchicus*, reinforcing that an increase in metabolic rate of fed copepods is linked to assimilation efficiency and cost of growth.

Variation in metabolic rates has also been associated with the quality of food ingested by the organism. Thor (2002) for instance, suggests that the energy required for biomass formation is dependent on the biochemical composition of the eggs of the copepod and importantly on the quality and biochemical signature of the food ingested (independent of concentration). His study shows that *Acartia tonsa* exhibited higher ingestion rates and consequently higher respiration rates and SDA values, when fed on similar concentrations of the flagellate *Tetraselmis impellucida* compared to a lower quality diet of the flagellate *Dunaliella tertiolecta* (Thor 2002).

### 1.2.2 Copepod basal respiratory cost

The basal or routine metabolic rates, respectively the rate of inactive and minimally active organisms, are typically measured, under constant laboratory conditions, to estimate basic energetic and carbon demands. However, in their natural environment, copepods experience considerable fluctuation in environmental conditions and undergo a variety of physiologically demanding activities; therefore, respiratory costs would reflect that also including the energetic expenditures of feeding, growth and reproduction.

The resting metabolic rate (or basal metabolic rate) of a poikilotherm copepod is constrained by a number of biotic and abiotic factors. However the major determinants of these basal metabolic requirements are the laws of thermodynamics and allometric relationships (Ikeda et al. 2001).

Copepod body mass must be taken into account as respiration rates in larger animals are higher than those in smaller ones. The range of allometric exponents highlight the fact that weight-specific respiration rates decrease with increasing body mass, making smaller copepods metabolically more active than larger ones (Kleiber 1947). This relationship is demonstrated by Kleiber's law describing how metabolic rates (R) scale with body size (or mass) (M) based on an exponential allometric relationship (b) (equation 1.1).

$$R = R_0 M^b \quad (1.1)$$

Where;

$R_0$  =normalisation constant independent of body mass

M = body mass

b = allometric exponent

Importantly, copepods are poikilotherms therefore the primary environmental factor affecting their oxygen consumption is temperature, with respiration rates increasing as temperature increases. This is due to a thermal dependency of ATP synthesis in respiratory processes (Clarke 1987). Marshall and Orr (1972) found that the respiration rates of *Calanus finmarchicus* doubled from 0 to 10°C and above that the oxygen consumption increases at even greater rates. The effect of temperature on metabolic rates R can be described by the Arrhenius relationship or Boltzmann factor (1.2), valid only in temperatures ranging from 0 to 40 °C (range of normal biological activity), and the Q<sub>10</sub> approximation derived from the van't Hoff rule (1.3). The Arrhenius relationship is a formulation based on thermodynamic laws and analogous to the van't Hoff equation although the latter is a simple empirical formula.

$$R = R_0 e^{-E_a/kT} \quad (1.2)$$

Where;

R<sub>0</sub> =normalisation constant independent of temperature

E<sub>a</sub> = activation energy

k = Boltzmann constant (8.617x10<sup>-5</sup> eV k<sup>-1</sup>)

T = temperature in Kelvin °K

$$Q_{10} = (R_2/R_1)^{10/(t_2-t_1)} \quad (1.3)$$

Where;

R<sub>1</sub> and R<sub>2</sub> = respiration rates at temperatures t<sub>1</sub> and t<sub>2</sub> (°C) respectively

The Q<sub>10</sub> formula describes the effects of temperature on copepod metabolic rates (Harris et al. 2006); where higher Q<sub>10</sub> values in a species signify its greater sensitivity to temperature variation.

For copepods, Ikeda (1985) suggests that up to 95% of the variation in basal or routine oxygen consumption rates is due to the effect of temperature and body size (Harris et al, 2006) therefore suggesting that a mechanistic approach can account for most of the

variations. The above relationships combined underpin the Metabolic Theory of Ecology (MTE) as shown by equation 1.4 (Gillooly et al. 2001; Brown et al. 2004).

$$R = R_0 M^b e^{\frac{-E_a}{kT}} \quad (1.4)$$

Where;

R = metabolic rate/respiration

R<sub>0</sub> = normalisation constant independent of mass and temperature

M = body mass

b = allometric exponent

k = Boltzmann constant (8.617x10<sup>-5</sup> eV k<sup>-1</sup>)

E<sub>a</sub> = activation energy

T = temperature in Kelvin °K

The universal MTE has been proposed as an accurate predictive tool for an organism's metabolic coefficients, suggesting the application of a fixed allometric exponent *b* to the <sup>3</sup>/<sub>4</sub> power for all organisms and activation energy in the range of 0.6-0.7 eV (Gillooly et al. 2001; Brown et al. 2004). However, this has been heavily criticised by many scientists such as Clarke (2004) and Glazier (2010), arguing that the metabolic rate of an organism varies inter and intra-specifically and can be affected by a variety of other factors. The allometric exponent *b* has been shown to vary between 0.4 and 1.4 between different organisms and ontogenic stages of the same species (Ivleva 1980; Glazier 2005). For instance, the respiration rate of *T. longicornis* scaled isometrically with dry-weight to the power of 0.83 - 1.35 (Castellani and Altunbaş 2013).

Current evidence indicates that other biotic and abiotic parameters such as species, gender, light, salinity and feeding history (food quality and quantity) can play a role in basal metabolic regulation (Hernandez-Leon and Ikeda 2005b). For example, Marshall and Orr (1975) found that the oxygen consumption of *Calanus sp.* doubled when exposed to strong light and decreased under the effects of lower salinity. Feeding history can also affect basal metabolic rates since it reflects the amount of time necessary for digestion and assimilation processes to take place. Increasing food concentration and food quality therefore can prolong the organism's energetic demands increasing respiration rates,

although a dramatic decline in oxygen consumption rates, under the effects of starvation, can be seen after 8-10 hours (Kiorboe et al. 1985; Castellani and Altunbaş 2013).

For copepods additional factors such as diel vertical migration, development stage and oxygen partial pressure can also influence respiration rates (Hernandez-Leon and Ikeda 2005a). Recent studies also suggest that the presence/absence of myelin sheath around nerves contributes to the regulation of metabolic rates (Ikeda et al. 2006; Ikeda et al. 2007). An average of 50% of calanoid copepods have myelin-like sheaths enveloping their axons. This has been suggested to affect reaction times with non-myelinated species generally showing slower responses to stimuli (Davis et al. 1999; Lenz et al. 2000; Lenz 2012). However, Ikeda et al. (2006) and Schukat et al. (2013) found no significant difference between the respiration rates of myelinated and non-myelinated species.

### 1.2.3 Copepod production and egg production rates (EPR)

Copepod secondary production includes species biomass and growth. Growth is part of the assimilated energy, in excess of metabolic requirements (maintenance), concentrated into somatic growth and for non-moulting adults, reproduction in terms of number of eggs spawned (Huntley and Lopez 1992; Kiorboe 2008). The determination of EPR is therefore a useful indicator representing a species' ability to reproduce and the recruitment potential of a population. It is also a good indicator of fitness and health, where stressed and poorly fed females produce poorer quality and fewer eggs (Jónasdóttir 1994; Guisande and Harris 1995; Jónasdóttir and Kiorboe 1996; Kleppel et al. 1998; Dutz et al. 2008; Mayor et al. 2009a).

Copepod egg production rates (EPR) are influenced by a variety of biotic and abiotic factors such as temperature (e.g. Huntley and Lopez 1992; Calbet and Agustí 1999; Castellani and Altunbaş 2006), food concentration (e.g. Calbet and Agustí 1999; Guisande et al. 2000; Castellani and Altunbaş 2006) and quality in terms of mineral ratios and biochemical composition (e.g. Jónasdóttir 1994; Kiorboe 1985; Anderson and Pond 2000; Broglio et al. 2003; Arendt et al. 2005; Jónasdóttir 2005; Kattner et al. 2007; Jónasdóttir et al. 2009; Mayor et al. 2009a; Koski et al. 2010). As shown for respiration rates, body size can also affect breeding in copepods as it limits the amount of gametes that can be produced and carried by a female. Life-histories and reproductive strategies are also crucial since fecundity is 7.5 times higher in free spawning species than brooding species which carry their eggs in external sacs (Mauchline 1998).

In the field, seasonal changes in environmental conditions influence the reproductive dynamics of zooplankton. Seasonal environmental conditions include temporal and spatial

differences in temperature gradients and food availability in terms of quantity and quality. These variables can affect not only the frequency of spawning but also the brood size produced by female copepods (Hirche et al. 1997).

The effects of seasonal processes on zooplankton are more pronounced in temperate and higher latitudes where the peak breeding season is typically restricted to a bimodal (temperate) or unimodal (high latitudes) response and where development time and copepod growth rates are slower (Kiorboe and Nielsen 1994; Mauchline 1998). On the other hand, epipelagic tropical copepods, generally smaller than those in higher latitudes, experience reduced variations in temperature and food availability on a temporal scale. These regions (except upwelling areas) are little affected by seasonal changes and therefore breeding tends to be spread throughout the year (Mauchline 1998).

Studies on the dynamics of phytoplankton blooms and temporal changes in food concentration reveal that copepod production and abundance in temperate ecosystems coincides with peaks in food availability and optimal temperature ranges, highlighting how the competition for limiting resources drives the physiological response of the copepods to the environment. Spatial variations in reproduction due to temperature variation and diet have also been observed by Calbet and Agustí (1999), who found that on an Atlantic latitudinal transect the copepod distribution was determined mainly by phytoplankton abundance, while EPR depended on chlorophyll-a (chl-a) concentration (as a proxy of food quantity) and temperature. In their study EPR increased with both temperature and food concentration up to a maximum threshold, then it declined indicating that EPR can be food-limited and/or temperature-limited.

Species-specific reproductive responses regulated by a multiplicity of environmental factors in the field have also been investigated. Castellani and Altunbaş (2006) for instance, found an annual maximum EPR of the neritic copepod *Temora longicornis* during spring/summer (9-11°C) and minimum in autumn/winter in the Irish Sea; the highest EPR values also coincided with higher *in situ* chl-a concentrations from ~1 to 3.5 µg L<sup>-1</sup>. However, the production rates of the higher-latitude *Calanus finmarchicus* were found to be principally food limited (Hirche et al. 1997; Jónasdóttir et al. 2008); for this key North Atlantic species when reproduction cannot be supported by *in situ* food availability, the animals accumulate lipid reserves and undergo diapause, overwintering in deeper waters (Jónasdóttir et al. 2008; Mayor et al. 2009b).

Nutrition is of primary importance in reproduction since diet-specific effects of not only food quantity, but also food quality, are important factors affecting copepod reproductive success. Hessen (1992) stated that seston biomass is not in fact always correlated with

zooplankton production and studies (e.g. Jónasdóttir et al. 1995; Pond et al. 1996; Arendt et al. 2005; Mayor et al. 2009a; Koski et al. 2010), carried out on a variety of neritic and higher latitude copepods, highlight the importance of a chemically rich and varied diet. Several studies have found a positive correlation between reproductive success and the organic content of the egg as the sum of protein, carbohydrate, and lipid (e.g. Lacoste et al. 2001; Ceballos and Álvarez-marqués 2006).

Most of these studies correlate the presence of a higher concentration of polyunsaturated fatty acids (PUFA), such as n-3, in the diet with higher fecundity and reproductive rates in copepods such as *Calanus finmarchicus* (Mayor et al. 2009a) and *Temora longicornis* (Jónasdóttir et al. 1995; Arendt et al. 2005). Kleppel et al. (1998) also found that EPR in *Acartia tonsa* was proportionally affected by the variation in concentration of 3 different fatty acids and 4 amino acids in the diet.

Some studies correlated EPR to the mineral concentration of the food; Checkley (1980) and Kiorboe (1989) for instance, found that reproduction in *Paracalanus parvus* and *Acartia tonsa* respectively, positively increased with the nitrogen content of the food ingested. Whereas, the production of some freshwater cladocerans has been found to be primarily limited by the phosphorus content of their food instead (Sterner and Hessen 1994).

A combination of mineral and biochemical substrates in the diet of copepods are therefore necessary to satisfy their growth requirements. This is dictated by the composition of their structural components which regulate the physiological demand for the compounds necessary for biosynthesis. Guisande (1999) for instance, observed higher reproductive success as the amino acid composition of the food *Euterpina acutifrons* preyed upon became closer to the amino acid composition of the copepod species' body. Therefore a diet, where the biochemical composition of the food is closer to the biochemical composition of the copepod, can be more balanced for the organism.

#### 1.2.4 Copepod feeding

Feeding is one of the physiological rates most extensively studied and examined experimentally in the field of zooplankton ecology. This is since grazing is the process through which zooplankton have a direct trophic impact on primary producers and through their growth and reproduction on secondary consumers. Copepods are hard-bodied animals and as a result have little or no ability to take up dissolved organic compounds from the surroundings through osmotic processes (Mauchline 1998). Copepods have access to a variety of food sources, resulting in a diverse range of methods and strategies

for food capture and acquisition. Ingested food is the only source of energy and material for their basal metabolic processes and growth (Bamstedt et al. 2000). Therefore food availability is one of the most important factors affecting the population dynamics of any zooplankton species (Guisande et al. 2000).

The portion of the organic matter that is not assimilated by zooplankton is packaged into sinking faecal pellets ( $5\text{-}220\text{ m d}^{-1}$  (Turner 2002)), while the portion of organic matter assimilated is turned into energy to sustain basal maintenance (respiration) and growth (somatic growth and eggs). The ingested material is also excreted in waste dissolved inorganic and organic compounds that contribute to sustain nutrient biogeochemical cycling in the ocean (Longhurst and Harrison 1989). Therefore knowledge of the feeding processes of zooplankton is crucial to understanding the mechanisms behind ecosystem function.

The early observations, as summarised by Huntley (1988), led to the description of a passive feeding response of copepods, known as “automatic feeding” (Fuller 1937), even describing copepods as “leaky-sieves” (Boyd 1976) and restricting feeding to a function of particle size and concentration (Frost 1972). Subsequent evidence suggested that this mechanistic approach was an incorrect and inadequate description of zooplankton feeding. In a study by Ryther (1954) it became apparent that some zooplankton feeding rates were inhibited in the presence of senescent algae. In the 1980’s research began on copepod behavioural food selection, particularly after morphological evidence of chemoreceptors on the body of copepods was found (Poulet and Marsot 1978; Friedman 1980).

Since then, a number of studies have shown that copepods have the ability to actively select their food based on increasing particle size (Poulet 1978; Paffenhofer and Van Sant 1985; Tackx et al. 1989; Cowles and Strickler 1983), particle abundance (Frost 1972; Poulet 1978; Turner and Tester 1989; DeMott 1989) and the quality of the food, determined by the biochemical composition of the particles (Poulet and Marsot 1978; Cowles et al. 1988; DeMott 1989; Paffenhofer et al. 1995; Cotonnect et al. 2001).

Copepods exhibit highly developed reactions to different sensory stimuli and present a complex pattern of behavioural responses to the physical properties of food particles (Poulet and Marsot 1978; Paffenhofer and Van Sant 1985). Calanoids and other copepods have evolved the ability to detect their food/prey using chemosensors and mechanoreceptors. The first is used to detect chemical signals mainly during particle-feeding (herbivory, detritivory); the latter is more functional in predatory (carnivory) feeding, to detect disturbance in the water (Mauchline 1998). The ability of copepods to

discriminate between food sources is complex and this process is very dynamic. Copepods respond and consequently adjust their selection responses to the relevant environmental and physiological functions they are exposed to, in agreement with the optimal foraging theory; this therefore suggests behavioural adaptation in favour of maximisation of nutritional gain (DeMott 1989).

Copepods prey on the seston which includes microalgae (autotrophs and mixotrophs), ciliates (heterotrophs and mixotrophs), other smaller zooplankton and detritus. Saiz and Calbet (2007 and 2011) summarised the current knowledge on marine copepod feeding rates, considering both auto- and hetero-trophic prey, searching for general patterns and limiting factors of ecological relevance. Their study concluded that food availability and body weight are major factors shaping copepod feeding rates in the field, with a relatively minor role of temperature (Saiz and Calbet 2007 and 2011). They also found that the major components of copepod diets included ciliates and dinoflagellates particularly in oligotrophic environments, 19% and 43% respectively compared to 3.9% and 2.8% in eutrophic systems respectively; whereas diatoms emerged as small contributors to the diet of copepods, except in some eutrophic ecosystems where they increased to a maximum of 19% (Saiz and Calbet 2011).

The mechanics of ingestion differ between herbivorous or omnivorous feeding and between suspension or raptorial feeding, depending on the preferred prey type and prey motility (Bamstedt et al. 2000). However copepod feeding behaviour does not usually follow only one type of feeding strategy (Kleppel 1993). For instance, in temperate and higher-latitudes areas, copepod species-specific feeding strategies can also vary with season, different feeding strategies can develop during winter in response to the strong decrease in primary production, ranging from increased carnivory to diapause (larger oceanic species) (Oresland and Ward 1993).

The temperate copepod *T. longicornis* for instance, can follow a seasonal succession in the diet composition; from omnivorous feeding during late winter and early spring, switching to a predominantly herbivorous diet with increasing phytoplankton stock in spring (Gentsch et al. 2008; Peters et al. 2013). The ubiquitous copepod *Metridia pacifica* also switched from herbivory to carnivory in response to declining chl-a concentrations and occasionally utilised detrital sources (El-Sabaawi et al. 2010). Feeding doesn't just vary interspecifically but also intraspecifically between different ontogenetic stages, with nauplii larvae and copepodite stages feeding on a different variety of food in comparison to adults (Paffenhofer 1988).

### 1.3 Copepod nutritional requirements

Zooplankton live in a heterogeneous world and therefore the availability of food varies on spatial and temporal scales (Calbet 2001; Kiorboe 2008). For instance, in upwelling ecosystems, diets can vary swiftly, in response to wind-driven regimes (Hutchings et al. 1995), in temperate domains it varies seasonally, whilst in more stable tropical domains the diet varies little throughout the year although the supply of food can be scarce (Mauchline 1998). As a result, copepods have developed a range of tolerances and the ability to adapt their metabolic energy expenditures to maximise energy utilisation and to cope with resource variations and limitation.

Copepods adjust their responses by means of biochemical, physical and behavioural reactions which allow them to survive periods with little or no food and quickly take advantage of periods with abundant resources. For instance, as mentioned in section 1.2.3, during periods of famine some species of medium to large calanoids such as *Calanus finmarchicus*, will migrate to deep waters and undergo diapause. For such organisms dormancy is the only strategy to bridge adverse circumstances and it is not simply a cessation of development, but involves structural and physiological changes (Dahms 1995; Hairston and Munns 1984). In this instance, copepods turn down their metabolic activity at the cost of growth and in order to fulfil their basic metabolic demands they utilize their lipid reserves accumulated as food storage (Dahms 1995).

Copepods fuel the synthesis of new organic compounds for reproduction and somatic growth by oxidizing, in different proportions, carbohydrates, lipids and proteins in their diet (Hernandez-Leon and Gomez 1996). The dietary requirements and the distribution of the various essential nutritional components varies within the body of copepods which in turn, changes through the different ontogenetic stages of the same species (Kleppel 1993), from nauplii to adults.

Proteins are the major organic components in copepods and are the fundamental building blocks for tissue and enzyme production. Protein is generally considered important for somatic growth of juvenile life stages (nauplii and copepodites) and for adults during gametogenesis. Carbohydrate content in copepods is generally low and most of it is structural. However, carbohydrates are an important component especially in eggs of species with fast development times, such as *Calanus helgolandicus* (Guisande and Harris 1995). They are a very important energy source, particularly during embryonic development and during the first stages of naupliar growth. Lipid and specific polyunsaturated fatty acids (PUFAs) play an important role in animal nutrition since they are considered essential during the process of gametogenesis. Triacylglycerols and/or

wax esters are the major constituent of crustacean eggs and female gonads, making them one of the main nutritional requirements of copepods (Gatten et al. 1980; Jónasdóttir, 1994; Mayor 2005). Proteins are essential for all animals and their concentrations vary as the animal grows (Kleppel 1993). Lipids are mainly used to store energy, and the specific energy storage needs can vary enormously and ultimately determine the success of important physiological activity such as diapause (Ohman 1987) and production (Roman 1991).

While all organic compounds include carbon, the occurrence of nitrogen is mainly restricted to protein, and that of phosphorus to lipid, nucleic acids and enzymes (Postel et al. 2000). It is generally accepted (Hessen and Lyche 1991; Sterner and Elser 2002) that other elements and micronutrients play no significant role as biomass proxies. On average copepods' dry mass contains about 40% C and 10% N. Although Calanoid copepods can have higher specific N-content compared to other zooplanktonic taxa, between copepod species C and N concentrations are nearly constant (Hessen and Lyche 1991).

In contrast, the P content is quite variable between zooplankton taxa, particularly in freshwater (Hessen and Lyche 1991; Postel, et al. 2000; Main et al. 1997). Although, generally, less than 1% of the total dry biomass of a copepod is composed of P, the macronutrient is of significance in storage compounds and skeletal material (Postel, et al. 2000; Bamstedt 1986). P plays a major role in the synthesis of RNA and therefore proteins, directly affecting zooplankton growth rates (Main et al. 1997; Carrillo et al. 2001); where an increased growth rate requires greater ribosomal RNA, which should result in increased %P (Main et al. 1997; Vrede et al. 2004).

Copepod basic food demands are therefore a function of their metabolism and growth and are driven by the physiological requirement for macro-, micro-nutrient and biochemical components such as protein, carbohydrate, lipid and essential vitamins. Following the concept of homeostasis most copepods are not able to store nutrients in excess and what is not assimilated is egested; hence their health and elemental balance is dependent on the chemical and biochemical composition of their food source. Therefore, if the nutritional demands of an organism are not met, the consumer will face nutritional imbalance (Anderson and Pond 2000). This “nutritional deficiency” theory states that lack of essential elements and macromolecules in the diet of copepods leads to decreased growth rates, EPR, reduces egg hatching success, and ultimately decreases nauplii survival rates (Pond et al. 1996; Anderson and Pond 2000; Jónasdóttir et al. 2002; Vargas et al. 2006). While a sufficient supply of poor-quality food may sustain the survival of an organism (maintenance), species success (high growth rate and reproduction) relies on a

high-quality diet that meets the consumer requirements for nutrients and compounds (Andersen et al. 2007).

## 1.4 Food quality

In the seston microalgae are the major suppliers of organic matter and energy in marine ecosystems, a source of protein, carbohydrate and lipid for zooplankton. Generally the nutritional value of any algal species is variable and often imbalanced for copepods, depending on its cell size, production of toxic compounds, and biochemical composition (carbohydrate, protein and lipid content); this is related to the organic macronutrient concentrations (carbon (C), nitrogen (N), phosphorus (P)) and in particular the mineral stoichiometry (C:N:P ratio) of the cell (Gnaiger and Bitterlich 1984; Sterner and Elser 2002).

Whilst biochemistry can help characterise the nature of the carbon containing compounds in the seston, the primary purposes of studying seston stoichiometry is to quantify the relationship between constituents in a chemical substance (Sterner and Elser 2002). Some studies argue that stoichiometry, in particular the organic C:N ratio of the food alone (Anderson 1992; Acheampong et al. 2012), does not fully represent “food quality” or the nutritional adequacy of phytoplankton and seston (Mayzaud et al. 1989; Acheampong et al. 2012). This is because mineral ratios alone do not fully characterise the nature of the food ingested by zooplankton, such as the quality of the carbon, therefore underestimating the importance of biochemical characterisation (Tang and Dam 1999; Cahoon 1981; Sterner and Schulz 1998; Broglio et al. 2003; Acheampong et al. 2012). As a consequence, the use of essential biochemical compounds such as fatty acids and amino acids, as proxies of food quality has been incorporated in several studies e.g. Graeve et al. (1994), Guisande and Harris (1995), Pond et al. (1998), Anderson and Pond (2000), Cotonnect et al. (2001), Hazzard and Kleppel (2003), Arendt et al. (2005), Evjemo et al. (2008), Wilson et al. (2010).

### 1.4.1 Phytoplankton nutritional value

Living organisms are products of their environment; changes in their environment therefore induce changes in their chemical composition (Corner and O'Hara, 1986). Since phytoplankton are osmotically balanced, their nutritional value and biochemical complexity can vary considerably according to the ambient conditions the cells grow in, therefore offering a wide range of natural diets to zooplankton. Kattner (1983) and Mayzaud et al. (1989) have shown that in the natural environment phytoplankton undergo compositional changes in their lipid classes as the availability of nutrients changes throughout the

seasons. This also applies to a laboratory setting where the culture medium, temperature and light exposure chosen for the cultures greatly affect the biochemical composition of phytoplankton (Hitchcock 1982).

Food quality and the organism's nutritional requirement have a direct influence on copepod metabolism, fecundity and the embryo's hatching success, since eggs are composed of a variety of essential elements, all supplied by food (Jónasdóttir 1994; Guisande and Harris 1995; Jónasdóttir and Kiorboe 1996; Kleppel et al. 1998; Dutz et al. 2008; Mayor et al. 2009a and 2009b). The compositional changes of algal food are therefore directly related to the physiological performance of the organism. Such differences in nutritional quality found in the natural environment, exist not only between but also within taxonomic groups. Hitchcock (1982) compared axenic cultures of dinoflagellates and diatoms of the same size, grown under identical conditions and estimated that dinoflagellates provide 2 to 6 times more protein, 2.5 to 3.5 times more carbohydrate, and 1.1 to 3 times more lipid than diatoms.

Investigations into the effects of diet on copepod physiology have shown that a mixed-algal diet provides a better nutritional balance for copepods (Hitchcock 1982; Brown et al. 1997; Cahoon 1981). For instance, Cahoon (1981) found that the reproductive rate of *Acartia tonsa* varied, in the laboratory, when fed on six different species of phytoplankton, suggesting that monospecific algal diets did not satisfy the complex nutritional requirements of the species. Kleppel (1993) argued that in research carried out by Roman (1984) *Acartia tonsa* survived longer and grew at higher rates when its diet consisted of a mixture of the diatom *Thalassiosira weissflogii* and detritus than when each food was provided alone; although *T. weissflogii* provided the majority of the nutrients required, the detritus supplied saturated and unsaturated fatty acids and several amino acids that were scarce or lacking in the diatom (Kleppel 1993). Mayor (2009a) noted that the addition of ciliates or rotifers, an important source of PUFA, to monospecific algal diets of copepods caused a reduction in development time, increased longevity in females, and also increased egg production (Bonnet and Carlotti 2001; Stoecker and Egglof 1987).

Copepods in their natural environment experience a much greater rate of change, in space and time, of the food offered compared with laboratory experiments (Mauchline 1998). Therefore, the feeding selectivity which enables the copepod to sample a variety of foods may permit nutrients lacking in one source to be obtained from others, hence maximising nutritional gain and species success (Kleppel 1993).

### 1.4.2 Fatty acids

Fatty acids are described here as:

$$X:Y_n - z$$

Where; x = number of carbon atoms, y = number of double bonds, n = “omega” and z = omega type.

Essential biochemical compounds are those that can be converted but cannot be synthesised *de novo* by the organism (or not in a sufficient amount) and include certain vitamins, amino acids, and fatty acids (Sterner and Schulz 1998; Cotonnect et al. 2001; Dunstan et al. 1992; Guisande and Harris 1995).

Fatty acids are building blocks of larger lipid molecules such as triglycerides, waxes and phospholipids which contribute significantly to copepod biomass (Berg et al. 2007; Christie 1989; Sterner and Elser 2002). Interestingly, some species of the genus *Calanus* have been found to have the highest lipid reserves in the animal kingdom, with a total content which can vary from 5% to 70% of the body mass, depending on ontogenic stage and food availability (Bamstedt 1986).

Lipids as components of many cellular functions, such as energy reserves for neutral lipids (wax esters and triacylglycerols), membrane components for polar lipids (phospholipids), buoyancy aids and hormones (Sargent and Falk-Petersen 1988; Sargent and Henderson 1986; Sterner and Elser 2002; Kattner et al. 2007). Copepods that have low wax ester levels, such as tropical species, have lower total lipid content which is mostly composed of other neutral lipids in the form of triacylglycerols (Fraser et al. 1989).

Polyunsaturated fatty acids (PUFA, fatty acids with 2 or more double bonds) are of particular importance for zooplankton physiology and can only be obtained and transferred to the organism from the diet. The requirement for these fatty acids is driven by the organism’s need to sustain its metabolic and physiological activities as they regulate growth, healthy development, diapause and gametogenesis (Kattner et al. 2007; Christie 1989; Sterner and Schulz 1998). For instance, the lipid concentration in eggs and gonads is higher than that of the whole individual (Gatten et al. 1980; Mayor 2005).

Essential PUFA of plant origin type *n*-3 and *n*-6, such as C18 (e.g.  $\alpha$ -linolenic acid “ALA” 18:3*n*-3), C20 (e.g. Eicosapentaenoic acid “EPA” 20:5*n*-3, Arachidonic acid “AA” 20:4*n*-6) and C22 (e.g. Docosahexaenoic acid “DHA” 22:6*n*-3) are necessary components of all animal diets. Sterner and Shulz (1998) explain that 18:3*n*-3 and 20:5*n*-3 in particular,

serve as precursors to the synthesis of a variety of molecules, such as prostaglandins, that are involved in regulation of egg production and laying. 22:6*n*-3 is also essential for neural development.

Sargent and Falk-Petersen (1988) found that the PUFA abundance and composition in the wax esters of calanoids corresponded to the PUFA abundance and composition in the algal lipids ingested. As a consequence, neutral lipids found in copepods are rich in *n*-3 PUFA such as 18:4, 20:5 and 22:6 (Fraser et al. 1989). Depending on the diet, the 18:4 form can account for about 20% and *n*-3 PUFA collectively for about 40% of the total fatty acids present in the wax esters (Sargent and Falk-Petersen 1988). Plant lipid has a distinctive intraspecific fatty acid composition, as shown in table 1.1, which after assimilation by the copepod can be detected in the animals. It can therefore be used to investigate the feeding history and trophic transfer of energy within the zooplankton population (Wilson et al. 2010).

**Table 1.1.** Fatty acids in phytoplankton and detritus.

Phytoplankton Class	PUFA	Other Fatty Acids	Source
Bacillariophyceae	16:4 <i>n</i> -1, 20:5 <i>n</i> -3	C <sub>16</sub> , 16:1 <i>n</i> -7	Pond et al. (1998) and references therein; Graeve et al. (1994).
Cryptophyceae	18:3 <i>n</i> -3, 18:4 <i>n</i> -3, 20:5 <i>n</i> -3, 22:6 <i>n</i> -3	C <sub>18</sub>	Zhukova and Aizdaicher (1995)
Dinophyceae	18:4 <i>n</i> -3, 18:5 <i>n</i> -3, 22:6 <i>n</i> -3	C <sub>18</sub>	Pond et al. (1998) and references therein; Graeve et al. (1994)
Prymnesiophyceae	18:3 <i>n</i> -3, 18:4 <i>n</i> -3, 22:6 <i>n</i> -3	18:1 <i>n</i> -9	Pond et al. (1998) and references therein; Zhukova and Aizdaicher (1995);
Chlorophyceae	16:2 <i>n</i> -6, 16:3 <i>n</i> -3, 16:4 <i>n</i> -3, 18:2 <i>n</i> -6, 18:3 <i>n</i> -3		Zhukova and Aizdaicher (1995)
Eustigmatophyceae	20:5 <i>n</i> -3, 20:4 <i>n</i> -6	C <sub>16</sub> , 16:1 <i>n</i> -7	Zhukova and Aizdaicher (1995)
Detritus/ bacteria	-	C <sub>18</sub> , 18:1 <i>n</i> -9	Pond et al. (1998); Mayzaud et al. (1989)

Different classes of phytoplankton have different PUFA compositions; therefore fatty acids can be employed as trophic biomarkers (Sterner and Shulz, 1998) (Table 1.1). For instance, bacillariophyceae (diatoms) are rich in C<sub>16</sub>, in particular 16:1*n*-7 and 20:5*n*-3

PUFAs while dinophyceae (dinoflagellates) and prymnesiophyceae (coccolithophores) are 18:4*n*-3 (SDA) and 22:6*n*-3 PUFA rich (Pond et al. 1998; Graeve et al. 1994; Zhukova and Aizdaicher 1995). In general, cryptophytes and chrysophyceae (including diatoms) are PUFA-rich, while cyanobacteria (and prokaryotes in general) are PUFA-poor (Ahlgren et al. 1990). Since a single species of algae can have a completely different food quality depending on the conditions under which it was grown, algal taxonomy alone is insufficient to determine food quality (Sterner and Shulz 1998).

Sargent and Falk-Petersen (1988) suggest that actively growing algae can contain up to 20% of their total dry weight as polar glycolipids rich in *n*-3 PUFA. However, the amount of neutral and polar lipids can vary. For instance, phytoplankton grown under N-limited conditions (e.g. the end of a bloom), accumulate mostly triacylglycerols. These are low in *n*-3 and high in saturated and monosaturated fatty acids (SAFA) compared to the accumulation of glycolipids when grown under N replete conditions (Kattner et al. 2007).

PUFA have been widely used as a measure of food quality and index of nutritional value where, the higher the PUFA concentration in the algae the more nutritious is the food. PUFA can also reveal information on zooplankton feeding preferences (Kattner 2007). Fatty acid biomarkers can therefore provide quantitative and qualitative estimates of algal quality and species composition in cultured and natural phytoplankton communities, ultimately helping to evaluate food web relationships between primary producers and higher trophic levels.

#### 1.4.3 Stoichiometry

The biochemical constituents of the biomass of copepods; carbohydrate, protein and lipid are ultimately affected by the stoichiometric composition of the major nutrients in their food which contain a variable amount of elements such as C, N and P.

Phytoplankton grow by taking up multiple inorganic nutrients and trace elements from the surrounding environment through osmotic and photosynthetic processes. These processes therefore determine the elemental composition of primary producers. The most widely used empirical stoichiometric relationship reported for marine phytoplankton is the C:N:P ratio, where healthy natural communities of marine plankton tend to have an organic C:N:P ratio of around 106:16:1 by atoms (approximately 40:7:1 by weight) (Tezuka 1989). This is referred to as the Redfield ratio since its original description in the 1930s by Redfield (1934).

The Redfield ratio was previously considered to be a constant relationship between N and P, however recent research has determined its variability throughout the global oceans (Klausmeier et al. 2004a; Sterner and Hessen 1994; Geider and La Roche 2002; Leonardos and Geider 2004; Deutsch and Weber 2012; Martiny et al. 2013). 16:1 is defined as the guideline at which limitation by one nutrient switches over to another within the phytoplankton cell (Rhee and Gotham 1980; Wynne and Rhee 1986; Terry et al. 1985; Geider and La Roche 2002). The elemental composition of individual species of phytoplankton grown under N or P limitation can vary from around 6:1 to 60:1 (N:P ratio) (Rhee 1978; Leonardos and Geider 2004; Goldman et al. 1979).

Temporal and spatial variation in nutrient supply ratios (generally dissolved inorganic nitrate  $\text{NO}_3^-$  and nitrite  $\text{NO}_2^-$  to phosphate  $\text{PO}_4^{3-}$  ratio) and inorganic nutrient biogeochemical dynamics are significant sources of phytoplankton stoichiometric deviation. Inorganic nutrients such as P and N are used until they become limiting and consequently inhibit further algal growth; their proportions determine which nutrient will limit biological productivity, where higher N:P ratios suggest P-limitation and lower ratios denote N-limitation (Deutsch and Weber 2012). For many decades, Liebig's law of the minimum was the dominant theory stating that only a single factor, or a single nutrient, limits algal growth at any given time (Arrigo 2005). Recent studies have demonstrated that algal growth rates can be limited by one nutrient in the lowest amount in relation to the cell physiological requirements, in addition to one other or more environmental resource (Rhee and Gotham 1981, Rhee and Gotham 1980; de Baar 1994).

Growth limitation by different nutrients in the same mixed layer was also shown to be affected by changes in light intensity (Rhee and Gotham 1981). In their natural habitat planktonic algae are transported vertically by physical and/or biological mechanisms exposing them to various light climates (Wynne and Rhee 1986). Light intensity (irradiance) is an important parameter regulating primary production and is affected by factors such as particulate matter and dissolved substances in the water. Rhee and Gotham (1981) found that nutrient requirements increase as light intensity decreases. These variations of the optimum N:P ratio with light intensity indicate that the degree and even the kind of nutrient limitation of phytoplankton can change with their vertical distribution and according to the optical characteristics of the water.

Interspecific differences have been identified as one of the causes of C:N:P ratio variations in phytoplankton cells (Quigg et al. 2003; Arrigo 2005); this is since species-specific optimum nutrient ratios are variable (Rhee and Gotham 1980; Quigg et al. 2003; Lagus 2004; Arrigo 2005). For instance, Quigg et al. (2003) and Arrigo (2005) state that

the two major phytoplanktonic superfamilies green and red (defined by Quigg et al. (2003) based on plastids differences) differ noticeably in their cellular N:P ratios, with the green superfamily showing an empirical N:P ratio of 27 and exhibiting significantly higher ratios than the red superfamily with a N:P ratio of 10. These species differ in their kinetics of nutrient uptake, assimilation and storage capacities, and therefore, have different nutrient requirements as well as different cellular concentrations of nutrients (Rhee and Gotham 1980; Hecky and Kilham 1988). The species-specific optimum nutrient ratio may change depending on the species' ecological niche and consequently on factors such as growth rate, temperature, light availability and nutrient concentrations (Lagus 2004).

Shifts in nutrient limitation patterns have also been noted to follow salinity gradients and seasonal phytoplankton succession; hence, a whole range of biotic and abiotic factors affecting algal habitats are the cause of variation in phytoplankton stoichiometry and are found to limit autotrophic primary production (Klausmeier et al. 2004b).

### **1.5 Variable N:P ratio**

The abundance of inorganic and organic nutrients is regulated by dynamical chemical and biological forces varying on seasonal and latitudinal scales. These variations have been widely recognised. For instance, Longhurst et al. (1995) subdivided the oceans into 56 biogeochemical provinces based on regional differences in primary production affected by the physical properties of the water masses and ecological variables. Since Longhurst's definition, others have found that these geographic boundaries exhibit considerable physical and biological variability on a variety of time scales (Rodríguez and Mullin 1986; Marañón et al. 2001; McClain et al. 2004).

The distribution of nutrients on a global scale is also driven by ocean circulation and physical forces such as temperature, and density or eddy driven mixing which constrain large areas of the low-latitude oceans to oligotrophic conditions (Deutsch and Weber 2012; Weber and Deutsch 2010). Different spatial distributions of N and P are seen, not only on latitudinal but also on vertical scales (Weber and Deutsch 2010).

The organic Redfield ratio exhibits large spatial variations although some global patterns have been identified (Table 1.2). Martiny et al. (2013) suggest that the seston N:P ratios in the global ocean (surface only) exhibit a strong latitudinal pattern and can range from 5:1 to 316:1 with a mean of ~20:1.

**Table 1.2.** Distribution of N:P and C:N ratios (molar) throughout the world's oceans. The ratios are approximate values and the type of ratio is specified as follows PO: Particulate Organic, DO: Dissolved Organic, DI: Dissolved Inorganic.

Location	N:P Ratio	C:N ratio	Source
Arctic & Sub-Arctic Surface		5-7.8:1 PO	Tamelaender et al. (2012) (Berent Sea)
Antarctic & Sub-Antarctic Surface	15:1 DI 15:1 PO	7.13:1* PO 5.56:1 PO	Arrigo (1999) - disappearance ratios Copin-montegut and Copin-montegut (1983)
Mediterranean Surface	26:1PO	8.3:1 PO	Copin-montegut and Copin-montegut (1983)
Deep	30:1PO 21-23:1 PO 28:1 DI		Thingstad et al. (2012) Copin-montegut and Copin-montegut (1983) Krom et al. (2004)
North Sea Surface	17:1 PO 15:1 PO	7.6:1 PO 6.7 to 7.8:1 PO 5.6 to 7.2:1 PO	Sterner et al. (2008) Frigstad et al. (2011) Koski et al. (2010)
North Atlantic Surface	17:1 (Apr), 5:1 (Jan) PO 13-14:1 PO	5.3-5.6:1 PO	Menzel and Ryther (1964) Copin-montegut and Copin-montegut (1983)
250-700m	>30:1 PO* 16-19:1 DI	5-6:1 PO Bloom 10-16:1PO postbloom	Kortzinger et al. (2001) Martiny et al. (2013) - Sargasso Sea Takahashi et al. (1985)
South Atlantic Surface	17:1 PO	6.7:1 PO	Copin-montegut and Copin-montegut (1983)
400-1000m 300-700m	16:1 PO 14.5-18:1 DI	7.8:1 PO	Schneider and Schlitzer (2003) Anderson and Sarmiento (1994) Takahashi et al. (1985)
Indian Ocean Surface	18-21:1 PO	6.5:1 PO	Copin-montegut and Copin-montegut (1983)
400-1000m	11-26:1 15:1 PO 16:1 PO 12-16 DI		Martiny et al. (2013) Sterner et al. (2008) Anderson Sarmiento (1994) Takahashi et al. (1985)
Deep	13:1 PO		Anderson Sarmiento (1994)
Pacific Ocean Surface	>30:1PO*		Nobili et al. (2013); Martiny et al. (2013)
400-1000m	16:1 PO	8-10:1 PO	Schneider and Schlitzer (2003)
Deep	16:1		Anderson Sarmiento (1994)

\* Oligotrophic Gyres

Generally the subtropical gyres are areas where nutrient supply is minimal and concentrations of nutrients and primary production are characteristically low throughout the year, causing nutrient limitation in phytoplankton. For instance The North Pacific

Subtropical Gyre and the Sargasso Sea are P-limited (Martiny et al. 2013; Krom et al. 2004). In contrast, some temperate and higher latitude areas follow a seasonal pattern of eutrophic conditions and have replete (Redfield values) nutrient ratios (Frigstad et al. 2011).

## 1.6 Thesis objectives

The overall aim of this research is to investigate the effects of a selected number of biotic and abiotic environmental variables on production, consumption and metabolism of copepods. In chapter 2 we detail the methods and the techniques employed during laboratory and field work and review some of the methods available to measure zooplankton respiration. The results in chapter 3 focus on the effects of food quality on copepod feeding, EPR and respiration rates in the laboratory; whereas chapter 4 assesses the variability and distribution of organic nutrients and food quality (stoichiometry and biochemistry) in the Atlantic Ocean. Chapter 5 investigates the effects of temperature on the respiration and EPR of some migratory mesopelagic copepods in the field.

The hypotheses tested in chapter 3 include:

1. Maximum metabolic and growth rates occur when copepods are fed on phytoplankton which have an optimal food quality.
2. The effects of food mineral N:P ratio on copepod biomass can be seen in the field.
3. A balanced diet for all copepods corresponds to an elemental ratio of 16N:1P (molar) (Redfield ratio).

To test the hypotheses, the following objectives were defined:

- Undertake controlled laboratory experiments to isolate the effects of food quality on the physiology of the neritic copepod *Temora longicornis*.
- Investigate how the characteristics of the food affect copepod metabolic rate. Does this response vary between copepod species?
- Determine possible effects of food quality on zooplankton ecology in the field and Investigate potential implications on a global scale.

In chapter 4 the following objectives were defined:

- Assess and compare different indicators of food quality in the field.
- Assess empirical relationships between organic elements and environmental parameters and evaluate the predictability of organic elements.
- Determine latitudinal and temporal variation in copepod diet across an Atlantic Meridional Transect.

In order to test four hypotheses:

4. Food quality is lower in oligotrophic domains and higher in upwelling and temperate regions of the Atlantic Ocean.
5. Particulate organic nutrients can be predicted from environmental parameters measured by sensors deployed on the CTD rosette.
6. Empirical relationships between particulate organic nutrients and environmental factors allow the determination and the prediction of food quality when *in situ* data are not available.
7. Food quality has deteriorated over time in the Atlantic Ocean.

The following objectives were defined for chapter 5:

- Investigate the relationship between copepod metabolism, temperature and body size in the Atlantic Ocean.
- Investigate variation in egg production rates between species and/or with latitude.
- Compare responses to temperature changes at population and species-specific level and estimate potential future impacts of global ocean warming.

In order to test the following hypotheses:

8. The respiration rates, carbon demand and egg production rates of different mesopelagic species of copepod vary differently in response to latitudinal variations in temperature.
9. Body size and temperature are not the only factors affecting copepod metabolism in the Atlantic Ocean.

10. Mesopelagic copepods have higher sensitivities to a temperature increase than epipelagic species

Chapter 6 discusses the overall findings, the lessons learnt during this study and suggests future research objectives. The objectives of chapter 6 include:

- Assess the consequences of our findings on ocean ecology and biogeochemical cycles. We ask the following questions:
  - What are the ecological implications and the effects of nutritional imbalance in copepods on biogeochemical cycles and trophic transfer of energy?
  - What effect will ocean warming have on copepod physiology?
  - Can copepod respiration, under different ecological constraints, be used as an indicator to define the species response to environmental change?
- Propose an experimental approach to investigate the effects of food quality on copepod respiration in the field alongside the variation of other environmental parameters.

## **CHAPTER 2**

## 2. Experimental and analytical methods

### 2.1 Field and experimental work overview

This project included both field and laboratory based experimental work. Initial field and laboratory training on zooplankton physiology measurement was undertaken in Plymouth at the SAHFOS laboratory. The main laboratory work for this project was carried out at the UEA laboratories where the zooplankton were obtained from the North Sea, off the coast of Great Yarmouth (UK) (52°41.9N, 1°48.5E) with the help of Gardline Environmental Ltd. Field work also took place during an Atlantic Meridional Transect (AMT20) cruise. Similar techniques and experimental methodologies were used throughout the study. However, these were adapted and refined to address each separate scientific question.

### 2.2 Algal cultures and food quality experiments

The general procedure for this set of experiments involved the set up of three algal continuous cultures at different nutrient ratios. This allowed a constant supply of food for the zooplankton in which the quality was biochemically pre-determined (see section 2.2.1) and kept in a steady equilibrium over the period of a few months.

Once the cultures achieved steady state, live zooplankton were collected from the North Sea and adult females of *Temora longicornis* were incubated with the different food types. In order to determine the effects of food quality on the copepods, metabolic rates; respiration, feeding and egg production rates were measured and the quality of the food ingested was monitored.

#### 2.2.1 Continuous cultures

Continuous cultures of the free-swimming cryptophyte *Rhodomonas salina*, obtained from the Plymouth Culture Collection PLY544, were set-up in order to maintain a constant supply of food for the zooplankton.

The production of different phytoplankton 'quality' was accomplished by stoichiometrically manipulating the inorganic N:P supply ratio in the medium in which the phytoplankton cells were grown. Three cultures were established under different nutrient conditions: no nutrient limitation, nitrogen (N) limited and phosphorus (P) limited.

In continuous cultures, a fresh supply of medium is added continuously at the same rate at which it is withdrawn. At steady state the specific growth rate ( $\mu$ ) of the population within the continuous culture is determined by the dilution rate as shown in equation (2.1) (Andersen 2005):

$$\mu = \left(\frac{f}{V}\right) \quad \text{hence} = D \quad (2.1)$$

Where;

$\mu$  = growth rate

f = medium flow rate

V = volume

D = dilution rate

In order to determine the appropriate dilution rates of the continuous cultures, growth rates  $\mu$  were measured on batch cultures first. The specific growth rates of *R. salina* were derived from preliminary batch culture experiments where the cells' growth rates were measured in triplicate 25 mL glass tubes at  $13 \pm 0.5$  °C on a 24 hour light cycle with an irradiance of  $300 \mu\text{E m}^{-2}\text{s}^{-1}$ , at the same conditions chosen for the chemostats.

The batch cultures were grown in ESAW medium without silica as described in Berges et al. (2001) (Enriched Seawater, Artificial Water; pH = ~ 7.8).

The growth rates were determined by measuring daily in vivo fluorescence (F), as a proxy for cell number (n), using a Turner 10-AU design Fluorometer.

A 24 hour light cycle was selected in order to minimize the effects of diel cycle and circadian rhythm on the cells' physiology. Irradiance was measured using a Biospherical Instruments inc. QSL 2101 light meter.

The temperature of the laboratory 'constant temperature room' was initially verified and monitored with a Grant ® squirrel type temperature logger over a period of 24 hours to determine any fluctuations in the ambient conditions. The temperature averaged  $13 \pm 0.5$ °C. During the experiments the room temperature was monitored using mercury based thermometers and hand held temperature probes.

The batch cultures' growth rates  $\mu$  were calculated according to the slope of equation (2.2):

$$\mu = \frac{\text{Ln}F_1 - \text{Ln}F_0}{T_1 - T_0} \quad (2.2)$$

Where;

$F_0$  and  $F_1$  = fluorescence at time  $T_0$  and  $T_1$  respectively

Having established the growth rate of the selected species under constant conditions, the final dilution rate  $D$  of the chemostats was calculated by the following equation (2.3).

$$D = \frac{\left(\frac{\mu}{2}\right)}{V} \quad (2.3)$$

Where;

$D$  = dilution rate

$\mu$  = growth rates

$V$  = volume

*R. salina* was grown in 1.5 L chemostats in ESAW medium without silica supplied at 540 mL d<sup>-1</sup> at 13° ± 0.5 °C on a 24 hour light cycle with an irradiance of 300 μE m<sup>-1</sup>s<sup>-1</sup>.

Three cultures (Figure 2.1) were established under different nutrient conditions: no nutrient limitation with a 16:1 N:P ratio, N-limited with a 3:1 N:P ratio and P-limited with a 80:1 N:P ratio. The culture media were prepared in 20 litre carboys by adding a measured amount of the respective salts as described in Berges et al. (2001). However the concentration and addition of N and P salts to the different media was modified and the final amounts of salts were calculated stoichiometrically as described in table 2.1.



**Figure 2.1.** Chemostats. From the left; 80:1 N:P ratio culture, 3:1 N:P ratio culture and 16:1 N:P ratio culture.

**Table 2.1.** N and P added in ESAW medium per chemostat.  $\text{NaNO}_3$  molecular weight = 84.99 g.  $\text{NaH}_2\text{PO}_4$  molecular weight = 156.01 g.

N:P ratio	$\text{NaNO}_3$ g L <sup>-1</sup>	N mol L <sup>-1</sup>	$\text{NaH}_2\text{PO}_4$ g L <sup>-1</sup>	P mol L <sup>-1</sup>
Standard Recipe	$4.67 \times 10^{-2}$	$5.49 \times 10^{-4}$	$3.09 \times 10^{-3}$	$1.98 \times 10^{-5}$
16:1	$2.70 \times 10^{-2}$	$3.17 \times 10^{-4}$	$3.09 \times 10^{-3}$	$1.98 \times 10^{-5}$
3:1	$2.70 \times 10^{-2}$	$3.17 \times 10^{-4}$	$1.64 \times 10^{-2}$	$1.05 \times 10^{-4}$
80:1	$1.35 \times 10^{-1}$	$1.59 \times 10^{-3}$	$3.09 \times 10^{-3}$	$1.98 \times 10^{-5}$

Figure 2.2 shows schematically the continuous cultures' apparatus and the principles of the system. The system's headspace was internally pressurized by blowing air and medium into the culture vessel through the medium + air inlet. With the sampling outlet valve closed, the headspace pressure inside the culture's chamber P1 channels the extra fluid through the outflow tube at pressure P2 and into the waste outflow at pressure P3 where;  $P1 (=P2) > P3$ .

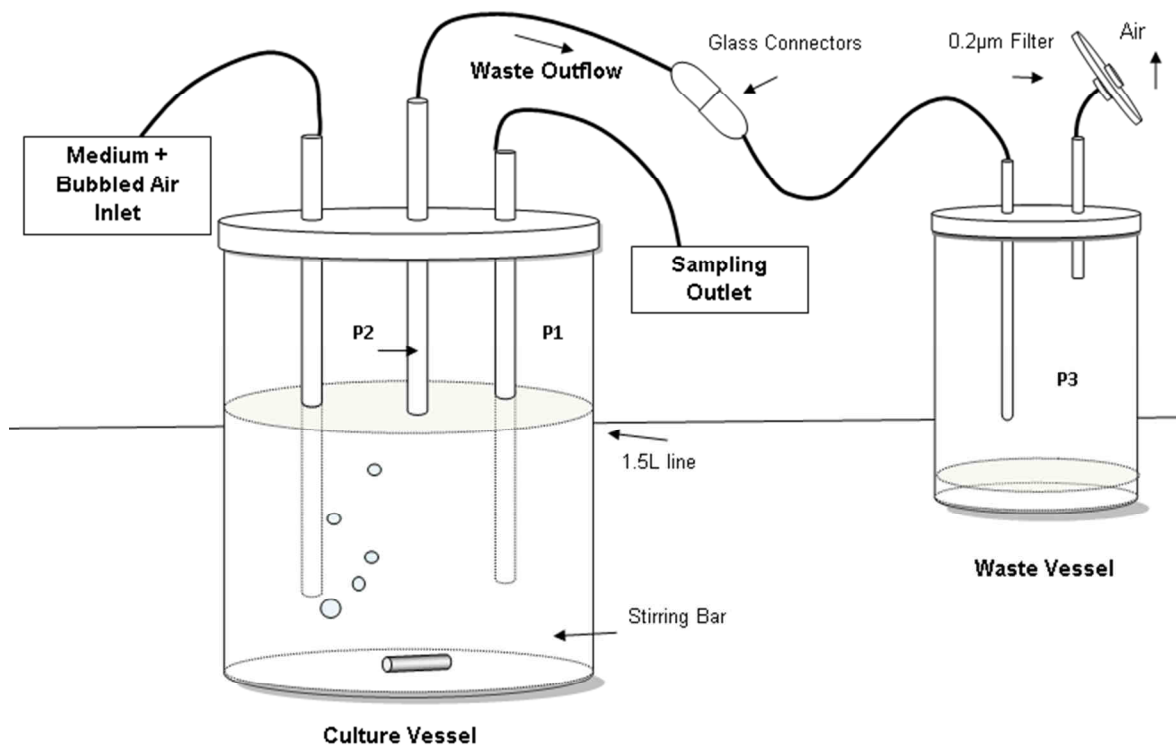


**Figure 2.2.** Continuous culture apparatus and principles of the system. P1: pressure of the culture vessel's headspace. P2: pressure of the waste outflow's tube headspace. P3: pressure of the waste outflow's headspace.

The waste vessel is connected to the culture chamber via male to female glass connectors which allow the easy replacement of the container with a clean one as and when necessary. The waste bottles are changed under aseptic conditions by sterilizing the glass connectors over a blue flame before and after the replacement.

The culture is kept in suspension by stirring it continuously with a magnetic stirrer bar activated by an underlying ESP Velp Scientifica magnetic stirring plate without motor, which does not generate heat and hence allowing for a better temperature controlled environment.

Flux rates of different sized tubing at different pumping speeds were initially measured and calculated in order to determine the apparatus' potential dilution rates. The final tubing size was selected and marprene autoclavable double manifold tubing 0.88 mm bore was fitted to a 323 series Watson and Marlow peristaltic pump; the medium was pumped into the cultures at the speed of 6 rpm (revolutions per minute).

## Notes for future set up:

- pH: In cultures at cell densities  $>4 \times 10^5$  cells mL<sup>-1</sup> an increase in pH  $>9$  was observed therefore the cultures needed constant pH monitoring and adjustment. We opted for manual addition of concentrated HCl or 10 M NaOH solutions since Crawford et al. (2011) suggests that the use of buffer solutions such as Tris or HEPES in the medium, at the concentration required for such large volumes, leads to adverse effects on growth rates.
- Wall growth: In high cell density cultures with cell number mL<sup>-1</sup>  $>1 \times 10^6$ , wall growth was observed. Depending on the severity, this phenomenon can lead to cell shading ultimately affecting the culture's growth rates. Frequent changes in the culture vessels can help reduce this and should be taken into account when designing experiments. A different approach to be considered is that a calculated reduction in cell density within the culture will prevent wall growth from occurring altogether.
- Volume: When choosing the total volume of the culture, several factors need to be taken into account as the larger the volume, the more time will be needed for the culture to reach steady state. The cultures took up to 2 months to reach a steady state.

## Lessons learnt:

- With the aim of minimizing continuous culture volumes along with experimental time, preliminary experiments were carried out and 35 mL continuous cultures were set up. Mercuric chloride (HgCl<sub>2</sub>) at a concentration of  $4 \times 10^{-4}$  mL mL<sup>-1</sup> was used to preserve the material accumulating in the outflow vessel. Live culture and HgCl<sub>2</sub> fixed culture were filtered to measure particulate organic nutrients (CHN analysis), and compared in order to determine the effect of the poison on the culture's biochemistry. The results show a significant loss of carbon in the samples of ~15%, consequently this poison method was not continued.
- The continuous culture's volume should be decided by prior estimation of the amount of material needed for sample collection and food necessary for the incubation experiments. This is since, in order to maintain the culture in equilibrium, less than the daily amount of medium pumped into the culture can be taken out.

### 2.2.2 Zooplankton collection

Although culturing copepods in the laboratory was initially considered and attempted, due to time constraints limiting the creation of an established culture and questions regarding how well cultured copepods represent an *in situ* population, we decided to use natural copepods. For instance, copepods grown in the laboratory are affected by inbreeding reducing the genetic variability (Tiselius et al. 1995), also affecting the physiology of the organisms causing a reduction in animal size and fecundity (Klein Breteler and Gonzalez 1982; Koski et al. 2010). Only healthy animals collected from the North Sea were utilized throughout this research. To reduce the effects of variable environmental conditions and animal size the animals were acclimatised for a few days at  $13^{\circ}\text{C} \pm 0.5^{\circ}\text{C}$  and the rates were dry-weight adjusted.

The sampling was carried out with the help of Gardline Environmental Ltd and a 120  $\mu\text{m}$  plankton net was deployed when possible  $\pm 1$  nautical mile off the coast of Great Yarmouth (Norfolk, UK) from April 2011 to December 2011. 20 minute horizontal net tows were carried out in the mornings at  $\sim 10$  am. Upon recovery, the catch was diluted into 20 L containers, stored in a sealed coolbox and transported to the University facilities within 2 hours.

The animals were then gently siphoned out of the containers into a semi- submerged 200  $\mu\text{m}$  sieve. To avoid overcrowding, excess light and oxygen depletion, the copepods were transferred to gently aerated 30 L buckets, darkened and kept at  $13^{\circ}\text{C} \pm 0.5^{\circ}\text{C}$  in 0.2  $\mu\text{m}$  filtered seawater (salinity = 32) .

The copepods were kept for up to three weeks and/or up to when the animals were deemed unhealthy. The animals were fed three times a week with a mixture of the cryptophyte *Rhodomonas salina*, the dinoflagellate *Oxyrrhis marina* (fed twice a week with the chlorophyte *Dunaliella marina*) and the diatom *Thalassiosira weissflogii*.

The health state of the copepod *Temora longicornis* was checked prior to each experiment by inspecting them under the microscope for anatomical damage. We also examined the animals' behavioural response to external stimuli including the verification of normal swimming patterns and/or escape responses. Occasionally the copepod respiration rates were measured, if the rates showed abnormally low values (lower than average basal  $3 \mu\text{L O}_2 \text{ dw}^{-1} \text{ h}^{-1}$ ), the animals were discarded.

Data obtained from animals deemed unhealthy are not included in this thesis.

### 2.2.3 Experimental protocol

In order to avoid biases caused by abrupt changes in food type and concentration, prior to determination of physiological rates, the animals underwent pre-conditioning and acclimation to the food quality selected for the experiment.

Up to 70 adult females of *T. longicornis* were randomly selected for each experiment and picked out using a stereo microscope and a glass wide-bore Pasteur pipette. All the copepods selected were carefully inspected to ensure the absence of parasites and for any sign of anatomical damage.

The copepods were grouped into darkened Duran bottles containing 1.5 L of 0.2  $\mu\text{m}$  filtered seawater to which the food was added. The animals were fed *R. salina* from the chemostats diluted to an amount corresponding to a final cell concentration of  $5 \times 10^6 \mu\text{m}^3 \text{mL}^{-1}$  (Jónasdóttir and Kiorboe 1996). The water and the food in the pre-conditioning chambers were changed every 24 hours for 48 hours prior to determination of physiological rates to minimize food quality deterioration and changes.

During the experiment, the animals were fed the same amount as they had received during pre-conditioning. In general the food dilution was calculated proportionally using the following formula (2.4):

$$x = \frac{V_{\text{btl}}}{(V_{\text{cc}}/5 \times 10^6)} \quad (2.4)$$

Where;

$x$  = mL of culture to dilute

$V_{\text{btl}}$  = Volume of incubation chamber in mL

$V_{\text{cc}}$  = Continuous culture volume ( $\mu\text{m}^3 \text{mL}^{-1}$ )

### 2.2.4 Respiration rates

Respiration rates were measured by means of the Winkler Oxygen titration technique (Winkler 1888; Robinson et al. 2002, Strickland and Parsons 1972). Dissolved  $\text{O}_2$  was determined by automated Winkler titration using photometric end-point detection as described in Williams and Jenkinson (1981). The sodium thiosulphate was calibrated,

prior to analysis, with 0.1 N potassium iodate standard. The salinity of the seawater used in the incubation was also measured with a portable salinometer fitted with a salinity/temperature sensor to enable oxygen concentration and saturation to be calculated from the equation of Garcia and Gordon (1992).

A preliminary experiment was carried out incubating single adult females *Temora longicornis* at  $13 \pm 0.5^\circ\text{C}$  in  $\sim 60$  mL chambers containing  $0.2 \mu\text{m}$  FSW. There was no significant difference (Student t-test  $p = 0.6$ ,  $n = 13$ ,  $df = 11$ ) between the respiration rate of copepods incubated over 18 and the more usual 24 h as shown in Table 2.2. Therefore we measured copepod respiration over the shorter incubation time of 18 h.

**Table 2.2.** 18 vs 24 hour respiration experiment. The results show there was no difference between the respiration rates of *T. longicornis* incubated for 18 hours and *T. longicornis* incubated for 24 hours at  $13^\circ\text{C}$  ( $\text{nL O}_2 \mu\text{g DW}^{-1} \text{h}^{-1}$ )  $\pm$  SD.

Incubation time (hr)	nL O <sub>2</sub> $\mu\text{g DW}^{-1} \text{h}^{-1}$	Replicates n
18	5.17 $\pm$ 1.43	7
24	5.64 $\pm$ 1.76	6

For the experiments the female *T. longicornis* were transferred from the preconditioning chamber to a smaller beaker containing 100 mL of  $0.2 \mu\text{m}$  filtered seawater. Actively swimming animals were selected and with the help of a wide bore pipette, single individuals were delicately inserted into the appropriate calibrated respiration bottles with an average volume of  $\sim 60$  mL. This process was carried out with particular care in order to avoid the formation of bubbles in the respiration bottles which would have affected the amount of dissolved oxygen. The bottles were all initially filled with oxygen saturated  $0.2 \mu\text{m}$  filtered seawater. Unfed and fed respiration rates were measured. In the latter, food from the chemostats with cell concentrations of  $5 \times 10^6 \mu\text{m}^3 \text{mL}^{-1}$  (Jónasdóttir and Kiorboe 1996) were added by removing a calculated quantity of filtered seawater and by carefully adding the same quantity of phytoplankton as per equation (2.4).

Four bottles containing  $0.2 \mu\text{m}$  filtered seawater and four bottles containing  $0.2 \mu\text{m}$  filtered seawater and food were fixed at the start of the incubation as  $T_0$  (time zero). Another four bottles containing  $0.2 \mu\text{m}$  filtered seawater (control bottles), four bottles containing  $0.2 \mu\text{m}$  filtered seawater and copepods (basal respiration), four bottles containing  $0.2 \mu\text{m}$  filtered

seawater and food (food control) and at least four bottles containing 0.2 µm filtered seawater, food and copepods (feeding respiration) were placed underwater in the dark at 13 °C ± 0.5 °C for 18 hours.

The respiration bottles containing food and copepods with food were positioned on a plankton wheel rotating at <2 rpm to keep the phytoplankton cells suspended. At the end of the 18 hours ( $T_{18}$ ) the bottles were removed from the incubator and the wheel, fixed with a solution of  $MnSO_4$  (manganese sulphate) and a solution of  $NaI+NaOH$  (sodium iodide + sodium hydroxide respectively) as described in Appendix A (which killed the animals) and analysed for oxygen concentration as described in Appendix A (chapter 7). At the end of the analysis each copepod was removed from the respiration bottles, fixed in 4% formalin and stored for later size determination.

The rates were calculated from the difference in dissolved oxygen between the mean of the controls and the mean of the experimental bottles at the end of the incubation. The rates are calculated with an associated standard error. Data where the rates were less than twice the standard error were not used ( $n=1$ ).

When applicable, oxygen consumption rates were converted into carbon demand. Respiration rates expressed in units of carbon represent the carbon requirement for zooplankton metabolism and can be used as an index of minimum food requirements when assimilation efficiency and growth are not taken into account (Omori and Ikeda 1992).

Respiration rates (R) were converted to carbon units using Omori and Ikeda (1992) protein based respiratory quotient (RQ) of 0.97 as shown in equation 2.5:

$$R (\mu\text{L ind}^{-1}\text{h}^{-1}) \times \text{RQ} \times \left(\frac{12}{22.4}\right) = \mu\text{g C ind}^{-1}\text{h}^{-1} \quad (2.5)$$

### 2.2.5 Egg production

Egg production experiments were carried out in 100 mL amber high-grade polystyrene plastic containers. An internal separation system, comprising a 200 µm net glued to the lower end of a plexiglass tube, was devised. The screen was small enough to prevent the adults reaching and potentially cannibalising the eggs sinking to the bottom of the chamber (eggs size ± 80 µm).

Single females, in at least triplicate samples for each experiment, were incubated in 0.2 µm filtered seawater for 24 hours in the dark. At the end of the incubation the net

separator was removed and the females were washed back into the container. Two drops of lugol iodine were added to kill the animals and stain the eggs to aid their visual detection. The eggs were counted the next day under a stereo microscope.

### 2.2.6 Feeding rates

To determine the quantity of food ingested, for each of the different qualities, copepod feeding rates over the period of 24 hours were measured.

Groups of up to 12 females selected from the pre-conditioning bottles (2.1.3) were placed into 1 to 3 x 500 mL bottles filled with 0.2µm filtered seawater and a volume of  $5 \times 10^6 \mu\text{m}^3 \text{mL}^{-1}$  of food from one of the 3 cultures (2.1.3). Six control bottles without copepods were filled with the same seawater and food, 3 of the bottles were sampled at  $T_0$  and the remaining 3 were allocated as “incubation controls” and sampled at the end of the 24 hours ( $T_{24}$ ).

The bottles were sealed with parafilm to stop the formation of a headspace and all the bottles, except the  $T_0$ , were mounted on a slowly rotating plankton wheel (<2 rpm) in the dark for 24 hours.

Food concentration measurements and the biochemical analyses; particulate organic carbon, nitrogen and phosphorus, fatty acids were carried out at the beginning and at the end of the incubations. The experimental bottles were sampled for cell counts.

At the end of the incubation the females were removed; a number of individuals were kept for dry weight determination, carbon content and fatty acid analysis. Clearance  $C$  and ingestion  $I$  rates, equation (2.6) and (2.7) respectively, were calculated according to Frost (1972):

$$C = V \left( \frac{g}{N} \right) \text{ (mL copepod}^{-1} \text{ hr}^{-1}) \quad (2.6)$$

$$I = nC \text{ (cells eaten copepod}^{-1} \text{ hr}^{-1}) \quad (2.7)$$

Where;

$n$  = average cell concentration

$g$  = grazing coefficient

$V$  = volume of the incubation chamber (mL)

$N$  = number of copepods

The grazing coefficient  $g$  was calculated from equation (2.8):

$$g = k_g - \frac{\ln\left(\frac{n_0}{n_1}\right)}{T_1 - T_0} \quad (2.8)$$

Where;

$k_g$  = growth constant

$n_1$  and  $n_0$  = cell concentration at time  $t_1$  and  $t_0$  respectively

$T_1 - T_0$  = incubation time

The growth constant  $k_g$  was calculated from equation (2.9):

$$k_g = \frac{\ln\left(\frac{n_0}{n_1}\right)}{T_1 - T_0} \quad (2.9)$$

Where;

$n_1$  and  $n_0$  = cell concentration at time  $t_1$  and the control at  $t_0$  respectively

$T_1 - T_0$  = incubation time

### 2.2.7 Biochemical Analysis

To determine the composition of the food and monitor the food quality change over time, undiluted culture, the feeding bottles at  $T_0$  and the control bottles  $T_{24}$  were filtered under low vacuum (<5 in Hg) and analysed for the following:

- Particulate organic carbon and nitrogen (POC/PON)
- Particulate organic phosphorus (POP)
- Fatty Acids

The water in the bottles containing *T. longicornis* was analysed for cell abundance and cell volume using a Beckman Coulter Multisizer 3 coulter counter.

A number of copepod specimens were retained for the analysis of:

- Average individual size and dry weight
- Organic carbon and nitrogen content (C and N)

### Particulate Organic Carbon and Nitrogen (C, N).

Samples for phytoplankton particulate organic C and particulate organic N were collected on pre-combusted (450°C for 4 h) 25 mm GF/F filters under low vacuum. The sample filters and filter blanks (minimum 3 per each experiment) were immediately dried at 60°C for 24 hours and stored in a sealed container in the dark until analysis via the combustion technique on an Exeter 440 Elemental Analyzer calibrated with the aid of pre-weighed standards (1600-2000 µg Acetanilide) prior to analysis of the filters.

### Particulate Organic Phosphorus. (POP)

Phytoplankton samples and blanks (minimum 3) for POP were collected on pre-combusted (450°C for 4 h) 25 mm GF/F filters under low vacuum. The filters were immediately dried at 60°C for 24 hours and stored at -20°C until analysis. The samples were processed following the Potassium Persulfate ( $K_2S_2O_8$ ) digestion method of Suzumura (2008) and analysed with the colorimetric method of Strickland and Parsons (1972) (Appendix B, chapter 7) using a PerkinElmer Lambda 25 UV/Vis Spectrometer provided with a PerkinElmer S10 autosampler and a 4 cm<sup>3</sup> cell. A calibration was run prior to each set of analyses using  $PO_4$  standards diluted from a 1000 µmol L<sup>-1</sup> concentrated stock of  $KH_2PO_4$ .

### Fatty acids.

Triplicate samples for FA analysis were collected on pre-combusted (450°C for 4 h) 25mm GF/F filters under low vacuum and immediately immersed and extracted in a solution of chloroform:methanol (2:1 by volume) in 4 mL vials, then stored at -80°C prior to analysis. The samples were transported to the British Antarctic Survey laboratory in Cambridge, processed and extracted by the method of Folch et al. (1957) and Pond (1996). The vials were initially supplemented with an internal FA standard (23:0). The lipids were separated from the non-fatty acid fraction and then transmethylated to fatty acid methyl esters (FAME). FA were then saponified in hexane:diethylether (1:1v/v) and purified via Thin Layer Chromatography (TLC) prior to analysis. FAMES were measured using a Thermo Finnigan Gas Chromatogram (GC) equipped with an FID (Flame Ionisation Detector). Hydrogen was used as the carrier gas.

The final amount of fatty acids per sample was quantified by comparing the retention time with that of the internal standard using equation (2.10):

$$S_M = \frac{S_A}{23:0_A} 23:0_M \quad (2.10)$$

Where;

S = fatty acid,

<sub>M</sub> = molar concentration

A = area of the peak.

Fatty acids are described here as x:y(n-z) where x = number of carbon atoms, y = number of double bonds (saturation) and n-z is used for unsaturated fatty acids where z = location of first double bond on the carbon chain after CH<sub>3</sub>.

### 2.2.8 Zooplankton size and dry weight

The prosome length (PL  $\mu\text{m}$ ) of copepod specimens preserved in 4% buffered formalin was measured under a stereo microscope with a calibrated reticule. Dry weight (dw) in mg was estimated using equation (2.11) (Castellani and Altunbaş 2013):

$$\text{Lndw} = 2.18 \text{LnPL} - 15.9 \quad (2.11)$$

Respiration rates were individually dry-weight adjusted (using the copepods from the oxygen bottles), whilst feeding and EPR were adjusted based on the average dry-weight of the copepods used during the respective experiments.

## 2.3 The Atlantic Meridional Transect (AMT)

The Atlantic Meridional Transect (AMT) is a multidisciplinary time-series ocean observation programme (Figure 2.3) funded by NERC, and coordinated by PML (Plymouth Marine Laboratory) in collaboration with NOCS (National Oceanography Centre Southampton). Details about the programme can be found on the website [www.amt-uk.org](http://www.amt-uk.org).

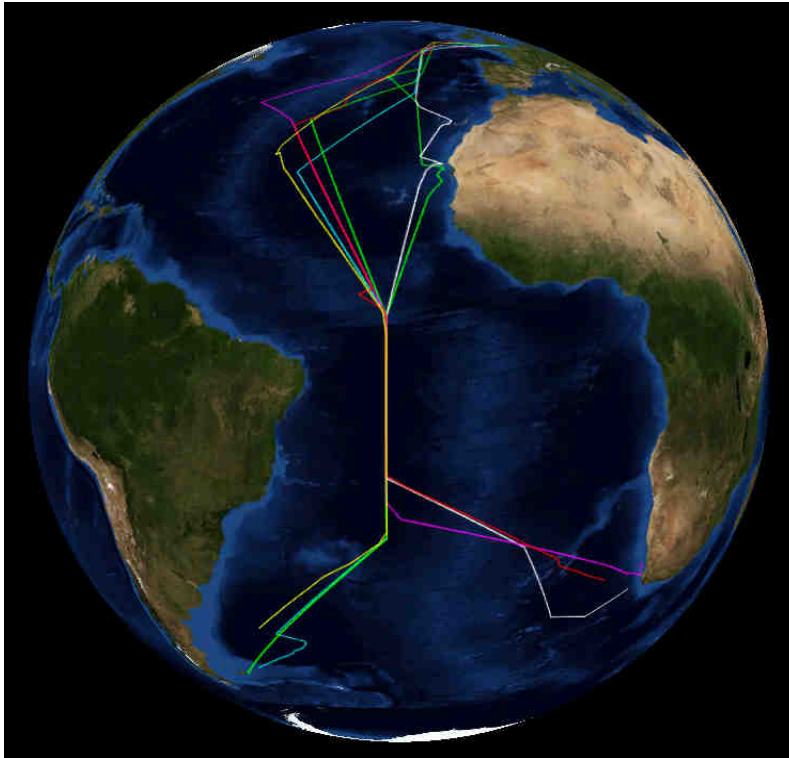


**Figure 2.3.** AMT cruises from 1995 to 2010. View from space of the different transects covered during the AMT programme (PML, 2010).

### 2.3.1 AMT20

Field data for this thesis were collected on board the RRS James Cook from the 13<sup>th</sup> of October 2010 to the 21<sup>st</sup> of November 2010 as part of the Atlantic Meridional Transect cruise AMT20 between Southampton (UK) and Punta Arenas (Chile).

Routine data on biological, chemical and physical oceanographic variability across the planktonic systems of the Atlantic Ocean collected during the cruise were also used in this thesis. Data sets are held at the British Oceanographic Data Centre (BODC 2012) and include:

- Vertical CTD profiles and continuous underway data.
- Optical characteristics of the water column.
- Biogeochemical measurements including nutrients, pigments (chl-a), dissolved gases ( $[O_2]$  used for calibration) and particulate carbon and nitrogen.

### 2.3.2 The Atlantic Ocean and oceanic biogeochemical provinces

The Atlantic Meridional Transect programme is a project of particular interest for the study of food quality variation since it is latitudinally spread, incorporating a variety of oceanic biogeochemical regions and domains (Banse 1974; Longhurst 1995; Marañon et al. 2001). These are split following hydrographic (depth, proximity to the coast and currents) and hydrological (water quality) characteristics.

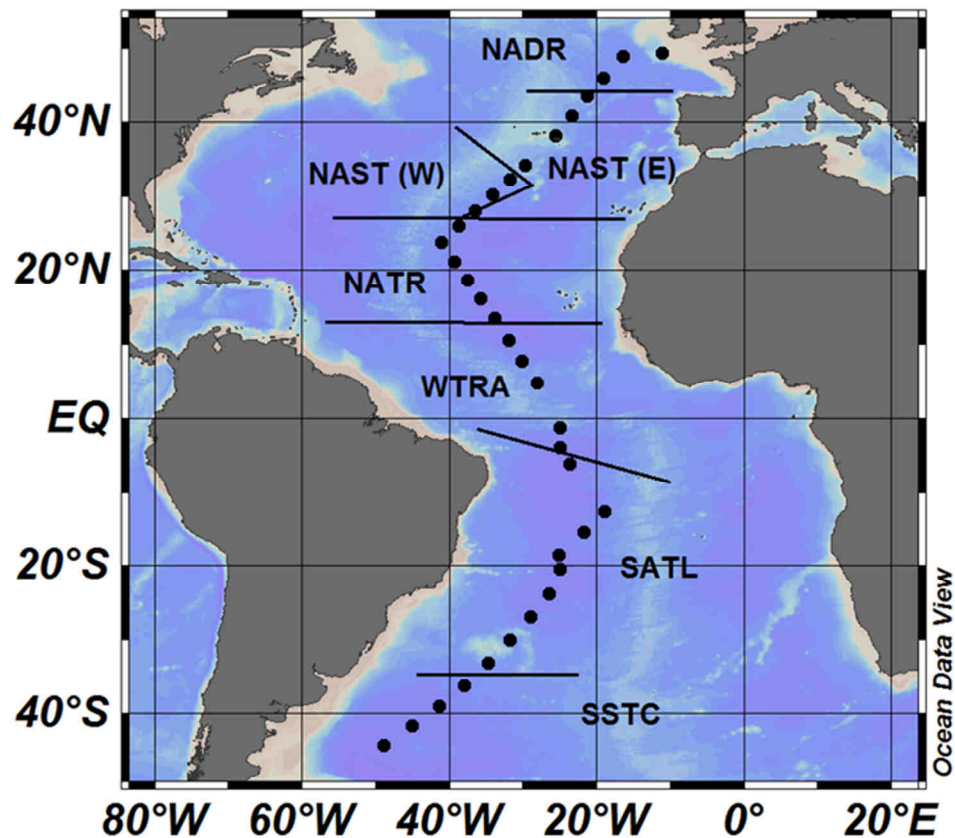


**Figure 2.4.** AMT20 stations sampled and biogeochemical provinces crossed. Provinces (Longhurst 1995): South Subtropical Convergence (SSTC), South Atlantic Gyre (SATL), Western Tropical Atlantic (WTRA), North Atlantic Tropical Gyre (NATR), North Atlantic Subtropical Gyre (NAST), North Atlantic Drift East and West (NADR).

The biogeochemical provinces, described by Longhurst (1995), and crossed during AMT20 include the coastal, westerlies and trades domains separated as follows (Figure 2.4):

- NECS: North East Atlantic Continental Shelf. From the narrow shelf of western France, north across the British shelf and North Sea, including also the Baltic Sea seasonally covered by ice.
- NADR: North Atlantic Drift
- NAST: North Atlantic Subtropical Gyre
- NATR: North Atlantic Tropical Gyre
- WTRA: Western Tropical Atlantic
- SATL: South Atlantic Tropical Gyre

### 2.3.3 Sample collection

In order to determine the effects of temperature and food quality on copepod physiology, respiration and egg production rates were measured on adult female copepods of different species and the quantity and quality of the phytoplankton (at the deep chlorophyll maximum (CM)) was biochemically determined.

#### Zooplankton sampling

A 200  $\mu\text{m}$  WP2 bongo net was deployed daily. 200 m vertical net hauls were carried out at pre-dawn. Upon recovery, the catch was diluted into darkened 10 L buckets and immediately transferred to the laboratory. Every other day live zooplankton specimens were selected for metabolic rate experiments. One of the net samples was immediately preserved in 4% formaldehyde solution and stored for possible future taxonomic identification.

#### Water sampling

The water samples collected were used for food quality analysis and experiments. 60 litres of CM seawater was collected every other day from the Niskin bottles on the pre-dawn CTD cast and gently siphoned into 20 L acid-washed carboys. The water was gently screened through a 200  $\mu\text{m}$  sieve while decanted to remove larger grazers and then filtered through GF/F filters for the following analyses:

- Particulate Organic Carbon and Nitrogen (POC/PON)
- Particulate Organic Phosphorus (POP)

- Chlorophyll-a (chl-a)
- Fatty Acids

#### 2.3.4 Experimental protocols

In the laboratory, the zooplankton were gently taken out of the container in 100 mL batches and were carefully pre-screened through a 200  $\mu\text{m}$  mesh. Then they were washed and diluted with 0.2  $\mu\text{m}$  FSW at in situ temperature. CM water was used for the incubations which was filtered by gravity through 0.8-0.2  $\mu\text{m}$  Acro-Pack® (100 L capacity) cartridges.

Adult females of different species and size ranges were selected with the aid of a field stereo microscope and then, using soft tweezers, were picked by their antennae and placed directly in the relevant incubation chambers. All the copepods selected were carefully inspected to ensure the absence of parasites and for any sign of physical damage.

Respiration, feeding and egg production rates were measured through a series of acclimatised (*in situ*) conditions and temperature outside the sampling range, varying over  $\pm 10^\circ\text{C}$ . Incubators were maintained at 3 different temperatures based on the daily temperatures at the CM, the surface and at 200 m. Temperatures outside the *in situ* range were also selected. The animals were incubated for 24 hours and the incubators were kept in the dark.

#### 2.3.5 Metabolic rates

##### Respiration rates

Respiration rates were measured via Winkler titration (Winkler 1888) as per section 2.1.4 and following the protocol in Appendix A, chapter 7.

The females were subjected to short-term acclimation to laboratory conditions in natural seawater and then moved to 0.2  $\mu\text{m}$  filtered CM water (less than 9 hours). The temperature was maintained close to that of either surface or CM waters depending on the temperatures (CM water temperature was selected when surface temperature  $>20^\circ\text{C}$ ). The copepods were incubated for a 24 hour period in the dark in 0.2  $\mu\text{m}$  filtered CM water at 3 different temperatures as stated in section 2.3.4.

## Egg production rates (EPR)

EPR were determined as stated in section 2.1.5. At the end of the 24 hour incubation the net separator was removed, the females washed back into the container and preserved in 4% formaldehyde solution for later egg count under a dissecting microscope.

### 2.3.6 Taxonomic determination and dry weight

The specimens kept and preserved after respiration and EPR determination were taken back to the laboratory and identified.

The dry weight (mg) of each copepod was estimated using the following procedure:

- 1- For each copepod, prosome length (PL  $\mu\text{m}$ ), urosome length (UL  $\mu\text{m}$ ), prosome width (PW  $\mu\text{m}$ ) and urosome width (UW  $\mu\text{m}$ ) were measured.
- 2- The shape of a prolated spheroid for the copepod prosome and a cylinder for the copepod urosome were assumed and the total volume (V) for each copepod was calculated using equation (2.12) (Weisstein 2011).

$$V = \left[\left(\frac{1}{6}\pi\right)PL(PW^2)\right] + \left[\left(\frac{1}{4}\pi\right)UL(UW^2)\right] \quad (2.12)$$

- 3- The copepod volume was converted to carbon (C) and corrected using formula (2.13):

$$C = 0.026 + [1.49(0.0475V)] \quad (2.13)$$

Where 0.0475 represents the calculated Optical Plankton Counter biovolume conversion to C from Gallienne et al. (2001), corrected for shrinkage caused by formalin (Alcaraz et al. 2003).

### 2.3.7 Chemical and biochemical analysis

To determine the biochemical composition of CM phytoplankton the samples collected as per section 2.2.1 were analysed as per section 2.1.7 unless otherwise stated.

## Particulate Organic Carbon and Nitrogen (C, N).

Due to the potential presence of calcite forming phytoplankton in the water, prior to POC/PON analysis, the inorganic carbon (PIC) in the particulate material was removed via HCl acidification.

Preliminary tests to determine the required duration of the fuming were carried out on coccolithophorid cultures (Heinle, unpublished data).  $\text{Ca}^{2+}$  analysis (PIC) were carried out via flame atomic absorption spectrometry whilst POC analysis was carried out as stated in section 2.1.7. It was found that after 24 hour fumigation, as per standard UNESCO (1994) protocol, a -41% loss of POC was experienced. After 12 hours no significant loss of POC was detected therefore the filters were fumed with concentrated HCl in a glass desiccator for 12 h.

## Chlorophyll-a

Samples for fluorimetric determination of pigment concentration (Loftus and Carpenter 1971) were collected on 25mm GF/F filters under low vacuum, immediately flash frozen in liquid nitrogen and then stored at  $-20^{\circ}\text{C}$  prior to analysis. Chlorophyll a was extracted in 90% acetone for 24 hours and analysed using a Turner designs fluorometer pre-calibrated with chl-a standards by A. Rees.

Inorganic nutrient data and CTD data collected during AMT were obtained from the BODC (British Oceanographic Data Centre).

Inorganic nutrient data included:

- Dissolved Inorganic Nitrogen: nitrate ( $\text{NO}_3^-$ ) + nitrite ( $\text{NO}_2^-$ ) (N+N)
- Dissolved Inorganic Phosphorus: soluble reactive phosphate ( $\text{PO}_4$ ) (SRP)

Dissolved inorganic nutrient samples were collected and analysed by C. Harris from Plymouth Marine Laboratory (PML). Single samples for nitrate ( $\text{NO}_3^-$ ) + nitrite ( $\text{NO}_2^-$ ) (N+N) and soluble reactive phosphate ( $\text{PO}_4$ ) (SRP) were collected by Niskin bottles and analysed using a 5 channel Bran and Luebbe AAIII segmented flow, colorimetric, autoanalyser. Data for nitrate was analysed following the Brewer and Riley (1965) protocol, nitrite using Grasshoff' (1976) and phosphate by the method of Kirkwood (1989).

CTD data from the stainless steel CTD frame included 0 to 300 or 500m depth profiles of:

- Depth (m). From Pressure data. Manufacturer's calibration applied.

- Temperature (°C). SBE 3P Temperature Sensor s/n 03P-4116 manufacturer's calibration applied.
- Salinity (no unit). SBE 4C Conductivity Sensor s/n 04C-2580 calibrated using salinometer data (PML).
- Photosynthetically Available Radiation PAR ( $\text{Wm}^{-2}$ ). 2PI PAR (DWIRR) s/n PML10 manufacturer's calibration applied.
- Dissolved oxygen ( $\mu\text{mol L}^{-1}$ ). SBE 43 Oxygen s/n 43-0862 calibrated against discrete dissolved oxygen analyses (Winkler titrations) (PML).
- Oxygen saturation (%). Derived from oxygen sensor data calibrated against discrete dissolved oxygen analyses (Winkler titrations) and computed using the Garcia and Gorgon (1992) algorithm with Benson and Krause (1984) constants.
- Sigma-theta ( $\text{kg m}^{-3}$ ). Computed using UNESCO SVAN function.
- Backscatter ( $\nu$ ). Wetlabs BBRTD backscatter s/n 182 manufacturer's calibration applied.

Hydrographic data of temperature and fluorescence were acquired from pre-dawn stainless steel frame CTD casts made with a Sea-Bird 911 plus fitted with an SBE 32 Carousel and a Chelsea MkIII Aquatracka Fluorometer. The CTD fluorometer was calibrated against chlorophyll a (chl-a) measurements extracted from filtered sea water samples collected by Niskin bottles and determined by fluorimetric analysis by A. Rees from PML. The calibration data is shown in Table 2.3.

**Table 2.3.** Fluorometer calibration on AMT20. Stainless CTD fluorometer – due to large offsets making the low values unreasonable the regressions were forced through 0.

	Calibration factor	SE	n	p-value	$r^2$
CTD 4-7	1.45	0.033	9	<0.001	0.79
CTD 10-13	2.04	0.01	10	<0.001	0.89
CTD16-79	3.06	0.01	110	<0.001	0.97
CTD80-85	2.07	0.01	22	<0.001	0.94
CTD86	No calibration - fluorometer failed during upcast				
CTD087s	2.04	0.02	3	0.03	0.50
CTD088s	1.42	0.008	3	0.02	0.50
CTD089s	1.99	0.02	4	0.002	0.66

## 2.4 Planar Optode

Recent developments in sensor technology are giving scientists the opportunity to advance their current research methods, making them more practical and improve the accuracy of estimates compared to the old techniques. The application of new *in vivo* dissolved oxygen sensors in the field of ecology for instance could reduce the need for bulky equipment, a large amount of laboratory space (particularly in the field), long incubation times and the need for a large volume of water; therefore adding methodological flexibility.

We therefore set out to evaluate and compare a number of dissolved oxygen determination techniques and tested the respective accuracies and stability of the different instruments available.

### 2.4.1 Zooplankton respiration

The optode (Ocean Optics NeoFox system) was tested in the field, comparing the performance of one sensor to the Winkler technique (Winkler 1888) for copepod respiration measurements. Single copepod respiration measurements were undertaken during AMT20. The probe was set up using the manufacturer's calibration and then single-point calibrated at the beginning of the experiments with 100% saturated (bubbled) milliQ water.

The manufacturer's multipoint calibration is based on a measured and calculated Tau ( $\tau$ ) - partial pressure of oxygen - temperature °C quadratic (second order polynomial) relationship as shown in Figure 2.5.

The difference between a two-point calibration and a multipoint calibration method is that the two-point calibration does not consider variable temperature when calculating the partial pressure of oxygen from Tau ( $\tau$ ), but the multipoint conversion includes this variation (Ocean Optics manual 2011). Therefore the choice of calibration will vary depending on the required application. For instance, during zooplankton respiration measurements, the need for a fixed incubation temperature suggests that a two-point calibration is acceptable. Whilst for dissolved oxygen measurement in the field, under variable temperature conditions, using a multipoint calibration would improve accuracy.

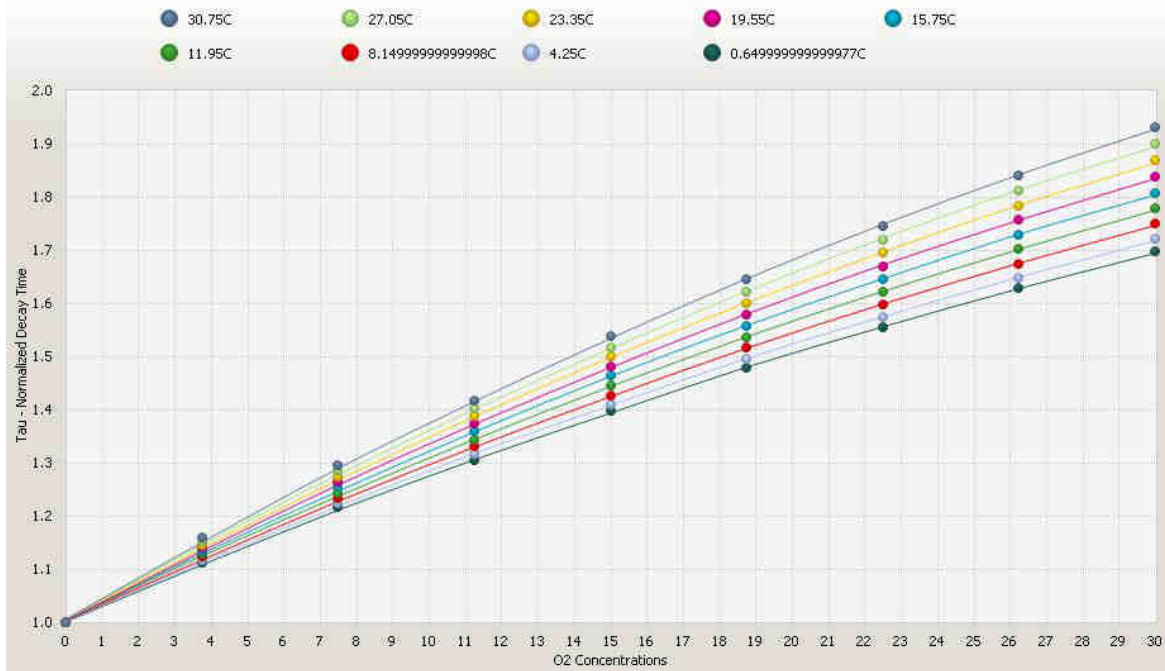


**Figure 2.5.** Manufacturer's calibration curve. Quadratic relationship between Tau ( $\tau$ ) partial, pressure of oxygen and temperature  $^{\circ}\text{C}$ .

A series of 7 mL glass chambers with water-tight stoppers were designed. The stoppers included a silicon coated hole in the middle for the insertion of the optode needle. During incubations the chamber was kept air-tight by sealing the needle in the hole with extra silicon tubing and parafilm.

The experimental set up included the measurement of a control bottle alongside a bottle containing a copepod for a period of 6 hours. Single adult female copepods were incubated at in situ temperature in the dark for 2-3 hours in  $0.2\ \mu\text{m}$  filtered chlorophyll maximum water. At the beginning and at the end of the 6 hours period a 7 mL control bottle with  $0.2\ \mu\text{m}$  FSW was set up in the dark and monitored. Dissolved oxygen concentration was semicontinuously recorded with the LED cycle of the optode set to 1 second on and 3 seconds off to decrease sensor drift. The calculated drift for our experiments was 0.003%.

Temperature was kept as stable as possible in the sample (mean  $\text{SD} \pm 0.5\ ^{\circ}\text{C}$ ) by a continuous flow of water between the water bath and a cooling system. The water in the chambers was not stirred to avoid stress and damage to the animal. At the end of the incubation the specimen was picked and fixed in 4% formalin then stored for later taxonomic and dry weight determination as described in section 2.2.4.

The copepod respiration experiments were deemed unsuccessful since the noise in the optode signal was greater than the respiration signal. This was possibly caused by variations in temperature  $>0.2$  °C and the inability to stir the water in the incubation chambers. This was also due to the inability to measure the concentration of dissolved oxygen in the control at the same time as that in the bottle containing the copepod; thus, resulting in further ineffective attempts to detect any significant differences between incubation chambers.

Suggestions for future improvements include:

- 1- The use of a greater number of animals in larger incubation chambers (Alcaraz et al. 2010). However this contradicts one of the reasons we might want to use an optode.
- 2- Improve the system to include the possibility of stirring the water to homogenise the sample; therefore avoiding the formation of temperature and oxygen gradients in the chambers. This could be achieved by including a magnetic stirrer in the bottle.
- 3- Work in a temperature controlled room as at present even small changes in ambient temperature appeared to affect the optode signal.
- 4- Set up a multiple-array system for the simultaneous measurement of respiration chamber and control bottle according to Alcaraz et al. (2010). Although this would be costly.
- 5- Increase incubation times to allow animal acclimation and exclusion of any diel rhythm effects (Alcaraz et al. 2010; Pavlova 1994). This also would contradict one of the reasons we might want to use an optode, we also recommend undertaking preliminary experiments to assess species size-specific minimum incubation times and the smallest incubation volume that would allow precise results.

The main downside of an optode system is that the sensors are potentially expensive to maintain since the probes need yearly reconditioning. Along with yearly maintenance, it is necessary to separately purchase the factory recalibrations each time.

Based on this experience and considering the above suggestions we believe that zooplankton respiration measurements carried out via Winkler technique can still be more fruitful and in most field-related occasions, practical. This is since the Winkler technique

allows dissolved oxygen determination on an unlimited number of replicates, at the same time and under a variety of experimental set ups.

#### 2.4.2 Instrument inter-comparison

In collaboration with colleagues from the University of Vigo (Spain), a set of experiments designed to compare dissolved oxygen techniques was carried out and written up in Garcia-Martin et al. (in prep.) (paper in preparation shown in Appendix C (Section 8 of this thesis)). This included comparing the performance of three different sensors for phytoplankton PI (photosynthesis /irradiance) measurements: Clark type microelectrode probe (Unisense S.A), Clark type (Clark 1959) electrode disc (Oxygraph, Hansatech instruments) and our group's needle-supported optode probe with a silicone overcoat (FOXY-AF-MG, NeoFox, Ocean Optics sensors). Dissolved O<sub>2</sub> concentration was determined inside a 5 mL Oxygraph jacketed chamber. Optode sensors experience some drift as they use an LED to excite the fluorescence in the oxygen sensitive coating, hence rates are semicontinuously recorded. The LED cycle of the optode was set to 1 second on and 3 seconds off. The calculated drift for our experiments was 0.003%.

Dissolved oxygen concentration was calculated from Temperature (°C) and Tau (τ) data using a modified Stern-Volmer equation (2.14) by Glud et al. (2000) and corrected for the probe drift calculated using equation (2.15).

$$[O_2]\mu M = \frac{\tau_0/\tau_{100}-1}{k_{sv}} \quad (2.14)$$

Where;

$\tau_{100}$  = Tau at 100% O<sub>2</sub>

$\tau_0$  = Tau at 0% O<sub>2</sub>

$K_{sv}$  = Quenching coefficient = slope ( $\tau_0/\tau_{100}$ ) vs 0-100% [O<sub>2</sub>] μM (Benson and Krause 1984).

The signal drift was calculated as per equation (2.15):

$$\text{Drift} = 0.01 \left( \frac{a_{on}}{a_{off}} \right) \quad (2.15)$$

Where;

0.01 = factory calculated stability O<sub>2</sub> % per hour

a = cycle time (sec) on and off respectively

For consistency between instruments a two-point calibration was chosen. The probe was two-point calibrated assuming a linear relationship between partial pressure of oxygen and Tau ( $\tau$ ) at a fixed temperature. The calibration was carried out at the same time as that for the electrodes, at the beginning of the experiment with a 0% (2-5% sodium dithionite leeching agent) and 100% saturated (bubbled) milliQ water at a fixed temperature  $SD \pm 0.02$  °C.

Temperature was kept stable in the sample (mean  $SD$  0.02 °C) by a continuous flow of water between the Oxygraph chambers' jacket and a water bath cooling system. The temperature was recorded continuously with a temperature data logger. The samples were continuously stirred in all the experiments to minimise the formation of oxygen gradients.

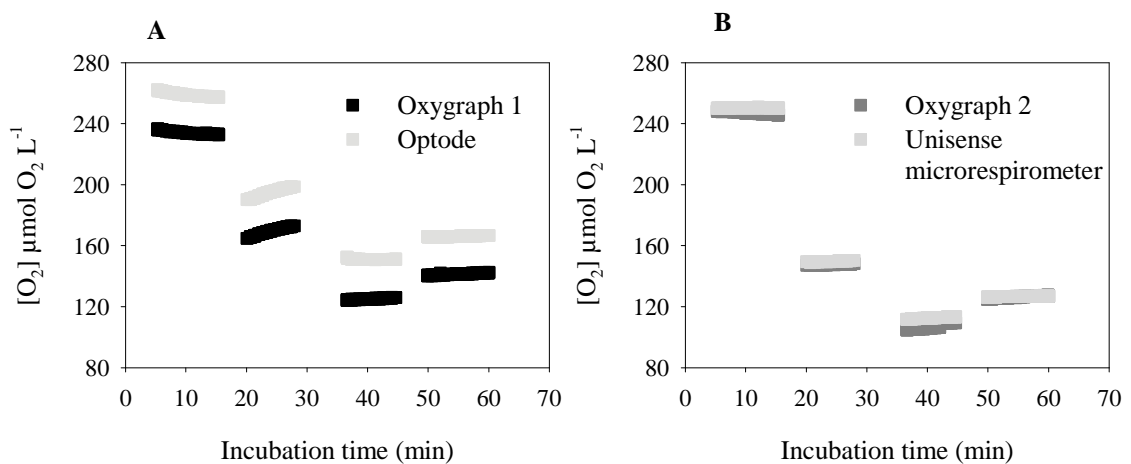


**Figure 2.6.** Precision test results. A) O<sub>2</sub> concentration recorded in oxygraph chamber 1 with optode. B) O<sub>2</sub> concentration recorded in Oxygraph chamber 2 with Unisense electrode.

A precision test was performed, to compare measurements of O<sub>2</sub> concentration between instruments (Figure 2.6). Different proportions of air bubbled (O<sub>2</sub> saturated) deionized water and N<sub>2</sub> bubbled (O<sub>2</sub> sub saturated) deionized water were mixed in the incubation chambers and O<sub>2</sub> concentration was determined. The temperature was kept stable at 16.99 °C,  $SD$  0.02. The oxygen concentration recorded in chamber 1 with the Oxygraph

and the Neofox optode (Figure 2.6A) showed a slight decrease and a minor increase of the oxygen concentration in the first and second set of measurements (Garcia-Martin et al. In prep.).

PI curves for *Emiliana huxleyi* culture (strain RCC1229) were produced from comparisons between the variations in O<sub>2</sub> concentration with changing light intensity (Figure 2.7). Phytoplankton cultures were incubated in the chambers and exposed to 8-9 increasing light intensities (0, 2, 25, 65, 135, 315, 600, 1300, 2000  $\mu\text{E m}^{-2} \text{s}^{-1}$ ).

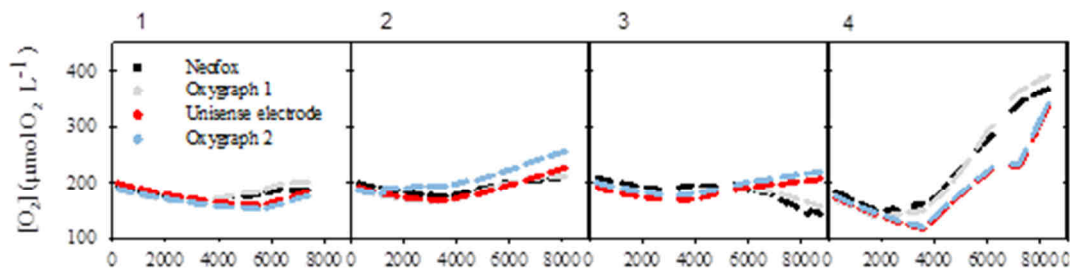


**Figure 2.7.** Variations in O<sub>2</sub> concentration for *Emiliana huxleyi* (strain RCC1229) culture under increasing light intensities. Experiments 1-4 of the thirteen carried out.

Details on the results and methodology are discussed in Garcia-Martin et al. (In prep.) and can be found in Chapter 8, Appendix C.

## 2.5 Data processing and error propagation

The errors in our estimates of stoichiometry were calculated through error propagation. SD (Standard Deviation) of measured C, N and P concentrations were propagated to calculate C:N, N:P and C:P mol mol<sup>-1</sup> ratios. The SD of the ratio was propagated using equation (2.16).

$$\sigma_{AB} = AB \sqrt{\left(\frac{\sigma_A}{A}\right)^2 + \left(\frac{\sigma_B}{B}\right)^2} \quad (2.16)$$

Where;

$\sigma$  = Standard Deviation

A = first variable

B = second variable

## **2.6 Statistical analysis**

Statistical analyses were carried out using SigmaPlot® v12.0 and MyStat®. Data were tested for parametric or non-parametric distribution. The use of dummy variables was occasionally implemented to test variability within relevant groups and plan further analyses. The data was normalised when required and as specified in each chapter. Standard regression or multiple regression analyses were carried out alongside appropriate correlation analyses where applicable and as stated in each chapter of this thesis.

## **CHAPTER 3**

### 3. Food quality regulates the metabolism and reproduction of *Temora longicornis* (Copepoda: Calanoida)

As submitted to Biogeosciences May 2013.

#### 3.1 Introduction

The physiology of copepods is affected by seasonal and latitudinal changes in environmental conditions (Mauchline 1998). Alongside body mass and temperature, food quantity and quality play important roles in regulating copepod physiology (Ambler 1986; Urabe and Watanabe 1992; Jónasdóttir et al. 1995; Guisande et al. 2000). The elemental content of the food available to copepods (seston) varies significantly with light availability, temperature and inorganic nutrients (Sterner and Elser 2002; Geider and La Roche 2002). Therefore food quality can become a significant factor limiting copepod production, by reducing efficient nutrient uptake and energy availability (Hessen and Anderson, 2008 and references therein).

Nutritious food is defined by the presence of a range of nutrients and organic compounds, which occur at optimal concentrations and proportions required to provide a balanced diet. Stoichiometric determination of the organic nutrients present in the copepod's diet is therefore a reliable indicator of food quality (Sterner and Elser 2002). Although elemental analyses are known to lack information on the nature of the different carbon-containing compounds (Tang and Dam 1999), their ease of measurement can provide a practical approach to the determination of food quality, and allow an important link to nutrient biogeochemical cycles.

The C:N ratio of phytoplankton is typically used to determine the quality of the diet of copepods in the marine environment, whereas C:P and N:P ratios are not routinely measured (e.g. Touratier et al. 1999; Jones et al. 2002; Mayor et al. 2009a). However, although phosphorus constitutes only ~1% of the total dry biomass of adult marine calanoid copepods (Bamstedt 1986), it plays a major role in the synthesis of cellular ATP and RNA. As a consequence, this macronutrient is essential for protein synthesis and thus copepod production and growth (Sterner and Elser 2002). Hence, using N:P as a food quality determinant alongside the C:N ratios, should provide a more complete measure of the nutritional value of the food (Vrede et al. 2004).

Copepod growth and egg production rate are influenced by food quality in terms of protein, amino acid and fatty acid composition (e.g. Jónasdóttir 1994; Kleppel and Burkart 1995; Koski et al. 1998; Guisande et al. 2000). However, little is known of the effects of

food quality on metabolism. Copepod metabolism, determined as oxygen uptake, increases during feeding, in relation to a high protein diet, and decreases to basal rates when starved (e.g. Vidal 1980; Kiorboe et al. 1985; Thor 2000); but, to the best of our knowledge, no information is available on the effect of the organic nutrient ratio of the food on the respiration rate of copepods.

To assess the effects of food stoichiometry on the physiology of the neritic copepod *T. longicornis*, we measured feeding, respiration, and egg production rates at a range of phytoplankton N:P, C:N and C:P nutrient ratios. We test the hypothesis that maximum physiological rates occur when *T. longicornis* is fed on phytoplankton which have an elemental ratio of 16N:1P (molar). This corresponds to the global average elemental ratio of marine particulate matter (Redfield 1958) and may be expected to provide a balanced diet for copepods since phytoplankton with an N:P ratio above or below 16, are considered to be P or N limited respectively (Geider and La Roche 2002 and references therein). We then assess the effect of food quality on growth and biomass by calculating copepod carbon budgets. Finally, we consider the ecological implications of food quality on ecosystem productivity by investigating the possibility of N:P limitation in the field. We apply our laboratory findings to field data in order to determine how current and future changes in the interaction between primary producers and grazers could impact ocean biogeochemistry and the trophic transfer of energy.

## 3.2 Methods

### 3.2.1 Algal Cultures

The cryptophyte *Rhodomonas salina*, equivalent spherical diameter  $\sim 7\mu\text{m}$  (CCMP 1319) was grown in 1.5 L continuous cultures in ESAW medium (Berges et al. 2001) without silicate, supplied at  $540\text{ mL d}^{-1}$  (growth rate =  $0.36\text{ cell d}^{-1}$ ) at  $13 \pm 0.5^\circ\text{C}$  in continuous light with an irradiance of  $300\ \mu\text{mol photons m}^{-2}\text{s}^{-1}$ . Cultures were established under different nutrient conditions: balanced growth, N-limited and P-limited. The steady state of the cultures was monitored using cell abundance and cell volume measured with a Beckman multisizer 3 coulter counter and their state of health was determined using a Walz PhytoPAM phytoplankton analyser every three days.

For each experiment, seawater, obtained at the same time as the copepods, was  $0.2\ \mu\text{m}$  filtered and used to dilute one of the stock cultures to create a consistent *R. salina* concentration with a particular N:P ratio, which could then be used as the food source for *T. longicornis*. We aimed for an algal concentration of  $5 \pm 0.5 \times 10^6\ \mu\text{m}^3\ \text{mL}^{-1}$ , as this reflects saturating food concentration (O' Connors 1980) and bloom conditions in the

North Sea (Jónasdóttir and Kiorboe 1996). Due to a malfunction of the coulter counter, on three occasions (11, 20 and 23 July) the dilution of *R. salina* was prepared based on measurements made with a Becton Dickinson FACS Calibur flow cytometer, and on 11 and 20 July, the samples were fixed in 2% lugol and stored prior to enumeration.

### 3.2.2 Elemental Composition of the Diet

Triplicate samples (70-120 mL) of the *R. salina* fed to the copepods were collected for analysis of particulate organic carbon (C), nitrogen (N), and phosphorus (P). Samples were filtered through pre-combusted (450°C for 4 h) 25mm GF/F filters under <5 mmHg vacuum. POC and PON filters were immediately dried at 60°C for 24 h and stored until analysis on an Exeter 440 Elemental Analyzer. Particulate P filters were dried at 60°C for 24h, and stored at -20°C prior to analysis. The samples were processed following the potassium persulfate ( $K_2S_2O_8$ ) digestion method of Suzumura (2008) and analysed with the colorimetric method of Strickland and Parsons (1972) using a PerkinElmer Lambda 25 UV/Vis Spectrometer equipped with a PerkinElmer S10 autosampler and a 4 cm<sup>3</sup> cell.

The C, N and P concentrations and C:N, N:P and C:P mol mol<sup>-1</sup> ratios of *R. salina* were calculated as the average of the measurements made at the beginning ( $T_0$ ) and end ( $T_{24}$ ) of the incubations  $\pm$  SD. Where applicable the standard deviation was calculated via error propagation.

### 3.2.3 *T. longicornis* sampling and maintenance

Experiments were carried out on natural zooplankton due to time constraints in setting up an established culture of copepods and since the physiological responses of cultured copepods have been found to be reduced, and therefore unrepresentative of the in situ population (Klein Breteler and Gonzalez 1982; Tiselius et al. 1995; Koski et al. 2010)

Individuals of *T. longicornis*, were collected from the North Sea off the coast of Great Yarmouth (UK) (52° 41.9'N, 1° 48.5'E) between June and December 2011 using a 120- $\mu$ m plankton net towed horizontally for ~20 min. The sample was brought back to the laboratory and kept at  $13 \pm 0.5^\circ\text{C}$  in salinity 34.0-34.2 FSW in a darkened 30 L bucket for up to 2 weeks. The animals were fed three times a week with a mixture of the cryptophyte *Rhodomonas salina*, the dinoflagellate *Oxyrrhis marina* (fed twice a week with the chlorophyte *Dunaliella marina*) and the diatom *Thalassiosira weissflogii*.

### 3.2.4 Physiological rates

Adult females of *T. longicornis* were isolated and acclimated for 48 h to the experimental conditions (13°C in the dark) in 4 L 0.2 µm FSW at the food quality and quantity to be used during the incubations. During this acclimation period the females were transferred daily to new medium and fed at an *R. salina* cell concentration corresponding to a saturating biovolume of  $5 \pm 0.5 \times 10^6 \mu\text{m}^3 \text{mL}^{-1}$  (Jónasdóttir and Kiorboe 1996; O'Connors et al. 1980). Feeding, egg production and respiration rates were measured at  $13 \pm 0.5^\circ\text{C}$ . Copepods found dead or moribund at the end of the incubations were not included in the analysis.

### 3.2.5 Feeding rates

Up to 9 x 500 mL amber glass bottles were filled with *R. salina* in 0.2 µm FSW. A number of female *T. longicornis* (8-12) were placed in 3 of these bottles and 6 without copepods were used as controls. The bottles were sealed with parafilm (to avoid bubbles), capped and mounted on a slowly rotating plankton wheel (1rpm) for 24 h. Three control bottles were sampled at the beginning ( $T_0$ ) and three at the end ( $T_{24}$ ) of the incubation for cell abundance, volume and elemental composition of *R. salina* as described in section 3.2.1. At the end of the incubation *T. longicornis* clearance and ingestion rates were calculated according to Frost (1972).

### 3.2.6 Respiration rates

Copepod respiration rates were derived from the consumption of oxygen during an *in vitro* incubation in 100% oxygen saturated 0.2 µm FSW. A preliminary experiment showed that there was no significant difference (Student t-test  $p = 0.55$   $n = 16$ ) between the respiration rate of copepods incubated over 18 and the more usual 24 h. Therefore we measured copepod respiration over the shorter incubation time of 18 h.

Single adult *T. longicornis* females were incubated in triplicate 60 mL borosilicate glass bottles in 0.2 µm FSW containing *R. salina* to determine the respiration rates of feeding copepods ( $R_f$ ). Triplicate bottles containing *R. salina* in 0.2 µm FSW were incubated in order to determine the respiration rate of the algal food and any bacteria remaining in the 0.2 µm FSW (fed control). Additionally, *T. longicornis* females were incubated in 0.2 µm FSW without *R. salina* to determine the unfed respiration rates ( $R_u$ ), alongside triplicate bottles of 0.2 µm FSW as a control. All the respiration bottles were incubated in the dark for 18 h and the bottles containing the copepods with the food were placed on a rotating plankton wheel (1rpm).

Measurements of dissolved oxygen concentration were made with an automated Winkler titration system with a photometric endpoint (Robinson et al. 2002). The sodium thiosulphate titrant was calibrated with 0.1N potassium iodate standard (replicates average SD  $\pm$  0.0001 N) (Carrut and Carpenter 1966). The salinity of the seawater used in the incubation was measured with a portable salinometer fitted with a salinity/temperature sensor to enable oxygen concentration and saturation to be calculated from the equation of Garcia and Gordon (1992) using the equilibrium constants of Benson and Krause (1984).

The respiration rates for the fed and unfed animals in nL O<sub>2</sub> female<sup>-1</sup> h<sup>-1</sup> were calculated as the difference between the means of the triplicate zero time bottles and the triplicate incubated bottles corrected for the controls.

The respiration rates were normalised to the dry weight (*dw*) of each individual. The dry weight (in  $\mu$ g) was calculated by measuring the prosome length (*PL*, in  $\mu$ m) of 4% formaldehyde preserved specimens collected at the end of the feeding and respiration incubations. This was then converted to dry weight using Eq. (3.1) (Castellani and Altunbaş 2013):

$$\ln dw = 2.78 \ln PL - 15.9 \quad (3.1)$$

### 3.2.7 Egg production rates (EPR)

Single adult females (n=2 to 7; Table 3.1) were incubated for 24 h in the dark in plexiglass tubes which had a 200  $\mu$ m nylon screen attached at their lower end. The tubes were inserted in 90 mL amber plastic vessels and filled with 0.2  $\mu$ m FSW. The nylon screen was small enough to allow the eggs to sink to the bottom of the chamber yet prevent the adults from cannibalising them. At the end of the incubation the number of eggs female<sup>-1</sup> day<sup>-1</sup> were counted using a stereoscopic microscope.

### 3.2.8 Experimental protocol

Fifteen single-diet experiments were carried out between June 2011 and December 2011. In the initial 4 experiments only ingestion, clearance rates and respiration were measured, however in the remaining 11 experiments (between 23 October and 15 December 2011), ingestion, clearance rates, respiration and EPR were measured (Table 3.1).

### 3.2.9 Carbon Budget

Copepod budgets were calculated in carbon units, and where possible rates and efficiencies were calculated in N and P units. Respiration rates were converted into

carbon using a protein based respiratory quotient (RQ) of 0.97 (Omori and Ikeda 1992). This adoption of a fixed RQ can result in an uncertainty of about 20% in the oxygen to carbon dioxide conversion since the quotient varies with the substrate metabolised (Hernandez-Leon and Ikeda 2005).

Since *T. longicornis* adults do not undergo moulting, egg production was used as an index for growth (G) (Mauchline 1998). Egg production rate (EPR) was converted to G in units of carbon assuming an egg carbon content of  $0.0833 \mu\text{g C egg}^{-1}$  (Dam and Lopes 2003) and an average egg diameter of  $80 \mu\text{m}$  ( $\pm 4 \mu\text{m}$  SD) (Dam and Lopes 2003). G was calculated in units of N using an egg nitrogen content of  $0.015 \mu\text{g N egg}^{-1}$  (Dam and Lopes 2003). Ingestion (I; feeding rate x time) in units of carbon was calculated according to Frost (1972). Ingestion in units of N and P was calculated using the N and P concentration per cell measured as described in section 3.2.1. For the experiments on 11 and 20 July, due to the issues discussed in section 3.2.1, the average ingestion rate from all the other experiments was used to calculate assimilation efficiency (AE) in carbon units and gross growth efficiency (GGE) in carbon and nitrogen units. Where applicable the standard deviation was calculated via error propagation.

Assimilation efficiency ( $AE = 100 \cdot (G + R_{\text{unfed}}) / I$ ) and gross growth efficiency ( $GGE_{\text{C}} = 100 \cdot G / I$ ) were determined using  $\mu\text{g Carbon (food)} \mu\text{g Carbon (copepod)}^{-1}$ . The carbon content of *T. longicornis* was calculated assuming that the carbon content is 40% of the dry weight (Omori and Ikeda, 1992).  $GGE_{\text{N}}$  was calculated following  $GGE_{\text{C}}$  using  $\mu\text{g Nitrogen (food)} \mu\text{g Carbon (copepod)}^{-1}$ .

The metabolic increment (MI) of fed copepods was determined as the % increase in carbon consumption between unfed ( $R_{\text{u}}$ ) and fed ( $R_{\text{f}}$ ) copepods for each of the *R. salina* N:P ratios ( $MI = 100 \cdot (R_{\text{f}} - R_{\text{u}}) / R_{\text{u}}$ ). In this study MI characterizes the increase in metabolic rate of the organism during feeding.

The cost of egg production (CoE) was calculated as the amount of C expended in respiration ( $\mu\text{g C} \mu\text{g C d}^{-1}$ ) to produce eggs, based on the assumption that the respiration while feeding is a proxy for the carbon requirement, in excess of basal metabolism, necessary for growth, therefore  $CoE = (R_{\text{f}} - R_{\text{u}}) / \text{Egg n}$ .

### 3.2.10 Time Series Data

We used time-series data to test whether the ecological implications that are suggested by our laboratory results are consistent with field data. We obtained particulate organic N:P data from the Norwegian Coastal Surveillance Program at Arendal station ( $58^{\circ} 23'N$ ,

08° 48'E) in the North Sea, between 1991 and 2010. For each of the available years, monthly average particulate organic N and P concentrations ( $\mu\text{g L}^{-1}$ ) were calculated. Since co-located zooplankton biomass data were not available, we used Continuous Plankton Recorder (CPR) data to calculate *T. longicornis* abundance from 1991 to 2010 in a 2° latitude x 2° longitude area around the Arendal station.

To investigate whether other copepod species have a response to the N:P ratio of their food similar to that of *T. longicornis*, we searched for co-located data for seston N:P ratios and zooplankton biomass. We obtained seston N:P ratios and night time size fractionated zooplankton biomass (0.2-0.5, 0.5-1, 1-2 and 2-5) from the North Pacific Subtropical Gyre (NPSG), between 1994 and 2010, from the Hawaii Ocean Time-series Data Organization and Graphical System (HOT-DOGS) website. We made the assumption that copepods dominate the zooplankton biomass in the 0.2 to 5 mm size fractions. According to Landry et al. (2001), copepods account for an average of 77% of the zooplankton community at night at the Hawaii Ocean Time series station (HOT) and do not contribute to the fraction >5 mm. We used a binomial fit for the biomass of each of the zooplankton size classes, as a function of time, to calculate the year in which the biomass of each of the individual size-fractions reached a maximum. For each of the biomass peak years we determined the corresponding annual mean seston organic N:P ratio for the upper 150 m of the euphotic zone. This seston N:P ratio was compared with the N:P ratio for each zooplankton size fraction, obtained from Hannides et al. (2009).

### 3.3 Results

#### 3.3.1 *R. salina* quantity and quality

In order to determine the influence of food N:P ratio rather than food quantity or cell size, we aimed to provide *T. longicornis* with a saturating concentration ( $5 \times 10^6 \mu\text{m}^3 \text{mL}^{-1}$ ) of *R. salina* cells of a constant size. However, due to a malfunction of the coulter counter, on 11, 20 and 23 July, the food concentration supplied to the copepods was significantly higher or lower than anticipated (Table 3.1), and on 11 and 20 July cell volume could only be estimated from samples fixed in 2% lugol (data not shown). We therefore assessed whether these three data should be included or removed from further analysis.

**Table 3.1.** Stoichiometric ratios (N:P, C:N and C:P mol mol<sup>-1</sup>), carbon, nitrogen and phosphorus content (pg cell<sup>-1</sup>), cell volume (μm<sup>3</sup>) and concentration (cell mL<sup>-1</sup>) of *R. salina* and number of replicates for each respiration (R), egg production (EPR) and feeding experiment (F). Data are the means of measurements taken at the beginning (T<sub>0</sub>) and at the end (T<sub>24</sub>) of the feeding incubation ± SD. NA = data not available.

Date	Stoichiometry			Nutrient measurements			Size	Food conc	Replicates		
	N:P	C:N	C:P	C pg cell <sup>-1</sup>	N pg cell <sup>-1</sup>	P pg cell <sup>-1</sup>	Cell μm <sup>3</sup>	cells mL <sup>-1</sup>	R	EPR	F
29/06	14.8:1 ± 0.7	6.2:1 ± 0.2	92.2:1 ± 2.9	35.1 ± 0.7	6.5 ± 0.3	1.0 ± 0.06	98 ± 2	30369 ± 4025	NA	NA	1
11/07	10.2:1 ± 0.7	7.5:1 ± 0.3	77.4:1 ± 3.9	38.8 ± 1.0	6.0 ± 0.2	1.3 ± 0.12	NA	15815 ± 2355	5	NA	2
20/07	22.8:1 ± 0.5	7.4:1 ± 0.2	168:1 ± 3.4	45.2 ± 0.9	7.1 ± 0.1	0.7 ± 0.01	NA	48675 ± 4447	5	NA	2
23/07	15.6:1 ± 0.8	8.3:1 ± 0.2	128:1 ± 5.6	45.0 ± 0.6	6.3 ± 0.1	0.9 ± 0.05	123 ± 2	47298 ± 6782	5	NA	2
23/10	9.6:1 ± 0.6	9.9:1 ± 0.7	94.3:1 ± 4.1	55.2 ± 2.0	6.5 ± 0.5	1.6 ± 0.05	198 ± 6	25841 ± 1864	7	3	2
26/10	15.5:1 ± 0.4	5.9:1 ± 0.2	92:1 ± 2.0	34.7 ± 0.6	6.8 ± 0.2	1.0 ± 0.02	173 ± 13	32704 ± 1592	5	2	2
31/10	14.2:1 ± 1.0	6.7:1 ± 0.2	90.9:1 ± 4.3	33.8 ± 0.4	5.9 ± 0.1	1.0 ± 0.07	181 ± 10	29619 ± 2965	8	2	2
05/11	12.3:1 ± 0.6	7.9:1 ± 0.2	94.2:1 ± 3.5	50.9 ± 0.8	7.5 ± 0.2	1.4 ± 0.06	205 ± 6	26041 ± 4067	4	3	1
11/11	13.3:1 ± 0.7	5.8:1 ± 0.3	76.4:1 ± 2.1	33.5 ± 0.6	6.8 ± 0.3	1.1 ± 0.04	170 ± 14	26037 ± 1588	6	4	2
14/11	17.3:1 ± 0.8	8.1:1 ± 0.2	138:1 ± 4.8	46.8 ± 0.6	6.8 ± 0.1	0.9 ± 0.04	201 ± 6	28059 ± 5035	7	2	1
17/11	20.3:1 ± 0.5	5.3:1 ± 0.1	108:1 ± 1.6	38.4 ± 0.5	8.5 ± 0.2	0.9 ± 0.01	178 ± 3	31645 ± 2366	5	4	1
26/11	16.5:1 ± 0.5	5.2:1 ± 0.1	86.5:1 ± 1.7	33.4 ± 0.4	7.4 ± 0.2	1.0 ± 0.03	173 ± 9	25727 ± 1737	7	4	2
29/11	17.2:1 ± 0.9	6.7:1 ± 0.2	115:1 ± 3.8	39.9 ± 0.5	7.0 ± 0.2	0.9 ± 0.05	177 ± 8	29985 ± 4063	6	2	2
13/12	19.9:1 ± 0.7	6.0:1 ± 0.1	122:1 ± 2.2	37.5 ± 0.2	7.2 ± 0.2	0.8 ± NA	186 ± 6	26090 ± 2725	9	7	2
15/12	18.9:1 ± 1.2	6.2:1 ± 0.1	118:1 ± 6.7	41.2 ± 0.6	7.7 ± 0.1	0.9 ± 0.06	193 ± 12	27307 ± 3001	6	2	2

With these three data removed, the food concentration varied between 0.9 and 1.4  $\mu\text{g C mL}^{-1}$ , and so we investigated whether the metabolism of *T. longicornis* was related to this variability in food concentration. Clearance rates varied between 0.2 and 0.4  $\text{mL } \mu\text{g dw}^{-1} \text{d}^{-1}$  and were not related to food concentration ( $r^2=0.05$   $p=0.48$ ); ingestion varied between 0.2 and 0.5  $\mu\text{g C } \mu\text{g dw}^{-1} \text{d}^{-1}$  and was significantly related to food concentration ( $r^2 =0.35$   $p= 0.04$ ) (Figure 3.5 in Supplementary Material). However, neither EPR ( $r^2=0.2$   $p=0.17$ ) nor respiration rate ( $R_f$   $r^2=0.24$   $p=0.12$ ) were related to ingestion rate (Figure 3.6 in Supplementary Material). The EPR of *Paracalanus parvus* and the EPR and respiration rate of *Temora stylifera* have previously been shown to be independent of ingestion above a critical rate of ingestion and food concentration (Checkley 1980; Abu Debs 1984). We suggest that by maintaining the food concentration at saturating levels, we achieved an analogous critical ingestion rate where ingestion was not related to respiration or egg production rates, and therefore *T. longicornis* metabolism was not related to food concentration.

When data from 11, 20 and 23 July were included in the analysis, the outcome was not affected. Ingestion was significantly related to food concentration ( $r^2=0.74$   $p<0.001$ ) and clearance rates were not ( $r^2<0.01$   $p=0.9$ ), and neither respiration ( $r^2=0.18$   $p=0.13$ ) nor EPR ( $r^2=0.2$   $p=0.17$ ) were related to ingestion.

Neither ingestion ( $r^2=0.05$   $p=0.8$ ) nor clearance ( $r^2=0.1$   $p=0.29$ ) rates were related to cell volume (Figure 3.6 in Supplementary Material). Cell volume was not measured on the 11 and 20 July. In addition, neither food concentration ( $r^2<0.2$   $p>0.08$ ) nor cell volume ( $r^2<0.03$   $p>0.4$ ) were related to the N:P, C:N or C:P ratio of the *R. salina* cells.

The particulate organic matter content (C, N and P) of *R. salina* cells during each of the experiments is presented in Table 3.1. The N:P ratios of *R. salina* varied from a minimum value of 9.6:1 to a maximum value of 22.8:1  $\text{mol mol}^{-1}$ . The C:N ratios ranged from 5.2:1 to 9.9:1  $\text{mol mol}^{-1}$  and the C:P ratios varied from 76.4:1 to 166.7:1  $\text{mol mol}^{-1}$ .

### 3.3.2 *T. longicornis* size and physiological rates

Female prosome length (PL) ranged from 650  $\mu\text{m}$  to 900  $\mu\text{m}$  and did not differ significantly between experiments (1-way ANOVA  $F = 0.89$ ;  $p = 0.57$ ;  $df = 14$ ). Figures 3.1a, 3.2a and 3.3a show that neither the clearance nor ingestion rates ( $\mu\text{g C } \mu\text{g dw}^{-1} \text{d}^{-1}$ ) of *T. longicornis* were related to the N:P, C:N or C:P ratios of *R. salina* ( $r^2 <0.25$ ;  $p >0.08$ ; data from 11, 20 and 23 July not included). Ingestion varied between 0.2 and 0.5  $\mu\text{g C } \mu\text{g dw}^{-1} \text{d}^{-1}$ , 0.03 and 0.1  $\mu\text{g N } \mu\text{g dw}^{-1} \text{d}^{-1}$  and 0.005 and 0.01  $\mu\text{g P } \mu\text{g dw}^{-1} \text{d}^{-1}$  and was not related to either EPR or respiration (Figure 3.7 in Supplementary Material).

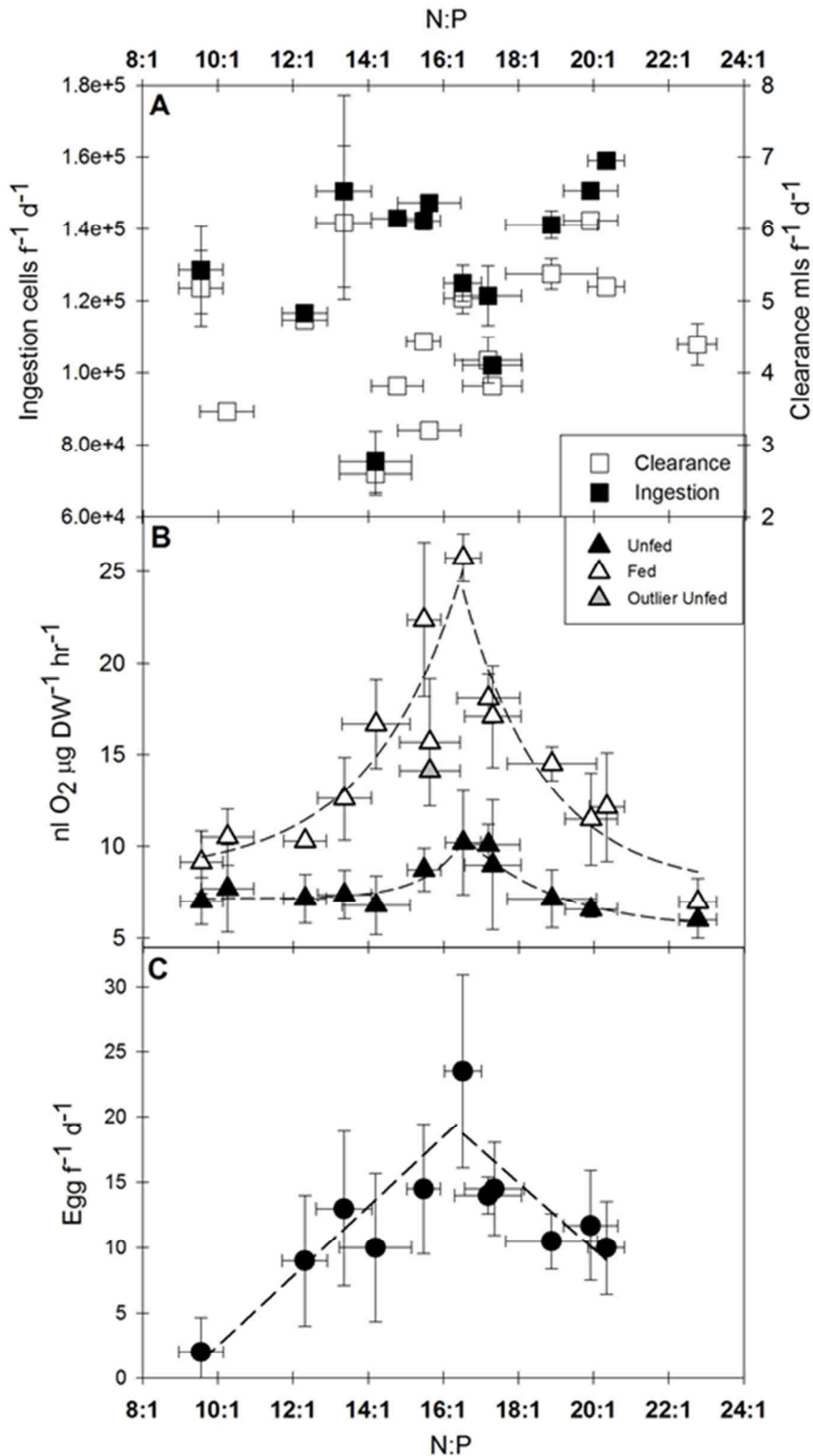


**Figure. 3.1.** (A) Relationship between the molar N:P ratio of *R. salina* and clearance and ingestion rates of *T. longicornis*. (B) Relationship between the molar N:P ratio of *R. salina* and respiration rate of *T. longicornis* (normalised by dry weight). (C) Relationship between the molar N:P ratio of *R. salina* and EPR of *T. longicornis*. The dashed lines represent the regression lines B) non-linear and C) linear fits. All errors are  $\pm$  SD.

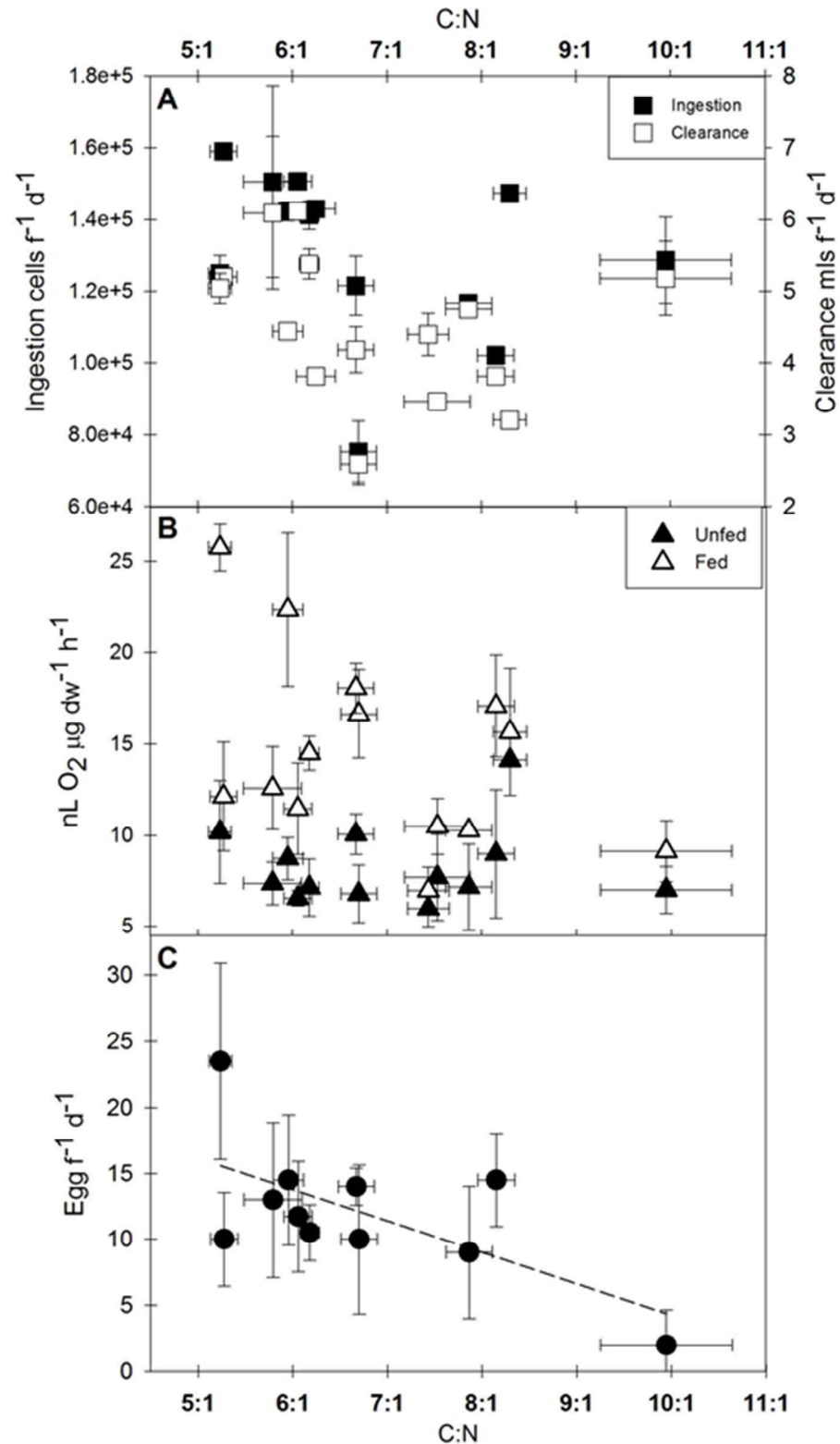


**Figure 3.2.** (A) Relationship between the molar C:N ratio of *R. salina* and clearance and ingestion rates of *T. longicornis*. (B) Relationship between the molar C:N ratio of *R. salina* and respiration rate of *T. longicornis* (normalised by dry weight). (C) Relationship between the molar N:P ratio of *R. salina* and EPR of *T. longicornis*. The dashed line represents the linear regression line. All errors are  $\pm$  SD.

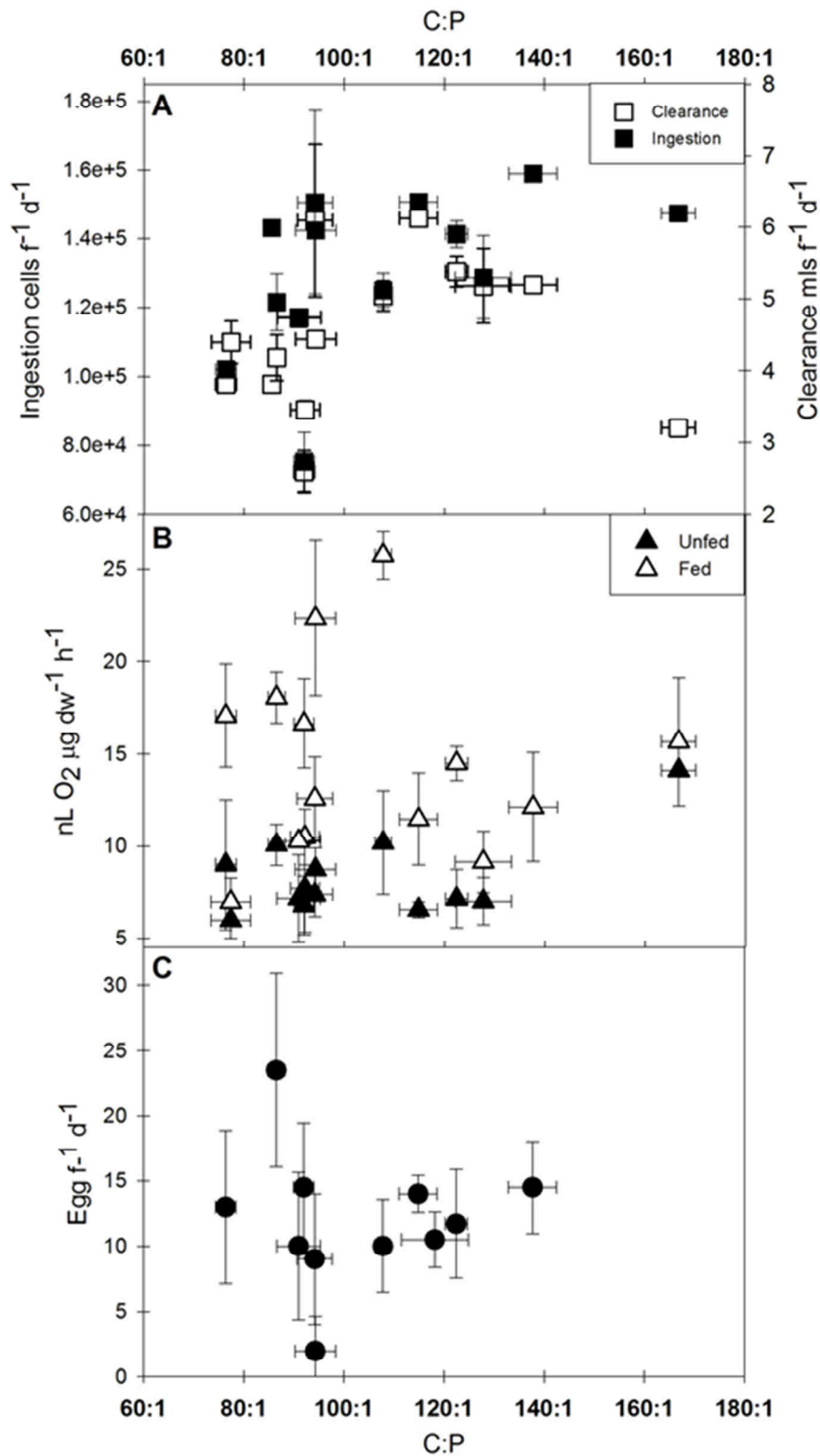


**Figure 3.3.** (A) Relationship between the molar C:P ratio of *R. salina* and clearance and ingestion rates of *T. longicornis*. (B) Relationship between the molar C:P ratio of *R. salina* and respiration rate of *T. longicornis* (normalised by dry weight). (C) Relationship between the molar N:P ratio of *R. salina* and EPR of *T. longicornis*. All errors are  $\pm$  SD.

EPR was not measured on 11, 20 or 23 July, however respiration was (Table 3.1). We examined the relationship between *T. longicornis* respiration rates and *R. salina* stoichiometry with and without the data included and found no difference in the overall trends. For completeness, we included all respiration data in the figures and analysis.

The respiration rates of feeding ( $R_f$ ) *T. longicornis* increased exponentially with the N:P ratio of *R. salina* (Fig. 3.1b). The average respiration rates increased to a maximum of  $25.8 \pm 1.3$  nL O<sub>2</sub>  $\mu\text{g dw}^{-1} \text{h}^{-1}$  at 16.5:1 N:P and exponentially decayed as the food N:P increased above 16.5:1, reaching a minimum respiration rate of  $7 \pm 1.3$  nL O<sub>2</sub>  $\mu\text{g dw}^{-1} \text{h}^{-1}$  at an N:P ratio of 22.8:1.

The respiration of unfed ( $R_u$ ) copepods ranged from  $6 \pm 1$  to  $10.2 \pm 2.8$  nL O<sub>2</sub>  $\mu\text{g dw}^{-1} \text{h}^{-1}$  (Fig. 1b). The response followed a similar pattern to the respiration of fed animals with an exponential increase at N:P  $\leq 16.5:1$  and an exponential decay at N:P  $\geq 16.5:1$ . The maximum fed respiration rate (at saturating food concentrations) of 25.8 nL O<sub>2</sub>  $\mu\text{g dw}^{-1} \text{h}^{-1}$  is 2.5-fold higher than the maximum unfed rate and 8.6-fold higher than the published average routine respiration rate of starved *T. longicornis* of  $\sim 3$  nL O<sub>2</sub>  $\mu\text{g dw}^{-1} \text{h}^{-1}$  (Castellani and Altunbaş, 2013).

Egg production rates also showed a response to *R. salina* N:P ratio (Fig. 3.1c), linearly increasing from a minimum of  $2 \pm 2.6$  eggs female<sup>-1</sup> day<sup>-1</sup> at N:P 9.6:1 to a maximum of  $23.5 \pm 7.4$  eggs female<sup>-1</sup> day<sup>-1</sup> at N:P 16.5:1 and then linearly decreasing to a minimum of  $10 \pm 3.6$  eggs female<sup>-1</sup> day<sup>-1</sup> at N:P 20.3:1. All significant relationships between respiration rate, egg production rate and food quality are given in Table 3.2.

**Table 3.2.** Significant regression analyses of fed ( $R_f$ ) and unfed ( $R_u$ ) respiration rates (nL O<sub>2</sub>  $\text{dw}^{-1} \text{h}^{-1}$ ) and egg production rates (EPR; eggs female<sup>-1</sup> day<sup>-1</sup>) versus food quality (separated into N:P < 16:1 and N:P > 16:1). Exponential relationship  $y = ae^{bx} + c$  for  $R_f$  and  $R_u$  and linear relationship  $y = ax + c$  for EPR.

Variables	n	Slope (a)	(b)	Intercept (c)	r <sup>2</sup>	p
$R_f$ vs N:P $\leq 16:1$	7	0.019	0.410	8.464	0.09	0.007
$R_f$ vs N:P $\geq 16:1$	7	33817	-0.462	7.698	0.92	0.006
$R_u$ vs N:P $\leq 16:1$	7	$3.86 \times 10^7$	0.963	7.162	0.89	0.013
$R_u$ vs N:P $\geq 16:1$	6	3922	-0.402	5.417	0.95	0.011
EPR vs N:P $\leq 16:1$	6	2.661	NA	-24.104	0.86	0.008
EPR vs N:P $\geq 16:1$	6	-2.527	NA	60.452	0.75	0.027
EPR vs C:N	11	-2.380	NA	28.038	0.43	0.029

Figure 3.2b and 3.3b show that there was no significant relationship between respiration rates and the C:N (fed  $r^2 = 0.2$ ,  $p = 0.1$  a negative trend; unfed  $r^2 = 0.086$ ,  $p = 0.36$ ) or C:P ratios (fed  $r^2 < 0.001$ ,  $p = 0.9$ ; unfed  $r^2 = 0.03$ ,  $p = 0.6$ ) of *R. salina*. Figures 3.2c and 3.3c show no relation between EPR and *R. salina* C:P ( $r^2 = 0.001$ ,  $p = 0.92$ ) but a negative relationship with C:N where the minimum of  $2 \pm 2.6$  eggs female<sup>-1</sup> day<sup>-1</sup> occurred at a C:N of 10:1 and the maximum of  $23.5 \pm 7.4$  eggs female<sup>-1</sup> day<sup>-1</sup> occurred at a C:N ratio of 5.2:1.

*T. longicornis* fed and unfed respiration rates were positively correlated with egg production rates (fed:  $r^2 = 0.77$ ,  $p < 0.001$ ; unfed:  $r^2 = 0.60$ ,  $p = 0.008$ ), consistent with a common physiological response to *R. salina* nutrient ratios.

### 3.3.3 *T. longicornis* carbon budget

A carbon budget of *T. longicornis* fed on *R. salina* was calculated from I, G, R<sub>f</sub>, R<sub>u</sub>, AE and GGE<sub>c</sub> (Table 3.3). Table 3.4 summarises the significant relationships between the carbon budget of *T. longicornis* and the N:P and C:N ratios of *R. salina*. GGE<sub>c</sub>, and AE were highest at an N:P ratio of 16.5:1 at 50% and 93% respectively (Table 3.3; Figure 3.8 in Supplementary Material), and followed a similar biphasic pattern to the physiological rates. AE and GGE<sub>c</sub> were lowest at an N:P ratio of 9.6:1. In the same manner as EPR, GGE<sub>c</sub> showed a weak significant relationship with the C:N of *R. salina*, linearly decreasing as diet C:N increased (Table 3.4). AE and GGE<sub>c</sub> showed no significant relationship with C:P ( $r^2 < 0.01$ ;  $p > 0.7$ ). MI ranged from 16% at an *R. salina* N:P ratio of 22.8:1 to 156% at an *R. salina* N:P ratio of 15.5:1. MI was related to C:N (Table 3.4) but not related to C:P ( $r^2 < 0.001$ ;  $p = 0.95$ ).

CoE decreased significantly with increasing N:P ratio, ranging from 33 ng C μg C<sup>-1</sup> egg<sup>-1</sup> d<sup>-1</sup> at an *R. salina* N:P ratio of 9.6:1 to 10 ng C μg C<sup>-1</sup> egg<sup>-1</sup> d<sup>-1</sup> at an N:P ratio of 22.8:1 (Tables 3.3 and 3.4). There was no significant relationship between CoE and C:N, C:P or the number of eggs produced female<sup>-1</sup> day<sup>-1</sup> ( $r^2 < 0.09$ ;  $p > 0.3$ ).

**Table 3.3.** Average carbon budget of *T. longicornis* fed on *R. salina* at different N:P ratios. G EPR: Growth determined as egg production rates, AE: assimilation efficiency, GGE<sub>c</sub>: gross growth efficiency, R: respiration, MI: metabolic increment, CoE: cost of egg production. The measurements made on 26 November with an N:P ratio of 16.5 are given in bold. The shaded numbers represent calculated values using the fitted regression relationships given in Table 3.2. For the experiments of the 11 and 20 July the average ingestion rate was used to calculate AE and GGE<sub>c</sub>. Data are mean ± SD.

Date	N:P	I Ingestion μgCμgC <sup>-1</sup> d <sup>-1</sup>	G EPR %	AE % = G+R <sub>f</sub> /I	GGE % = G/I	R Fed %	R Unfed %	MI %	CoE ngCμgC <sup>-1</sup> egg <sup>-1</sup> d <sup>-1</sup>
23/10	9.6:1	1.28 ± 0.17	3 ± 4	19.53 ± 8.67	2.49 ± 3.32	28.5 ± 5.3	21.8 ± 4.0	30.31 ± 0.20	33.1 ± 0.002
11/07	10.2:1	NA	5 ± NA	33.30 ± NA	5.82 ± NA	32.7 ± 4.8	24.0 ± 7.4	36.35 ± 0.17	27.6 ± NA
05/11	12.3:1	0.88 ± 0.10	12 ± 8	38.76 ± 6.61	13.37 ± 8.57	32.0 ± NA	22.3 ± 10	43.65 ± NA	10.8 ± 0.012
11/11	13.4:1	0.82 ± 0.21	19 ± 10	50.77 ± 9.90	22.72 ± 12.00	39.2 ± 7.0	23.0 ± 3.7	70.81 ± 0.46	12.5 ± 0.015
31/10	14.2:1	0.42 ± 0.08	14 ± 9	85.32 ± 4.99	34.68 ± 22.20	51.9 ± 7.5	21.2 ± 5.0	145.3 ± 0.81	30.8 ± 0.013
29/06	14.8:1	0.76 ± 0.07	20 ± NA	58.67 ± NA	26.79 ± NA	51.8 ± NA	24.1 ± NA	114.8 ± NA	18.2 ± NA
26/10	15.5:1	0.85 ± 0.12	22 ± 11	57.86 ± 14.47	25.96 ± 12.61	69.7 ± 13.1	27.2 ± 3.6	156.3 ± 0.99	29.3 ± 0.030
23/07	15.6:1	1.27 ± 0.11	30 ± NA	63.65 ± NA	23.30 ± NA	48.8 ± 14.9	26.4 ± N	84.7 ± NA	12.8 ± NA
26/11	<b>16.5:1</b>	<b>0.74 ± 0.09</b>	<b>37 ± 15</b>	<b>92.87 ± 11.67</b>	<b>49.74 ± 20.83</b>	<b>80.3 ± 4.0</b>	<b>31.7 ± 8.8</b>	<b>152.9 ± 0.49</b>	<b>20.7 ± 0.035</b>
29/11	17.2:1	0.80 ± 0.16	20 ± 8	64.73 ± 7.03	25.50 ± 9.59	56.3 ± 4.3	31.4 ± 3.5	79.36 ± 0.31	17.8 ± 0.011
14/11	17.3:1	0.78 ± 0.08	21 ± 8	62.80 ± 9.18	26.81 ± 10.23	53.2 ± 8.7	28.0 ± 11	90.09 ± 0.35	17.4 ± 0.029
15/12	18.9:1	0.88 ± 0.08	14 ± 4	41.23 ± 4.58	15.93 ± 4.92	45.2 ± 2.9	22.3 ± 4.9	103.0 ± 0.48	21.8 ± 0.008
13/12	19.9:1	0.82 ± 0.04	15 ± 6	43.16 ± 8.24	18.33 ± 7.64	35.8 ± 7.8	20.4 ± 1.3	75.10 ± 1.27	13.1 ± 0.012
17/11	20.3:1	1.14 ± 0.18	16 ± 9	32.33 ± 14.31	14.48 ± 7.48	37.8 ± 9.3	20.3 ± NA	86.09 ± NA	17.5 ± NA
20/07	22.8:1	NA	5 ± NA	26.86 ± NA	5.45 ± NA	21.7 ± 4.0	18.7 ± 3.1	16.39 ± 0.13	10.4 ± NA

**Table 3.4.** Regression analyses of significant relationships between *T. longicornis* AE (%),  $GGE_c$  (%), MI (%) and CoE (%) and *R. salina* N:P (separated into > 16:1 and < 16:1) and C:N ratios. Linear relationship  $y = ax + c$ . AE: assimilation efficiency,  $GGE_c$ : gross growth efficiency (carbon), MI: metabolic increment, CoE: cost of egg production.

Variables	n	Slope (a)	Intercept (c)	$r^2$	P
AE vs N:P ≤ 16:1	9	8.35	-57.60	0.74	0.003
AE vs N:P ≥ 16:1	7	-9.29	228.48	0.80	0.007
GGE vs N:P ≤ 16:1	9	5.26	-48.63	0.78	0.002
GGE vs N:P ≥ 16:1	7	-5.44	125.60	0.73	0.015
MI vs N:P ≤ 16:1	9	17.91	-150.17	0.73	0.004
MI vs N:P ≥ 16:1	7	-14.94	369.75	0.66	0.026
MI vs C:N	15	-19.79	222.03	0.35	0.021
CoE vs N:P	14*	-1.30	41.19	0.43	0.011
GGE vs C:N	15	-4.92	54.66	0.28	0.044

\* 1 outlier removed (N:P 12.3:1)

### 3.3.4 Time series data

At and around Arendal station in the North Sea, the abundance of *T. longicornis* showed an abundance maximum when in situ temperature was 11-13°C, chlorophyll a concentrations were 1-2  $\mu\text{g L}^{-1}$  and the N:P ratio of particulate organic matter was ~16:1 (Fig. 3.4a).

At HOT, regression analyses showed no significant relationship between seston N:P and total zooplankton biomass ( $r^2 = 0.04$ ;  $p = 0.45$ ). However, the binomial relationship between zooplankton biomass and time (year) for the individual size fractions <5 mm was significant ( $r^2 > 0.5$ ;  $p < 0.02$ ), showing progressively later biomass peak years for smaller size-classes. The smallest size fraction peaked in 2006-2007, while the 2-5 mm biomass peaked in 2001-2002 (data not shown).

Figure 3.4b shows the significant relationship between the N:P ratio of each zooplankton size class and the N:P ratio of the food available in the year of the biomass peak of the respective zooplankton size class, for the size fractions < 5 mm ( $r^2 = 0.96$ ;  $p = 0.02$ ). The N:P of the seston corresponding to the year of the peak was calculated following the positive linear relationship between the average N:P and time (year) ( $r^2 = 0.75$ ;  $p < 0.001$ ).

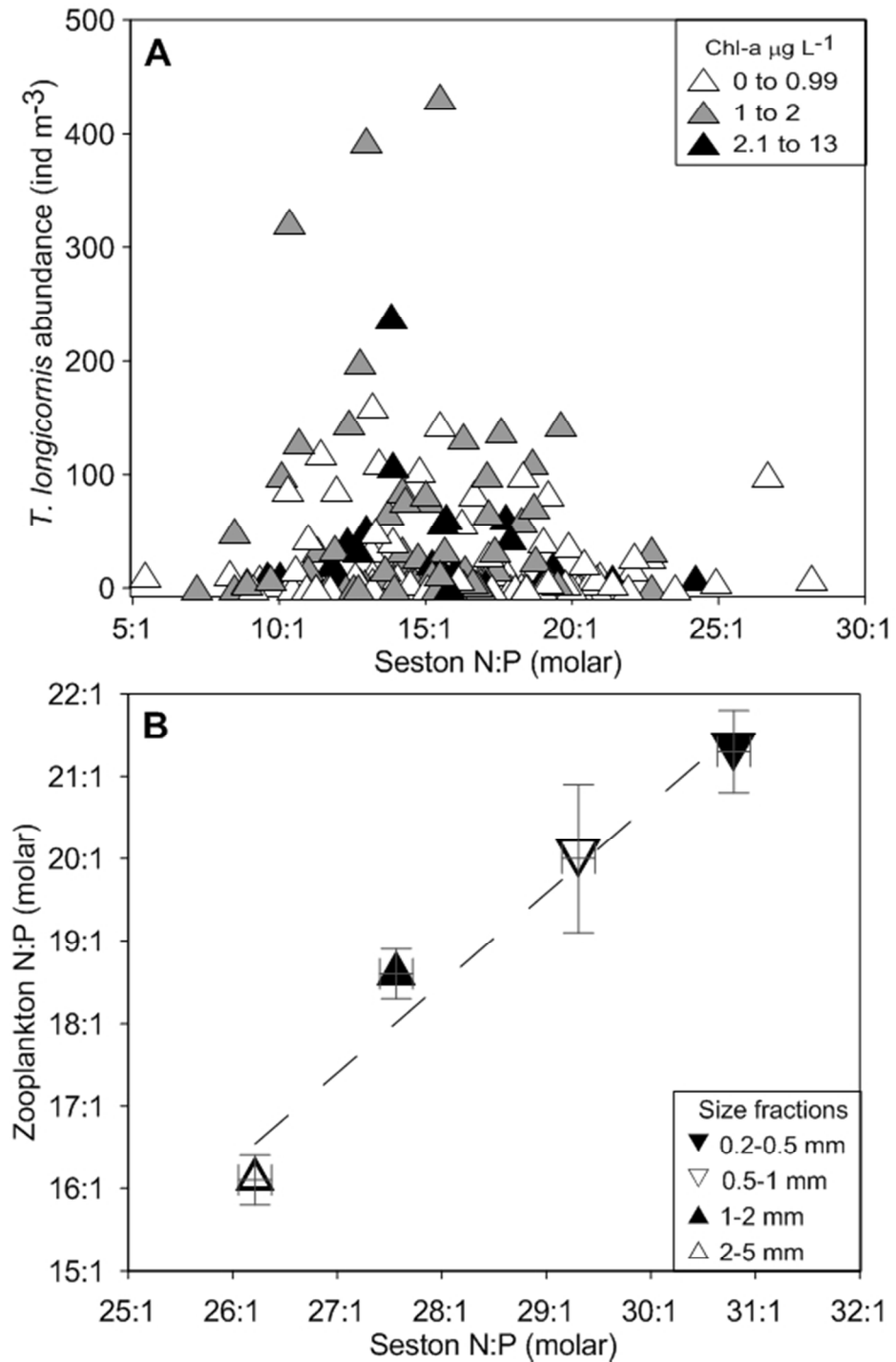


**Figure 3.4.** (A) Relationship between monthly *T. longicornis* abundance (ind m<sup>-3</sup>), monthly average seston N:P ratio (molar) and chlorophyll a concentration ( $\mu\text{g L}^{-1}$ ) in the North Sea (Arendal station 58° 23'N, 08° 48'E) between 1991 and 2010. (B) Relationship between the N:P ratio of size fractionated zooplankton (Hannides et al. 2009) and the corresponding food N:P ratio in the year when the biomass of that zooplankton size-fraction reached a maximum. HOT data from 1994 to 2010. The dashed line represents the regression line. Errors are  $\pm$  SE of the mean for zooplankton N:P and SE of the slope for the calculated seston N:P.

### 3.4 Discussion

#### 3.4.1 Effects of the diet on physiological rates

The main variables affecting copepod physiological rates are body size, food quantity, food quality and temperature (Kiorboe et al. 1985; Mauchline 1998; Ikeda et al. 2001). Therefore, in our laboratory study, to control for the effect of body size, food quantity and temperature on metabolism we used similar sized copepods, maintained the animals at 13°C and provided saturating food conditions (O' Connors 1980; Jónasdóttir and Kiorboe 1996). At this saturating food abundance, feeding rates did not affect the  $R_f$  or EPR of *T. longicornis*. The only variable that changed in the experiments was food quality, in terms of stoichiometric ratios. In this way, any measured change in metabolism could be attributed to changes in food N:P, C:N and C:P ratios (molar).

*R. salina* N:P ratios ranged from 9.6:1 to 22.8:1 N:P, C:N ratios ranged from 5.2:1 to 9.9:1 and C:P ratios ranged from 76.4:1 to 166.7:1. This is within the range (5:1 to 38:1) of naturally occurring particulate N:P (Figure 4; Geider and La Roche 2002) and C:N (5:1 to 30:1) ratios (Tang and Dam 1999) in the ocean. Phytoplankton N:P, C:N and C:P did not affect *T. longicornis*' ingestion rates, indicating that grazing rates did not increase to compensate for low quality food. Clearance rates were not affected by food N:P, C:N or C:P ratios and remained low and within the values found previously by Dam and Lopes (2003) for *T. longicornis* feeding on a monospecific algal diet.

Respiration and reproduction were similarly affected by phytoplankton quality, each showing a marked biphasic response to N:P ratio. This is because the growth and reproduction of small neritic copepods are tightly linked to the availability of energy obtained from metabolising organic compounds (Kiorboe et al. 1985; Thor 2000).

$R_u$  also showed a biphasic response to N:P ratio, likely due to the residual effect of the nutritional conditions experienced during 48 h acclimation prior to the rate measurements (Checkley, 1980; Tester and Turner, 1990). The copepods used for measurement of  $R_u$  were not starved prior to the incubation. Since copepod respiration rates decline 8-12 hours after they stop feeding (Kiorboe et al. 1985; Thor 2000; Castellani and Altunbaş 2013) the measured unfed respiration rates were greater than basal respiration rates. Average  $R_u$  rates (7.8 nL O<sub>2</sub> dw<sup>-1</sup> h<sup>-1</sup>) measured at 13°C were 2.6-fold higher than basal metabolic rates of *T. longicornis* (3 nL O<sub>2</sub> dw<sup>-1</sup> h<sup>-1</sup> at 13 °C; Castellani and Altunbaş 2013).

$R_f$  rates reached a maximum at an *R. salina* N:P ratio of 16.5:1 and exponentially decreased to within the range of  $R_u$  either side of the peak. The maximum increase (2.5-

fold) in  $R_f$  above  $R_u$  for *T. longicornis* agrees with published values of maximum specific dynamic action (SDA) which are typically two to four times higher than oxygen uptake rates of starved copepods (Kiorboe et al. 1985; Thor 2000).

Egg production rates reached a maximum of 32 eggs female<sup>-1</sup> day<sup>-1</sup>, agreeing with previous laboratory studies where *T. longicornis* fed on monospecific algal diets produced 15-30 eggs female<sup>-1</sup> day<sup>-1</sup> (Jónasdóttir et al., 2009; Dam and Lopes, 2003). Nevertheless, these laboratory rates are lower than maximum rates of production measured in the field (40-60 eggs female<sup>-1</sup> day<sup>-1</sup>; Castellani and Altunbaş, 2006). The lower rates we found in our study may be due to the fact that copepods generally produce more eggs on mixed-food diets than on single-food diets (Dam and Lopes 2003).

Our study showed that egg production rates declined linearly with dietary deficiency. Thus, our results agree with previous studies where females fed on a low quality diet produced fewer eggs (e.g. Ianora and Poulet 1993; Jónasdóttir and Kiorboe 1996; Kleppel et al. 1998). This follows the concept of optimal nutrition (Hessen and Anderson, 2008) where diet deficiency can cause a shortage in energy and nutrient supply in the organism therefore limiting growth. Our study shows that *R. salina* characterised by an N:P ratio lower and higher than 16.5:1, does not provide the necessary balance of N and P for *T. longicornis* to achieve maximum rates of egg production.

While nitrogen may be the primary limiting nutrient for marine zooplankton (Sterner and Elser, 2002), phosphorus limitation, by inhibiting RNA synthesis (Elser et al. 2003), can also cause protein limited production (Tang and Dam 1999; Sterner and Elser 2002; Malzhan and Boersma 2012). Our data confirm that N and P stoichiometry is an important food quality determinant and that the variation in metabolic performance is related to the quality of food ingested. The scale of these responses is presumably dependent on the availability of the necessary constituents in the diet (e.g. Cowles et al. 1988; Sterner and Schulz 1998; Mitra and Flynn 2005), driven by the physiological and structural requirements for biochemical constituents such as protein, carbohydrate and lipid.

In this study the C:N ratio of *R. salina* varied from 5:1 to 10:1 (mol<sup>-1</sup> mol<sup>-1</sup>). EPR decreased with increasing C:N in agreement with previous studies where EPR also decreased with increasing C:N ratios and therefore diet induced nitrogen-limitation, (e.g. Checkley 1980; Ambler 1986; Kiorboe 1989), suggesting that algal cells with lower C:N ratios represent greater nutritional value to copepods (Ambler 1986; Tang and Dam 1999). However, C:N ratio alone does not fully characterise the effects of food quality on copepod physiology, as C:N was not significantly related to *T. longicornis* respiration (though a weak decreasing trend can be seen). Respiration integrates different costs besides that of

producing eggs, hence the two patterns may not always coincide (Kiorboe 2008). In addition, respiratory processes can preferentially metabolise different substrates whereas during egg production, nitrogen requirements are constantly high since eggs are composed of ~55% protein, all of which is derived from the food source (Kiorboe 2008). Therefore, under food quality constraints, egg production is potentially more limited by nitrogen than respiration. Overall, the N:P ratio of *R. salina* had a greater impact on EPR than the C:N ratio, and since all the C:N ratios, except the lowest 5.2:1, correspond to either N or P limited values, we investigated whether the relationship between EPR and C:N was an artefact of the influence of the N:P ratio. This was not the case, as even when the lowest C:N ratio of 5.2:1 which corresponds to the optimum N:P of 16.5, was excluded from the regression, the linear relationship between EPR and C:N was still significant (data not shown).

### 3.4.2 Effects of food quality on copepod carbon budgets

Basal metabolism and growth are the major fates of assimilated energy in any organism (Kiorboe et al. 1985; Withers 1992). Therefore AE is a proxy for the material available for biosynthesis and with increasing AE, more eggs are produced, increasing GGE. Conversely, when AE decreases, more material is lost through excretion and faecal pellet production (Ianora and Poulet 1993). This follows the concept of homeostasis, where copepods excrete nutrients which occur in excess, while retaining nutrients that are limiting.

AE increased when *T. longicornis* was fed on *R. salina* with optimal elemental composition and was not affected by food concentration. This concurs with previous studies on neritic copepods such as *Temora stylifera* and *Acartia clausi* (Ianora and Poulet 1993; Mayzaud et al. 1998). Our maximum AE of 93% is greater than that (81-84%) reported by Kiorboe et al. (1985) for *A. tonsa* fed on a monospecific diet (at  $92 \mu\text{g C L}^{-1}$ ), however, AE as high as 90% and as low as 10% have been reported for herbivorous copepod species (Mauchline, 1998). Our mid-range AE values, which occur at N:P ratios between 13.4:1 and 17.3:1, fall within the range of 50-80% calculated by Kiorboe et al. (1985), but our lowest value (19.5%) is below this range. The low AE values (Table 3.3) could indicate some dietary deficiency, showing indirectly that poor quality algae are not metabolised, as seen from the correspondingly lower EPR, GGE and  $R_f$  (Table 3.3), but rather egested as organic material.

$\text{GGE}_c$  reached a maximum of 50% at the highest AE, when the food N:P ratio was 16.5:1 and C:N was at its lowest of 5.2:1. This agrees with a previous study which calculated a  $\text{GGE}_c$  of 49% at high AE (81-84%) (Kiorboe et al. 1985). The  $\text{GGE}_c$  values which occurred

at *R. salina* N:P ratios between 13.4:1 and 17.3:1 agree with Straile (1997) who suggested that copepod GGE<sub>c</sub>s typically average 25%. Both AE and GGE<sub>c</sub> decreased with increasing algal C:N as previously shown by Tang and Dam (1999), but were not related to ingestion or food concentration, in contrast to measurements with freshwater Daphnids (Urabe and Watanabe 1992). Importantly, AE and GGE<sub>c</sub> showed the same biphasic relationship with food N:P ratio as respiration and egg production rates, demonstrating a strong dependence of physiological response on nutrition and therefore N and P limitation.

The results of the present study clearly show that copepod metabolism and carbon budgets are influenced by food quality; as respiration decreased, egg production, GGE<sub>c</sub> and AE also decreased. As far as we are aware, this is the first study to show a biphasic response in copepod GGE<sub>c</sub>, AE, respiration and egg production rates to the N:P ratio of their food. We define the N:P ratio at which GGE<sub>c</sub>, AE, R<sub>f</sub>, R<sub>u</sub> and EPR reached a maximum as the Threshold Nutrient Ratio (TNR<sub>N:P</sub>) in an analogous way to the Threshold Elemental Ratio (TER) which defines the C:P or C:N ratio at which P or N limits growth (e.g. Urabe and Watanabe 1992) and physiological rates. This TNR<sub>N:P</sub> defines the switch from nitrogen limitation to phosphorus limitation at an N:P ratio of ~16:1 for *T. longicornis*. The TNR<sub>N:P</sub> of 16 thus defines the optimum metabolic requirement for *T. longicornis* to maximise reproduction.

MI increased with AE and GGE<sub>c</sub>, showing a strong dependency on food quality with a linear biphasic response to food N:P and a negative linear response to C:N. MI is usually associated with the cost of protein biosynthesis and reflects the increased energy demand of the organism above routine metabolism (Thor 2000; Secor 2008; Kiorboe 2008). Thus, the increase in respiration rate above the routine rate measured in the present study probably represents the additional energy required for the biosynthesis of eggs.

The CoE represents the amount of energy necessary to produce eggs. CoE shows a significant linear decrease with increasing N:P ratio. This indicates that nitrogen plays a major role in the cost of egg production, even above an N:P ratio of 16.5:1 where both the numerator (R<sub>f</sub>-R<sub>u</sub>) and the denominator (EPR) indicate P limitation.

### 3.4.3 Ecological implications

Marine ecosystems and so algal stoichiometry are changing with global warming. Changes in inorganic nutrient concentrations (Falkowski and Davis 2004; Sarmiento 2004; Arrigo 2005) and phytoplankton community structure (Edwards and Richardson 2004; Arrigo, 2005; Hays et al. 2005) have altered the nutritional value and particulate organic

nutrient ratios of algae (Geider and La Roche 2002; Falkowski and Davis 2004; Arrigo 2005). Assuming that algae are a major component of the diet of copepods, then any change in algal stoichiometry will impact the quality of food available to copepods. Based on our laboratory results, the GGE of *T. longicornis* will decrease rapidly with decreasing food quality and this may have a significant negative impact on zooplankton biomass (Buitenhuis et al., 2006) with consequences for oceanic biogeochemical cycles and trophic transfer of energy. Thus it is relevant to interrogate available field data to assess any co-variance between copepod biomass and seston organic N:P ratios.

Data from the Norwegian Coastal Surveillance Program highlight strong interannual variation in seston N:P ratios (variance of annual averages= 8.6 mol mol<sup>-1</sup> n=21; variance of a climatological year with averages for each month= 0.68 mol mol<sup>-1</sup> n=12) in the mesotrophic North Sea (58° 23'N, 08° 48'E). Spring bloom data show an increase in the seston organic N:P ratio from ~10:1 in 1991 to ~22:1 in 2004, and then a decrease to 11:1 in 2010 (data not shown). These trends are consistent with changes in phytoplankton community composition observed in the nearby waters of the NE Atlantic and northern North Sea. Between 1958 and 2002, phytoplankton community structure shifted from being dominated by diatoms (average group N:P ratio of ~10:1 (Quigg et al. 2003)) to being dominated by dinoflagellates (average phylum N:P ratio ~30:1 and higher C:N ratio (Quigg et al. 2003)) (Leterme et al. 2006). From 2006 onwards, there was a significant decline in dinoflagellate abundance, resulting in diatom dominance once again (Hinder et al. 2012).

Our analysis suggests that temperature and food quantity were not the only factors influencing *T. longicornis* abundance; the annual maximum chlorophyll-a (chl-a) concentration (as a proxy of food quantity) occurred in February-March (maximum 12.8 µg L<sup>-1</sup>) whereas the highest temperature of ~17°C was recorded in August. In contrast, the highest abundance of *T. longicornis* in the vicinity of the Arendal station over the period of investigation occurred in June-July when temperature ranged between 11°C and 13°C, chl-a ranged between 1 µg L<sup>-1</sup> and 2 µg L<sup>-1</sup> and seston N:P averaged ~16:1 (Fig. 3.4a). Interestingly a secondary, smaller peak of abundance often took place in October-November at the same temperatures recorded for the June-July peak of copepod abundance but at higher chl-a concentrations of ~4 µg L<sup>-1</sup>. During the autumn bloom, however, the average N:P ratio was 13.7:1 which our laboratory experiments have indicated is a poorer food quality for this species. Therefore, although we cannot rule out the effect of predation, the lower population abundance we found in autumn may be the result of the lower quality of the food available to the copepods at this time of the year compared to June-July. Using different indicators of food quality, such as fatty acids,

proteins and C:N ratios, previous studies have also shown for a number of calanoid copepod species that the chemical composition of the food can affect copepod population abundance and reproduction (e.g. Pond et al. 1996; Guisande et al. 2000; Vargas et al. 2006; Koski et al. 2010). Jónasdóttir et al. (1995) for instance, argued that in the field, polyunsaturated fatty acids are important for the reproductive success of *T. longicornis*, as EPR increased with increasing n-3:n-6 ratios and decreasing 20:5 to 22:6 ratios. Therefore, food quantity and temperature don't exclusively account for the pattern in *T. longicornis* abundance and the biphasic relationship we find between *T. longicornis* physiology and the food N:P ratio in the laboratory may also be important in the field.

Shifts in the phenology of a phytoplankton species, associated with increasing temperature (Edwards and Richardson 2004), could cause changes in the particulate N:P ratio of the phytoplankton present in a particular month of the year. Our laboratory data suggest that if the N:P ratio of the algal food during the months of maximal *T. longicornis* growth were to increase by 0.5 N:P from the optimal of 16.5:1 (due to a change in the dominant phytoplankton species present), then the GGE would decrease by ~39% (calculated using data from Table 3.3 and equations from Table 3.4). Therefore changes in food quality, even when food quantity and temperature remain optimal, could affect the seasonal distribution of copepods, impacting production of higher trophic levels.

In order to determine whether the biomass of copepods other than *T. longicornis* is influenced by food quality, and if so, if a  $TNR_{N:P}$  of 16 is ubiquitous, we searched for data showing long-term trends in copepod abundance and seston N:P at a range of locations. Unfortunately, few of the existing time series studies measure both organic phosphorus and zooplankton biomass. We were only able to find such concurrent data within the HOT program.

In the NPSG between 1994 and 2010, the annual average particulate organic N:P in the upper 150 m of the water column has increased from 17:1 in 1990 to 38:1 in 2010 (variance of annual averages of N:P= 44 mol mol<sup>-1</sup> n=21), triggered by increased stratification, increasing N<sub>2</sub> fixation and inorganic phosphorus limitation (Karl and Yanagi 1997). These changes were accompanied by a shift in phytoplankton community structure towards dominance by smaller prokaryotic primary producers (Karl et al. 2001) and an increase in smaller sized zooplankton. For example, the biomass of the largest zooplankton size class of 2-5 mm peaked in 2001-2002 while the biomass of the smallest mm size class of 0.2-0.5 mm peaked in 2006-2007.

Since small prokaryotic primary producers have generally higher N:P ratios (Geider and La Roche 2002), we investigated whether changes in food quality could be contributing to

these peaks in size fractionated zooplankton biomass. By comparing seston N:P with the N:P ratio of the zooplankton size fractions (from Hannides et al. 2009), and assuming that the seston is the major food source of the zooplankton size fractions we considered here, we show that these temporal changes in biomass peaks are consistently coupled with variations in food quality. The biomass of the smallest zooplankton size fraction (0.2-0.5 mm) with a higher body N:P ratio (~21.3:1 N:P), peaked towards the end of the time series when food with a higher N:P ratio was available (~30.8:1 N:P). The peak in biomass of each zooplankton size fraction occurred when the N:P ratio of the food was ~9.5 higher than the N:P ratio of the zooplankton (Fig. 3.4b). This constant offset between the stoichiometry of consumer and prey links this co-variance between food quality and mesozooplankton abundance, in agreement with stoichiometric theory which suggests that homeostasis and the elemental ratio of the consumer drives its growth requirements (Urabe and Watanabe 1992; Plath and Boersma 2001; Sterner and Elser 2002). This could also indicate species-specific  $TNR_{N:P}$ ; different species may respond differently to ecosystem variability, depending on their specific physiological requirements.

#### 3.4.4 Summary and conclusions

This study shows that the physiological responses of copepods can be constrained by food quality and the efficiencies with which macronutrients are assimilated and used. If the relationship we show between copepod growth, biomass and the N:P ratio of their food holds for the natural environment, then this has implications for zooplankton mediated carbon export, nutrient cycling through the release of dissolved organic and inorganic nutrients, respiratory production of  $CO_2$  and transfer of energy to higher trophic levels including commercial fisheries. Thus we argue that the study of climate driven changes in nutrient and phytoplankton distributions (Beaugrand and Reid 2003), should be extended to include the impact of changing seston stoichiometry and nutrient limitation on zooplankton dynamics.

The key findings of this study are:

- 1- A combination of nutrient ratios provides a comprehensive description of the effects of nutrient limitation on copepod metabolism. Increased consideration of P limitation is required in future studies.
- 2- The biphasic response of the metabolism of *T. longicornis* to the N:P ratio of the available food, shows that algae with an elemental composition of 16.5N:1P are the optimum diet for this species.

- 3- Our laboratory results are consistent with time series data which show that highest *T. longicornis* abundance in the North Sea occurs when seston N:P ratios are ~16:1.
- 4- The co-occurrence of an increasing trend in seston N:P ratios and a decrease in abundance of larger copepod species in the NPSG hints at the influence of food quality on the GGE of copepods other than *T. longicornis*.
- 5- Since shifts in zooplankton community structure to smaller species and reduced zooplankton biomass could cause reduced faecal pellet carbon export, increased respiratory CO<sub>2</sub> evasion and reduced prey for fisheries, a field study to investigate the influence of food quality, in addition to temperature and food quantity, on zooplankton biomass and community structure is now warranted.

## 3.5 Supplementary Material Nobili et al. BG-2013-79

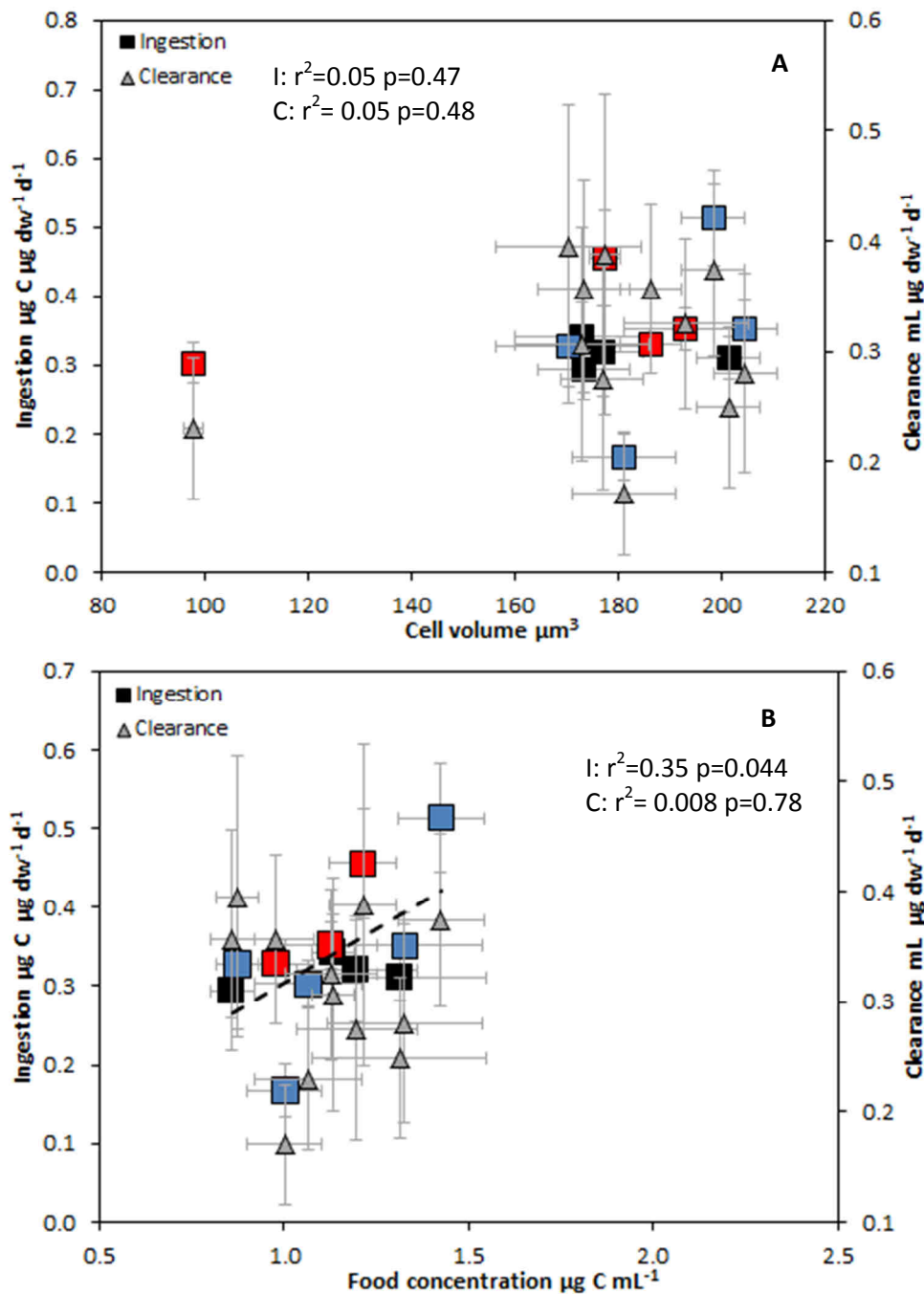


**Figure 3.5.** Ingestion and clearance rates as a function of A) cell volume and B) food concentration. The dashed line represents the significant regression between ingestion and food concentration. The ingestion data are coloured according to high (red N:P>17.5:1), low (blue N:P<15.5:1) and balanced (black 15.5:1>N:P<17.5:1) N:P ratios. Measurements of cell volume derived from 2% lugols fixed samples (11, 20 July) and of food concentration prepared when the coulter counter was broken (11, 20, 23 July) are not shown. Errors are + SD.

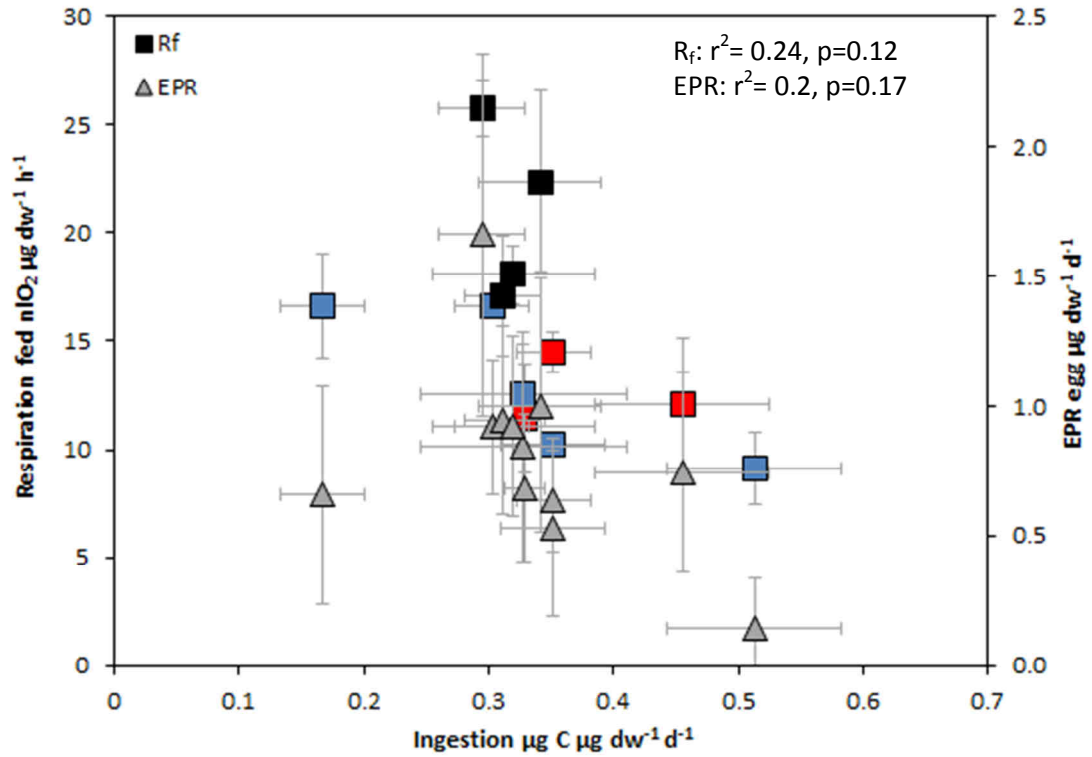


**Figure 3.6.** R and EPR as a function of carbon ingestion. Ingestion rates determined on 11, 20 and 23 July are not shown. The respiration data are coloured according to high (red N:P>17.5:1), low (blue N:P<15.5:1) and balanced (black 15.5:1>N:P<17.5:1) N:P ratios. Errors are + SD.

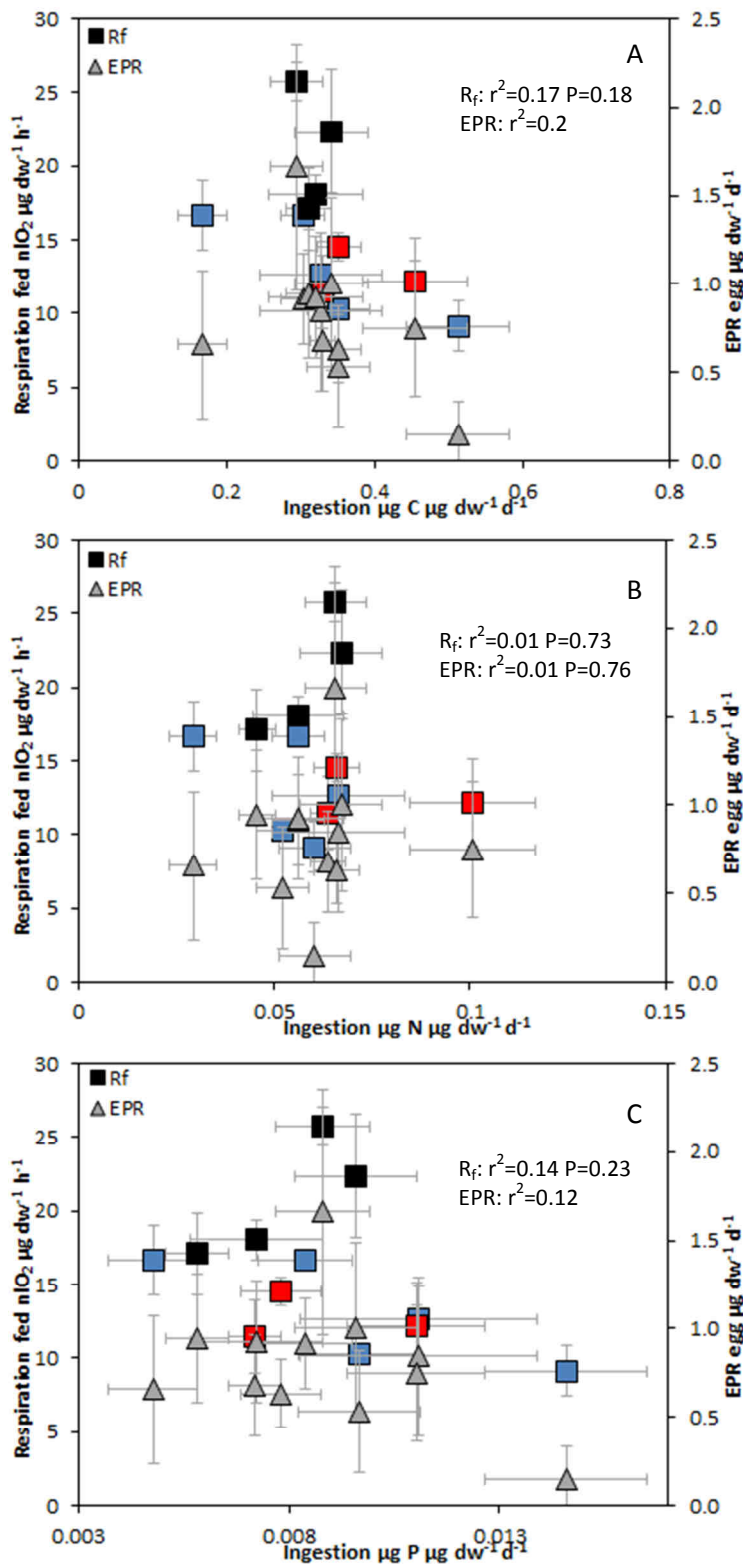


**Figure 3.7.** R and EPR as a function of A) carbon ingestion, B) nitrogen ingestion, and C) phosphorus ingestion. The respiration data are coloured according to balanced (black, 5.5:1 > N:P < 17.5:1), limited (blue, N:P 12-15 and 17-20) and extremely limited (red, N:P < 12:1 and N:P > 20:1) N:P ratios. Data from 11, 20 and 23 July are not shown. Errors are + SD.

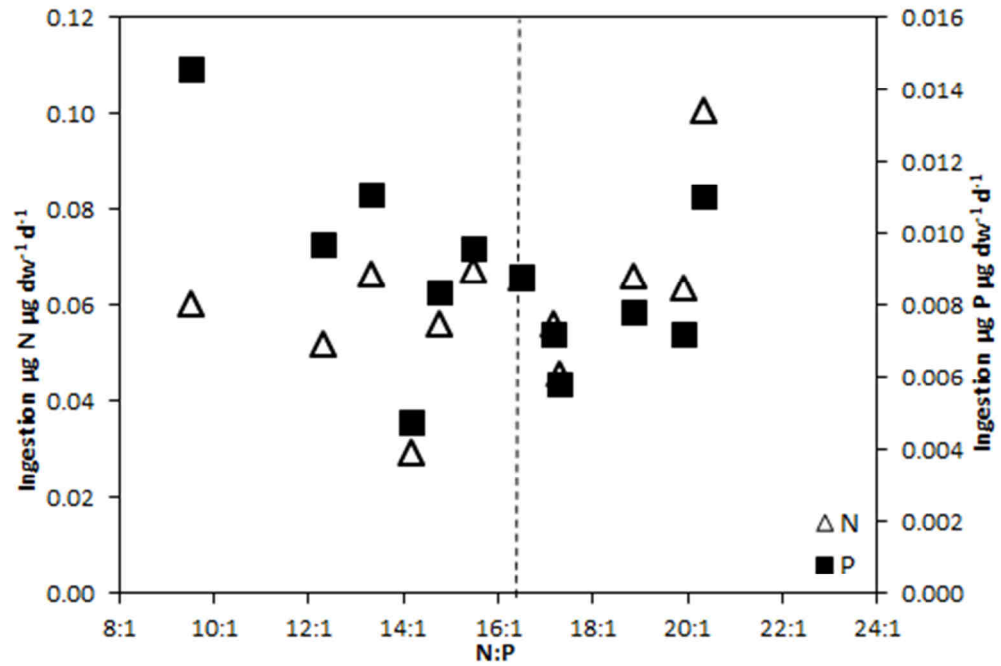


**Figure 3.8.** N and P ingestion rates as a function of *R. salina* N:P ratio. The dashed line marks the 16.5:1 N:P ratio. Calculated data from 11, 20 and 23 July are not included.

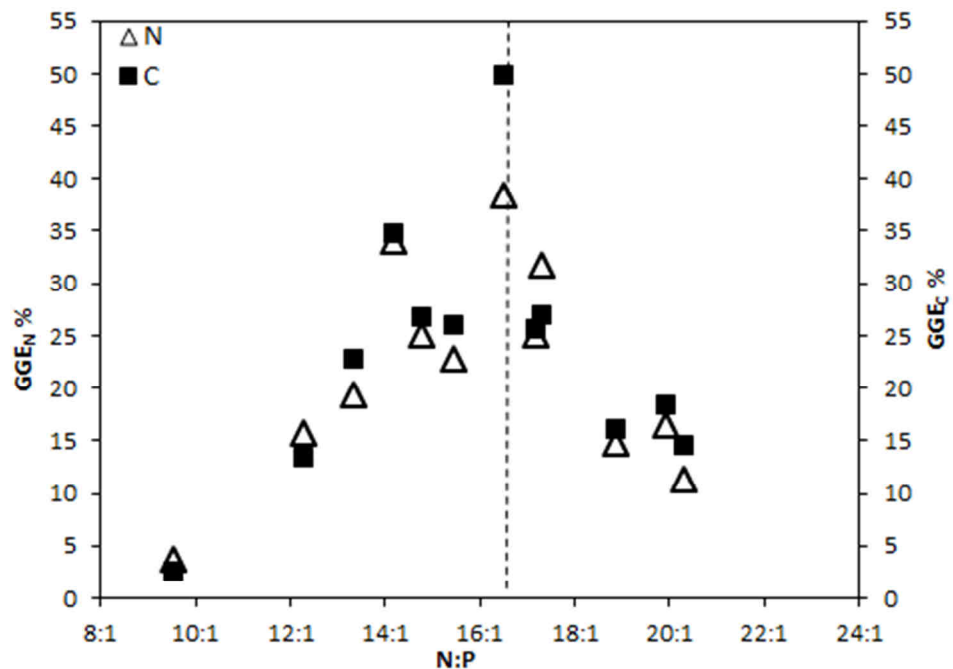


**Figure 3.9.** Gross Growth Efficiency in terms of carbon ( $GGE_C$ ) and nitrogen ( $GGE_N$ ) as a function of *R. salina* N:P ratio. The dashed line marks the 16.5:1 N:P ratio. Calculated  $GGE$  data from 11, 20 and 23 July are not shown.

### 3.5.1 Supplementary results on fatty acids (FA)

Although not discussed in this chapter, interesting correlations between FA classes and *T. longicornis* physiological rates were identified and summarised in Table 3.5. A positive trend between *T. longicornis* EPR and *R. salina* n-3/n-6 ratio was identified and a weaker increasing trend with total %PolyUnsaturated Fatty Acids (PUFA) can also be seen. Moreover fed respiration rates ( $R_f$ ) were negatively correlated to the content (%) of monounsaturated fatty acids (MUFA) in the food.

This relationship between n-3/n-6 ratio, PUFA content of the food and *T. longicornis* EPR had already been highlighted by Jónasdóttir et al. (1995), however at the best of our knowledge, this is the first time that a correlation between the fed respiration rates of copepods and the fatty acids (MUFA) content of the food has been identified.

**Table 3.5.** Regression analyses of fed ( $R_f$ ) respiration rates ( $\text{nL O}_2 \text{ dw}^{-1} \text{ h}^{-1}$ ) and egg production rates (EPR;  $\text{eggs female}^{-1} \text{ day}^{-1}$ ) versus the content (%) of major fatty acid classes in *R. salina*. Saturated fatty acids (SAFA), polyunsaturated fatty acids (PUFA), monounsaturated fatty acids (MUFA) and n-3:n-6 ratio (weight).

	SAFA	PUFA	MUFA	n-3/n-6
$R_f$	$r^2=0.1$ $p=0.29$	$r^2=0.21$ $p=0.1$	$r^2=0.036$ $p=0.03$	$r^2=0.24$ $p=0.09$
EPR	$r^2=0.21$ $p=0.15$	$r^2=0.27$ $p=0.1$	$r^2=0.21$ $p=0.16$	$r^2=0.34$ $p=0.06$

Significant relationships between mineral C:N ratio of *R. salina* and the concentration of the major fatty acids classes were identified during this study (Table 3.6), indicating a correlation between the carbon stoichiometry and the biochemistry of the food. Saturated Fatty Acids (SAFA) and MUFA % were increased as the C:N of the algae increased, whilst PUFA and n-3/n-6 ratio decreased as the C:N of *R. salina* increased. FA were not correlated to N:P ratio ( $r^2 < 0.2$   $p > 0.8$ ).

**Table 3.6.** Significant regression analyses of C:N ratio versus the content (%) of major fatty acid (FA) classes in *R. salina*. Saturated fatty acids (SAFA), polyunsaturated fatty acids (PUFA), monounsaturated fatty acids (MUFA) and n-3:n-6 ratio. Yellow= positive relationship, orange = negative relationship.

FA	C:N
SAFA	$r^2=0.35$ $p=0.027$
PUFA	$r^2=0.52$ $p=0.004$
MUFA	$r^2=0.46$ $p=0.007$
n-3/n-6	$r^2=0.47$ $p=0.007$

The concentrations (%) of major FA classes and individual FA in *R.salina* are presented in table 3.7 overleaf.

**Table 3.7.** Major fatty acids (FA) as a proportion of total FA, ratios and nutrients by concentration at different N:P (molar) ratios of *R. salina*. Error  $\pm$  SD. NA= data not available.

Average Fatty Acids %	Experiment Average time 0 vs ctrl N:P ratio (molar)							
	9.6:1	10.2:1	12.3:1	13.4:1	14.2:1	14.8:1	15.5:1	15.6:1
<b>14:0</b>	9.36 $\pm$ 0.39	6.10 $\pm$ 0.54	5.42 $\pm$ 0.43	3.92 $\pm$ 0.66	6.32 $\pm$ 0.29	3.92 $\pm$ 0.52	4.54 $\pm$ 0.43	11.43 $\pm$ 0.39
<b>16:0</b>	16.77 $\pm$ 1.45	28.83 $\pm$ 0.44	23.94 $\pm$ 0.72	6.42 $\pm$ 4.07	17.04 $\pm$ 0.76	22.29 $\pm$ 0.95	17.49 $\pm$ 1.63	14.99 $\pm$ 0.45
<b>16:1(n-7)</b>	2.89 $\pm$ 0.92	1.81 $\pm$ 0.36	1.39 $\pm$ 0.12	3.50 $\pm$ 0.24	1.13 $\pm$ 0.05	1.85 $\pm$ 0.23	2.87 $\pm$ 0.31	2.04 $\pm$ 0.13
<b>16:2(n-4)</b>	1.17 $\pm$ 0.15	1.03 $\pm$ 0.23	0.66 $\pm$ 0.14	1.25 $\pm$ 0.37	1.40 $\pm$ 0.19	0.77 $\pm$ 0.20	1.62 $\pm$ 0.33	0.82 $\pm$ 0.06
<b>18:0</b>	5.00 $\pm$ 1.16	15.53 $\pm$ 0.45	6.03 $\pm$ 0.22	3.32 $\pm$ 0.16	8.84 $\pm$ 0.89	12.46 $\pm$ 0.64	8.19 $\pm$ 0.48	2.17 $\pm$ 0.22
<b>18:1(n-9)</b>	7.94 $\pm$ 0.86	9.34 $\pm$ 0.38	11.46 $\pm$ 0.27	2.08 $\pm$ 0.15	4.42 $\pm$ 0.51	7.03 $\pm$ 0.38	4.07 $\pm$ 0.57	14.08 $\pm$ 0.57
<b>18:1(n-7)</b>	5.16 $\pm$ 0.20	3.05 $\pm$ 0.18	5.79 $\pm$ 0.22	7.42 $\pm$ 0.39	4.04 $\pm$ 0.20	4.35 $\pm$ 0.40	5.76 $\pm$ 0.67	4.85 $\pm$ 0.13
<b>18:2(n-6)</b>	5.77 $\pm$ 0.24	4.87 $\pm$ 0.15	7.89 $\pm$ 0.03	2.34 $\pm$ 0.22	3.20 $\pm$ 0.24	5.23 $\pm$ 0.24	4.88 $\pm$ 6.92	8.07 $\pm$ 0.13
<b>18:3(n-3) ALA</b>	22.22 $\pm$ 1.26	14.79 $\pm$ 0.19	18.95 $\pm$ 0.59	19.33 $\pm$ 0.77	22.32 $\pm$ 0.59	19.22 $\pm$ 0.98	10.96 $\pm$ 1.47	21.75 $\pm$ 0.28
<b>18:4(n-3)</b>	11.20 $\pm$ 0.47	7.42 $\pm$ 0.41	10.25 $\pm$ 0.12	27.13 $\pm$ 1.77	15.42 $\pm$ 0.53	10.73 $\pm$ 0.40	19.81 $\pm$ 2.85	9.60 $\pm$ 0.62
<b>20:4(n-6) ARA</b>	0.40 $\pm$ 0.06	0.37 $\pm$ 0.01	0.53 $\pm$ 0.01	0.32 $\pm$ 0.02	0.31 $\pm$ 0.06	0.51 $\pm$ 0.03	2.57 $\pm$ 0.75	0.63 $\pm$ 0.02
<b>20:4(n-3)</b>	0.34 $\pm$ 0.05	0.17 $\pm$ 0.01	0.22 $\pm$ 0.03	0.39 $\pm$ 0.06	0.23 $\pm$ 0.06	0.18 $\pm$ 0.06	0.45 $\pm$ 0.35	0.25 $\pm$ 0.02
<b>20:5(n-3) EPA</b>	7.20 $\pm$ 0.42	3.90 $\pm$ 0.15	4.44 $\pm$ 0.18	12.57 $\pm$ 0.95	8.69 $\pm$ 0.38	6.40 $\pm$ 0.20	9.33 $\pm$ 1.52	5.60 $\pm$ 0.39
<b>22:6(n-3) DHA</b>	4.58 $\pm$ 0.38	2.80 $\pm$ 0.08	3.02 $\pm$ 0.25	10.03 $\pm$ 0.86	6.63 $\pm$ 0.55	5.03 $\pm$ 0.24	7.44 $\pm$ 1.54	3.71 $\pm$ 0.25
<b>Total SAFA</b>	31.13 $\pm$ 1.90	50.46 $\pm$ 0.83	35.39 $\pm$ 0.87	13.65 $\pm$ 4.12	32.20 $\pm$ 1.21	38.67 $\pm$ 1.26	30.22 $\pm$ 1.76	28.60 $\pm$ 0.64
<b>total PUFA</b>	52.88 $\pm$ 1.49	35.35 $\pm$ 0.56	45.97 $\pm$ 0.69	73.36 $\pm$ 2.35	58.20 $\pm$ 1.09	48.09 $\pm$ 1.15	57.07 $\pm$ 7.98	50.43 $\pm$ 0.83
<b>Total MUFA</b>	15.99 $\pm$ 1.27	14.19 $\pm$ 0.55	18.64 $\pm$ 0.37	12.99 $\pm$ 0.48	9.60 $\pm$ 0.55	13.24 $\pm$ 0.60	12.71 $\pm$ 0.93	20.97 $\pm$ 0.60
<b>Total n-3</b>	8.23 $\pm$ 0.05	7.77 $\pm$ 0.06	7.05 $\pm$ 0.20	4.22 $\pm$ 0.20	5.24 $\pm$ 0.24	5.59 $\pm$ 0.12	3.90 $\pm$ 0.10	8.35 $\pm$ 0.21
<b>Total n-6</b>	1.11 $\pm$ 0.03	1.42 $\pm$ 0.03	1.62 $\pm$ 0.04	0.17 $\pm$ 0.01	0.36 $\pm$ 0.01	0.80 $\pm$ 0.01	0.64 $\pm$ 0.63	1.78 $\pm$ 0.04
<b>n-3/n-6</b>	7.40 $\pm$ 0.04	5.48 $\pm$ 0.04	4.34 $\pm$ 0.12	25.24 $\pm$ 0.10	14.41 $\pm$ 0.13	6.97 $\pm$ 0.06	6.12 $\pm$ 0.36	4.70 $\pm$ 0.12
<b>DHA/EPA</b>	0.64 $\pm$ 0.03	0.72 $\pm$ 0.01	0.68 $\pm$ 0.01	0.80 $\pm$ 0.05	0.76 $\pm$ 0.04	0.79 $\pm$ 0.01	0.80 $\pm$ 0.06	0.67 $\pm$ 0.06
<b>Total FA (pg cell<sup>-1</sup>)</b>	18.09 $\pm$ 0.62	26.83 $\pm$ 0.22	19.26 $\pm$ 0.24	6.06 $\pm$ 0.25	9.87 $\pm$ 0.26	13.41 $\pm$ 0.14	8.17 $\pm$ 0.64	20.36 $\pm$ 0.28
<b>C (pg cell<sup>-1</sup>)</b>	55.15 $\pm$ 2.04	38.77 $\pm$ 0.98	50.95 $\pm$ 0.84	33.54 $\pm$ 0.57	33.84 $\pm$ 0.38	35.07 $\pm$ 0.69	34.65 $\pm$ 0.59	44.97 $\pm$ 0.58
<b>N (pg cell<sup>-1</sup>)</b>	6.48 $\pm$ 0.48	5.99 $\pm$ 0.22	7.54 $\pm$ 0.21	6.79 $\pm$ 0.31	5.94 $\pm$ 0.15	6.48 $\pm$ 0.27	6.81 $\pm$ 0.20	6.28 $\pm$ 0.09
<b>P (pg cell<sup>-1</sup>)</b>	1.57 $\pm$ 0.05	1.29 $\pm$ 0.12	1.40 $\pm$ 0.06	1.14 $\pm$ 0.04	0.96 $\pm$ 0.07	0.97 $\pm$ 0.06	0.97 $\pm$ 0.02	0.93 $\pm$ 0.05
<b>C:N (molar)</b>	9.95 $\pm$ 0.69	7.53 $\pm$ 0.35	7.86 $\pm$ 0.24	5.79 $\pm$ 0.31	6.70 $\pm$ 0.19	6.25 $\pm$ 0.21	5.95 $\pm$ 0.16	8.30 $\pm$ 0.17
<b>%FA of total C</b>	32.79 $\pm$ 1.66	69.19 $\pm$ 1.83	37.81 $\pm$ 0.78	18.07 $\pm$ 0.82	29.16 $\pm$ 0.83	38.22 $\pm$ 0.86	23.59 $\pm$ 1.89	45.26 $\pm$ 0.85

Table 3.7. Cont'

Average Fatty Acids %	Experiment Average time 0 vs ctrl N:P ratio (molar)						
	16.5:1	17.2:1	17.3:1	18.9:1	19.9:1	20.3:1	22.8:1
<b>14:0</b>	5.02 ± 0.46	6.09 ± 1.26	5.74 ± 0.23	7.63 ± 0.55	6.93 ± 0.33	4.31 ± 0.37	8.98 ± 0.54
<b>16:0</b>	7.39 ± 0.53	12.87 ± 1.43	21.32 ± 0.22	12.48 ± 0.24	12.20 ± 0.47	7.48 ± 0.37	18.95 ± 0.44
<b>16:1(n-7)</b>	1.26 ± 0.11	2.51 ± 0.07	1.91 ± 0.08	3.07 ± 0.50	1.81 ± 0.18	1.37 ± 0.03	1.80 ± 0.36
<b>16:2(n-4)</b>	1.45 ± 0.07	0.84 ± 0.16	0.68 ± 0.09	1.38 ± 0.22	1.43 ± 0.10	1.24 ± 0.13	0.56 ± 0.23
<b>18:0</b>	3.60 ± 0.60	2.25 ± 0.46	2.76 ± 0.21	3.84 ± 0.10	4.11 ± 0.69	3.08 ± 0.39	1.90 ± 0.45
<b>18:1(n-9)</b>	1.63 ± 0.29	6.24 ± 0.81	11.72 ± 0.19	4.88 ± 0.42	4.96 ± 0.30	2.01 ± 0.13	16.37 ± 0.38
<b>18:1(n-7)</b>	5.21 ± 0.09	6.66 ± 0.64	4.00 ± 0.20	4.69 ± 0.26	4.86 ± 0.26	8.31 ± 0.16	3.72 ± 0.18
<b>18:2(n-6)</b>	1.36 ± 0.13	4.53 ± 0.65	7.38 ± 0.08	3.61 ± 0.18	4.20 ± 0.17	1.88 ± 0.04	9.61 ± 0.15
<b>18:3(n-3) ALA</b>	18.04 ± 0.59	20.25 ± 2.83	22.74 ± 0.22	27.50 ± 0.63	27.06 ± 0.66	20.85 ± 0.23	21.54 ± 0.19
<b>18:4(n-3)</b>	31.18 ± 0.37	19.08 ± 2.40	11.70 ± 0.09	15.07 ± 0.47	15.63 ± 0.47	28.00 ± 0.31	8.31 ± 0.41
<b>20:4(n-6) ARA</b>	0.12 ± 0.02	0.33 ± 10.39	0.50 ± 0.01	0.23 ± 0.03	0.32 ± 0.05	0.26 ± 0.02	0.64 ± 0.01
<b>20:4(n-3)</b>	0.37 ± 0.05	0.46 ± 0.07	0.30 ± 0.01	0.21 ± 0.01	0.20 ± 0.02	0.35 ± 0.02	0.31 ± 0.01
<b>20:5(n-3) EPA</b>	13.09 ± 0.44	11.19 ± 1.24	5.47 ± 0.14	8.09 ± 0.53	8.99 ± 0.22	11.64 ± 0.09	4.06 ± 0.15
<b>22:6(n-3) DHA</b>	10.26 ± 0.40	6.70 ± 1.06	3.78 ± 0.10	7.31 ± 0.48	7.29 ± 0.17	9.22 ± 0.38	3.23 ± 0.08
<b>Total SAFA</b>	16.02 ± 0.92	21.21 ± 1.96	29.82 ± 0.38	23.96 ± 0.61	23.24 ± 0.90	14.87 ± 0.65	29.83 ± 0.83
<b>total PUFA</b>	75.88 ± 0.93	63.38 ± 11.17	52.55 ± 0.32	63.41 ± 1.11	65.14 ± 0.88	73.43 ± 0.57	48.27 ± 0.56
<b>Total MUFA</b>	8.10 ± 0.32	15.40 ± 1.04	17.62 ± 0.29	12.64 ± 0.70	11.62 ± 0.43	11.69 ± 0.21	21.90 ± 0.55
<b>Total n-3</b>	4.69 ± 0.02	6.07 ± 0.05	7.76 ± 0.15	5.94 ± 0.05	5.66 ± 0.06	4.59 ± 0.12	7.54 ± 0.35
<b>Total n-6</b>	0.10 ± 0.002	0.52 ± 0.004	1.43 ± 0.04	0.41 ± 0.004	0.46 ± 0.02	0.14 ± 0.004	2.07 ± 0.13
<b>n-3/n-6</b>	47.24 ± 0.01	11.63 ± 0.03	5.43 ± 0.10	14.60 ± 0.03	12.36 ± 0.04	32.14 ± 0.06	3.65 ± 0.24
<b>DHA/EPA</b>	0.79 ± 0.01	0.60 ± 0.03	0.70 ± 0.03	0.91 ± 0.02	0.81 ± 0.01	0.79 ± 0.04	0.79 ± 0.06
<b>Total FA (pg cell<sup>-1</sup>)</b>	6.44 ± 0.05	10.61 ± 0.11	18.05 ± 0.22	10.37 ± 0.10	9.70 ± 0.10	6.54 ± 0.12	20.17 ± 0.49
<b>C (pg cell<sup>-1</sup>)</b>	33.39 ± 0.38	39.90 ± 0.52	46.81 ± 0.59	41.22 ± 0.58	37.45 ± 0.17	38.35 ± 0.54	45.21 ± 0.91
<b>N (pg cell<sup>-1</sup>)</b>	7.45 ± 0.15	6.99 ± 0.22	6.84 ± 0.12	7.74 ± 0.14	7.24 ± 0.17	8.48 ± 0.18	7.11 ± 0.13
<b>P (pg cell<sup>-1</sup>)</b>	1.00 ± 0.03	0.90 ± 0.05	0.88 ± 0.04	0.91 ± 0.06	0.82 ± NA	0.93 ± 0.01	0.70 ± 0.01
<b>C:N (molar)</b>	5.24 ± 0.12	6.67 ± 0.19	8.15 ± 0.19	6.18 ± 0.10	6.06 ± 0.15	5.27 ± 0.14	7.43 ± 0.22
<b>%FA of total C</b>	19.30 ± 0.26	26.59 ± 0.44	38.57 ± 0.67	25.17 ± 0.43	25.91 ± 0.29	17.06 ± 0.39	44.60 ± 1.41

# **CHAPTER 4**

## **4. Seston quantity and quality in the chlorophyll maximum along an Atlantic Meridional Transect**

### **4.1 Introduction**

The quantity and the quality of particulate organic matter (hereafter termed seston) are important indicators of large-scale variability in environmental conditions. This is because the biochemistry and nutrient composition of the seston change on latitudinal and temporal scales to reflect the habitat hydrography and hydrology (e.g. Lunghurst and Harrison 1989; Sterner and Elser 2002; Arrigo 2005). Biotic and abiotic environmental factors regulate phytoplankton abundance, species succession and hence chemical and biochemical characteristics (e.g. Geider and La Roche 2002; Sterner and Elser 2002; Arrigo 2005).

Organic matter is composed on average of 63% protein, 5-41% carbohydrate and 5-31% lipid (Anderson 1995; Hedges et al. 2002) which in turn are all composed of particulate organic macronutrients; carbon (POC), nitrogen (PON) and phosphorus (POP) in various proportions. Hence stoichiometry and the biochemical concentration of primary metabolites are commonly used to define and measure the quality of the seston (Tang and Dam 1999). Presently the global average organic 16:1 N:P (Redfield ratio) is defined as the point at which phytoplankton limitation by N switches over to limitation by P (Falkowski 1997, Tyrrell 1999; Geider and La Roche 2002). Based on this theory and the suggestion that low C:N ratios are better for the ecosystem overall (Tang and Dam 1999; Sterner and Elser 2002), optimal seston quality can be defined by low C:N and C:P ratios ( $\leq$  than Redfield 6.6 and 106:1 respectively) and N:P values approaching the Redfield ratio (16:1). This is accompanied by high concentrations of essential fatty acids (FA) and amino acids, important contributors to the maximisation of a consumer's growth and reproductive success (Sterner and Elser 2002).

Particulate organic matter from the euphotic zone has a key role in determining the amount, proportions and chemical complexity of the compounds exported to the deep ocean, which also affects the efficiency of bacterial remineralisation (e.g. Pahlow and Riebesell 2000; Sterner and Elser 2002; Dunne et al. 2007). For instance, Wolff et al. (2011) found that nutrient enriched new primary production in surface waters caused an increase in exported organic matter quantity and quality on the seafloor, lowering the C:N ratio of the sedimented matter and also increasing the amount of polyunsaturated fatty acids (PUFA, fatty acids with 2 or more double bonds).

Another reason for studying organic matter quality, is to aid the understanding of relationships between nutrient limitation and the production of an ecosystem (Cavender-Bares et al. 2001), since food quality changes the ecological balance (Klausmier 2004) and is a key bottom-up regulator of trophic dynamics. For instance, <10% to >100% of total primary production of cells  $\geq 2 \mu\text{m}$  (size potentially ingestible by copepods) is consumed daily by zooplankton in the Atlantic Ocean (Huskin et al. 2001), making it an important food source for secondary producers. In ecological terms, population shifts due to possible variations in food supply and quality, have been previously suggested (Vargas et al 2006; Piontkovski and Castellani 2009; Wolff et al. 2011; Nobili et al. 2013). For instance, on a seasonal basis, temperate and higher latitude zooplankton maximise population growth during a window of reproductive opportunity which coincides with optimum food quality related to the spring phytoplankton bloom (e.g. Vargas et al. 2006; Koski et al. 2010).

Importantly, food quality can be used to define food-web interactions via trophic transfer of compounds. Primary producers provide energy and essential elements to higher trophic levels, identifiable via their biochemical composition. FA biomarkers specific to different algal taxa such as 16:1(*n*-7) and 20:5(*n*-3) for diatoms (Ackman et al. 1968), 18:4(*n*-3) and 22:6(*n*-3) for dinoflagellates (Ackman et al. 1968) are indicators of distinct communities and therefore diets when found within consumers. For this reason, FA determination of different trophic levels reveals quantitative and qualitative information on *in situ* community interactions and biological processes.

The variability of seston quality has also been used as an indicator of ecosystem health; a recent study shows that as food quality decreases, the physiological strategy of copepods shifts from resource allocation to growth, to allocation of resources to maintenance, ultimately causing a species-specific decline in gross growth efficiency and biomass (Nobili et al 2013; chapter 3). This is because poorer quality food causes a decrease in organic matter assimilation, negatively affecting the energetic input driving metabolic responses in feeding organisms. Piontkovski and Castellani (2009) show that zooplankton biomass declines in the Atlantic, related to the NAO-index and to phosphate concentration, and propose this is due to a decline in food quality. Therefore, monitoring seasonal, interannual and decadal changes in seston stoichiometry and biochemistry could give an indication of zooplankton ecology.

The Atlantic Ocean is an area of particular interest for the study of food quality variation since it covers  $\sim 120^\circ$  degrees of latitude, and crosses a range of biogeochemical “domains”

(Banse 1974; Longhurst 1995; Marañon et al. 2001). The Redfield ratio is known to vary with latitude and environmental parameters (Osterroht and Thomas 2000; Martiny et al. 2013). Nutrient limitation can permanently affect phytoplankton biomass and growth (Howarth 1988) particularly in oligotrophic gyres (Moore et al. 2008). In contrast, temperate and higher latitude areas follow a seasonal eutrophic pattern of seston quality, corresponding to the timing of the spring phytoplankton bloom (Koski et al. 2010; Frigstad et al. 2011).

The pelagic ecosystem has a strongly layered structure (Longhurst and Harrison 1989) and food quality can also vary vertically, affected by currents and /or stratification/mixing events. For instance, an important feature in stratified waters is the formation of higher phytoplankton biomass at a deep Chlorophyll Maximum (CM), usually associated with a density discontinuity and between the 0.1 and 10% light depths (Longhurst and Harrison 1989). Throughout much of the tropical ocean, the CM is a permanent feature, while at higher latitudes, it occurs seasonally (Longhurst and Harrison 1989). The CM appears between the nutrient-depleted upper layer and light-limited lower layer of the euphotic zone (within or below the mixed layer), and contains most of the organic matter available for export from the surface to deeper waters (Cullen 1982; Weber and Deutsch 2010) and most of the organic nutrients available for primary consumers (Harris 1988).

The aim of this study was to examine the variability of food quantity and quality, using organic nutrient concentrations, stoichiometry and fatty acid concentrations, across a range of ecological domains in the North and South Atlantic Ocean. As such we hypothesise that low food quality and organic nutrient limitation are restricted to oligotrophic domains; while temperate areas sampled during austral spring and boreal autumn and the equatorial upwelling domain provide a more balanced diet for higher trophic levels. Nutritious food includes seston with lower C:N ratios, N:P ratios close to Redfield values and a higher proportion of essential fatty acids such as 20:5(*n*-3) and 22:6(*n*-3), high (*n*-3):(n-6) ratios and low proportions of Saturated Fatty Acids (SAFA). Additionally we hypothesise that particulate organic nutrient concentrations can be predicted from observed environmental parameters collected from sensors attached to the CTD rosette and that these empirical relationships can be used to estimate food quantity and quality on latitudinal and temporal scales. We also investigated whether as a result of climatic variation, food quality deteriorated over time in the Atlantic basin.

## 4.2 Methods

Data were collected on board RRS James Cook between the 13<sup>th</sup> of October and the 21<sup>st</sup> of November 2010 as part of the Atlantic Meridional Transect programme (AMT cruise 20) (<http://www.amt-uk.org/>) between Southampton (UK) and Punta Arenas (Chile) (Figure 4.1).

### 4.2.1 Ecological Domains

The stations sampled (Figure 4.1) were partitioned according to the ecological domains defined by Marañón et al. (2001). The domains were differentiated based on surface chl-a, dissolved inorganic nutrient concentrations and the presence, depth and intensity of the thermocline. Six major domains were identified as shown in Table 4.1

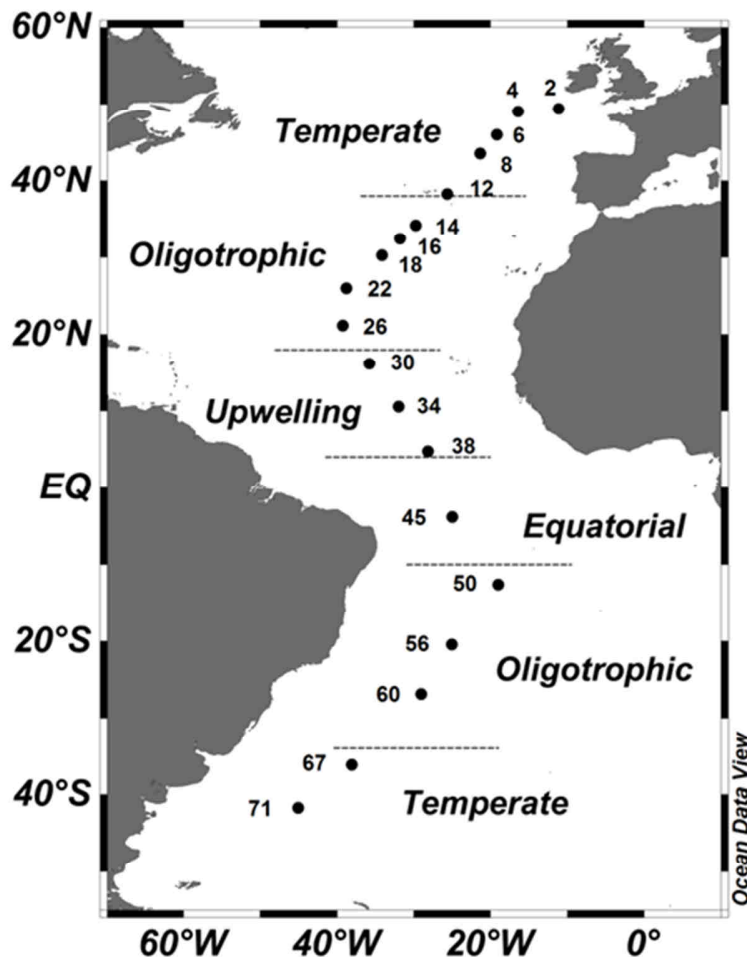


**Figure 4.1.** Stations sampled during AMT20, divided into six ecological domains.

The domains characterised by Marañón et al. (2001) are similar to the biogeochemical provinces distinguished by Longhurst (1995). The temperate south corresponds to Longhurst's (1995) South Subtropical Convergence (SSTC), the oligotrophic southern gyre to the South Atlantic Gyre (SATL), the equatorial region to the Western Tropical Atlantic (WTRA), the upwelling to the North Atlantic Tropical Gyre (NATR), the oligotrophic northern gyre to the North Atlantic Subtropical Gyre (NAST) and finally the temperate north domain corresponds to Longhurst's (1995) North Atlantic Drift East and West (NADR). There are some differences between the boundaries of the respective NADR, NAST and NATR regions.

**Table 4.1.** AMT20 Ecological domains, defined according to Marañón et al. (2001).

<i>Domain</i>	<i>Surface Chl a</i>	<i>NO<sub>3</sub> concentration</i>	<i>Thermocline</i>	<i>AMT20 Latitudinal distribution</i>
Temperate N	>0.2 µg L <sup>-1</sup>	Present throughout	Weak or absent	50 - 38°N
Oligotrophic N	<0.2 µg L <sup>-1</sup>	<0.05 µM	Developed at depth >50m	38 - 18°N
Upwelling	Shallow DCM	>1 µM	Very shallow	18 - 4°N
Equatorial	Shallow DCM		Shallower than gyres	4 - 10°S
Oligotrophic S	<0.2 µg L <sup>-1</sup>	<0.05 µM	Developed at depth >50m	10 - 34°S
Temperate S	>0.2 µg L <sup>-1</sup>	Present throughout	Weak or absent	34 - 45°S

#### 4.2.2 Chemistry and hydrography

Fluorescence maxima, near the bottom of the euphotic zone, was sampled for food quality and quantity determination. This was based on the assumption that the main source of carbon and nutrients for oceanic zooplankton might come from the CM (Longhurst and Harrison 1989).

Dissolved inorganic nutrients (nitrate NO<sub>3</sub><sup>-</sup> + nitrite NO<sub>2</sub><sup>-</sup>: N+N), particulate organic carbon, nitrogen, phosphorus (POC, PON and POP) and fatty acids (FA) were determined as stated in sections 2.2.7 and 2.3.7.

The Mixed Layer Depth (MLD) at each of the sampled stations was estimated using temperature (T) and density (Sigma-theta σ) data and the threshold method where MLD = depth at which ΔT = 0.1°C or Δσ = 0.035 kgm<sup>-3</sup> (Hooker et al. 2000).

### 4.2.3 Data analysis

We aimed to calculate empirical relationships and predict food quality within each of the domains sampled on AMT20, however too few data were available in each of the 6 domains. Therefore the transect data were aggregated into higher productivity (Temperate N and S, Upwelling and Equatorial domains) and lower productivity (Oligotrophic N and S domains) regions.

Table 4.2 summarises the abiotic and biotic parameters considered during forward stepwise and multiple linear regression analyses to test the predictability of organic matter characteristics from CTD measured or derived variables. A calculated distance between the chlorophyll maximum and the mixed layer (dMLCM hereafter) was included in the predictor parameters. The dMLCM is an indicator of the level nutrient stress, highlighting patterns of phytoplankton vertical distribution with variations in light gradients and in relation to the depth of the nitracline and therefore the vertical extent of the nitrate-depleted waters (Gist et al. 2009). Stations where the CM lay within the MLD, or the dMLCM was small, were assumed to be under low nutrient stress, whereas those stations with CM lying below the MLD were defined as under high nutrient stress with greater the distance the greater the stress.

**Table 4.2.** List of variables considered in the forward stepwise and multiple linear regression analyses. CM= chlorophyll maximum.

Variable	Symbol	Unit
CM Nitrate + Nitrate	N+N	} $\mu\text{g L}^{-1}$
CM Soluble reactive phosphorous	SRP	
CM Chlorophyll-a	chl-a	
CM particulate organic carbon	POC	
CM particulate organic nitrogen	PON	
CM particulate organic phosphorous	POP	}
CM Total fatty acids	FA	
CM Temperature	CMT	$^{\circ}\text{C}$
CM Salinity	S	
CM Backscatter	BS	volts (v)
Mixed layer depth	MLD	m
Distance between CM and MLD	dMLCM	m
CM Saturated fatty acids	SAFA	} % Total FA
CM Polyunsaturated fatty acids	PUFA	
CM Monounsaturated fatty acids	MUFA	
CM DHA:EPA fatty acids ratio	DHA:EPA	
CM $\omega$ 3: $\omega$ 6 fatty acids ratio	(n-3):(n-6)	

Both simple and forward stepwise multiple regression (OLS) were used to examine relationships between variables on AMT20. If a parameter did not contribute significantly to the prediction, it was excluded, and the regression was completed using the remaining variables. When the VIF (variance inflation factor) indicated strong collinearity between independent parameters, one was removed.

Additional datasets from previous AMT cruises (Table 4.3) were obtained from BODC in order to determine variations in organic nutrients and food quality over time. The cruises were selected based on the availability of inorganic nutrient data and the requirement for the cruise track to cross Oligotrophic, Upwelling and Temperate domains. No cruise data were available for years 2006, 2007 and 2009.

**Table 4.3.** List of AMT cruises with respective dates and routes.

<b>Cruise</b>	<b>Dates</b>	<b>Route</b>
AMT18	Oct-Nov 2008	UK-Chile
AMT17	Oct-Nov 2005	UK-South Africa
AMT16	May-June 2005	South Africa-UK
AMT15	Sept-Oct 2004	UK-South Africa
AMT14	April-May 2004	Chile-UK
AMT12	May-June 2003	Chile-UK

Due to issues with the instrumentation on board, optical data on transmission and backscatter (except for AMT20) were not available for analysis. Depth was not included as a predictor in multiple linear regression analyses, however it was considered in simple linear regression tests for nutrient distribution purposes.

N+N and SRP data below the limit of detection of  $<0.02 \mu\text{M}$  were considered as  $0.01 \mu\text{M}$  for statistical analysis purposes. All data except temperature and dMLCM were natural logarithm (Ln) transformed whilst percentage data were square root transformed. Pearson product-moment correlation coefficient (PCC) analysis was carried out to measure correlations between relevant variables and a 2-tailed Student t-test was used to query differences between the higher productivity and the oligotrophic regions on AMT20.

Data for POC and PON concentrations at the CM from this study were compared to the CM POC and PON concentrations determined by David Drapeau from the Bigelow Laboratory

during AMT20. The Bigelow data were collected at the same depths and same time but also included 10 extra stations. POP concentration data for comparison were not available.

### 4.3 Results

The AMT20 meridional transect crossed 6 ecological domains as shown in Figure 4.1 (above). Stations from the northern hemisphere were sampled during boreal autumn while stations from the southern hemisphere were sampled during austral spring. The sampling took place during a La Niña episode which developed in the eastern and central tropical Pacific in mid- 2010 and lasted until early 2011 (NOAA 2012) accompanied by temperature anomalies (above-normal) in the Atlantic Ocean (WMO 2012).

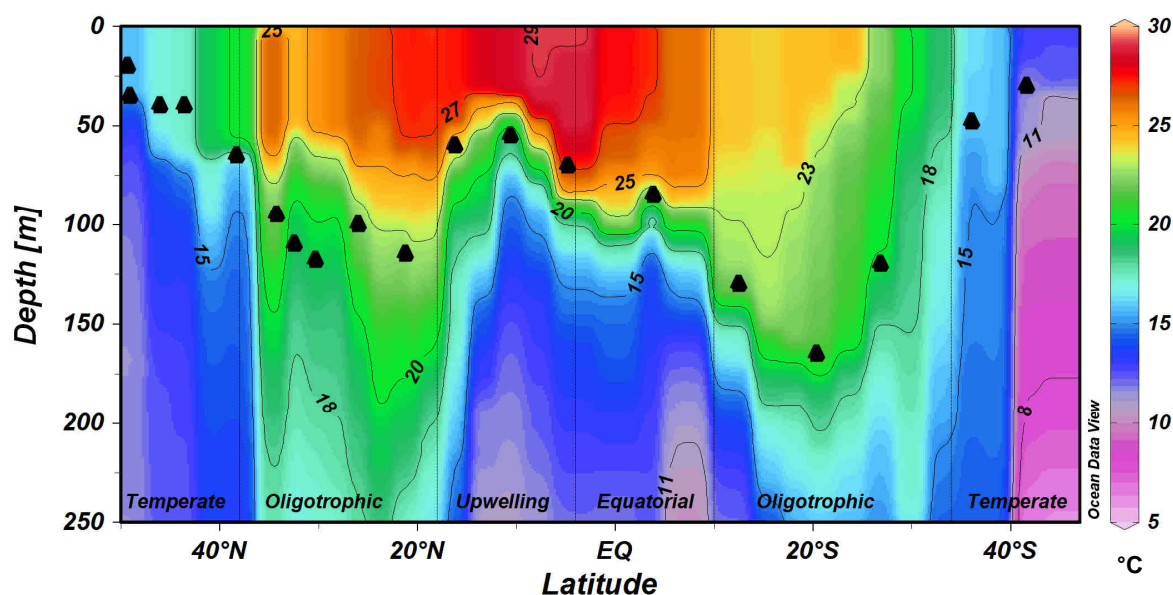


**Figure 4.2.** AMT20 Latitudinal distribution of temperature (°C) in the six ecological domains. The triangles represent the sampling locations at the CM.

Surface temperatures (SST) ranged from 11 to 29°C as shown in Figure 4.2 and salinity (S) ranged from 34.5 to 37.5. Mixed layer depth (MLD) varied from ~14 to ~59 m, with generally deeper values found in the oligotrophic domains. The water column depth at station 2 (Figure 4.1) was the shallowest sampling location at ~200 m; all the other stations had water column depths of >3000 m.

### 4.3.1 Dissolved inorganic nutrients

The distribution of dissolved inorganic nutrients at the CM is shown in Table 4.4. N+N and SRP were at their lowest in the Oligotrophic N domain, for the most part remaining below the limit of detection. N+N and SRP reached their highest in the Upwelling and Equatorial regions at stations 34 and 45 (N+N 7.48 and 7.68  $\mu\text{M}$ , SRP 0.38 and 0.69  $\mu\text{M}$  respectively) followed by station 71 (N+N 4.05  $\mu\text{M}$ , SRP 50.55  $\mu\text{M}$ ) in the Temperate S domain. Interestingly, SRP was high in the Oligotrophic S domain, reaching higher concentrations than N+N at stations 56 and 60. Stations 8 and 12, near the Azores system, showed increased N+N in comparison to other Temperate N locations.

**Table 4.4.** Chemical characteristics of water collected at the chlorophyll maximum. CTD Chl-a – chlorophyll a derived from the CTD fluorescence sensor, Discrete Chl-a – chlorophyll a measured by acetone extraction on a discrete water sample, POC= particulate organic carbon, PON= particulate organic nitrogen, POP= particulate organic phosphorus, N+N= nitrate + nitrite, SRP= soluble reactive phosphate. ND= below detection limit <0.02  $\mu\text{M}$ . NA= data not available. Errors are  $\pm$  SD of 2-3 replicates.

Domains	STN	CTD		Discrete			N+N $\mu\text{M}$	SRP $\mu\text{M}$	POC:Chl-a (g:g)
		Chl-a $\mu\text{g L}^{-1}$	Chl-a $\mu\text{g L}^{-1}$	POC $\mu\text{g L}^{-1}$	PON $\mu\text{g L}^{-1}$	POP $\mu\text{g L}^{-1}$			
Temp N	2	0.89 $\pm$	0.76 $\pm$ NA	98.93 $\pm$ 12.1	14.19 $\pm$ 0.38	1.98 $\pm$ 0.11	0.69 $\pm$ NA	0.09 $\pm$ NA	130:1 $\pm$ 15.91
	4	0.72 $\pm$	0.58 $\pm$ 0.01	113.71 $\pm$ 3.28	12.76 $\pm$ 0.45	2.00 $\pm$ 0.05	0.64 $\pm$ NA	0.07 $\pm$ NA	196:1 $\pm$ 6.59
	6	0.55 $\pm$ NA	0.46 $\pm$ 0.01	63.12 $\pm$ 0.04	6.06 $\pm$ 0.57	1.39 $\pm$ 0.05	0.49 $\pm$ NA	0.04 $\pm$ NA	137:1 $\pm$ 2.98
	8	0.59 $\pm$	0.37 $\pm$ 0.03	49.14 $\pm$ 2.16	4.72 $\pm$ 0.16	1.81 $\pm$ 0.10	2.60 $\pm$ NA	0.16 $\pm$ NA	133:1 $\pm$ 12.25
	12	0.78 $\pm$	0.57 $\pm$ 0.02	50.37 $\pm$ 1.92	5.36 $\pm$ 0.76	1.04 $\pm$ 0.02	1.71 $\pm$ NA	0.09 $\pm$ NA	88:1 $\pm$ 4.58
Oligo N	14	0.31 $\pm$	0.43 $\pm$ 0.03	38.10 $\pm$ 2.57	2.72 $\pm$ 0.15	0.67 $\pm$ 0.20	0.14 $\pm$ NA	0.03 $\pm$ NA	89:1 $\pm$ 8.60
	16	0.49 $\pm$	0.39 $\pm$ 0.00	48.18 $\pm$ 4.11	6.41 $\pm$ 1.03	1.17 $\pm$ 0.05			123:1 $\pm$ 10.54
	18	0.39 $\pm$ NA	0.41 $\pm$ 0.01	57.81 $\pm$ 3.88	3.18 $\pm$ 0.06	0.57 $\pm$ 0.03	ND	ND	141:1 $\pm$ 10.07
	22	0.31 $\pm$	0.43 $\pm$ 0.01	NA	3.92 $\pm$ 1.03	1.00 $\pm$ 0.16			NA
	26	0.36 $\pm$	0.69 $\pm$ 0.01	41.77 $\pm$ 5.31	2.68 $\pm$ 0.88	0.72 $\pm$ 0.04	0.04 $\pm$ NA		60:1 $\pm$ 7.75
Upw	30	0.71 $\pm$	0.73 $\pm$ 0.02	52.15 $\pm$ 6.14	7.50 $\pm$ 0.86	0.96 $\pm$ 0.04	0.19 $\pm$ NA	0.10 $\pm$	71:1 $\pm$ 8.64
	34	1.37 $\pm$ NA	1.15 $\pm$ 0.05	69.12 $\pm$ 1.61	9.84 $\pm$ 0.22	3.19 $\pm$ 0.17	7.48 $\pm$ NA	0.38 $\pm$ NA	60:1 $\pm$ 2.96
	38	0.99 $\pm$	0.92 $\pm$ 0.04	47.77 $\pm$ 0.55	6.48 $\pm$ 0.22	0.95 $\pm$ 0.11	1.23 $\pm$ NA	0.11 $\pm$	52:1 $\pm$ 2.34
Equ	45	0.81 $\pm$ NA	0.72 $\pm$ 0.03	35.25 $\pm$ 2.52	5.36 $\pm$ 0.34	1.04 $\pm$ 0.04	7.68 $\pm$ NA	0.69 $\pm$ NA	49:1 $\pm$ 4.05
Oligo S	50	0.54 $\pm$	0.47 $\pm$ 0.02	30.63 $\pm$ 1.02	3.21 $\pm$ 0.90	1.24 $\pm$ 0.05	0.51 $\pm$ NA	0.20 $\pm$	65:1 $\pm$ 3.52
	56	0.42 $\pm$ NA	0.42 $\pm$ 0.03	26.82 $\pm$ 0.39	2.91 $\pm$ 0.01	0.72 $\pm$ 0.06	0.06 $\pm$ NA	0.19 $\pm$ NA	64:1 $\pm$ 4.65
	60	0.43 $\pm$	0.46 $\pm$ 0.04	26.48 $\pm$ 4.43	2.98 $\pm$ 0.19	0.56 $\pm$ 0.05	0.09 $\pm$ NA	0.12 $\pm$	58:1 $\pm$ 10.85
Temp S	67	0.99 $\pm$	0.86 $\pm$ 0.02	83.86 $\pm$ 1.75	13.35 $\pm$ 0.98	2.43 $\pm$ 0.04	0.07 $\pm$ NA	0.17 $\pm$	97:1 $\pm$ 3.05
	71	2.07 $\pm$ NA	1.35 $\pm$ 0.01	132.89 $\pm$ 7.65	22.95 $\pm$ 3.25	3.35 $\pm$ 0.07	4.05 $\pm$ NA	0.55 $\pm$ NA	98:1 $\pm$ 5.71

**Table 4.5.** Forward stepwise and multiple regression analysis of nutrients to significant predictor variables. A) Includes data from all the domains. B) Data from the higher productivity domains. C) Oligotrophic domains only. Ln = natural log, N+N= nitrate + nitrite ( $\mu\text{M}$ ), SRP= soluble reactive phosphate ( $\mu\text{M}$ ), POC= particulate organic carbon ( $\mu\text{g L}^{-1}$ ), PON= particulate organic nitrogen ( $\mu\text{g L}^{-1}$ ), POP= particulate organic phosphorus ( $\mu\text{g L}^{-1}$ ), Chl-a= chlorophyll-a ( $\mu\text{g L}^{-1}$ ), CM T= in situ temperature at the chlorophyll maximum ( $^{\circ}\text{C}$ ), S= salinity (dimensionless), MLD= mixed layer depth (m), dMLCM= distance between the CM and the MLD (m), BS= backscatter (V). NA = data not available.

Nutrient	A) All Domains n=19		B) Higher Productivity Regions n=11		C) Oligotrophic Regions n=8	
	Forward Stepwise	Multiple regression	Forward Stepwise	Multiple regression	Forward Stepwise	Multiple regression
<b>lnN+N <math>\mu\text{M}</math></b>	CM T & S $r^2=0.53$ , $p=0.002$	$493 + (0.37 \times \text{CMT}) - (134 \times \ln\text{S})$	None	NA	None	NA
<b>lnSRP <math>\mu\text{M}</math></b>	S $r^2=0.32$ , $p=0.01$	$156 - (44.2 \times \ln\text{S})$	None	NA	None	NA
<b>lnPOC <math>\mu\text{g L}^{-1}</math></b>	BS & CM T $r^2=0.69$ $p<0.001$	$17.4 + (2.1 \times \ln\text{BS}) - (5 \times 10^{-2} \times \text{CMT})$	BS & CM T $r^2=0.56$ $p=0.027$	$17.4 + (2.1 \times \ln\text{BS}) - (0.046 \times \text{CMT})$	None	NA
<b>lnPON <math>\mu\text{g L}^{-1}</math></b>	dMLCM, N+N & chl-a $r^2=0.91$ $p<0.001$	$2.43 + (6.43 \times 10^{-3} \times \text{dMLCM}) - (0.138 \times \ln\text{N+N } \mu\text{M}) + (1.29 \times \ln\text{Chl-a } \mu\text{g L}^{-1})$	dMLCM, N+N & chl-a $r^2=0.82$ $p=0.006$	$2.46 + (7.92 \times 10^{-3} \times \text{dMLCM}) - (0.15 \times \ln\text{N+N } \mu\text{M}) + (1.35 \times \ln\text{Chl-a } \mu\text{g L}^{-1})$	None	NA
<b>lnPOP <math>\mu\text{g L}^{-1}</math></b>	dMLCM & chl-a $r^2=0.73$ $p<0.001$	$0.7 + (4.95 \times 10^{-3} \times \text{dMLCM m}) + (0.68 \times \ln\text{Chl-a } \mu\text{g L}^{-1})$	CMT & chl-a $r^2=0.64$ $p=0.017$	$1.68 + (0.62 \times \ln\text{Chl-a } \mu\text{g L}^{-1}) - (6.1 \times 10^{-2} \times \text{CMT})$	None	NA

A positive correlation between N+N and SRP (PCC  $r=0.81$ ,  $p<0.001$ ) indicates that the dissolved inorganic nutrients increased together. Multiple linear regression analysis, using only abiotic parameters, showed that N+N concentrations across the entire transect can be predicted by a linear combination of CM T and S, whilst SRP was mainly related to S (Table 4.5). However, when taking into consideration separate productivity regions no significant empirical relationships were found between N+N and SRP and the available observed parameters.

#### 4.3.2 Chl-a

Chl-a derived from calibrated CTD fluorescence data (Table 4.5) was used for the data analysis. A CM was present at all locations, which occurred below the MLD, except at station 2, 6 and 8 where the CM was located within the mixed layer (Figure 4.3). A well-developed deep CM was identified in the tropical and subtropical domains.

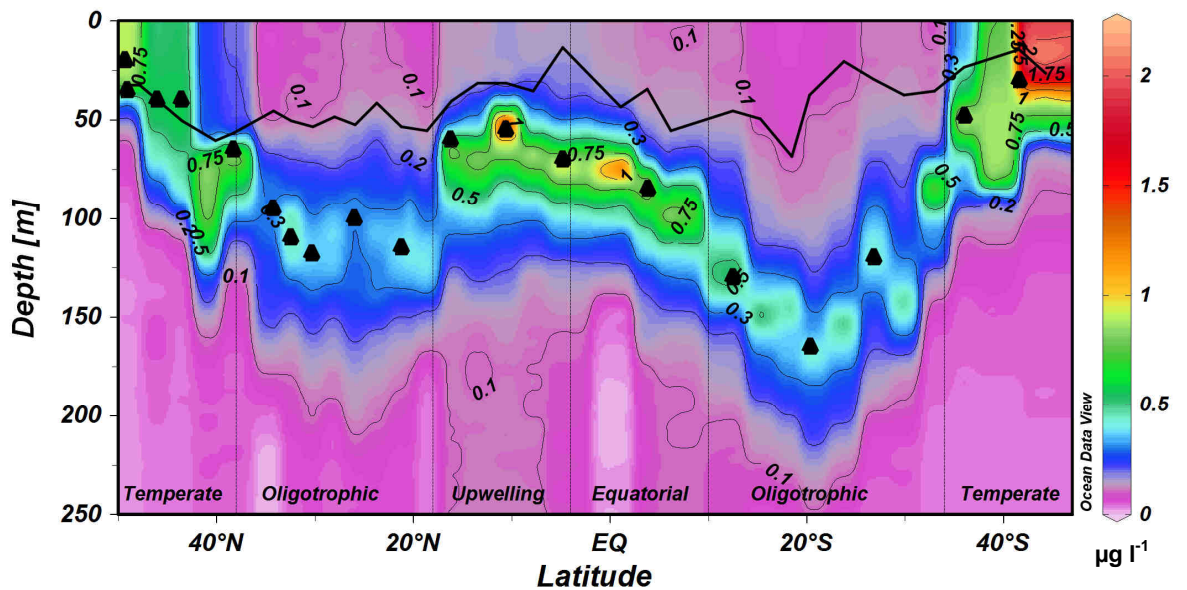


**Figure 4.3.** AMT20 Latitudinal distribution of chlorophyll a ( $\mu\text{g L}^{-1}$ ) and CM partitioned by ecological domains. The triangles represent the sampling locations at the CM. The black line represents the estimated MLD (mixed layer depth).

Across the meridional transect chl-a concentrations decreased significantly with increasing CM depth ( $r^2=0.44$ ,  $p=0.002$ ) however, chl-a was not related to CM T ( $r^2=0.15$ ,  $p=0.096$ ). The lowest chl-a concentrations and deepest CM were found in the Oligotrophic domains with a minimum of  $0.31\mu\text{g L}^{-1}$  at station 22 and the deepest CM at 165m at station 56. The highest CM and chl-a concentrations were found in the Upwelling and Temperate S domains. The CM identified at station 71 displayed the highest chl-a concentration of  $2.1\mu\text{g L}^{-1}$  coinciding with the lowest CM temperature of  $11.7^\circ\text{C}$  at 30 m depth. In the Upwelling domain, station 34 also exhibited elevated chl-a of  $1.37\mu\text{g L}^{-1}$  at  $19.8^\circ\text{C}$  at 55 m depth, representing the peak of productivity in the upwelling.

### 4.3.3 Particulate organic matter

The concentration of POC, PON and POP (Table 4.4) significantly decreased with increasing depth ( $r^2>0.6$ ,  $p<0.001$ ) and were statistically greater in the higher productivity areas compared to the Oligotrophic domains ( $t(16)>3.2$ ,  $p=0.005$ ). Overall all particulate organic nutrients were at their highest in the Temperate S and the northern part of the Temperate N domains. POC, PON and POP reached their maxima at station 71. The minimum POC concentrations were found at Stations 56 and 60 in the Oligotrophic S domain. The minimum PON concentrations occurred at stations 14 and 26 in the Oligotrophic N domain and the minimum POP concentrations occurred at stations 18 and 60 in the Oligotrophic N and S domains.

Strong positive correlations were found between all the particulate organic nutrients and chl-a. POC, PON, POP and chl-a increased together (PCC  $r>0.7$ ,  $p<0.003$ ). Forward stepwise and multiple regression analyses were used to create algorithms to estimate the concentration of organic nutrients from readily available CTD data. In this instance chl-a was included alongside the list of independent variables as a potential predictor. Table 4.5 shows the relationship between particulate organic nutrient and environmental variables. Backscatter data were used only for the prediction of POC. Salinity was shown to be a collinear factor and removed from the particulate nutrients multiple linear correlation analysis.

Stepwise regressions showed that no variables were significant predictors for the distribution of organic nutrients in the Oligotrophic domains (group C). The empirical relationships were different for the three groups (A, B and C), indicating that different processes drive nutrient distributions in the different domains. In both scenarios A and B (including and excluding

oligotrophic data respectively), PON was the parameter with the strongest multiple linear predictability, whereas POC had the weakest multiple linear relationship.

#### 4.3.4 Validation of the prediction of particulate organic nutrients

To validate the empirical models of POC and PON (all domains) shown in equation 4.2 and 4.3, data for measured and calculated POC and PON concentrations at the CM from this study were compared to the CM POC and PON concentrations determined by David Drapeau from the Bigelow Laboratory during AMT20.

$$\text{LnPOC} = 17.4 + (2.1 \text{ LnBS}) - (5 \times 10^{-2} \text{CM T}) \quad (4.2)$$

$$\text{LnPON} = 2.43 + (6.43 \times 10^{-3} \text{dMLCM}) - (0.138 \text{ LnN} + \text{N}) + (1.29 \text{ LnChl} - a) \quad (4.3)$$

The predictor parameters and therefore the model equations for the distribution of POC and PON based on the Bigelow POC and PON data which were collected at the same depths as data presented in Table 4.4 (Bigelow dataset 1), are given in equations 4.4 and 4.5. David Drapeau also determined POC and POC at the CM of an additional 10 stations on AMT20 (Bigelow dataset 2). In order to validate equations 4.2, 4.3, 4.4 and 4.5, predicted POC and PON from these equations were compared to measured POC and PON from this Bigelow dataset 2 (Big2) as shown in Table 4.6.

$$\text{LnPOC Big} = 4.56 + (8.32 \times 10^{-3} \text{ dMLCM}) + (0.77 \text{ LnChl} - a) \quad (4.4)$$

$$\text{LnPON Big} = 2.33 - (0.3 \text{ LnN} + \text{N}) + (2.03 \text{ LnChl} - a) \quad (4.5)$$

**Table 4.6.** Validation of POC and PON predictive equations for AMT20. Linear regression relationship between predicted (p) data from the Bigelow dataset 1 (Big1) and data from this study (Raf Nobili; RN) and measured (m) data from the Bigelow dataset 2 (Big2).

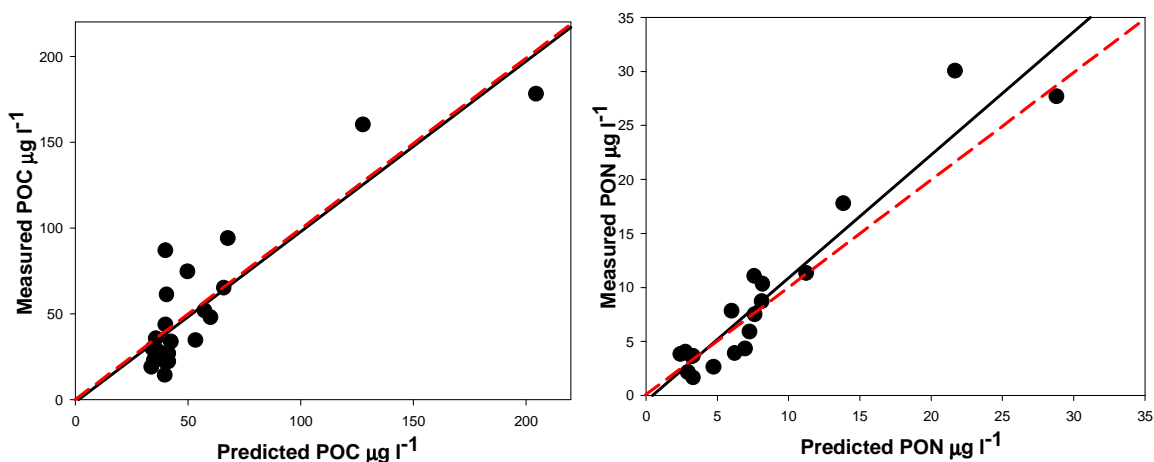
<b>Validation POC</b>	<b>r<sup>2</sup></b>	<b>p-value</b>
Big1 m- RN m	0.84	<0.001
Big1 p- Big2 m	0.88	<0.001
RN p <sup>1</sup> - Big2 m	0.94	<0.001
RN p - Big1+Big2 p	0.83	<0.001

<b>Validation PON</b>	<b>r<sup>2</sup></b>	<b>p-value</b>
Big1 m- RN m	0.9	<0.001
Big1 p- Big2 m	0.91	<0.001
RN p <sup>1</sup> - Big2 m	0.96	<0.001
RN p - Big1+Big2 p	0.92	<0.001

(1) Extra stations only

The measured POC and PON data from this study (RN) and Bigelow (Big1) had a positive linear relationship (Table 4.6 Big1m – RN m). Table 4.6 demonstrates that the predicted POC and PON values (RN dataset) compared well with the Bigelow2 dataset (RN p – Big2 m). Figure 4.5 shows that the predicted POC and PON (equations 4.2 and 4.3) compare well with the measured POC and PON data not included in the formulation of the equations (Bigelow datasets 1+2), approaching the 1:1 line. Additionally the significant positive relationship between RN p – Big1 p (Table 4.6) suggests that the POC and PON equations 4.2, 4.3 and the equations 4.4 and 4.5 are all valid predictors for nutrient concentrations along the AMT20 transect.



**Figure 4.4.** Linear regression (black line) and 1:1 relationship (red dashed line) between measured data from the Bigelow dataset 1 and 2 and predicted (from equations 4.2 and 4.3) A) POC=  $0.99x-1.24$  ( $r^2=0.78$   $p<0.0001$ ) B) PON=  $1.14x-0.51$  ( $r^2=0.91$   $p<0.0001$ ).

POP data were not available for equation validation purposes; therefore we assume the validity of equation in Table 4.5 for POP to be similar to that of POC and PON.

#### 4.3.5 Equations applicability

In order to estimate organic nutrient variation in the ecological domains over time, empirical equations for POC and PON were applied to AMT data collected during previous cruises which covered a 7 year timespan from 2003 to 2010 (Table 4.3). For each of these cruises POC, PON and N+N data were available.

The POC equation 4.2 was not applicable to the previous datasets due to the lack of backscatter data, therefore equation 4.4, calculated from the Bigelow dataset 1 (AMT20) was used. For PON equation 4.3 was applied. A minimum of 11 points (stations) were calculated for each cruise.

The predicted POC and PON values were compared to the measured POC and PON data from the same cruises. They were positively related (POC  $r^2=0.6$   $p<0.001$  and PON  $r^2=0.54$   $p<0.001$ ) however as shown in Figure 4.5, the predicted values were lower than the measured concentrations.

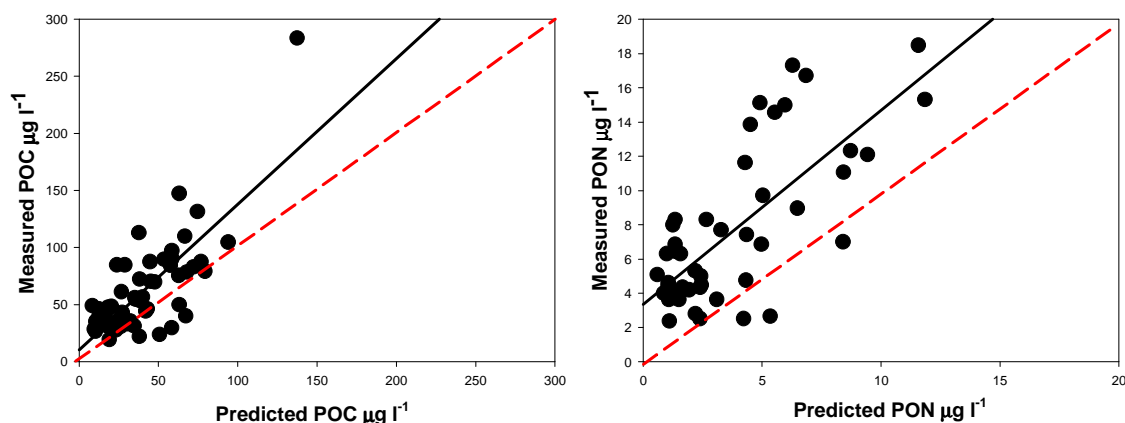


**Figure 4.5.** Linear regression (black line) and 1:1 relationship (red dashed line) between predicted and measured nutrient data from AMT12 to AMT18 according to equations 4.4 and 4.5. POC (A) and PON (B) at the CM depth of the sampling locations which included N+N, POC and PON data for each AMT transect.

The difference between predicted and measured POC and PON concentrations could be due to differences in the parameters used in the predictive equations between AMT20 and the previous cruises. In particular, differences between the dMLCM (data not shown) and the concentration of chl-a determined on AMT20 compared to the previous AMT cruises are shown in Figure 4.6.

In order to predict as accurately as possible the POC and PON concentrations on AMT12 to AMT18, empirical equations were calculated from POC (n=84) and PON (n=67) measured during these cruises. To validate equations 4.6 ( $r^2=0.58$   $p<0.001$ ) and 4.7 ( $r^2=$   $p<0.001$ ), predicted POC and PON derived from these equations were compared to some of the measured POC and PON which were not included in deriving the predictive equations. A total of n=11 POC and n=9 PON concentrations were randomly removed from the datasets and compared to predicted POC and PON concentrations for these locations as shown in Table 4.7

$$\text{LnPOC} = 6.4 - (0.52 \text{ LnCM}) + (0.22 \text{ LnChl} - a) \quad (4.6)$$

$$\text{LnPON} = 39.98 + (0.5 \text{ LnChl} - a) - (9.655 \text{ LnS}) \quad (4.7)$$

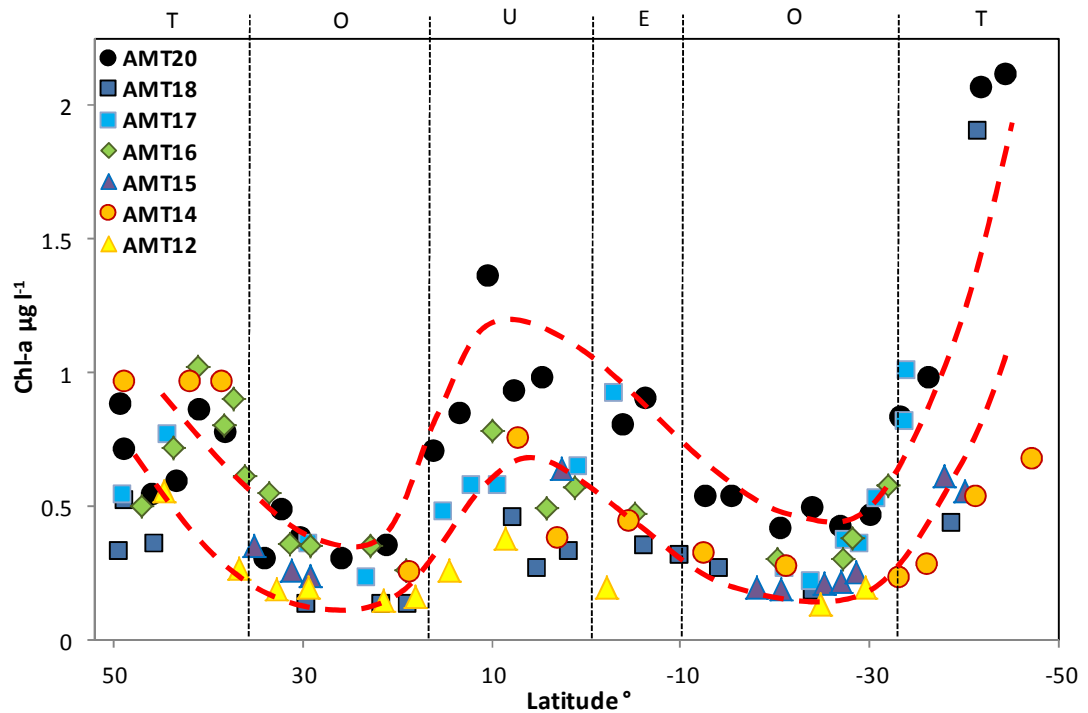


**Figure 4.6.** Chl-a  $\mu\text{g L}^{-1}$  during six AMT transects between 2003 and 2010. The markers represent the chl-a concentration at the CM depth of the sampling locations which included N+N, POC and PON data for each AMT transect. The red dashed lines trace the chl-a concentrations of AMT20 (top) and the previous AMT cruises (bottom) (indicative only). The vertical black dotted lines separate the ecological domains defined on AMT20 T= Temperate, O= Oligotrophic, U= Upwelling, E= Equatorial.

**Table 4.7.** Validation of POC and PON predictive equations for AMT12 to AMT18. Linear regression relationship between predicted (p) data (AMT p) and measured (m) data (AMT m).

<b>Validation POC</b>	<b><math>r^2</math></b>	<b>p-value</b>
AMT <sup>1</sup> m- AMT p	0.81	<0.001
AMT m - AMT p	0.84	<0.001
<b>Validation PON</b>	<b><math>r^2</math></b>	<b>p-value</b>
AMT <sup>1</sup> m- AMT p	0.82	<0.001
AMT m - AMT p	0.71	<0.001

(1) Extra stations only

Table 4.7 demonstrates that the predicted POC and PON values (AMT p) compared well with measured data at the stations not included in the formulation (AMT<sup>1</sup> m - AMT p) therefore suggesting that equation 4.6 and 4.7 are valid predictors for nutrient concentrations during previous AMT transects. Figure 4.7 also shows that the total predicted POC and PON (equations 4.6 and 4.7) compare well with the total measured POC and PON data, approaching the 1:1 line.

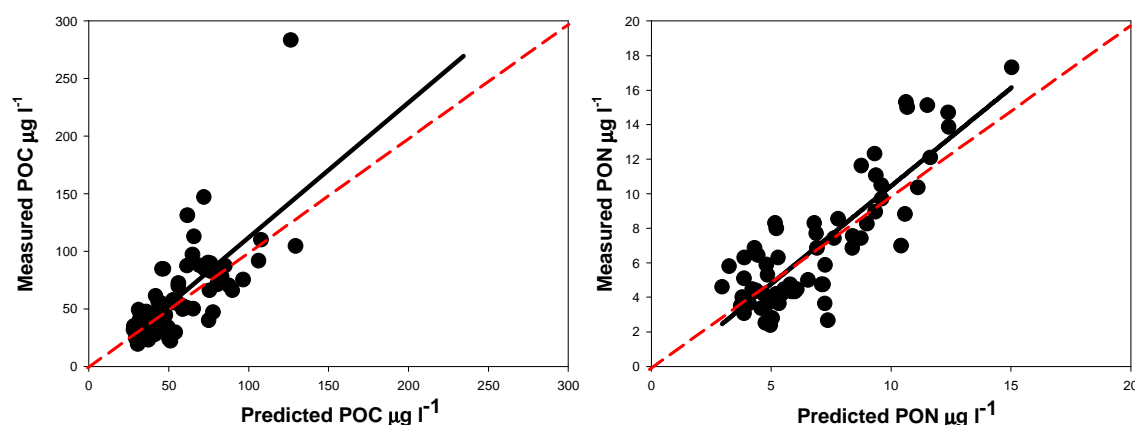


**Figure 4.7.** Linear regression (black line) and 1:1 relationship (red dashed line) between predicted and measured nutrient data from AMT12 to AMT18 according to equations 4.6 and 4.7. POC (A) and PON (B) at the CM depth of the sampling locations.

To estimate POC and PON variation from AMT12 to AMT20 we selected 1 location ( $\pm 4^\circ$  latitude) per latitudinal band, representative of Temperate, Oligotrophic and Upwelling domains for each of the cruises considered. In the Upwelling domain the station with the highest chl-a concentration was selected. At stations where measured data were not available, predicted values were used. The final part of the routes (where the station at  $40^\circ\text{S}$  occurs) for AMT17, 16 and 15 turned eastward towards South Africa rather than westward towards Chile. However, with the exception of AMT17 (where the  $40^\circ\text{S}$  station was removed), no differences were detected between these cruises' parameters (dMLCM, CM depth and MLD, eg. Figure 4.6) and those of AMT12, 14 and 18. Therefore the  $40^\circ\text{S}$  data were retained.

The estimated POC ( $\mu\text{g L}^{-1}$ ) variation at 5 indicative latitudes is shown in Figure 4.8.

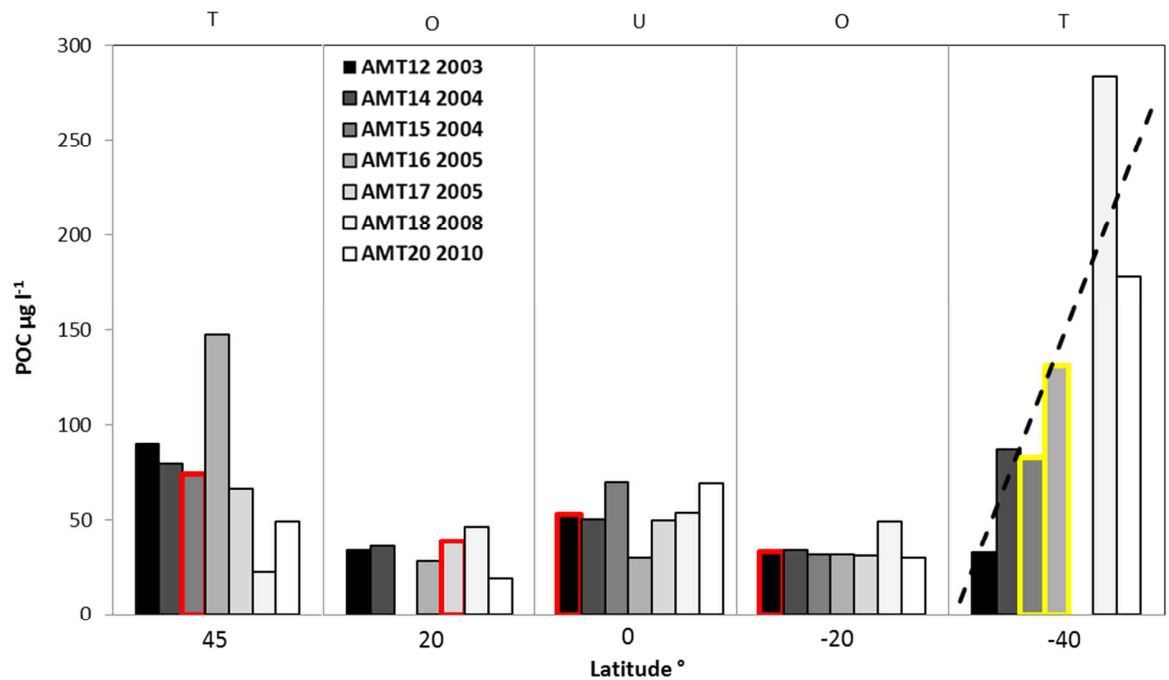


**Figure 4.8.** POC ( $\mu\text{g L}^{-1}$ ) from AMT12 to AMT20 at five locations along the Atlantic transect. The bars highlighted in red indicate predicted values (calculated as stated in section 4.3.4). The bars highlighted in yellow indicate stations sampled at a different longitude (east South Atlantic for AMT16 and 15). The dashed line represents the regression line versus time (corrected). The partition lines identify the ecological domains T= Temperate, O= Oligotrophic, U= Upwelling.

POC was generally higher in the higher productivity domains (Temperate and Upwelling) with the highest concentration found in the Temperate S domain ( $283.5 \mu\text{g L}^{-1}$ ). In comparison with other AMT transects, the POC concentrations during AMT20 and AMT18 appeared low at most locations with the exception of  $\sim 40^{\circ}\text{S}$  in the Temperate S, where a significant increase of POC from AMT12 in 2003 to AMT20 in 2010 was also observed ( $r^2=0.65$   $p=0.05$ ). At  $45^{\circ}\text{N}$  in the Temperate N no significant trend over time was detected ( $r^2=0.3$   $p=0.2$ ), the regression includes gaps for the years and months when no data is available, whilst at the Upwelling domain a POC minima corresponding to mid-2005 (AMT16) occurred

The estimated PON ( $\mu\text{g L}^{-1}$ ) variation at 5 indicative latitudes along the Atlantic transect is shown in Figure 4.9.

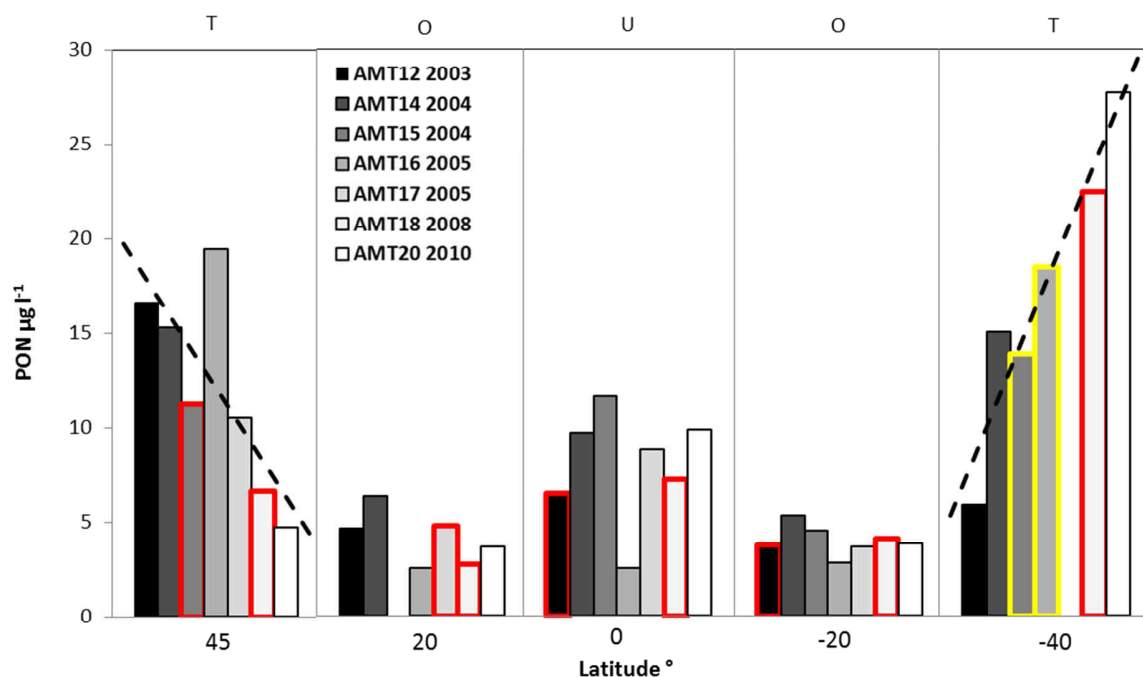


**Figure 4.9.** PON ( $\mu\text{g L}^{-1}$ ) from AMT12 to AMT20 at five locations along the Atlantic transect. The bars highlighted in red indicate predicted values (calculated as stated in section 4.3.4). The bars highlighted in yellow indicate stations sampled at a different longitude (east South Atlantic for AMT16 and 15). The dashed lines represent the regression lines versus time (corrected). The partition lines identify the ecological domains T= Temperate, O= Oligotrophic, U= Upwelling.

The distribution of PON along the meridional transects from 2003 to 2010 followed a similar pattern to the POC distribution in figure 4.9. PON was generally higher in the higher productivity domains (Temperate and Upwelling) with the highest concentration found in the Temperate S domain ( $27.7 \mu\text{g L}^{-1}$ ). In comparison with other AMT transects, the concentrations of PON during AMT20 and AMT18 appeared low at most locations with the exception of  $\sim 40^{\circ}\text{S}$  in the Temperate S, where a significant increase of PON from AMT12 in 2003 to AMT20 in 2010 was also observed ( $r^2=0.88$   $p=0.006$ ), the regression includes gaps for the years and months when no data is available. At  $\sim 45^{\circ}\text{N}$  in the Temperate N a significant decreasing trend over time was detected ( $r^2=0.6$   $p=0.03$ ) and at the Upwelling domain a PON minima corresponding to mid-2005 (AMT16) was noted.

No statistically significant trends were found in the Oligotrophic domains (20°N and 20°S), however between AMT12 (2003) and AMT20 (2010) POC and PON decreased 43% and 21% respectively in the Oligotrophic N whilst POC and PON appeared unchanged in the Oligotrophic S.

Overall the limited number of data and strong interannual variability due to sampling at different times of the year could have affected the relationships observed in the Temperate domains (Figure 4.8 and 4.9). In addition, a weaker equatorial upwelling (low chl-a concentrations) was detected during AMT12 and 18. This was possibly due to natural variations or the lack of measurements at the exact location of the phenomena. All these factors increase uncertainty in the highlighted trends; therefore more data are needed to confirm the validity of these observations.

#### 4.3.6 Nutrient ratios

The stoichiometry (molar ratios) of organic and inorganic nutrients at the CM are shown in Figures 4.10, 4.11 and 4.12.

N:P and C:P ratios were not correlated to chl-a (PCC  $r=0.35$ ,  $p=0.15$  and  $r=-0.4$ ,  $p=0.1$  respectively) while C:N significantly increased as chl-a decreased (PCC  $r=-0.8$ ,  $p<0.001$ ) indicating a dependence of the C:N ratio on phytoplankton concentration. The highest N:P ratios (Figure 4.10) were found in areas within the Temperate N and Upwelling domains. However, in general the N:P ratios were below Redfield (16:1) except at station 30 (17:1 N:P) and approached Redfield values at Stations 2, 4, 38 and 71 in the Temperate N, Upwelling and Temperate S domains. This indicates the presence of potentially higher quality seston at these locations. The lowest N:P ratios also occurred in areas of the Temperate N and Upwelling domains, at stations 8 and 34 respectively and at station 50 in the Oligotrophic S.

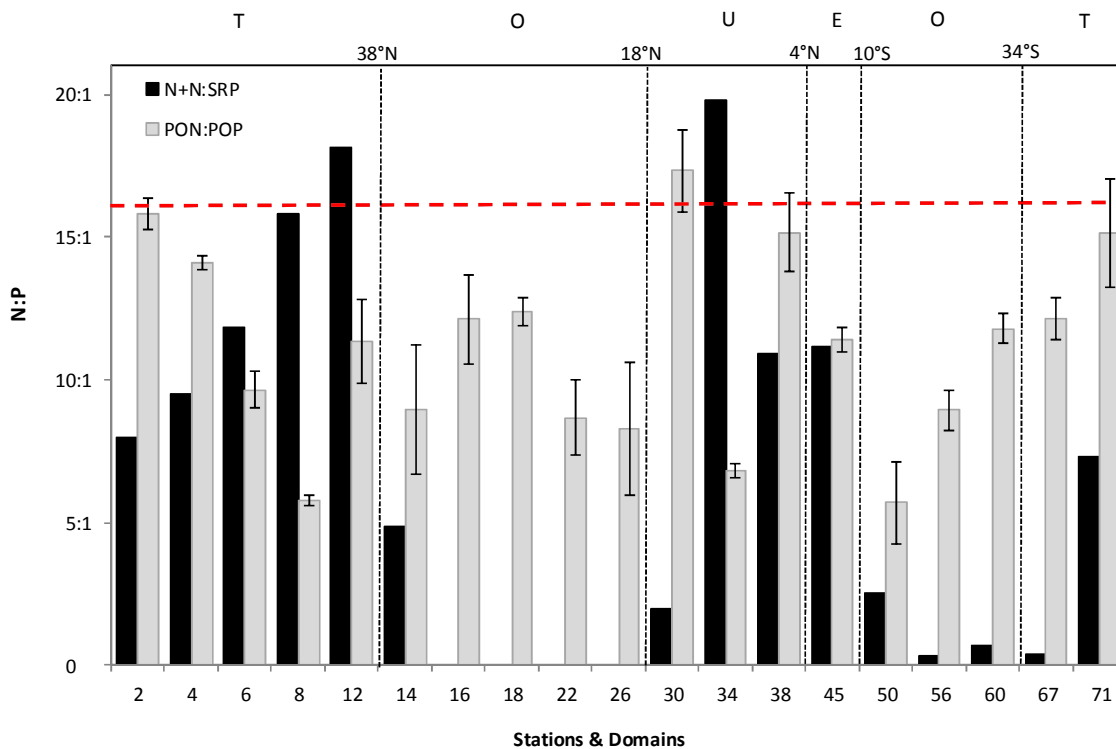


**Figure 4.10.** Organic (PON:POP) and inorganic (N+N:SRP) N:P ratios (mole:mole) at the depth of the chlorophyll maximum in the six ecological domains. The red dashed line represents the Redfield 16:1 N:P ratio. Error  $\pm$  SD. Ecological domains T= Temperate, O= Oligotrophic, U= Upwelling, E= Equatorial.

Organic (PON:POP) and inorganic (N+N:SRP) N:P ratios did not correspond to each other except at station 45 in the Equatorial domain. N+N:SRP ratios were significantly lower in the Oligotrophic S domain which were affected by the higher concentrations of SRP present in the area.

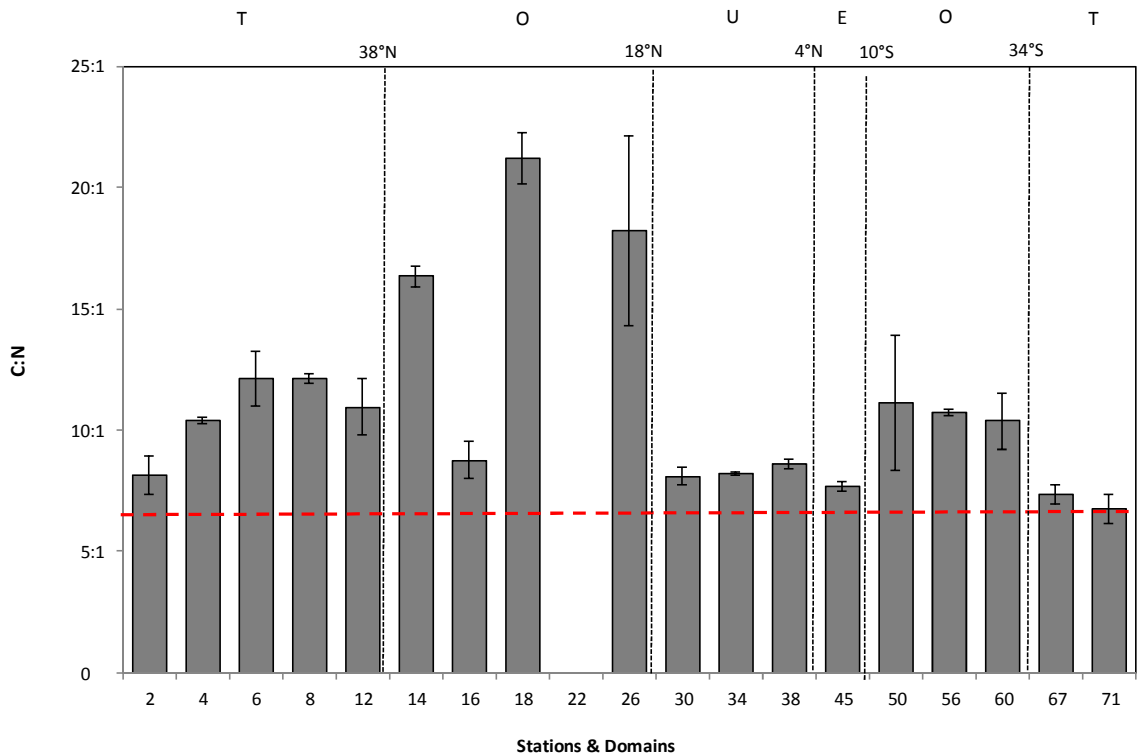


**Figure 4.11.** Organic C:N ratios (mole:mole) at the depth of the chlorophyll maximum in the six ecological domains. Error  $\pm$ SD. The red dashed line represents the Redfield 6.6:1 C:N ratio. Error  $\pm$  SD. Ecological domains T= Temperate, O= Oligotrophic, U= Upwelling, E= Equatorial.

The C:N ratios (Figure 4.11) were all above Redfield values (6.6:1); the most elevated C:N ratios occurred in the Oligotrophic N domain whilst lower values were found in the higher productivity domains of the Upwelling, Equatorial and Temperate S. C:N ratios reached their lowest, approaching Redfield values, at station 71 (6.8:1) coinciding with elevated chl-a concentrations. The C:P ratio (Figure 4.12) were mostly above Redfield (106:1) in the Northern hemisphere (except stations 8 and 34) and generally below Redfield in the Southern hemisphere (except station 60). In the Temperate S domain C:P ratios approached Redfield values indicating the presence of higher quality seston at these locations as also shown by the N:P and C:N ratios.

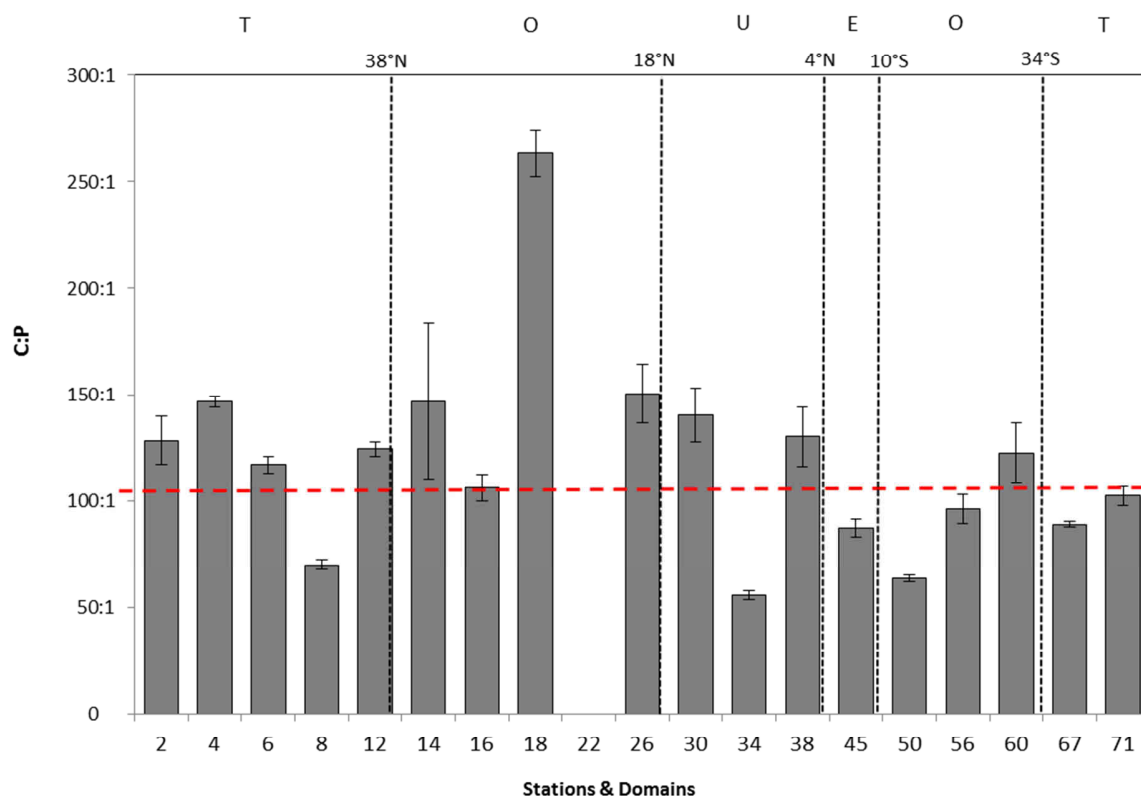


**Figure 4.12.** Organic C:P ratios (mole:mole) at the depth of the chlorophyll maximum in the six ecological domains. Error  $\pm$ SD. The red dashed line represents the Redfield 106:1 C:P ratio. Error  $\pm$  SD. Ecological domains T= Temperate, O= Oligotrophic, U= Upwelling, E= Equatorial.

The distributions of seston N:P and C:P ratios were not significantly different between the two productivity regions ( $t(16) < \pm 1$ ,  $p > 0.1$ ), however the C:N ratio was significantly higher in the Oligotrophic domains ( $t(16) = -3.9$ ,  $p = 0.008$ ) compared to the high productivity regions indicating decreased food quality in the oligotrophic locations.

To estimate food quality variation at the CM from 2003 to 2010 we used the available particulate organic nutrient concentrations measured during AMT12 to AMT20 (Figure 4.13). Data shown in Figure 4.7 and 4.8 were used to calculate the molar ratios at 5 representative locations within the Temperate, Oligotrophic and Upwelling domains for each of the cruises considered.

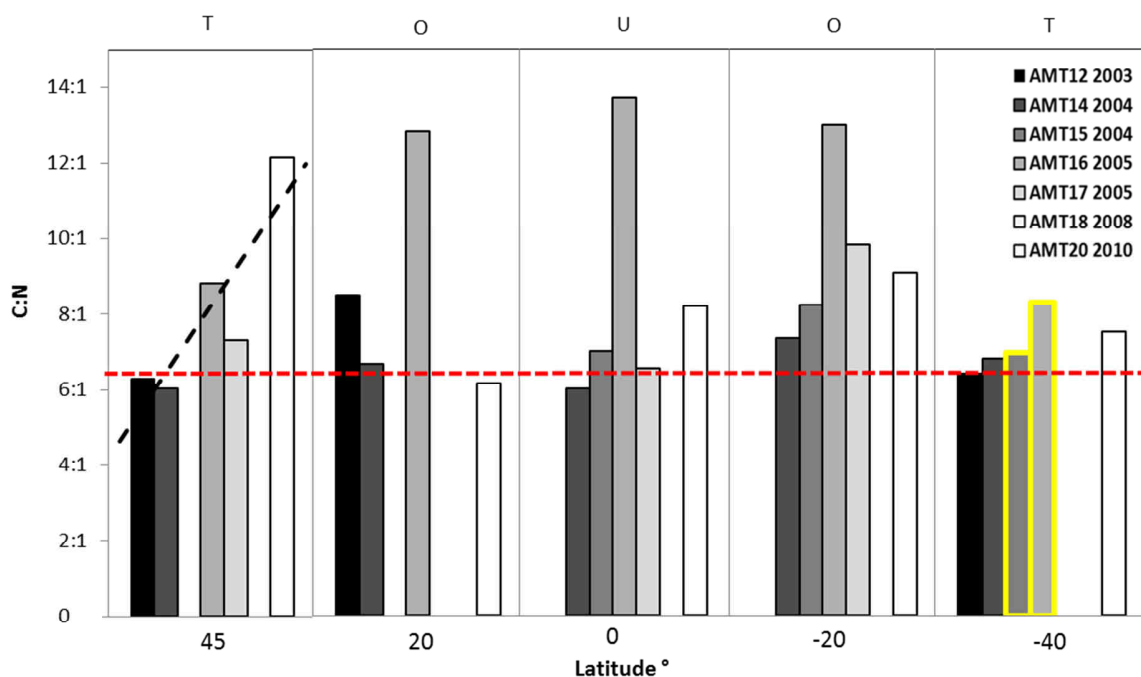


**Figure 4.13.** Organic C:N ratios (mole:mole) at the depth of the chlorophyll maximum from AMT12 to AMT20 at five locations along the Atlantic transect. The red dashed line represents the Redfield 6.6:1 C:N ratio. The black dashed line represents the regression line versus time. The bars highlighted in yellow indicate stations sampled at a different longitude (east South Atlantic for AMT16 and 15). The partition lines identify the ecological domains T= Temperate, O= Oligotrophic, U= Upwelling.

C:N ratios were generally high, peaking during 2005 (AMT16) in the Oligotrophic and the Upwelling domains, with the highest ratios reaching >12.5:1. A significant increase of C:N from AMT12 in 2003 to AMT20 in 2010 was observed ( $r^2=0.92$   $p=0.01$ ) at ~45°N in the Temperate N. Although a positive linear trend can be seen at 40°S, the relationship was not statistically significant ( $r^2=0.22$   $p=0.4$ ). The regression includes gaps for the years and months when no data is available.

#### 4.3.7 POC:Chl-a ratio

The POC:Chl-a ratios g:g (Table 4.3) were high (>123:1) in the majority of the Temperate N and Oligotrophic N domains (except at stations 12, 14 and 26), indicating that a large amount of the seston comprised detrital matter rather than living phytoplankton. This, alongside low

inorganic nutrient concentrations, suggests that the Temperate N domain exhibited post-bloom conditions. At station 12 (Temperate N) and 14 (Oligotrophic N) the POC:Chl-a ratio was lower (88-89:1 respectively). This was possibly caused by the Azores Current traversing the area, cooling the water column, supplying nutrients and therefore increasing the chl-a concentration. The lowest POC:Chl-a values were found in the Upwelling (<71:1), Equatorial (49:1) and the oligotrophic S domains (<97:1). The highest POC:Chl-a ratios were found in the Temperate N and Oligotrophic N domains, reaching a maximum of 196:1 g:g.

#### 4.3.8 Fatty acids

Total FA at the CM (Table 4.8) was at its highest at station 12 ( $30.16 \mu\text{g l}^{-1}$ ) (Figure 4.1) and at its lowest at station 45 ( $4.8 \mu\text{g L}^{-1}$ ). In all samples the total saturated fatty acids (SAFA) dominated, ranging from 59% of the total FA at station 71 to 97% of the total FA at station 18. Stations 18, 22 and 26 in the Oligotrophic N domain had the highest proportion of SAFA and highest C:N and C:P ratios of the entire transect; whereas stations 67 and 71 in the Temperate S domain had the lowest percentage of SAFA and lowest C:N ratios. The SAFA 16:0 and 18:0 dominated (abundant in detritus (Pond et al. 1998)), representing between 27-39% and 20-65% respectively of the total FA.

Polyunsaturated fatty acids (PUFA) were the second most abundant type of FA, reaching a maximum of 27% at station 71 in the Temperate S domain. The concentration of total FA was not significantly different between the higher productivity areas and the Oligotrophic domains ( $t(17)=0.53$ ,  $p=0.6$ ). However, %SAFA was higher in the Oligotrophic regions ( $t(17)=-3.18$ ,  $p=0.005$ ) while %PUFA and %MUFA were lower ( $t(17)>3.2$ ,  $p<0.005$ ) compared to the high productivity regions.

**Table 4.8.** Major fatty acids (FA) as a proportion of total FA and ratios by concentration for the seston at the chlorophyll maximum (CM) in different ecological domains. Error  $\pm$  SD of triplicate samples. NA= data not available.

Stations n Fatty Acids %	Temperate N					Oligotrophic N				
	2	4	6	8	12	14	16	18	22	26
<b>14:0</b>	3.22 $\pm$ NA	1.53 $\pm$ 0.33	1.61 $\pm$ 0.18	2.27 $\pm$ 0.17	2.32 $\pm$ 0.68	2.21 $\pm$ 0.33	2.80 $\pm$ 0.50	0.94 $\pm$ 0.09	1.41 $\pm$ 0.35	1.71 $\pm$ NA
<b>15:0</b>	1.23 $\pm$ 1.02	0.47 $\pm$ 0.06	0.57 $\pm$ 0.10	0.91 $\pm$ 0.09	0.97 $\pm$ 0.23	0.81 $\pm$ 0.10	1.15 $\pm$ 0.09	0.22 $\pm$ 0.01	0.48 $\pm$ 0.11	0.53 $\pm$ NA
<b>16:0</b>	37.86 $\pm$ 1.15	26.55 $\pm$ 2.32	31.80 $\pm$ 4.61	33.52 $\pm$ 2.24	32.76 $\pm$ 5.32	38.70 $\pm$ 0.68	39.76 $\pm$ 1.23	28.65 $\pm$ 1.07	28.81 $\pm$ 0.36	30.94 $\pm$ NA
<b>16:1(n-7)</b>	2.42 $\pm$ 0.25	1.16 $\pm$ 0.06	1.25 $\pm$ 0.04	2.51 $\pm$ 0.69	2.95 $\pm$ 0.98	1.42 $\pm$ 0.07	1.83 $\pm$ 0.23	0.20 $\pm$ 0.03	0.75 $\pm$ 0.16	0.71 $\pm$ NA
<b>16:2(n-4)</b>	1.69 $\pm$ 0.23	1.17 $\pm$ 0.12	1.40 $\pm$ 0.10	1.65 $\pm$ 0.45	2.60 $\pm$ 0.29	2.24 $\pm$ 0.18	2.56 $\pm$ 0.16	0.46 $\pm$ 0.03	0.56 $\pm$ 0.11	0.99 $\pm$ NA
<b>16:3(n-4)</b>	0.26 $\pm$ 0.04	0.15 $\pm$ 0.02	0.24 $\pm$ 0.08	0.62 $\pm$ 0.28	0.68 $\pm$ 0.20	0.39 $\pm$ 0.01	0.62 $\pm$ 0.05	0.05 $\pm$ 0.00	0.11 $\pm$ 0.09	0.18 $\pm$ NA
<b>16:4(n-1)</b>	0.31 $\pm$ 0.22	0.30 $\pm$ 0.23	0.29 $\pm$ 0.02	0.37 $\pm$ 0.05	0.36 $\pm$ 0.04	0.39 $\pm$ 0.01	0.39 $\pm$ 0.12	0.02 $\pm$ 0.02	0.06 $\pm$ 0.08	0.10 $\pm$ NA
<b>18:0</b>	29.34 $\pm$ 0.28	43.74 $\pm$ 3.74	42.09 $\pm$ 3.19	36.27 $\pm$ 4.86	33.52 $\pm$ 11.24	33.92 $\pm$ 0.24	28.90 $\pm$ 1.68	65.37 $\pm$ 1.14	61.41 $\pm$ 1.97	58.57 $\pm$ NA
<b>18:1(n-9)</b>	3.49 $\pm$ 0.01	6.80 $\pm$ 0.91	5.33 $\pm$ 1.16	6.31 $\pm$ 0.53	6.49 $\pm$ 1.09	5.17 $\pm$ 0.20	5.95 $\pm$ 0.75	0.54 $\pm$ 0.02	1.51 $\pm$ 0.26	1.82 $\pm$ NA
<b>18:1(n-7)</b>	0.90 $\pm$ 0.01	0.71 $\pm$ 0.07	0.67 $\pm$ 0.08	0.91 $\pm$ 0.30	0.69 $\pm$ 0.17	0.78 $\pm$ 0.12	1.00 $\pm$ 0.11	0.09 $\pm$ 0.02	0.24 $\pm$ 0.05	0.24 $\pm$ NA
<b>18:2(n-6)</b>	1.12 $\pm$ 0.02	1.81 $\pm$ 0.03	1.18 $\pm$ 0.02	1.53 $\pm$ 0.26	1.50 $\pm$ 0.04	1.09 $\pm$ 0.14	1.28 $\pm$ 0.03	0.13 $\pm$ 0.02	0.35 $\pm$ 0.06	0.37 $\pm$ NA
<b>18:3(n-6)</b>	0.19 $\pm$ 0.01	0.43 $\pm$ 0.32	0.20 $\pm$ 0.03	0.23 $\pm$ 0.02	0.25 $\pm$ 0.03	0.22 $\pm$ 0.01	0.29 $\pm$ 0.01	0.20 $\pm$ 0.01	0.20 $\pm$ 0.00	0.24 $\pm$ NA
<b>18:3(n-3)</b>	1.07 $\pm$ 0.12	0.27 $\pm$ 0.06	0.42 $\pm$ 0.06	0.34 $\pm$ 0.30	0.72 $\pm$ 0.02	0.58 $\pm$ 0.05	0.52 $\pm$ 0.06	0.05 $\pm$ 0.01	0.10 $\pm$ 0.05	0.17 $\pm$ NA
<b>18:4(n-3)</b>	2.99 $\pm$ 0.24	2.50 $\pm$ 1.15	2.69 $\pm$ 0.10	3.46 $\pm$ 0.04	3.90 $\pm$ 0.48	4.39 $\pm$ 0.01	3.89 $\pm$ 1.50	0.27 $\pm$ 0.01	0.60 $\pm$ 0.17	0.83 $\pm$ NA
<b>20:0</b>	0.90 $\pm$ 0.02	1.19 $\pm$ 0.28	1.11 $\pm$ 0.10	0.88 $\pm$ 0.01	0.89 $\pm$ 0.21	0.83 $\pm$ 0.01	0.86 $\pm$ 0.06	2.03 $\pm$ 0.09	1.79 $\pm$ 0.08	1.71 $\pm$ NA
<b>20:1(n-9)</b>	3.96 $\pm$ 0.24	1.89 $\pm$ 0.73	1.60 $\pm$ 0.27	1.32 $\pm$ 0.10	1.45 $\pm$ 0.34	1.05 $\pm$ 0.07	0.88 $\pm$ 0.21	0.09 $\pm$ 0.02	0.23 $\pm$ 0.07	0.25 $\pm$ NA
<b>20:5(n-3) EPA</b>	2.00 $\pm$ 0.28	2.21 $\pm$ 0.11	1.70 $\pm$ 0.13	1.75 $\pm$ 0.61	2.04 $\pm$ 0.04	1.36 $\pm$ 0.07	1.90 $\pm$ 0.87	0.22 $\pm$ 0.09	0.30 $\pm$ 0.00	0.32 $\pm$ NA
<b>22:5(n-3)</b>	0.22 $\pm$ 0.01	0.08 $\pm$ 0.00	1.35 $\pm$ 0.83	0.76 $\pm$ 0.36	2.13 $\pm$ 0.22	0.53 $\pm$ 0.02	0.80 $\pm$ 0.17	0.13 $\pm$ 0.02	0.28 $\pm$ 0.04	0.33 $\pm$ NA
<b>22:6(n-3) DHA</b>	6.91 $\pm$ 0.76	7.08 $\pm$ 0.53	4.49 $\pm$ 0.45	4.38 $\pm$ 0.60	3.79 $\pm$ 0.52	3.92 $\pm$ 0.48	4.62 $\pm$ 2.03	0.35 $\pm$ 0.03	0.82 $\pm$ 0.25	NA
<b>Total SAFA</b>	72.55 $\pm$ 1.56	73.48 $\pm$ 4.42	77.17 $\pm$ 5.61	73.86 $\pm$ 5.35	70.45 $\pm$ 12.5	76.48 $\pm$ 0.79	73.47 $\pm$ 2.15	97.20 $\pm$ 1.57	93.89 $\pm$ 2.04	93.46 $\pm$ NA
<b>total PUFA</b>	16.77 $\pm$ 0.91	15.99 $\pm$ 1.34	13.98 $\pm$ 0.97	15.09 $\pm$ 1.14	17.97 $\pm$ 0.83	15.10 $\pm$ 0.54	16.87 $\pm$ 2.69	1.88 $\pm$ 0.10	3.38 $\pm$ 0.35	3.52 $\pm$ NA
<b>Total MUFA</b>	10.76 $\pm$ 0.35	10.56 $\pm$ 1.17	8.85 $\pm$ 1.20	11.05 $\pm$ 0.93	11.58 $\pm$ 1.51	8.42 $\pm$ 0.25	9.66 $\pm$ 0.82	0.92 $\pm$ 0.05	2.73 $\pm$ 0.31	3.01 $\pm$ NA
<b>Total FA <math>\mu\text{g L}^{-1}</math></b>	15.68 $\pm$ 2.13	19.95 $\pm$ 0.97	11.31 $\pm$ 1.27	9.52 $\pm$ 1.62	30.16 $\pm$ 18.25	8.14 $\pm$ 0.25	6.62 $\pm$ 0.37	28.47 $\pm$ 0.73	21.53 $\pm$ 2.51	13.47 $\pm$ NA
<b>Fa % POC</b>	15.85 $\pm$ 2.89	17.54 $\pm$ 0.99	17.92 $\pm$ 2.02	19.37 $\pm$ 3.41	59.88 $\pm$ 36.30	21.36 $\pm$ 1.59	13.74 $\pm$ 1.40	49.25 $\pm$ 3.54	NA	32.26 $\pm$ NA
<b>DHA:EPA</b>	3 $\pm$ 0.88	3.20 $\pm$ 0.63	2.61 $\pm$ 0.71	2.58 $\pm$ 0.43	1.75 $\pm$ 3.25	2.89 $\pm$ 0.66	2.43 $\pm$ 1.94	1.59 $\pm$ 0.67	2.73 $\pm$ 0.61	NA
<b>(n-3):(n-6)</b>	9.79 $\pm$ 0.15	5.38 $\pm$ 0.37	7.79 $\pm$ 0.12	6.04 $\pm$ 0.13	7.14 $\pm$ 3.19	8.23 $\pm$ 0.09	7.48 $\pm$ 0.21	3.10 $\pm$ 0.03	3.84 $\pm$ 0.04	2.71 $\pm$ NA

Table 4.8: Cont'

Stations n Fatty Acids %	Upwelling			Equatorial	Oligotrophic S			Temperate S	
	30	34	38	45	50	56	60	67	71
<b>14:0</b>	3.10 ± 0.46	3.73 ± 0.20	4.05 ± 0.13	3.21 ± 0.17	2.88 ± 0.20	2.11 ± NA	2.24 ± 1.05	2.99 ± 1.00	4.66 ± 0.32
<b>15:0</b>	0.71 ± 0.04	0.76 ± 0.04	0.76 ± 0.01	0.88 ± 0.04	1.05 ± 0.11	0.73 ± NA	0.79 ± 0.35	0.61 ± 0.10	0.61 ± 0.03
<b>16:0</b>	33.22 ± 0.64	33.71 ± 0.03	34.01 ± 3.87	33.50 ± 0.39	39.12 ± 1.91	39.33 ± NA	31.15 ± 5.18	34.63 ± 3.21	32.30 ± 1.54
<b>16:1(n-7)</b>	1.11 ± 0.10	1.35 ± 0.19	1.46 ± 0.25	1.67 ± 0.11	2.34 ± 0.15	1.51 ± NA	1.27 ± 0.07	4.90 ± 0.21	3.27 ± 0.26
<b>16:2(n-4)</b>	1.98 ± 0.18	3.07 ± 0.20	1.50 ± 0.00	2.33 ± 0.14	2.00 ± 0.27	1.63 ± NA	1.19 ± 0.30	1.33 ± 0.47	1.07 ± 0.12
<b>16:3(n-4)</b>	0.25 ± 0.02	0.29 ± 0.08	0.41 ± 0.12	0.43 ± 0.05	0.58 ± 0.05	0.28 ± NA	0.30 ± 0.01	0.35 ± 0.00	0.26 ± 0.09
<b>16:4(n-1)</b>	0.20 ± 0.04	0.22 ± 0.06	0.24 ± 0.06	0.32 ± 0.03	0.26 ± 0.05	0.29 ± NA	0.14 ± 0.08	0.14 ± 0.01	0.22 ± 0.09
<b>18:0</b>	46.00 ± 2.25	34.45 ± 1.87	41.60 ± 5.26	35.92 ± 2.11	32.44 ± 3.82	38.94 ± NA	53.72 ± 8.17	26.76 ± 1.00	20.62 ± 3.04
<b>18:1(n-9)</b>	3.34 ± 0.40	5.21 ± 1.42	4.08 ± 0.17	5.30 ± 0.38	6.32 ± 0.93	4.42 ± NA	3.24 ± 0.14	6.10 ± 2.21	4.56 ± 0.03
<b>18:1(n-7)</b>	0.59 ± 0.07	0.79 ± 0.09	0.64 ± 0.08	1.13 ± 0.51	0.72 ± 0.10	0.48 ± NA	0.44 ± 0.09	1.15 ± 0.04	1.34 ± 0.02
<b>18:2(n-6)</b>	0.95 ± 0.07	1.85 ± 0.18	1.26 ± 0.13	1.64 ± 0.16	1.59 ± 0.50	1.33 ± NA	0.65 ± 0.10	1.73 ± 0.16	1.88 ± 0.01
<b>18:3(n-6)</b>	0.40 ± 0.02	0.35 ± 0.02	0.39 ± 0.04	0.51 ± 0.03	0.34 ± 0.04	0.32 ± NA	0.22 ± 0.04	0.22 ± 0.01	0.25 ± 0.02
<b>18:3(n-3)</b>	0.66 ± 0.06	1.28 ± 0.12	0.79 ± 0.01	0.90 ± 0.04	0.43 ± 0.05	0.37 ± NA	0.18 ± 0.03	0.92 ± 0.05	1.25 ± 0.05
<b>18:4(n-3)</b>	1.55 ± 0.00	2.28 ± 0.31	2.77 ± 1.27	2.84 ± 0.08	3.14 ± 0.14	3.40 ± NA	1.26 ± 0.29	3.36 ± 0.65	4.84 ± 1.90
<b>20:0</b>	1.39 ± 0.06	1.13 ± 0.06	1.07 ± 0.09	1.12 ± 0.08	0.95 ± 0.09	1.06 ± NA	0.77 ± 0.05	0.62 ± 0.06	0.61 ± 0.06
<b>20:1(n-9)</b>	1.15 ± 0.16	2.09 ± 0.19	1.09 ± 0.01	1.86 ± 0.12	0.75 ± 0.23	0.72 ± NA	0.40 ± 0.07	2.11 ± 0.15	4.60 ± 1.55
<b>20:5(n-3) EPA</b>	0.87 ± 0.13	1.99 ± 0.31	1.09 ± 0.03	1.79 ± 0.35	0.94 ± 0.01	0.64 ± NA	0.46 ± 0.12	3.35 ± 1.34	4.63 ± 0.41
<b>22:5(n-3)</b>	0.30 ± 0.08	0.44 ± 0.07	0.39 ± 0.09	0.43 ± 0.09	0.66 ± 0.09	0.43 ± NA	0.38 ± 0.15	1.73 ± 2.05	0.32 ± 0.08
<b>22:6(n-3) DHA</b>	2.77 ± 0.43	5.03 ± 0.53	2.39 ± 0.04	4.21 ± 0.27	3.47 ± 1.90	2.03 ± NA	1.21 ± 0.22	7.00 ± 0.63	12.70 ± 1.08
<b>Total SAFA</b>	84.42 ± 2.39	73.78 ± 1.88	81.49 ± 6.53	74.63 ± 2.15	76.45 ± 4.28	82.17 ± NA	88.67 ± 9.74	65.61 ± 3.51	58.81 ± 3.42
<b>total PUFA</b>	9.92 ± 0.51	16.78 ± 0.76	11.23 ± 1.29	15.40 ± 0.51	13.41 ± 2.00	10.71 ± NA	5.98 ± 0.53	20.13 ± 2.66	27.42 ± 2.24
<b>Total MUFA</b>	6.18 ± 0.45	9.44 ± 1.45	7.27 ± 0.31	9.97 ± 0.66	10.14 ± 0.98	7.12 ± NA	5.35 ± 0.19	14.26 ± 2.23	13.77 ± 1.57
<b>Total FA µg L<sup>-1</sup></b>	9.09 ± 0.49	9.78 ± 0.46	9.01 ± 0.86	4.79 ± 0.10	6.42 ± 0.35	5.72 ± NA	8.73 ± 1.64	13.00 ± 0.79	13.52 ± 0.45
<b>Fa % POC</b>	17.43 ± 2.26	14.14 ± 0.75	18.87 ± 1.81	13.60 ± 1.01	20.96 ± 1.34	21.34 ± NA	32.98 ± 8.28	15.51 ± 1.00	10.17 ± 0.67
<b>DHA:EPA</b>	3.20 ± 0.50	2.54 ± 0.24	2.21 ± 0.24	2.55 ± 0.21	3.67 ± 2.00	3.17 ± NA	2.63 ± 0.15	2.01 ± 1.10	2.74 ± 0.53
<b>(n-3):(n-6)</b>	4.57 ± 0.03	4.98 ± 0.08	4.49 ± 0.09	4.52 ± 0.02	4.47 ± 0.15	4.16 ± NA	4.02 ± 0.01	8.44 ± 0.35	11.20 ± 0.40

FA 22:6(n-3) (DHA), a biomarker for dinoflagellate taxa, and 20:5(n-3) (EPA), a biomarker for diatom taxa, were generally present in small quantities <8% of the total FA, at all locations except stations 2, 4, 67 and 71 where they exceeded 9% in the Temperate domains. The DHA/EPA ratio (low ratios being an index of diatoms) remained high and relatively constant throughout the AMT20 transect suggesting flagellates were dominant.

Other diatom biomarkers such as 16:1(n-7) (Ackman et al. 1968) and 16:2(n-4) (Volkman et al. 1989) were present in small amounts, <5% of the total FA, also suggesting that dinoflagellates were generally more abundant. DHA was the most abundant PUFA at most locations except stations 12, 14, 38 and 60 where 18:4(n-3) (biomarker for Prymnesiophyceae and other flagellates (Chuecas and Riley 1969)) dominated and station 18 where 16:2(n-4) dominated. Overall DHA was higher in the Temperate S domain where 20:5(n-3) and 18:4(n-3) were also abundant. At the same location the FA 16:2(n-4) was found to decrease in comparison to the other domains. The (n-3):(n-6) ratio was greater in the higher productivity domains compared to the Oligotrophic regions ( $t(17)=2.26$ ,  $p=0.037$ ).

**Table 4.9.** Simple regressions and correlations of fatty acids (FA) to individual variables. Sqrt= square root transformation, Ln= natural logarithm transformation. CM T= temperature, S= salinity, POC= particulate organic carbon, PON= particulate organic nitrogen, POP= particulate organic phosphorus, Chl-a= chlorophyll-a. Yellow= positive relationship, Orange= negative relationship.

FA	Simple regression				Correlation						
	CM T °C	lnS	lnMLD m	dMLCM m	lnPOC µg l <sup>-1</sup>	lnPON µg l <sup>-1</sup>	lnPOP µg l <sup>-1</sup>	lnChl-a µg l <sup>-1</sup>	LnC:N (molar)	LnC:P (molar)	LnN:P (molar)
sqrt SAFA %	r <sup>2</sup> = 0.48 p<0.001	r <sup>2</sup> =0.68 p<0.001	r <sup>2</sup> =0.18 p=0.074	r <sup>2</sup> =0.23 p=0.04	r=-0.56 p=0.017	r=-0.73 p<0.001	r=-0.78 p<0.001	r=-0.75 p<0.001	r=0.69 p=0.002	r=0.53 p=0.025	r=-0.13 p=0.6
sqrt PUFA %	r <sup>2</sup> =0.37 p=0.005	r <sup>2</sup> =0.62 p<0.001	r <sup>2</sup> =0.17 p=0.079	r <sup>2</sup> =0.21 p=0.048	r=0.48 p=0.04	r=0.69 p=0.001	r=0.74 p<0.001	r=0.72 p<0.001	r=-0.72 p<0.001	r=-0.57 p=0.015	r=0.12 p=0.62
sqrt MUFA % <sup>a</sup>	r <sup>2</sup> =0.41 p=0.03	r <sup>2</sup> =0.61 p<0.001	r <sup>2</sup> =0.15 p=0.11	r <sup>2</sup> =0.19 p=0.06	r=0.5 p=0.04	r=0.63 p=0.004	r=0.8 p<0.001	r=0.69 p=0.001	r=-0.45 p=0.06	r=-0.51 p=0.03	r=0.09 p=0.7
LnFA µg l <sup>-1</sup>	r <sup>2</sup> =0.001 p=0.89	r <sup>2</sup> =0.09 p=0.2	r <sup>2</sup> =0.05 p=0.36	r <sup>2</sup> =0.18 p=0.07	r=0.57 p=0.014	r=0.2 p=0.41	r=0.09 p=0.73	r=0.01 p=0.96	r=0.3 p=0.22	r=0.55 p=0.017	r=0.25 p=0.3
sqrtFa% POC <sup>a</sup>	r <sup>2</sup> =0.01 p=0.7	r <sup>2</sup> =0.15 p=0.11	r <sup>2</sup> =0.27 p=0.03	r <sup>2</sup> =0.04 p=0.43	r=-0.47 p=0.05	r=-0.74 p<0.001	r=-0.7 p=0.001	r=-0.67 p=0.003	r=0.79 p<0.001	r=0.46 p=0.05	r=-0.32 p=0.19
DHA /EPA	r <sup>2</sup> =0.02 p=0.6	r <sup>2</sup> =0.01 p=0.7	r <sup>2</sup> =0.01 p=0.7	r <sup>2</sup> =0.02 p=0.6	r=-0.13 p=0.63	r=-0.012 p=0.96	r=0.1 p=0.67	r=-0.09 p=0.7	r=-0.19 p=0.46	r=-0.34 p=0.19	r=-0.2 p=0.43
ln(n-3) /(n-6)	r <sup>2</sup> =0.57 p<0.001	r <sup>2</sup> =0.64 p<0.001	r <sup>2</sup> =0.06 p=0.3	r <sup>2</sup> =0.33 p=0.01	r=0.57 p=0.014	r=0.65 p=0.002	r=0.61 p=0.005	r=0.51 p=0.027	r=-0.49 p=0.04	r=-0.21 p=0.4	r=0.26 p=0.28

<sup>a</sup> Non-parametric data: Spearman correlation test used

**Table 4.10.** Forward stepwise and multiple regression analysis of FA to significant predictor variables. A) Includes data from all the domains. B) Data from the higher productivity domains. C) Oligotrophic domains only. Ln = natural logarithm, Chl-a= chlorophyll-a ( $\mu\text{g L}^{-1}$ ), CM T= temperature at the chlorophyll maximum ( $^{\circ}\text{C}$ ), MLD= mixed layer depth (m), dMLCM= distance between CM and MLD (m). NA = data not available.

FA	A) All domains n=19		B) Higher productivity domains n=11		C) Oligotrophic domains n=8	
	Forward Stepwise	Multiple regression	Forward Stepwise	Multiple regression	Forward Stepwise	Multiple regression
sqrt SAFA %	chl-a & CMT $r^2=0.75$ $p<0.001$	$7.11 - (0.61 \times \ln\text{Chl-a } \mu\text{g L}^{-1}) + (7.57 \times 10^{-2} \times \text{CMT})$	CMT, chl-a & dMLCM $r^2=0.95$ $p<0.001$	$6.77 + (0.1 \times \text{CMT}) - (0.29 \times \ln\text{Chl-a } \mu\text{g L}^{-1}) + (6.45 \times 10^{-3} \times \text{dMLCM m})$	None	NA
sqrt PUFA %	chl-a & CMT $r^2=0.65$ $p<0.001$	$6.13 + (1.1 \times \ln\text{Chl-a } \mu\text{g L}^{-1}) - (0.11 \times \text{CMT})$	CMT, chl-a & dMLCM $r^2=0.98$ $p<0.001$	$6.32 - (0.13 \times \text{CMT}) + (0.5 \times \ln\text{Chl-a } \mu\text{g L}^{-1}) - (7.3 \times 10^{-3} \times \text{dMLCM m})$	None	NA
sqrt MUFA %	chl-a $r^2=0.43$ $p=0.002$	$3.253 + (0.94 \times \ln\text{Chl-a } \mu\text{g L}^{-1})$	CMT & dMLCM $r^2=0.83$ $p<0.001$	$5 - (0.11 \times \text{CMT}) - (7.2 \times 10^{-3} \times \text{dMLCM m})$	None	NA
LnFA $\mu\text{g L}^{-1}$	None	NA	None	NA	None	NA
sqrtFa% POC	MLD $r^2=0.27$ $p=0.023$	$2.88 + (0.045 \times \ln\text{MLD m})$	MLD $r^2=0.33$ $p=0.065$	$2.75 + (0.045 \times \ln\text{MLD m})$	None	NA
DHA /EPA	None	NA	None	NA	None	NA
$\ln(n-3) / (n-6)$	CMT $r^2=0.57$ $p<0.001$	$3.33 - (0.085 \times \text{CMT})$	CMT $r^2=0.69$ $p=0.002$	$3.1 - (0.066 \times \text{CMT})$	None	NA

The relationships between FA parameters and environmental variables are shown in Table 4.9 (above). SAFA linearly increased with increasing CM T and S and decreased as the distance between CM and MLD decreased. Whereas PUFA, MUFA and (n-3):(n-6) decreased with increasing CM T and S.

Strong negative correlations were found between SAFA, the percentage of FA in POC (FA% POC) and organic nutrients + chl-a. SAFA and FA% of POC were positively correlated to the seston C:N and C:P ratio. This suggests that stoichiometric and biochemical indicators are tightly interlinked and that an increase in carbon based ratios indicates decreasing food quality. By contrast PUFA, MUFA and the (n-3):(n-6) ratio were positively correlated to seston organic nutrients + chl-a. PUFA was negatively correlated to the C:N and C:P ratios. This indicates better food quality was present at the station with lower C ratios and higher concentration of all organic nutrients and chl-a.

Forward stepwise and multiple regression analyses (Table 4.10) were used to create models able to estimate the proportions of FA from readily available CTD data. In this instance chl-a was included alongside the list of independent variables. Salinity was removed from multiple regressions after it was identified as a collinear predictor.

Stepwise regressions showed that not all the variables contributed significantly as predictors for the FA distribution, however CM T and chl-a concentration were consistent predictors for SAFA and PUFA variability in both scenarios A and B (including and excluding oligotrophic data respectively). The predictability of MUFA changed from chl-a based in scenario A (including data from all domains) to CM T based in scenario B (excluding oligotrophic data). FA% of POC was primarily driven by MLD while the (n-3):(n-6) ratio appeared to be affected mainly by CM T. No variables were significant predictors for organic nutrient distributions in the Oligotrophic domains.

## **4.4 Discussion**

### **4.4.1 Ecological Domains**

Our data show the latitudinal variability of seston macronutrients and FA at the CM across a meridional transect in the Atlantic Ocean during AMT20 (September-November 2010). We assessed this variability within six ecological domains classified following Marañón et al. (2001): Temperate N and S, Oligotrophic N and S, Upwelling and Equatorial. Shifts from the original domain boundaries were identified, highlighting a latitudinal expansion of the oligotrophic domains. The Oligotrophic N domain extended from 18° to 38°N compared to the division of Marañón et al. (2001) of 20° to 35°N. The Oligotrophic S

domain from 5° to 32°S was found to have shifted from 5° to 32°S with an expansion of the Equatorial domain from 5°N - 5°S to 4°N-18°S. This reflected temporal variations of the upwelling and equatorial zonal winds that follow the intertropical convergence zone seasonality (Grotsky et al. 2008) and the influence of a la Niña episode triggering increased SST in the Atlantic Ocean.

Strong food quality latitudinal variations occurred in response to phytoplankton distribution and production. The scale and structure of these variations are ecosystem-dependent, since each of the domains considered in this study is identified by particular hydrographical and hydrological characteristics affecting microplankton composition and its nutrients. For instance, temperate areas are generally cooler and characterised by a strong seasonal signal (light, temperature and nutrient variations) (Stramma 2001). In this study the Temperate N domain was sampled in boreal autumn, where low chl-a concentrations  $<1 \mu\text{g L}^{-1}$ , low inorganic nutrient concentrations ( $\text{N+N} \leq 2.6 \mu\text{M}$ ,  $\text{SRP} \leq 0.16 \mu\text{M}$ ) and higher POC:Chl-a ratios ( $>130:1$ ) indicating possible post-bloom conditions. Whereas the Temperate S was sampled during austral spring, in particular, the southernmost station (71) was characterised by a shallow mixed layer and higher inorganic nutrient concentrations ( $\text{N+N} = 4.05 \mu\text{M}$ ,  $\text{SRP} = 0.55 \mu\text{M}$ ), low POC:Chl-a ratios (98:1) and high chl-a concentration ( $2.1 \mu\text{g L}^{-1}$ ). These values were still lower than the maximum chl-a concentrations found in the surface waters off the Patagonian shelf during bloom conditions  $\geq 3\text{-}5 \mu\text{g L}^{-1}$  (Romero et al. 2006). This indicates that the southernmost stations of the transect represented the outer boundary of an austral spring bloom, affected by the colder subantarctic Falkland (Malvinas) and South Atlantic currents (Stramma 2001; Garcia et al. 2008).

The equatorial upwelling region is generally characterized by constant solar radiation and by a series of wind driven currents converging and pushing the water masses in separate directions (intertropical convergence zone) (Stramma 2001; Grotsky et al. 2008). This causes a shoaling of the chl-a maximum and of the thermocline producing a permanent uplifting of cold nutrient-rich waters into the mixed layer. During AMT20 the POC:Chl-a ratio was low at this location ( $<71:1$ ) whilst the chl-a concentration was high, reaching  $1.37 \mu\text{g L}^{-1}$ , within the values previously found by Marañón et al. (2000). This indicated the abundance of fresh material in the area.

The Upwelling domain is adjacent to regions of downwelling in the subtropical gyres in the Oligotrophic N and S domains, driven by Ekman pumping pushing nitrate-rich waters away from the surface waters (Sarmiento and Gruber 2006). These oligotrophic regions show only weak seasonal changes affected by the wind patterns and are characterised by

a permanently stratified water column with a deep CM (Stramma 2001). In oligotrophic domains during AMT20 the CM chl-a content was at its lowest, reaching maximum concentrations of 0.5 - 0.6  $\mu\text{g L}^{-1}$  as expected in these waters (Grotsky et al. 2008; Navarro et al. 2012). A few differences between the two oligotrophic areas were identified. Firstly the DCM (deep chl-a maximum) was much deeper in the Oligotrophic S. Secondly, contrarily to the N, the inorganic nutrient signal in the Oligotrophic S domain during AMT20 was detectable and therefore inorganic nutrients were still quantifiable (although still depleted). In particular, this domain was characterised by relatively high SRP values ( $\geq 1.2 \mu\text{M}$ ). This suggests that the Oligotrophic N and S domains have different biogeochemical regimes (Mather et al. 2008) and that in contrast to the North Atlantic gyre, new production in the Oligotrophic S is potentially limited by factors and/or nutrients other than N+N and SRP (Moore et al. 2009).

Little can be said about the Equatorial domain since only 1 sampling station was located within its boundaries (station 45). Overall, the tropical area that includes the Equatorial domain is characterised by a complicated circulation system, composed of several zonal currents and countercurrents moving in all directions (Stramma 2001) and affecting inorganic nutrient availability as well as primary production. The POC:Chl-a ratio and Chl-a concentrations at station 45 were low at 49:1 and 0.72  $\mu\text{g L}^{-1}$  respectively, indicating the presence of a limited amount of fresh material.

#### 4.4.2 Food Quality AMT20

The distribution of the different particulate organic nutrients was an important indicator of food quality across the AMT20 transect. POC, PON and POP at the CM increased with chl-a concentration and produced significant variability in food quality between the higher productivity (Temperate, Upwelling and Equatorial) and the oligotrophic domains (Oligotrophic N and S). This variability is caused by the lack of homeostasis in phytoplankton. Since the cell's nutrient uptake and growth varies with environmental conditions, in turn their biochemistry and stoichiometry varies according to the nutritional status (Geider and La Roche 2002; Sterner and Elser 2002). Therefore phytoplankton show strong fluctuations in their C:P and N:P ratios (less for C:N) (Geider and La Roche 2002; Sterner and Elser 2002) and also undergo composition changes in their lipid classes as the availability of nutrients changes throughout the season (Kattner 1983; Mayzaud et al. 1989).

Variations in organic nutrient concentrations and their proportions, along the AMT20 transect, were accompanied by large changes in CM stoichiometry. The C:N of the CM seston seemed to be the most consistent, suggesting SRP and POP triggered strong

fluctuations in N:P and C:P. Significantly higher C:N ratios were found in the oligotrophic domains, in agreement with Martiny et al. (2013) and some in the post-bloom area of the Temperate N. C:P ratios were higher in the Oligotrophic N but remained below Redfield in most of the Oligotrophic S. At the stations where N:P was at its lowest C:P was also lower, affected by the currents increasing SRP and consequently POP concentrations.

Although some of the highest N:P ratios of the transect were found in the Temperate and the Upwelling domains (higher productivity), overall the ratios remained low throughout, suggesting no dissimilarity between the two productivity areas and indicating widespread N-limitation of the seston at the CM in the Atlantic. This contrasts with the study of Martiny et al. (2013) who suggested that the stoichiometry of tropical and subtropical oceans generally coincides with higher N:P ratios, greater than the canonical Redfield ratio. Their observations suggest that communities dominated by diatoms had a lower N:P and C:P ratio compared with communities dominated by Cyanobacteria. Therefore latitudinal and depth related changes in phytoplankton assemblages could affect stoichiometric variation. Although cyanobacteria are abundant in the tropical and subtropical Atlantic Ocean, their biomass peaks at the surface (Goebel et al. 2010), therefore having a reduced effect on organic CM stoichiometry.

In addition, the concept of an N-limited Atlantic Ocean has already been proposed by Graziano et al. (1996), Mills et al. (2004), Moore et al. (2004) and Moore et al. (2008) based on inorganic nutrient distributions across the basin and their concentrations. This however excludes areas such as the Sargasso Sea and the subtropical N Atlantic off the Canaries, shown to be P-limited (Wu et al. 2000; Moore et al. 2008). In the current study, the lowest particulate organic N:P ratios were found in the middle of the upwelling (station 34), at station 8 affected by the North Atlantic Current and the northernmost part of the Oligotrophic S domain (station 50) affected by the South Equatorial Current and Countercurrent. Interestingly, during AMT20, organic N:P ratios did not correspond to the measured inorganic N+N:SRP ratios. Falkowski (1997) suggested these differences between organic and inorganic nutrient ratios may be caused by an imbalance between denitrification and N<sub>2</sub> fixation. Overall inorganic nutrient ratios (N+N:SRP) were found to be mostly below Redfield values except at two locations which corresponded to extremely low organic N:P (station 8 and 34). This could also indicate that, either N-uptake was limited by other environmental factors or that phytoplankton cells (such as diatoms) with lower cellular N:P ratios were abundant. The latter suggestion however was not corroborated by FA data. The FA signature of dinoflagellates (DHA and 18:4(n-3)), with generally a higher cellular N:P ratio (average phylum N:P ratio ~30:1 and higher C:N ratio (Quigg et al. 2003)), was more prevalent than that of the diatoms' (average group N:P

ratio of ~10:1 (Quigg et al. 2003)). The DHA:EPA was also generally >2 (except at station 12 and 18).

Therefore, with lower C:N ratios and with more stations with N:P ratios close to Redfield values, the CM seston in the Temperate S and the Upwelling domains was of better quality. This was supported by the FA data showing decreased SAFA and increased PUFA and (n-3):(n-6) ratios in the higher productivity domains and the Temperate S in particular. SAFA, total FA and % FA in POC were all positively correlated to C:N and C:P ratios, whereas PUFA, MUFA and (n-3):(n-6) all decreased as C:N and C:P increased. This indicates a close coupling between C stoichiometry and biochemistry. This is of particular interest since in recent years ecologists have been debating the definition of food quality. Criticisms over the use of stoichiometry (Tang and Dam 1999) as a standalone quality indicator have been common. We suggest that either indicator can be effective when assessing the effects of C on the ecosystem.

#### 4.4.3 Food Quantity and Quality Predictability on AMT20

Overall the variability of food quantity and quality (both stoichiometry and FA) across the AMT20 transect was primarily caused by chl-a, CM T and dMLCM. This is supported by previous studies which showed that latitudinal variations in seston organic nutrients, stoichiometry and biochemistry vary systematically by ecosystem (Martiny et al. 2013) and are driven by variations in primary production regulated by light availability (Geider and La Roche 2002), the distribution of inorganic nutrients and abiotic and biotic factors such as temperature, currents (Weber and Deutsch 2010) and phytoplankton species composition (Geider and La Roche 2002). The predictability of food quantity on AMT20, based on the relationships between organic nutrients and CTD measured environmental factors, was effective when considering the whole transect or just the higher productivity domains. In particular PON and POP concentrations appear to be confidently predictable ( $r^2 > 0.73$ ) from chl-a concentration (obtained from calibrated CTD fluorescence data), the distance of the CM from the MLD and inorganic nutrients (N+N for PON only).

In comparison POC from this study appeared to be affected by different environmental factors and the distribution of POC was best predicted by backscatter and CM T. This relationship supports previous findings that *in situ* optical parameters such as backscatter and transmission can be used as reliable indicators of POC concentration in the water column (Morel 1988; Stramski et al. 1998; Martinez-Vincente et al 2013). On the other hand, when considering the Bigelow Laboratory dataset, the predictive variables for POC were replaced with similar parameters to those predicting PON and POP as shown in Table 4.5. This could be due to potential disparity between methodological protocols and

analyses but it also suggests that optical parameters and the properties defining mixed layer depth and the chlorophyll maximum could be linked. This is since the relationship between bio-optical properties and measured properties of seawater can vary among datasets. The frequency over which the measurements are taken can also affect relationships between parameters and their statistical significance when comparing datasets from the same regions of the oceans. The latter also highlights that environmental predictors can differ between ecological domains.

The predictability of all particulate organic nutrients loses resolution ( $r^2$  decreases) when the higher productivity domains are considered separately. SAFA, PUFA, MUFA and (n-3):(n-6) were all confidently predicted from environmental variables and their predictability gained strength when the higher productivity domains were considered separately ( $r^2 \geq 0.7$ ).

#### 4.4.4 Food Quantity and Quality Variation Over Time

At lower food quantities carbon limitation reduces the substrate available to provide energy for the organism (Anderson and Hessen 1995). However, low food quality limits efficient nutrient uptake and reduces energy availability to the consumers independent of quantity (Hessen and Anderson 2008; Schoo et al. 2012). The quality and quantity of food available to consumers influences food web dynamics (Schoo et al. 2012) therefore affecting the biogeochemical cycles of the oceans through feedback mechanisms (Buitenhuis et al. 2006). Therefore monitoring food variability in the Atlantic Ocean over time can help quantify the effects of changing environmental conditions on the ecosystem.

The use of empirical models to predict organic nutrient distributions at the CM over time can be a useful tool to compensate for the lack of observational data. In this study, predicted POC and PON concentrations were successfully used in an investigation of long term trends of food quantity and quality over seven years in the Atlantic Ocean. Clear decreasing and increasing linear trends in particulate organic nutrient concentrations were seen from 2003 to 2010 at the Temperate N ( $\sim 45^\circ\text{N}$ ) and S ( $\sim 40^\circ\text{S}$ ) domains (respectively) of the Atlantic Ocean. At  $\sim 45^\circ\text{N}$ , between 2003 and 2010, POC and PON decreased 45% and 72% respectively whilst at  $\sim 40^\circ\text{S}$  POC and PON increased 450% and 370% respectively.

However, stations  $45^\circ\text{N}$  and  $40^\circ\text{S}$  shown in Figure 4.8 and 4.9 are strongly affected by seasonal variations in environmental parameters. Therefore the increasing and decreasing trends highlighted above should be interpreted with caution. AMT12, 14 and 16 took place during late boreal spring rather than boreal autumn when AMT 15, 17, 18

and 20 were sampled. Therefore some seasonality effects on phytoplankton production and chl-a, that reflected neither summer nor winter extreme conditions, are to be expected (Figure 4.6). However, Aiken et al. (2009) suggest that inter-annual variability of chl-a was low in all provinces during AMT1 to AMT17. Our data also suggests that the seasonal signal didn't appear to affect the overall trends in organic nutrient concentrations (Figure 4.8 and 4.9). This is since even after taking out the data from AMT12, 14 and 16, the linear relationships between POC and PON over time at ~45°N and ~40°S still persisted ( $r^2 \geq 0.5$ ); although, due to the reduced number of data points, the statistical significance decreased ( $p > 0.05$ ).

Extreme weather events can also have a significant impact on phytoplankton biomass. This is supported by previous findings suggesting that current climate trends (1998-2005) are coupled with a decrease in phytoplankton production in the North Atlantic Subtropical and Tropical Gyre (Temperate N and Oligotrophic N domains) (Tilstone et al. 2009). Aiken et al. (2009) also showed that between AMT1 to AMT17 there was evidence of perturbation from El Niño/La Niña–Southern Oscillation (ENSO) events in 1997-1998 and 1998-2000 causing a downward trend in chl-a concentration. Additionally Zhai et al. (2013) suggested a correlation between the variability of phytoplankton blooms in the North Atlantic and NAO. CM POC concentrations from AMT12 to AMT20 (2003–2010) in the North Atlantic at ~45°N show a positive trend with the Multivariate ENSO Index (MEI) (NOAA 2012) ( $r^2=0.42$   $p=0.1$ ) although, possibly due to the lack of a clear temporal trend as shown in Figure 4.8, the relationship was not statistically significant. On the other hand, CM PON concentrations at 45°N showed a clear positive relationship to MEI ( $r^2=0.7$   $p=0.02$ ) (data not shown). This suggests that food quantity in the North Atlantic could be affected by climate forcing and that the strong ENSO event in 2010 (NOAA 2012) could have contributed to lower POC and PON concentrations during AMT20.

Little information on food quality over time is available, however the CM C:N ratio in the North Atlantic at ~45°N from 2003 to 2010 was also related to MEI although possibly due to the small sample number, the trend was not statistically significant ( $r^2=0.62$   $p=0.1$ ). Interestingly, chl-a concentration at the CM in the Upwelling domain showed a weak decreasing trend with increasing MEI but again possibly due to the small sample number it was not statistically significant ( $r^2=0.36$   $p=0.16$ ). This could suggest that the intensity of the upwelling phenomena in the equatorial Atlantic could be affected by ENSO, however more data is necessary to test this hypothesis. In addition, we must point out that although Chl-a on AMT20 was calibrated following the method of previous cruises, it included unexplained systematic differences and the average values were 42% higher than the average values of AMT12–AMT18 (Figure 4.6). This difference was not reflected in

variations of POC concentrations between cruises, which in fact appeared mostly comparable or lower as shown in Figure 4.8 and 4.9, indicating a possible measurement error in chl-a.

#### 4.4.5 Summary and Conclusions

Data from the AMT20 cruise were used to examine the variability of food quantity (particulate organic nutrient concentrations) and quality (stoichiometry and fatty acid concentrations) along an Atlantic Meridional transect including six ecological domains. Nutritious food included seston with lower C:N ratios, N:P ratios close to Redfield values, a higher proportion of the essential key fatty acid markers PUFA and lower SAFA. Strong latitudinal food quantity and quality variations occurred as hypothesised at the CM in the Atlantic Ocean in response to changes in phytoplankton, organic matter and organic nutrients. Data from the AMT20 transect show that the subtropical and tropical Atlantic Ocean is characterised by warm, well-stratified and food quality-poor waters separated by the equatorial upwelling, a source of semi-permanent food quality-rich water near the Equator. At the 2 extremities of these oligotrophic domains the temperate regions of the North and South Atlantic are characterised by season-dependent food quality-rich waters.

Changes in food quantity, determined from POC and PON concentrations, during AMT20, were accompanied by variations in food quality across the ecological domains. Higher POC and PON content generally coincided with lower C:N ratios and N:P ratios closer to Redfield values throughout the transect, except for post-bloom areas. Additionally, as seston stoichiometry decreased, MUFA decreased and PUFA increased indicating a close coupling between C stoichiometry and biochemistry which are both effective food quality indicators.

Importantly, organic ratios were not related to the supply ratios and the low organic N:P ratios at the CM found across the entire meridional transect are possibly indicative of a nitrogen limited ocean as suggested by past studies focusing on inorganic nutrients (Graziano et al. 1996; Mills et al. 2004; Moore et al. 2008).

Overall POC and PON concentrations can be predicted from observed environmental parameters collected from CTD sensors and these empirical relationships can be used to estimate food quantity, verifying our second hypothesis. However, due to the uncertainties caused by variations in the measured parameters between cruises (Figure 4.6) food quality (C:N) appeared less straight forward to predict. Therefore more data are needed to reduce these uncertainties and determine the validity of these relationships between observations and food quality calculations to confidently predict stoichiometric ratios.

Food quantity and quality have declined over time in the temperate region of the North Atlantic whilst POC and PON concentrations appear to have increased in the South Atlantic temperate region. From 2003 to 2010 the PON concentration in the North Atlantic temperate domains appeared to be related to the MEI, indicating that current trends in climate affect the availability and the quality of the food available to secondary producers in the Atlantic Ocean. These changes in food availability and stoichiometry could therefore impact the ocean's ecosystems on many levels, such as altering oceanic nutrient cycles (Arrigo 2005), organic matter export (quality and rates) and zooplankton metabolism and productivity (Nobili et al. 2013, chapter 3) propagating higher up the food chain. Therefore, alongside latitudinal changes, monitoring temporal variations in food quality could help us identify the long term effects of climate change on oceanic ecosystems.

# **CHAPTER 5**

## 5. The respiration and egg production of some copepod species along an Atlantic Meridional Transect

### 5.1 Introduction

The basal metabolic rate of a copepod, measured via rates of oxygen consumption, reflects its minimal energy requirement for survival and therefore the maintenance of basic physiological processes (Withers 1992). Copepod egg production rates (EPR) denote the ability of the organism to allocate energy for growth, representing the reproductive success and the recruitment potential of a species. The respiration rates and EPR therefore, represent an organisms' health and well-being as well as their ability to acclimatise and their level of adaptation to the habitat, closely linked to their evolutionary history (Hernandez-leon and Ikeda 2005).

Since copepods can constitute up to 98% of total mesozooplankton biomass across the Atlantic Ocean (Isla et al. 2004), measuring their respiration rates and EPR can help evaluate the response of mesozooplankton to latitudinal variation in habitat conditions. Temperature and food (quantity and quality) are the major environmental factors affecting EPR (Calbet and Agustí 1999), whereas several biotic and abiotic factors can affect respiration rates. Overall Ikeda (1985) suggests that up to 95% of the variation in the basal or routine oxygen consumption rate of copepods is due to the effect of body size and temperature. These relationships underpin the Metabolic Theory of Ecology (MTE), summarised in eq. 5.1 (Gillooly et al. 2001; Brown et al. 2004), applicable to all organisms living within the range of biologically relevant temperatures from 0 to 40°C.

$$R = R_0 M^b e^{-E_a/kT} \quad (5.1)$$

where  $R$  is the metabolic rate here defined as respiration;  $R_0$  is a normalisation constant, independent of body size and temperature, in the same units as  $R$ ;  $M$  is the body mass and  $b$  is the allometric scaling exponent for body size (Kleiber's law);  $E_a$  in eV is the activation energy (Arrhenius relationship), calculated by the slope between the regression of  $\ln$  metabolic rate and the reciprocal of the absolute temperature  $1/kT$  (°K) and  $k$  is the Boltzmann or Gas constant ( $8.61731 \times 10^{-5}$  eV  $K^{-1}$ ).

In equation 5.1 the allometric effect on metabolic rates is described by Kleiber's law (equation 1.1 chapter 1) which assumes a constant mass exponent  $b$ , scaling to the

quarter power ( $b=3/4$ ) and therefore suggesting that inter- and intra-specific weight-normalised respiration rates decrease with increasing body size. This is supported by field data showing higher weight-specific respiration rates in smaller copepods (Ivleva 1980; Ikeda 1985). Interspecific body size variations are also known to vary geographically following temperature, latitudinal gradients and food availability (Ivleva 1980). For instance, mean body mass of epipelagic zooplankton in the Atlantic (Gallienne et al. 2001) and western Pacific Ocean (Ikeda et al. 2001; Ikeda 1985b) have been found to decrease latitudinally with increasing temperatures.

In the MTE, the relationship between temperature and metabolism is constrained by the Arrhenius equation (equation 1.2 chapter 1) with the parameter  $E_a$  (activation energy) indicating the sensitivity of the reaction rate to temperature. The higher the  $E_a$ , the greater the metabolic rate will increase with temperature (Vaquer-Sunyer et al. 2010; Yvon-Durocher et al. 2012). Temperature affects the respiration of aquatic organisms more than any other abiotic factor. Metabolic rates increase exponentially with temperature (e.g. Ivleva 1980; Ikeda 1985). In the ocean SST (Sea Surface Temperature) ranges from  $\sim -2$  to  $30^\circ\text{C}$ , varying on spatial and temporal scales. Annual changes in temperature are driven by seasonal processes which are in turn affected by latitudinal gradients. For instance, mid-latitude SST can vary up to  $9 - 10^\circ\text{C}$ , while in more stable polar and tropical regimes the seasonal effect ranges from  $0$  to  $2^\circ\text{C}$  (Hernandez-Leon and Ikeda 2005). Therefore, species living in polar and tropical regions are more specifically adapted to these conditions. This can result in species having limited ranges of physiological tolerance and therefore are less likely to endure prolonged exposure to unfavourable conditions and large habitat changes (Mauchline 1998). This sensitivity of a species to temperature variation can be estimated with the van't Hoff rule or  $Q_{10}$  index (equation 1.3 chapter 1) with the higher the index, the more sensitive the species is to temperature variations.

The competing hypothesis to the MTE is the Evolutionary trade-off theory (ETO) (Clarke 2004), suggesting that interspecific differences and other environmental factors must be taken into account when considering metabolic patterns. For instance, the value of the allometric exponential  $b$ , was found to vary significantly between animal taxa (Clarke 2004) rather than scaling consistently to the quarter power as previously suggested (Gillooly et al. 2001; Brown et al. 2004). Other studies have also shown that oxygen consumption rates of copepods can vary under a range of different environmental conditions such as salinity, pressure, light and in relation to the diel rhythms and swimming activity of the animal (Mauchline 1998; Hernandez-Leon and Ikeda 2005).

Feeding history can also play a role in regulating resting and routine metabolic rates as shown in Nobili et al. (2013) (chapter 3), Kiorboe et al. (1985) and Thor (2002, 2003).

In general, previous research has focused on the study of the response of mixed copepod populations to a variety of environmental factors. This helps in identifying patterns across a wide range of environmental gradients and in forming theories related to the effects of environmental variability on the metabolic response of a population (e.g. MTE). This generalisation is reflected in the mixed datasets available to date (e.g. Hernandez-Leon 2005; Ikeda 2007). However, the literature lacks information on the species-specific response of physiological rates to habitat changes.

The aim of this study was to examine the variability of respiration and EPR for different species across natural environmental gradients in the Atlantic Ocean. The AMT is an area of particular interest for the study of metabolic variation of copepod responses to biotic and abiotic factors since it covers  $\sim 120^\circ$  degrees of latitude, and crosses a range of biogeochemical “domains” (Banse 1974; Longhurst 1995; Marañón et al. 2001). EPR was measured in order to evaluate the effects of temperature on the overall productivity of the copepods and identify differences in species-specific reproductive strategies. We also aimed to examine and validate the temperature and mass dependency of copepod respiration with predicted MTE values and compare the calculated coefficients with those expected by the MTE hypothesising that body mass and temperature are not the only factors affecting copepod metabolic rates. Weight-specific respiration rates were expected to increase with temperature and to decrease with increasing body size. We also hypothesized that higher  $Q_{10}$  values would be found in mesopelagic species with a potentially lower tolerance to increasing temperatures.

## 5.2 Methods

Data were collected on board RRS James Cook between the 13<sup>th</sup> of October 2010 and the 21<sup>st</sup> of November 2010 as part of the Atlantic Meridional Transect programme (AMT 20) (<http://www.amt-uk.org/>) between Southampton (UK) and Punta Arenas (Chile) (Figure 4.1 in chapter 4).

Copepod respiration rates were measured across 5 ecological domains: Oligotrophic N and S, Upwelling, Equatorial, and Temperate S (Marañón et al. 2001) from station 14 to station 71. EPR rates were measured across 6 ecological domains: Oligotrophic N and S, Upwelling, Equatorial, and Temperate N and S (Marañón et al. 2001) from station 4 to station 71.

### 5.2.1 Experimental conditions

Copepods were obtained every other day with a 200 µm WP2 bongo net. Vertical net hauls from 200 m were carried out at pre-dawn (4-5 am GMT). Upon recovery, the sample was immediately diluted into darkened 10 L buckets and transferred to a temperature controlled laboratory. Adult females of different pelagic species and size ranges were selected for metabolic rate experiments and handled and acclimatised as described in section 2.3.4.

**Table 5.1.** *In situ* temperature at the surface, chlorophyll maximum (CM) and 200 m at the stations sampled during AMT20 for determination of copepod physiological rates.

Station	Temperature °C at depth		
	Surface	CM	200 m
4	15.7	16.5	11.65
8	17.24	16.62	12.66
12	20.1	16	13.83
14	23.4	18.2	18.5
22	26.5	22.7	18.6
26	27.2	22.3	19.1
30	27.4	23	15.9
34	28.4	19.8	11.6
38	29	26.8	13
45	27.2	20.1	13
50	24.1	22.2	13.6
56	24.3	21.1	18.8
60	22.4	19.8	16.2
67	16.3	16	14.5
71	12.9	11.7	7.7

Medium to large species were preferentially selected as these were considered to be stronger migrators (crossing a wider range of conditions) than smaller species which are predominantly found in the upper euphotic layer. Based on depth profiles of temperature, vertically migrating copepods may experience large temperature changes of up to 16°C within the upper 200 m (Table 5.1). The “*in situ*” range of incubation temperatures were therefore selected based on the water temperatures at 200 m, the chlorophyll-a maximum (CM) and the surface ( $\pm 0.3^\circ\text{C}$ ). For this reason, at each station, all temperatures within the sampled upper 200m were considered *in situ*, assuming that the selected copepods traversed this full depth range. Incubations also took place at temperatures outside the range experienced within the upper 200 m.

Routine oxygen consumption rates (24 hour incubation in the dark) were determined for individual copepods at a range of *in situ* and temperatures outside the sampling range (Table 5.6 in supplementary material section 5.5). Oxygen consumption was determined by Winkler titration and measured as described in section 2.3.5. Oxygen saturation at the end of the incubations was above 90%. After the analysis the specimens used in the incubations were picked and preserved in 4% formaldehyde solution for later identification and determination of dry weight as stated in section 2.3.6 of Ch. 2. The respiration was measured on individual copepods and the rates were all dry weight adjusted. For consistency throughout this thesis the respiration and mass units are reported in ( $\mu\text{l O}_2$ ) and (mg dw) respectively. Oxygen consumption rates expressed in units of carbon were used as an index of minimum food requirement (Omori and Ikeda 1992). Respiration rates were converted to carbon units using a protein based RQ of 0.97 with  $\mu\text{l O}_2 \text{ ind}^{-1} \text{ h}^{-1} \times \text{RQ} \times 12/22.4 = \mu\text{g C ind}^{-1} \text{ h}^{-1}$  (Omori and Ikeda 1992).

Egg production was determined when possible, at a range of *in situ* and temperatures outside the sampling range. The data are reported in supplementary Table 5.7 in section 5.5. Chlorophyll-a and nutrient concentrations ( $\mu\text{g L}^{-1}$ ) were also measured at the CM.

### 5.2.2 Temperature and allometric-dependent metabolic rates

Respiration rates were analysed as a function of body size and temperature, and compared with the MET-derived estimates of respiration (equation 5.1) (Gillooly et al. 2001; Brown et al. 2004). The values for the coefficients  $R_0$ ,  $b$  and  $E_a$  were empirically derived  $\pm$  SE (SyStat® software) using a non-linear least-squares method with a Gauss-Newton algorithm.

The 5 most re-occurring species within the dataset, covering a range of temperatures, were also considered separately.

The sensitivity of copepod respiration to temperature variation was calculated applying the  $Q_{10}$  index. This determines the factor by which a 10 °C rise in temperature will cause an exponential increase in respiration; the higher the values, the greater sensitivity of the species to temperature. There are several formulas used to calculate the  $Q_{10}$  index, all derivatives of the van't Hoff rule, although all vary on their respective approaches; for instance, in equation 5.2 (Ivleva 1980) and 5.3 (Raven and Geider 1988), contrarily to equations 5.4 (van't Hoff) and 5.5 (Hernandez-Leon and Ikeda 2005), the formulas assume that the  $Q_{10}$  coefficient can be derived by the Arrhenius relationship.

$$Q_{10} = \left( \frac{\text{Log}_{10} e \times 10}{k} \right) \frac{E_a}{T_1 T_2} \quad (5.2)$$

In equation 5.2 (Ivleva 1980)  $e$  is the base of the natural log,  $E_a$  is the activation energy,  $T_1$  and  $T_2$  correspond to the lowest and the highest absolute temperatures and  $k$  is the gas constant ( $8.62 \times 10^{-5} \text{ eV K}^{-1}$ ). The second derivative of the van't Hoff equation gives:

$$Q_{10} = e^{10 E_a / k T^2} \quad (5.3)$$

Here  $T$  is the average absolute temperature range (Kelvin). The most common version of the equation is given in 5.4:

$$Q_{10} = (R_2 / R_1)^{10 / (t_2 - t_1)} \quad (5.4)$$

Where  $R_2$  and  $R_1$  are the respiration rates corresponding to temperatures  $t_2$  and  $t_1$  in degrees Celsius (or Kelvin). Equation 5.4, contrarily to equation 5.2, 5.3 and 5.5 does not integrate the metabolic rates with a sequential increase in the independent variable value however; it is often used to adjust respiration rates from the measured temperature to a consistent temperature (e.g. 15 or 20°C). Alternatively the  $Q_{10}$  can be resolved graphically:

$$Q_{10} = e^{10 \times \text{slope}} \quad (5.5)$$

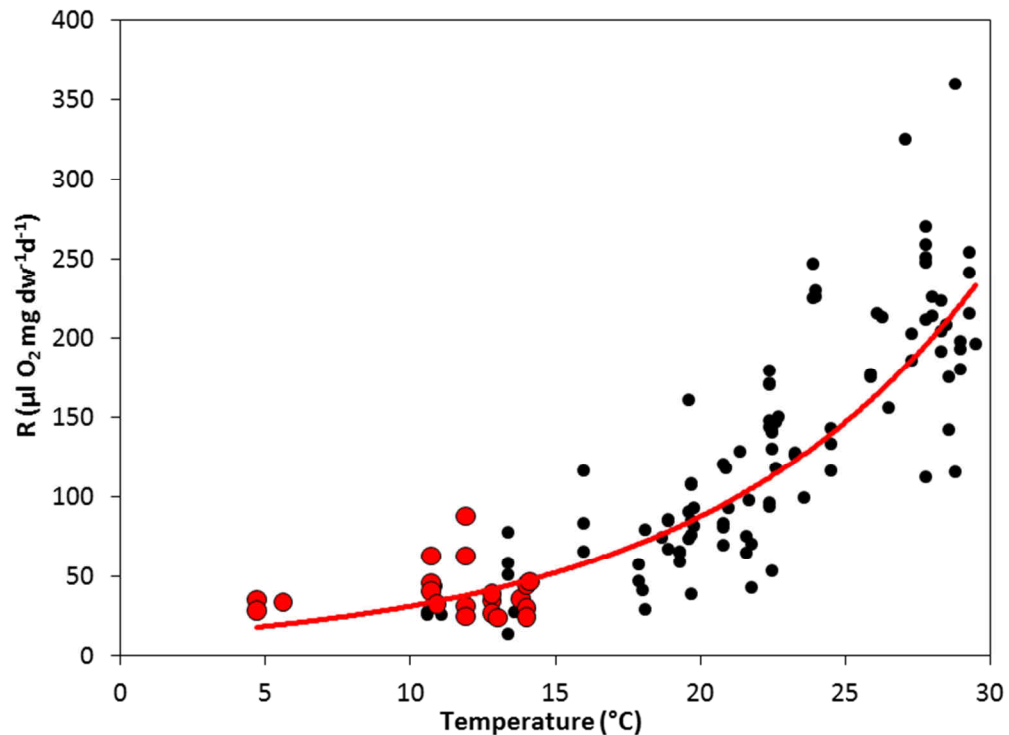
Where the slope is the gradient obtained from the linear regression between the natural log of the respiration rate and temperature (degrees Celsius). The results obtained from these different equations are compared and discussed below.

### 5.3 Results

The AMT20 meridional transect crossed 6 ecological domains partitioned according to Marañón et al. (2001) as discussed in chapter 4 and shown in Figure 5.1. Surface temperatures (SST) ranged from 11 to 29°C as shown in Table 5.1 and salinity (S) ranged from 34.5 to 37.5 (not shown). Stations from the northern hemisphere were sampled during boreal autumn while stations from the southern hemisphere were sampled during austral spring. The sampling took place during a La Niña episode which developed in the eastern and central tropical Pacific in mid-2010 and lasted until early 2011 (NOAA 2012) accompanied by temperature anomalies (above-normal) in the Atlantic Ocean (WMO 2012).

### 5.3.1 Temperature and allometric-dependent respiration rates

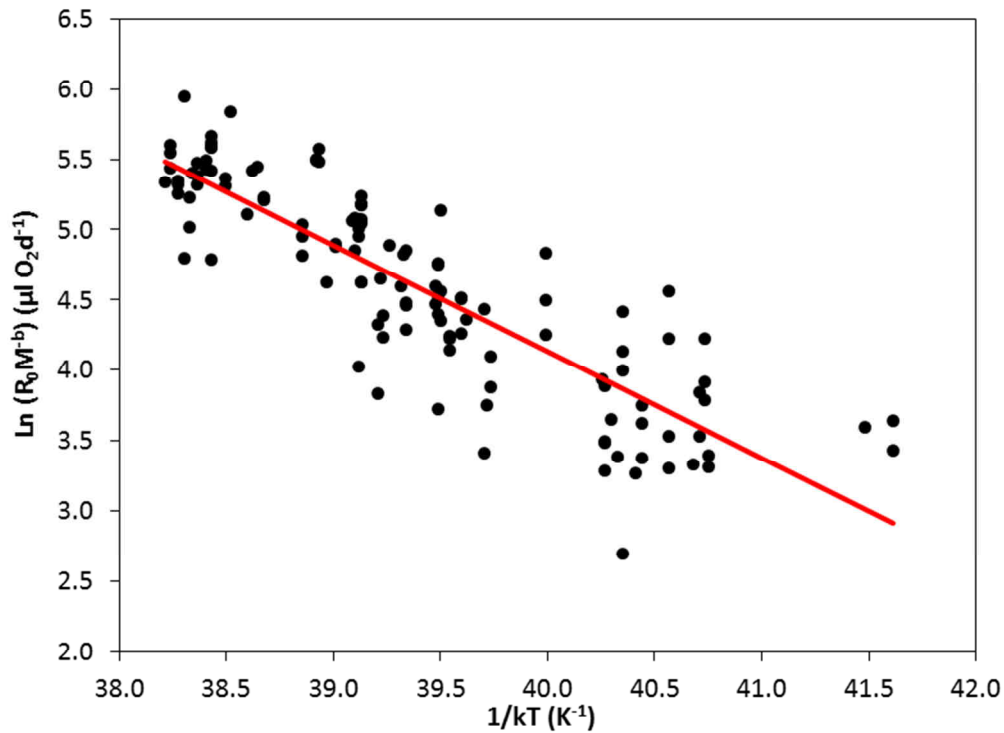
The body mass of the copepods selected for the experiments varied from 0.09 to 0.4 mg dry weight. All metabolic rates were dry weight normalised and reported in Table 5.6 (in the supplementary material section 5.5).



**Figure 5.1.** AMT20 relationship between temperature (°C) and copepod dry weight adjusted respiration rates ( $\mu\text{L O}_2 \text{ mg dw}^{-1} \text{ d}^{-1}$ ). The red line represent the exponential relationship fitted through all the data  $R = 9.4^{(0.11T)}$   $n=123$ . The red markers represent respiration rates at temperatures outside the sampled range, the black markers represent respiration rates measured at *in situ* temperatures.

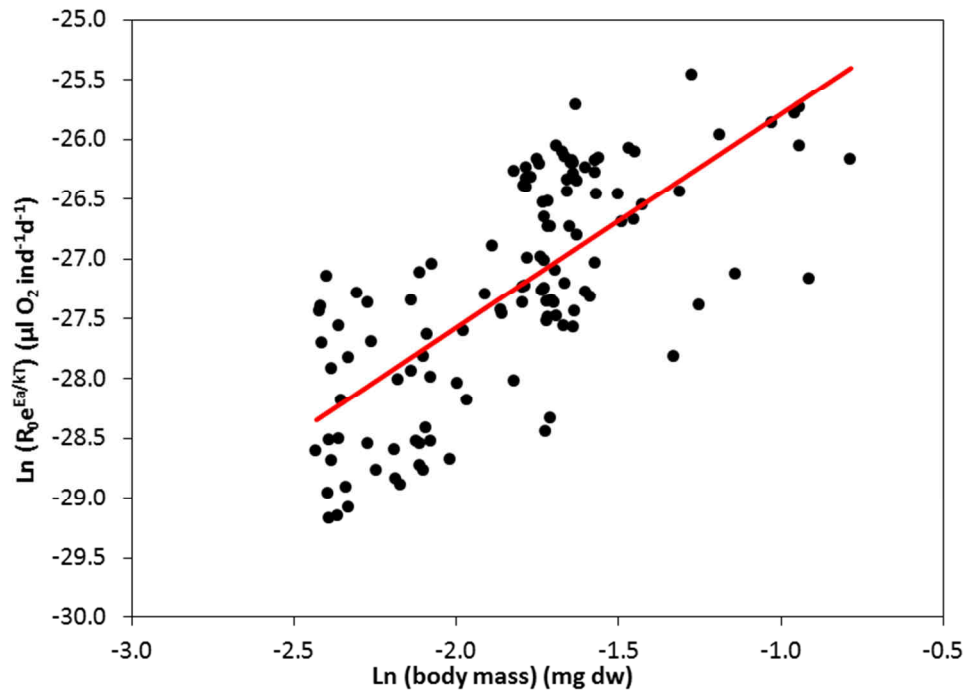
The overall relationship between copepod dry-weight normalised respiration and temperature is given in Figure 5.1. The respiration rate of several species of copepods increased exponentially with temperature across the Meridional transect ( $r^2=0.75$   $p<0.001$ ). The mean of the rates measured outside the sampled temperatures (red markers) did not differ significantly from the mean of the rates measured at *in situ* temperatures (black markers) (Mann-Whitney Rank Sum non-parametric test on rates measured between 4.7 to 16°C  $t = 194$   $p = 0.36$ ).

Figure 5.2 shows the linear relationship, calculated using equation 5.1, between copepod respiration and the reciprocal of  $kT$  ( $k$  = Boltzmann constant and  $T$  = absolute temperature). The slope of the relationship gives the activation energy  $E_a = -0.76 \text{ eV} \pm 0.063 \text{ SE}$ .



**Figure 5.2.** Arrhenius plot of copepod respiration during AMT20. Effect of temperature ( $1/kT$ ) on mass normalised and  $\ln$  transformed respiration rates ( $\mu\text{L O}_2 \text{ d}^{-1}$ ). The red line represents the linear regression  $r^2=0.75$   $p<0.001$   $n=123$ .

Using the Arrhenius equation and the calculated  $E_a$  from equation 5.1 (Figure 5.2) it is possible to estimate respiration corrected to a fixed common temperature of  $20^\circ\text{C}$  (arbitrary value corresponding to the average among the biologically relevant temperature range  $0\text{--}40^\circ\text{C}$ ), as a function of body mass. This allows a comparison of temperature standardised resting respiration as a function of body mass as shown in Figure 5.3. The slope of the relationship gives the allometric exponent  $M^b$  where  $b = 1.036 \pm 0.086 \text{ SE}$ .



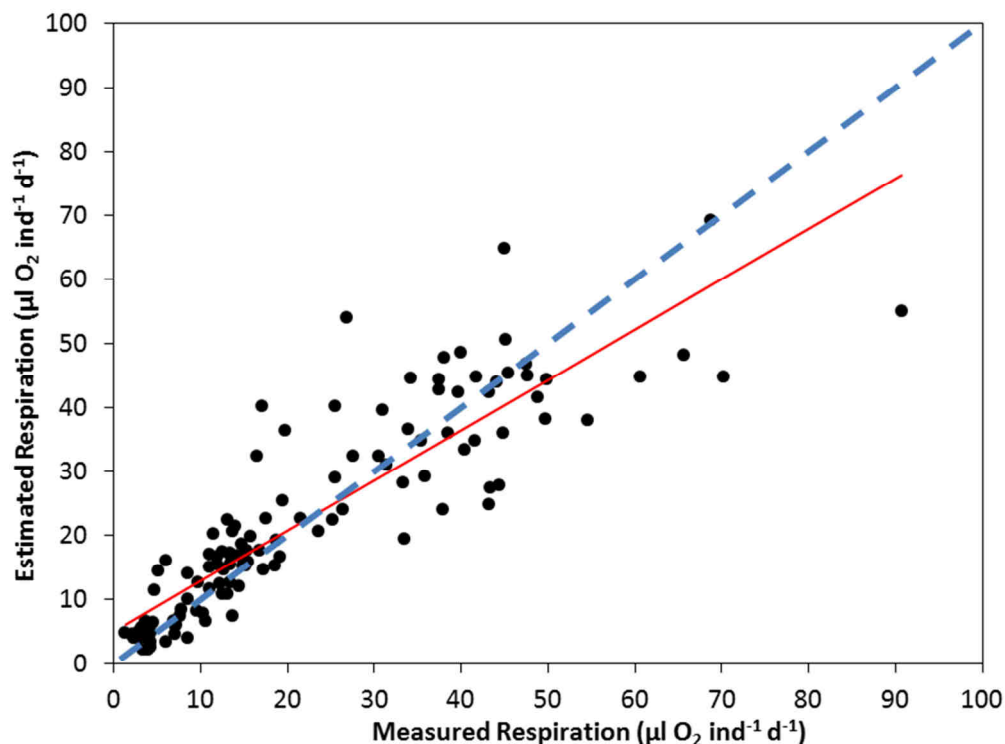
**Figure 5.3.** Relationship between temperature-corrected respiration rates ( $\mu\text{L}$  of oxygen individual $^{-1}$  day $^{-1}$ ) and copepod mass (mg dry weight). The red line represent the linear regression  $r^2=0.51$   $p<0.001$   $n=123$ .

Table 5.2 summarises the values of  $R_0$ ,  $b$  and  $E_a$  estimated through the MTE eq. 5.1 and the respiration data collected on AMT20 ( $n=123$ ).

**Table 5.2.** Estimates of the parameters describing the metabolic scaling of copepod respiration derived from measurements made during AMT20.  $R_0$ : normalisation constant,  $b$ : allometric exponent and  $E_a$ : activation energy (eV). Data shown are the values of each parameter, error  $\pm$  SE and 95% confidence interval. Expected values from the MTE from Gillooly et al. (2001) and Brown et al., (2004).

Parameter	Estimate	SE	95% Confidence Interval		MTE expected
			Lower	Upper	
$R_0$	$9.5 \times 10^{14}$	$2.35 \times 10^{15}$	$-3.71 \times 10^{15}$	$5.61 \times 10^{15}$	-
$b$	1.036	0.086	0.865	1.207	0.750
$E_a$	-0.757	0.063	-0.882	-0.632	-0.6 to -0.7

Figure 5.4 shows the linear relationship (calculated using equation 5.1) between the observed and the estimated respiration rates using the MTE (eq. 5.1) equation and the parameters shown in table 5.2. The data appear to be below the 1:1 line at the highest respiration rates. This suggests that respiration rates assumed by the MTE are underestimated at least for the largest sizes at higher temperatures. However, overall the measured and predicted rates compare well ( $r^2=0.79$   $p<0.001$ ) therefore consistent with the assumptions of the MTE eq 5.1. The empirically derived coefficient  $b$  on the other hand, did not compare well to the MTE expected value (Table 5.2).



**Figure 5.4.** Comparison between measured and MTE assumed respiration rates. The blue dashed line shows the 1:1 fit. The red line represents the linear regression  $n=123$ .

### 5.3.2 Species-specific metabolic responses

The 5 most frequently occurring species in the dataset were considered separately; *Undinula vulgaris* was found in abundance from station 26 to 60 in the northern and southern hemisphere in Oligotrophic, Upwelling and Equatorial domains where temperatures across 200 m depth ranged from 11°C to 29°C. The incubation temperatures varied from 11 to 30°C (Table 5.3) and were all within the *in situ* range.

*Pleuromamma gracilis* was found in abundance at most stations in the northern and southern hemisphere in the Temperate, Oligotrophic and Upwelling domains where across 200 m depth temperatures ranged from 7°C to 27°C. The incubation temperatures ranged from 5 to 27°C (Table 5.3) with the highest (13-27°C) being within the *in situ* temperature range whilst some of the lowest (5-13°C) were out of *in situ* ranges.

*Pleuromamma abdominalis* was found in the northern and southern hemisphere between stations 14 and 50 in the Temperate, Oligotrophic Upwelling and Equatorial domains where across 200 m depth temperatures ranged from 13°C to 27°C. The incubation temperatures ranged from 18 to 27°C and all were within the *in situ* temperature range.

*Nannocalanus minor* was found between stations 56 and 60 in the southern hemisphere in the Oligotrophic domain where across 200 m depth temperatures ranged from 16°C to 24°C. The incubation temperatures ranged from 13 to 22°C with the higher (14-22°C) within the *in situ* temperature range whilst some of the lowest (13-14°C) were outside this range.

*Euchirella sp.* was found between stations 26 and 50 in the northern and southern hemisphere in the Oligotrophic, Upwelling and Equatorial domains where across 200 m depth temperatures ranged from 13°C to 28°C. The incubation temperatures ranged from 20 to 29°C and were all within the *in situ* range.

**Table 5.3.** Exponential equations relating species- respiration rates ( $\mu\text{L O}_2 \text{ mg dw d}^{-1}$ ) to incubation temperature ( $^{\circ}\text{C}$ ). Coefficient (a) and exponent (b) values calculated from the fitted model equation  $R = a \times e^{(b \times t)}$  with R: respiration and t: temperature ( $^{\circ}\text{C}$ ). Error  $\pm$  SE.

Species	Temperature range $^{\circ}\text{C}$	Coefficient (a)	Exponent (b)	$r^2$	P
<i>U. vulgaris</i>	11-30	14.5 $\pm$ 5.2	0.095 $\pm$ 0.013	0.63	<0.001
<i>P. gracilis</i>	5-27	14.8 $\pm$ 2.86	0.096 $\pm$ 0.009	0.8	<0.001
<i>P. abdominalis</i>	18-28	4.7 $\pm$ 3.7	0.15 $\pm$ 0.03	0.76	<0.001
<i>N. minor</i>	13-22	10.2 $\pm$ 5.9	0.085 $\pm$ 0.03	0.58	0.017
<i>Euchirella sp.</i>	20-29	26.2 $\pm$ 17.2	0.075 $\pm$ 0.024	0.66	0.008

Table 5.3 summarises the equations describing the species-dependent relationship between temperature and dry weight adjusted respiration. Respiration was significantly

related to temperature in all species and respiration exponentially increased with exponents ranging from 0.075 (*Euchirella* sp.) to 0.15 (*P. abdominalis*).

Although some respiration rates were measured outside *in situ* temperature conditions, the overlap between all the respiration rates (for *P. gracilis* and *N. minor* in particular) measured at similar temperatures suggests that the temperature response measured was not an artefact of experimental conditions.

For each species the MTE equation was tested and the response of respiration to temperature (Arrhenius relationship) and body size (allometry) were analysed. Respiration rates as a function of body mass were corrected to a common temperature of 20°C using the Arrhenius relationship.

The Arrhenius and allometric relationships for *U. vulgaris* are shown in Figure 5.5. *U. vulgaris* mass adjusted respiration was significantly related to the reciprocal of  $kT$  as shown in Figure 5.5A ( $r^2=0.75$   $p<0.001$ ). The allometric exponent was not predictable (Figure 5.5B) ( $r^2=0.06$   $p=0.11$ ) due to the narrow range of body mass, therefore the general value of 1.036 shown in Table 5.2 was used to estimate  $E_a$ . The  $E_a$  (-0.7 eV  $\pm$  0.11 SE) was below the range estimated for the whole dataset.

The estimated MTE parameters are shown in Table 5.4. Although the predicted values appear to underestimate the higher respiration rates and overestimate the lower rates, overall they significantly correlated with the observed rates ( $r^2=0.62$   $p<0.001$ ) (Figure 5.5C) indicating a general agreement with the MTE. The difference noted above was possibly due to the general body mass coefficient used for the estimation, since a species-specific allometric exponent was not applicable.

The Arrhenius and allometric relationships for *P. gracilis* are shown in Figure 5.6. *P. gracilis* mass adjusted respiration was significantly related to the reciprocal of  $kT$  as shown in Figure 5.6A ( $r^2=0.58$   $p<0.001$ ). The allometric exponent was not predictable (Figure 5.6B) ( $r^2=0.03$   $p=0.35$ ) due to the narrow range of body mass, therefore the general value of 1.036 shown in Table 5.2 was used to estimate  $E_a$ . The  $E_a$  (-0.69 eV  $\pm$  0.06 SE) was below the range estimated for the whole dataset.

The estimated MTE parameters for the species are shown in Table 5.4. Overall the predicted values compared well with the observed ( $r^2=0.79$   $p<0.001$ ) (Figure 5.6C) indicating an agreement with the MTE and the general allometric exponent used for the prediction.

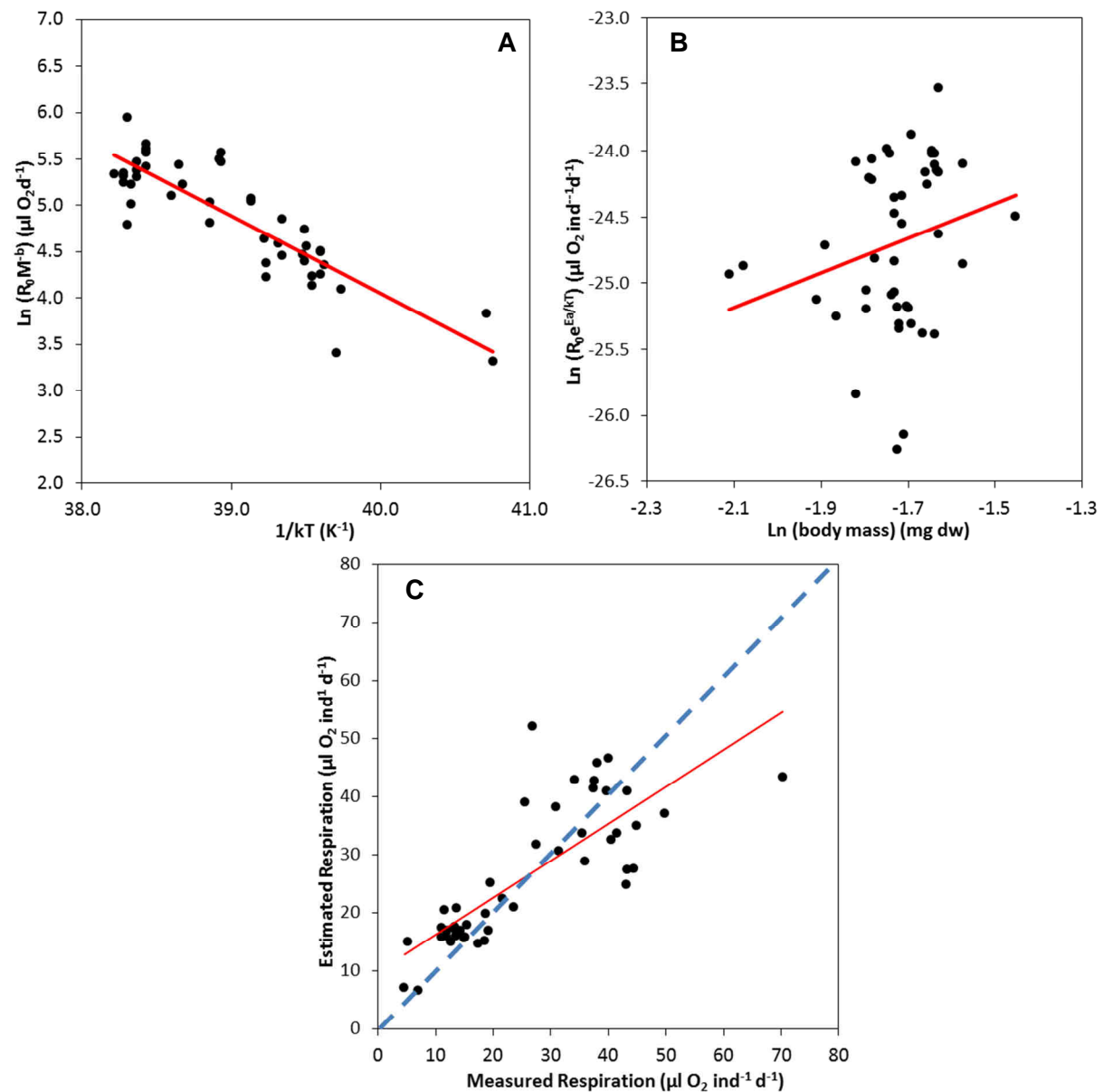


**Figure 5.5.** Responses of *Undinula vulgaris* respiration to temperature and body size  $n=46$ . A) Arrhenius plot of mass-normalised respiration rates  $r^2=0.75$   $p<0.001$ . B) Relationship between temperature-corrected respiration rates and copepod mass  $r^2=0.06$   $p=0.11$ . C) Comparison between measured and MTE assumed respiration rates  $r^2=0.62$   $p<0.001$ . The red lines represent the linear regressions. The blue dashed line shows the 1:1 fit.

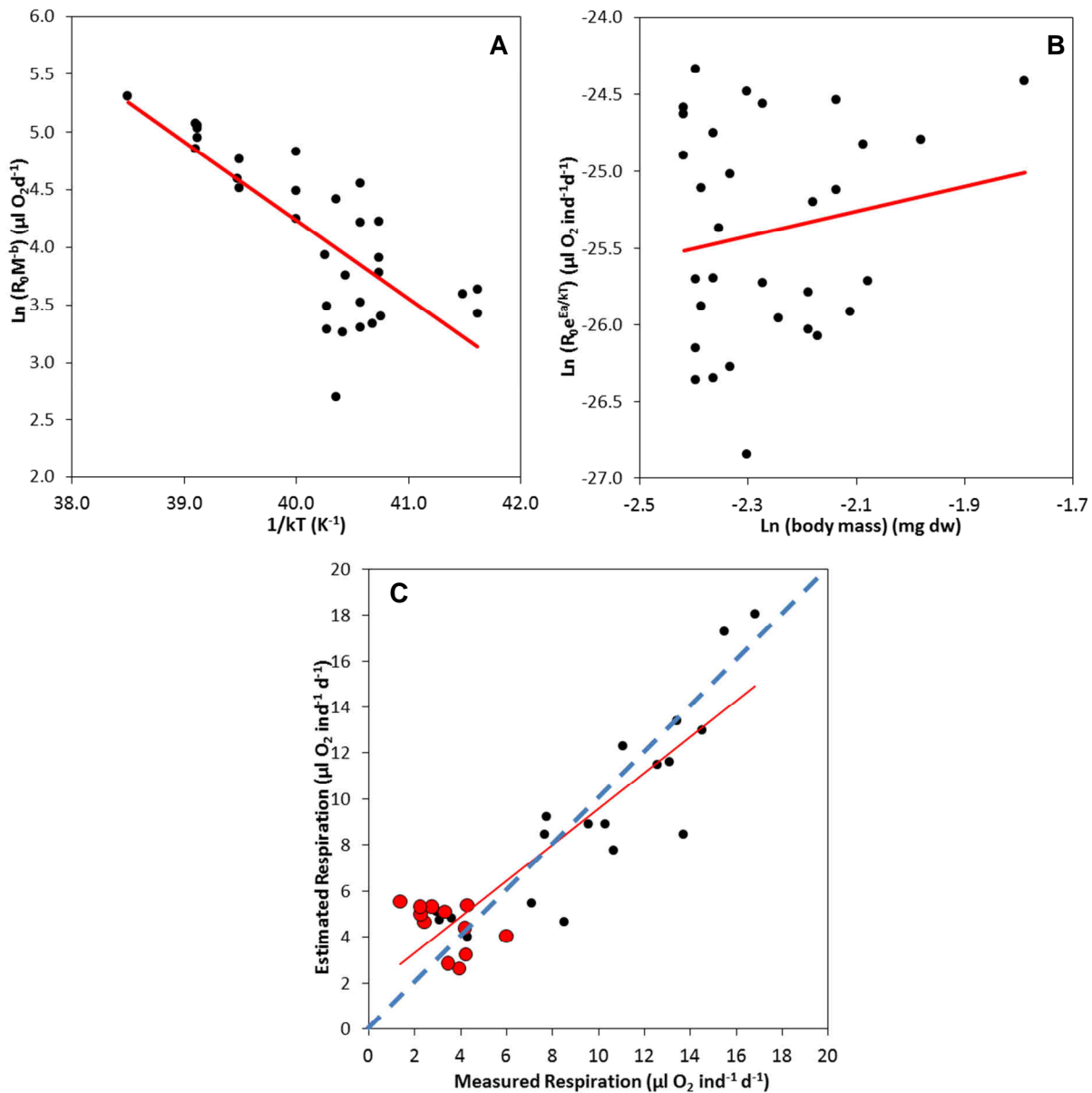


**Figure 5.6.** Responses of *Pleuromamma gracilis* respiration to temperature and body size  $n=31$ . A) Arrhenius plot of mass-normalised respiration rates  $r^2=0.58$   $p<0.001$ . B) Relationship between temperature-corrected respiration rates and copepod mass  $r^2=0.03$   $p=0.35$ . C) Comparison between measured and MTE assumed respiration rates  $r^2=0.79$   $p<0.001$ . The red markers represent respiration rates outside *in situ* temperatures. The red lines represent the linear regressions. The blue dashed line shows the 1:1 fit.

The Arrhenius and allometric relationships for *P. abdominalis* are shown in Figure 5.7. *P. abdominalis* mass adjusted respiration was significantly related to the reciprocal of  $kT$  as shown in Figure 5.7A ( $r^2=0.81$   $p<0.001$ ). The allometric exponent (Figure 5.7B) was extremely high  $2.09 \pm 0.6$  SE while the  $E_a$  ( $1.07$  eV  $\pm 0.02$  SE) was above the range estimated for the whole dataset.

The estimated MTE parameters for the species are shown in Table 5.4. Overall the predicted values compared well with the observed ( $r^2=0.9$   $p<0.001$ ) (Figure 5.7C) indicating a good agreement with the MTE, improved by the availability of the species-specific  $b$  exponent.

The Arrhenius and allometric relationships for *N. minor* are shown in Figure 5.8. *N. minor* mass adjusted respiration was significantly related to the reciprocal of  $kT$  as shown in Figure 5.9A ( $r^2=0.58$   $p=0.015$ ). The allometric exponent was not predictable (Figure 5.8B) ( $r^2=0.06$   $p=0.52$ ) due to the narrow range of body mass therefore the general value of 0.996 shown in Table 5.2 was used to estimate  $E_a$ . The  $E_a$  ( $-0.58$  eV  $\pm 0.2$  SE) was below the range estimated for the whole dataset.

The estimated MTE parameters for the species are shown in Table 5.4. Overall the predicted values were correlated to the observed ( $r^2=0.54$   $p=0.025$ ) (Figure 5.8C) however due to the considerable scatter in the data, measured and observed respiration did not agree, especially at higher respiration rates, possibly caused by the limited number of data points available.

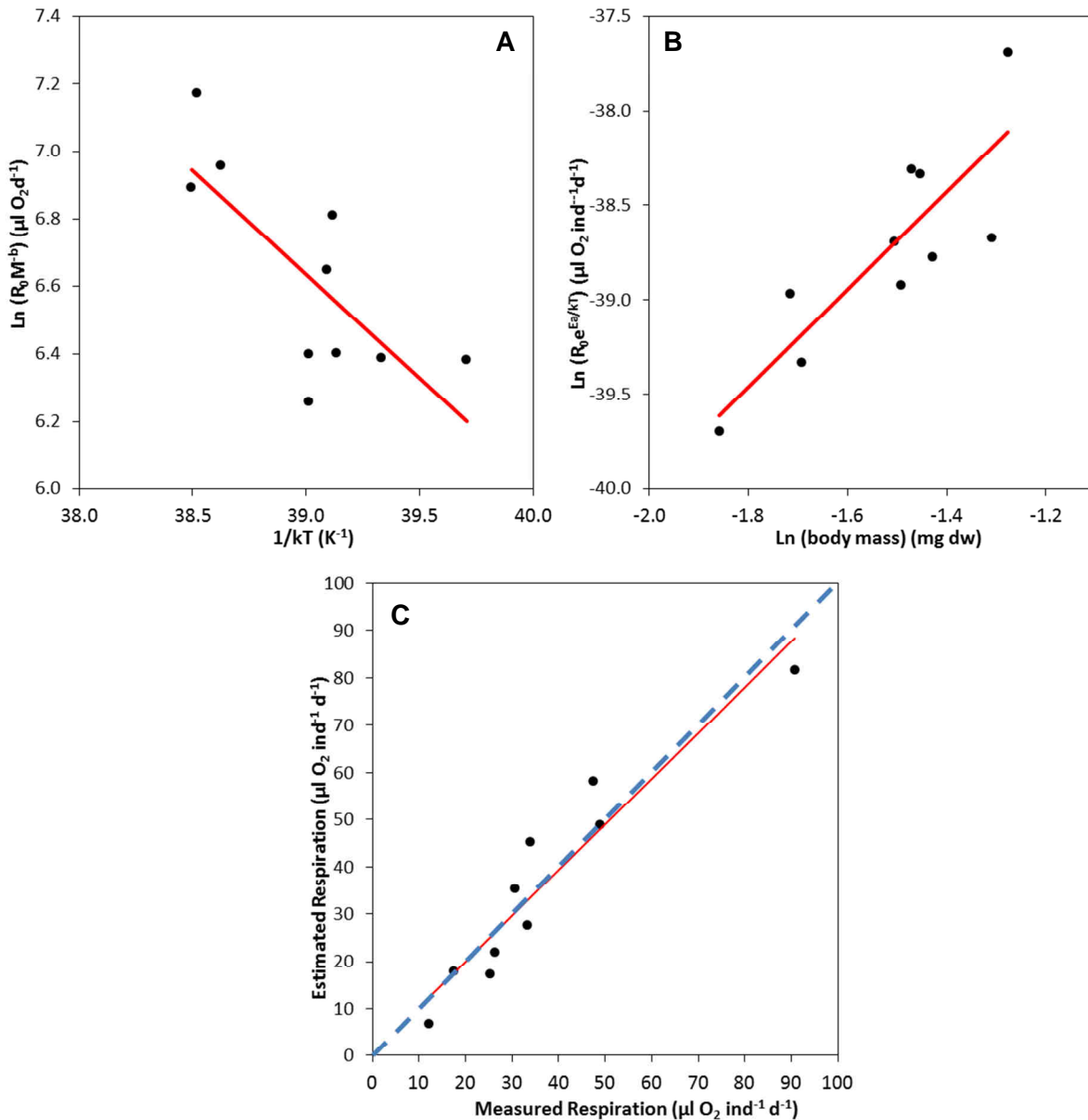


**Figure 5.7.** Responses of *Pleuromamma abdominalis* respiration to temperature and body size  $n=10$ . A) Arrhenius plot of mass-normalised respiration rates  $r^2=0.81$   $p<0.001$ . B) Relationship between temperature-corrected respiration rates and copepod mass  $r^2=0.72$   $p=0.002$ . C) Comparison between measured and MTE assumed respiration rates  $r^2=0.9$   $p<0.001$ . The red lines represent the linear regressions. The blue dashed line shows the 1:1 fit.

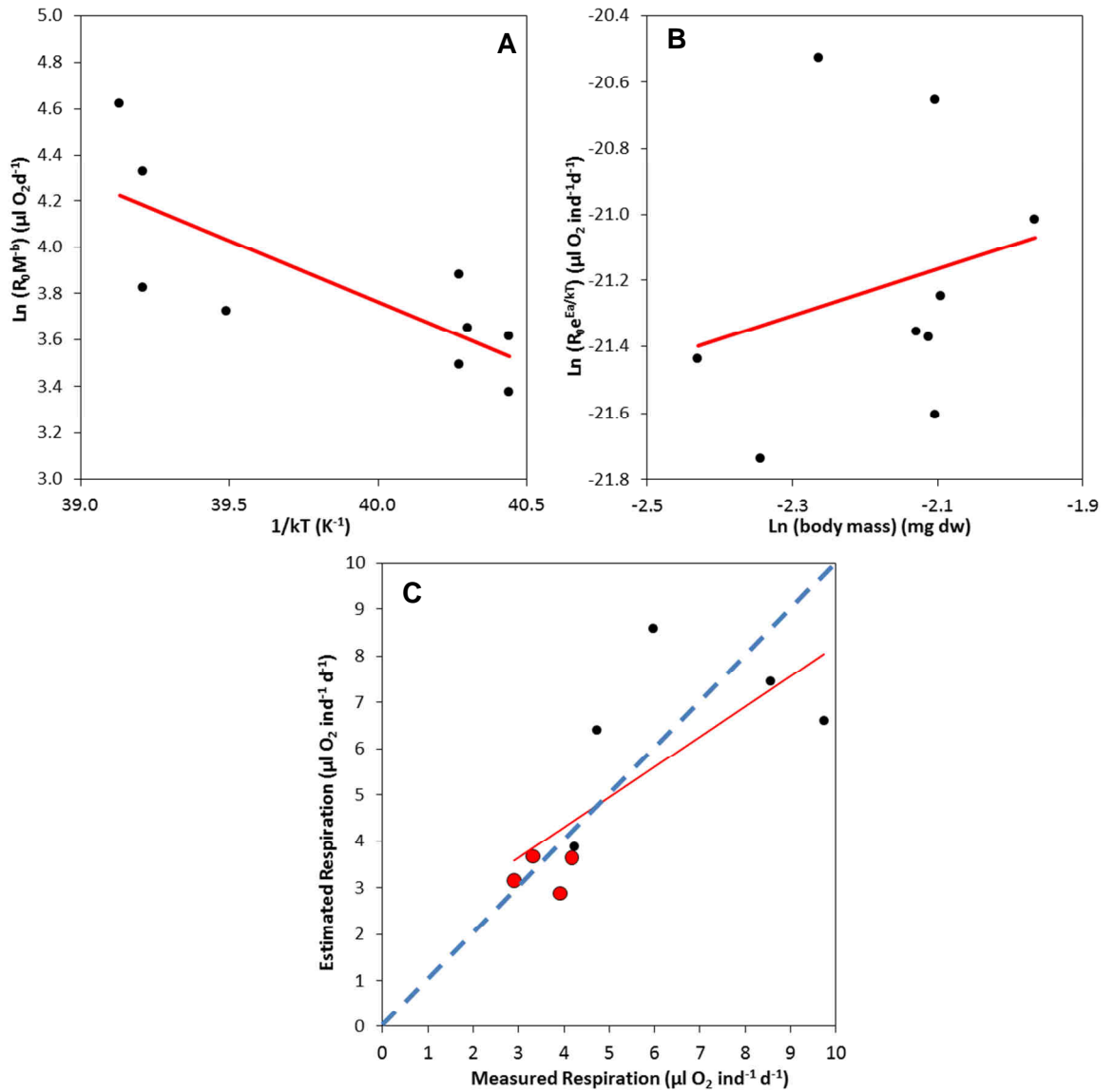


**Figure 5.8.** Responses of *Nannocalanus minor* respiration to temperature and body size  $n=9$ . A) Arrhenius plot of mass-normalised respiration rates ( $r^2=0.59$   $p=0.015$ ). B) Relationship between temperature-corrected respiration rates and copepod mass ( $r^2=0.06$   $p=0.52$ ). C) Comparison between measured and MTE assumed respiration rates ( $r^2=0.54$   $p=0.025$ ). The red markers represent respiration rates measured outside *in situ* temperatures. The red lines represent the linear regressions. The blue dashed line shows the 1:1 fit.

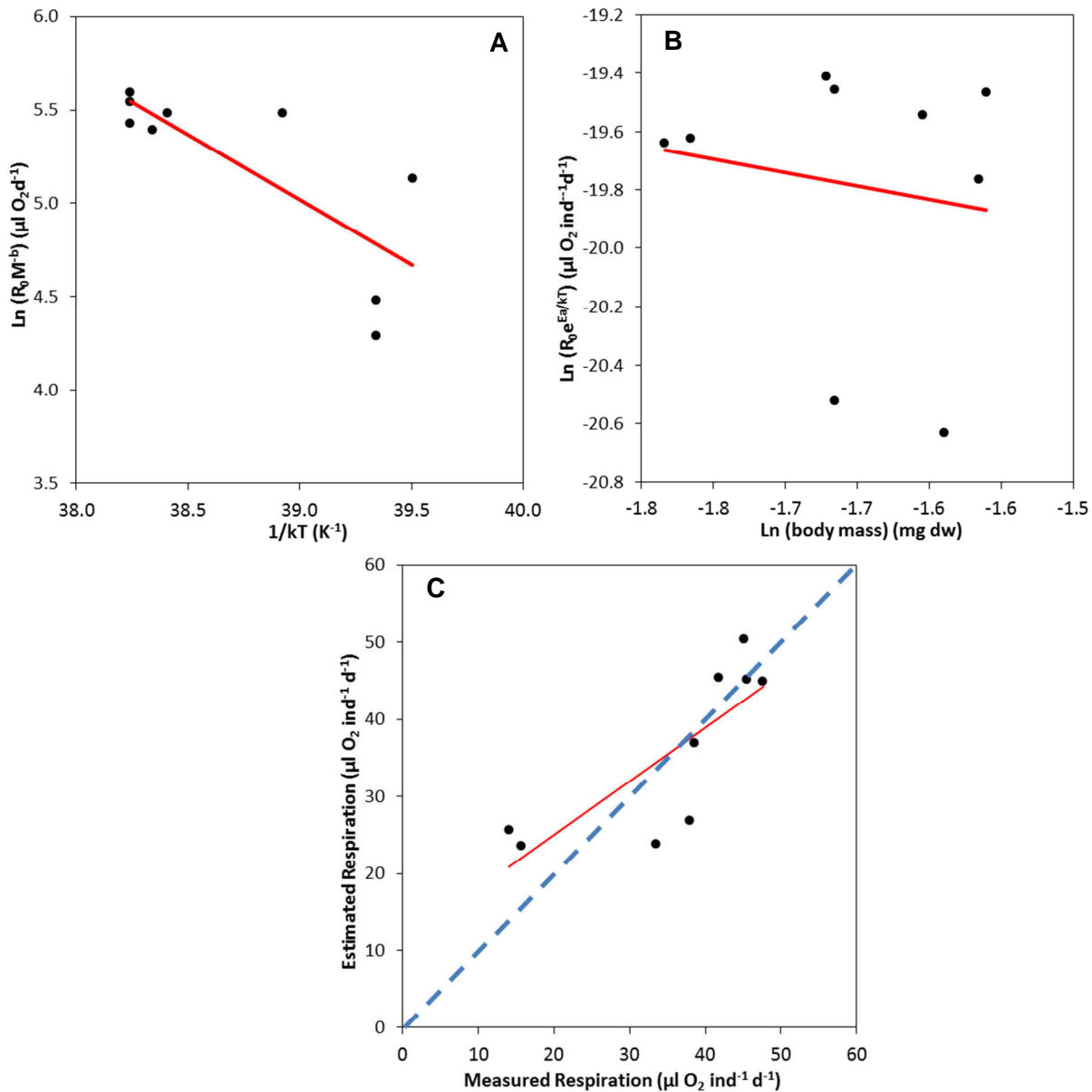


**Figure 5.9.** Responses of *Euchirella sp.* respiration to temperature and body size n=9. A) Arrhenius plot of mass-normalised respiration rates  $r^2=0.61$   $p=0.014$ . B) Relationship between temperature-corrected respiration rates and copepod mass  $r^2=0.027$   $p=0.67$ . C) Comparison between measured and MTE assumed respiration rates  $r^2=0.64$   $p=0.01$ . The red lines represent the linear regressions. The blue dashed line shows the 1:1 fit.

The Arrhenius and allometric relationships for *Euchirella sp.* are shown in Figure 5.9. *Euchirella sp.* mass adjusted respiration was significantly related to the reciprocal of  $kT$  as shown in Figure 5.9A ( $r^2=0.61$   $p=0.014$ ). The allometric exponent was not predictable (Figure 5.9B) ( $r^2=0.027$   $p=0.67$ ) due to the narrow range of body mass therefore the general coefficient value of 1.036 shown in Table 5.2 was used to estimate  $E_a$ . The  $E_a$  ( $-0.59$  eV  $\pm$  0.18 SE) was very low and well below the range estimated for the whole dataset ( $-0.76$  eV Table 5.2).

The estimated MTE parameters for the species are shown in Table 5.4. Although a limited number of data points was available, overall the predicted values were comparable to the observed ( $r^2=0.64$   $p=0.01$ ) (Figure 5.9C) indicating a general agreement with the MTE.

**Table 5.4.** Summary of estimates of the parameters describing the metabolic scaling of the respiration of the 5 copepod species measured during AMT20.  $R_0$ : temperature and body mass independent normalisation constant ( $\mu\text{L O}_2 \text{ d}^{-1}$ ),  $b$ : allometric exponent and  $E_a$ : activation energy (eV). Data are the values of each parameter  $\pm$ SE calculated with a non-linear least-square method using a Gauss-Newton model fit. NA: Data not available.

Species	$R_0$	$b$	$E_a$ eV
<i>U. vulgaris</i>	$1.12 \times 10^{14} \pm 4.76 \times 10^{14}$	NA	$-0.702 \pm 0.11$
<i>P. gracilis</i>	$6.37 \times 10^{13} \pm 1.72 \times 10^{14}$	NA	$-0.686 \pm 0.069$
<i>P. abdominalis</i>	$8 \times 10^{20} \pm \text{NA}$	2.09	$-1.066 \pm 0.021$
<i>N. minor</i>	$4.24 \times 10^{12} \pm 3.83 \times 10^{13}$	NA	$-0.576 \pm 0.229$
<i>Euchirella sp.</i>	$1.48 \times 10^{12} \pm 1.03 \times 10^{13}$	NA	$-0.588 \pm 0.181$

Table 5.4 summarises the species-dependent estimates for allometric and temperature-dependent relationships calculated with a non-linear model using a Gauss-Newton algorithm. Most of the species-specific allometric exponents were not derivable from the data available (NA) due to the limited size range of individuals incubated; therefore making the relationship between body mass and temperature adjusted respiration rates not significant.

Overall *P. abdominalis* had the highest activation energy ( $E_a = 1.07 \pm 0.02$  SE) meaning that respiration increased to a greater amount with increasing temperature, making the species most sensitive to temperature changes. *Euchirella sp.* and *N. minor* had the

lowest averaging  $0.58 (\pm 0.034 \text{ SD})$ . The  $E_a$  of *U. vulgaris* and *P. gracilis* averaged  $0.69 (\pm 0.011 \text{ SD})$  remaining below the  $E_a$  estimated for the whole dataset ( $0.76 \pm 0.06 \text{ SE}$ ).

### 5.3.3 $Q_{10}$ Estimates

The  $Q_{10}$  coefficients estimated from equations 5.2, 5.3, 5.4 and 5.5 all were compared as shown in Figure 5.10.

The  $Q_{10}$  estimated from copepod respiration rates across the meridional transect ranged from 2.0 (eq 5.4) to 2.82 (eq. 5.2). Of the 5 most frequently occurring species the mesopelagic *P. abdominalis* was the most sensitive to temperature variation with a  $Q_{10}$  ranging from 2.81 (eq. 5.4) to 4.07 (eq. 5.2) whilst *Euchirella sp.* was the least sensitive with a  $Q_{10}$  ranging from 1.52 (eq. 5.4) to 2.46 (eq.5.5). Most of the  $Q_{10}$  values were  $>2$  indicating a strong sensitivity to temperature.

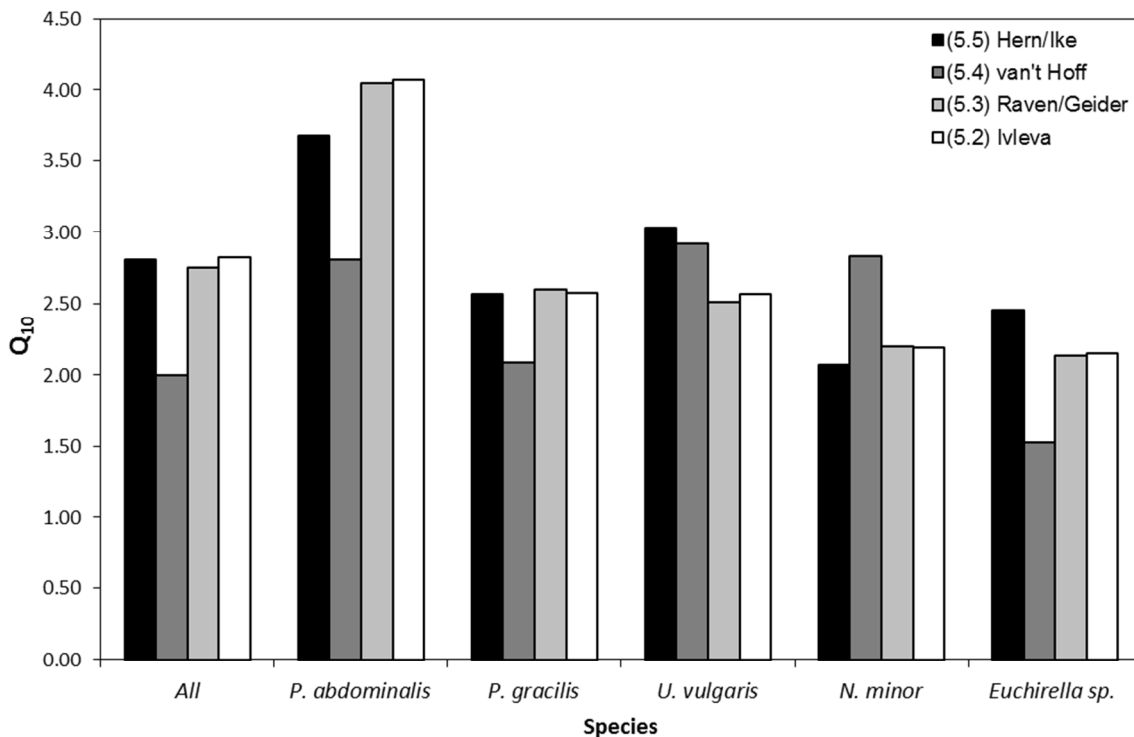


**Figure 5.10.**  $Q_{10}$  estimations using the whole dataset and 5 individual species of copepod. Different coloured bars represent the comparison between equations 5.2, 5.3, 5.4 and 5.5. Errors  $\pm$  SD.

All the  $Q_{10}$  estimates derived from equation 5.2 to 5.5 were compared and the difference between them was calculated as the average percentage of absolute change as shown in

Table 5.5. There was little variation (1.2% variation) between the  $E_a$  derived from equations 5.2 (Ivleva 1980) and 5.3 (Raven and Geider 1988). The largest variation in estimates (~31%) was found between equations 5.4 (van't Hoff) and 5.5 (Hernandez-Leon and Ikeda 2005), equations 5.4 and 5.3 (Raven and Geider 1988) and equations 5.4 and 5.2 (Ivleva 1980). This was possibly because equation 5.4 only considers the first and the last respiration measurements rather than allowing for a rate integrated approach as shown in the other equations.

**Table 5.5.** Difference between  $Q_{10}$  coefficients (average between whole dataset and species) from equation 5.2, 5.3, 5.4 and 5.5 in percentage of absolute change between estimates.

% Absolute Change	<b>5.4</b> (van't Hoff)	<b>5.3</b> (Raven & Geider 1988)	<b>5.2</b> (Ivleva 1980)
<b>5.5</b> (Hernandez-Leon & Ikeda 2005)	24.98	8.22	7.58
<b>5.4</b> (van't Hoff)	-	30.50	30.95
<b>5.3</b> (Raven & Geider 1988)	-	-	1.15
<b>5.2</b> (Ivleva 1980)	-	-	-

#### 5.3.4 Egg production rates (EPR)

EPR was measured between 11 to 29°C on the most re-occurring broadcast spawning species across the Atlantic Meridional Transect. Figure 5.11A shows that EPR was higher at lower temperatures (10-18°C) and declined at temperatures >18°C. The highest rate of 0.68 eggs  $\mu\text{g dw}^{-1} \text{d}^{-1}$  coincided with a temperature of ~11°C. The standard deviation in egg production rates was large at lower temperatures  $\pm 0.2$  eggs  $\mu\text{g dw}^{-1} \text{d}^{-1}$  (10-18°C), due to the frequency of females that failed to produce any eggs.

A weak linear decreasing trend ( $r^2=0.2$   $p=0.056$ ) between CM temperature and chl-a (natural log transformed) was identified. However figure 5.11B shows that EPR did not increase with chl-a concentration (CM depth), although since a limited number of species was incubated, in particular at the highest chl-a concentrations, this could have been due to the effects of species-specific responses.

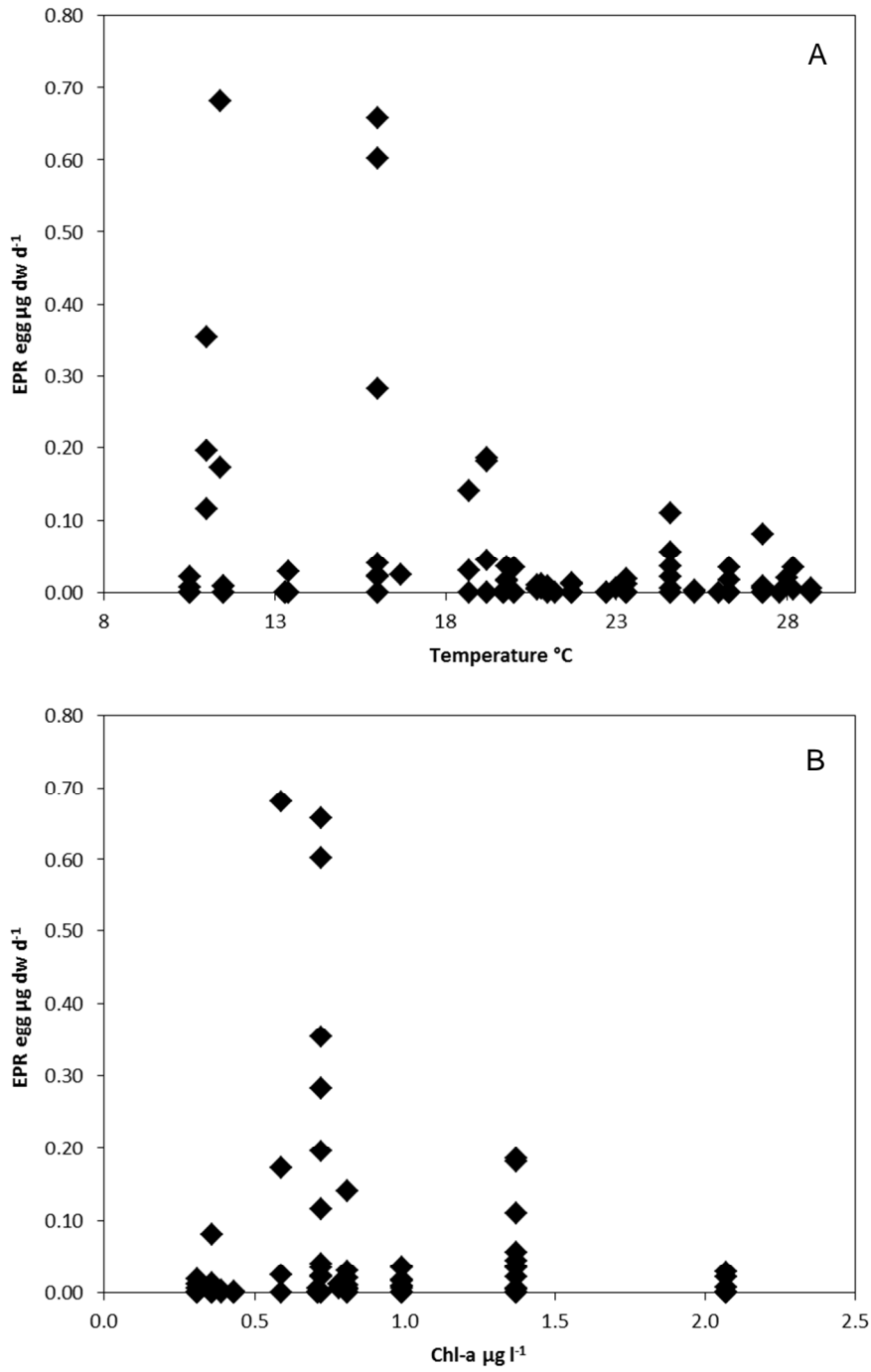


**Figure 5.11.** Egg production rates of larger copepod species on AMT20. A) EPR vs. temperature ( $^{\circ}\text{C}$ ). B) EPR vs. chlorophyll-a (CM) concentration ( $\text{Chl-a } \mu\text{g L}^{-1}$ ). Rates are dry weight adjusted.

Individual EPR measurements were statistically compared. The measurements were not averaged. This is because the limited number of species chosen for the incubation affected the overall randomness of the dataset, resulting in a methodological artefact as seen in the chl-a vs. EPR relationship. Single and multiple regression analyses were carried out to examine the relationships between EPR (dry weight adjusted) and environmental variables (temperature and chl-a concentration). However, due to the large incidence of zero values in the individual measurements, statistically there were no significant relationships between the parameters examined ( $r^2 < 0.1$ ,  $p > 0.4$ ). We should note that this high incidence of zero values could also be a result of a methodological artefact since females may need longer incubation times (>24h) to produce eggs (Tester and Turner 1990).

Species-specific reproductive responses (Table 5.7 supplementary material) show that the most fecund species was *Clausocalanus sp.* with a maximum of 0.68 eggs  $\mu\text{g dw}^{-1} \text{d}^{-1}$  corresponding to 53 egg  $\text{individual}^{-1} \text{d}^{-1}$  at 11°C at relatively constant chl-a concentrations (0.6-0.7  $\mu\text{g L}^{-1}$ ). Species of the genus *Pleuromamma* produced few eggs <4 eggs  $\text{individual}^{-1} \text{day}^{-1}$  at any given temperature (11-27°C) and chl-a (0.3-2.1  $\mu\text{g L}^{-1}$ ) throughout the Atlantic transect possibly indicating generally low reproduction potential. *Euchirella sp.* also appeared to have reduced fecundity levels on AMT20, producing <2 eggs  $\text{individual}^{-1} \text{day}^{-1}$ . *Euchirella sp.* eggs were the largest averaging 267  $\mu\text{m}$  in diameter (Table 5.7 supplementary material).

Of the species selected to measure respiration rates *U. vulgaris* was the species with the most number of EPR measurements and covering the widest range of temperature, 18 - 29°C, as shown in Figure 5.12. The species produced a maximum of ~0.18 eggs  $\mu\text{g dw}^{-1} \text{d}^{-1}$  corresponding to 33-35 eggs  $\text{individual}^{-1} \text{day}^{-1}$  at the lowest temperatures ~19°C and highest chl-a concentrations (1.4  $\mu\text{g L}^{-1}$ ) whereas EPR above 25°C and 0.8  $\mu\text{g L}^{-1}$  decreased considerably (Figure 5.12 A and B). At temperatures >20°C some eggs produced by *U. vulgaris* hatched into nauplii within the 24 hours.

Individual and averaged *U. vulgaris* EPR measurements were statistically compared. Single and multiple regression analysis were carried out to examine the relationships between *U. vulgaris* EPR (dry weight adjusted) and environmental variables (temperature and chl-a concentration). Possibly due to the large incidence of zero values in the individual measurements and the reduced sample size of the averaged values, statistically there was no significant relationship between the parameters examined ( $r^2 < 0.1$ ,  $p > 0.4$ ).

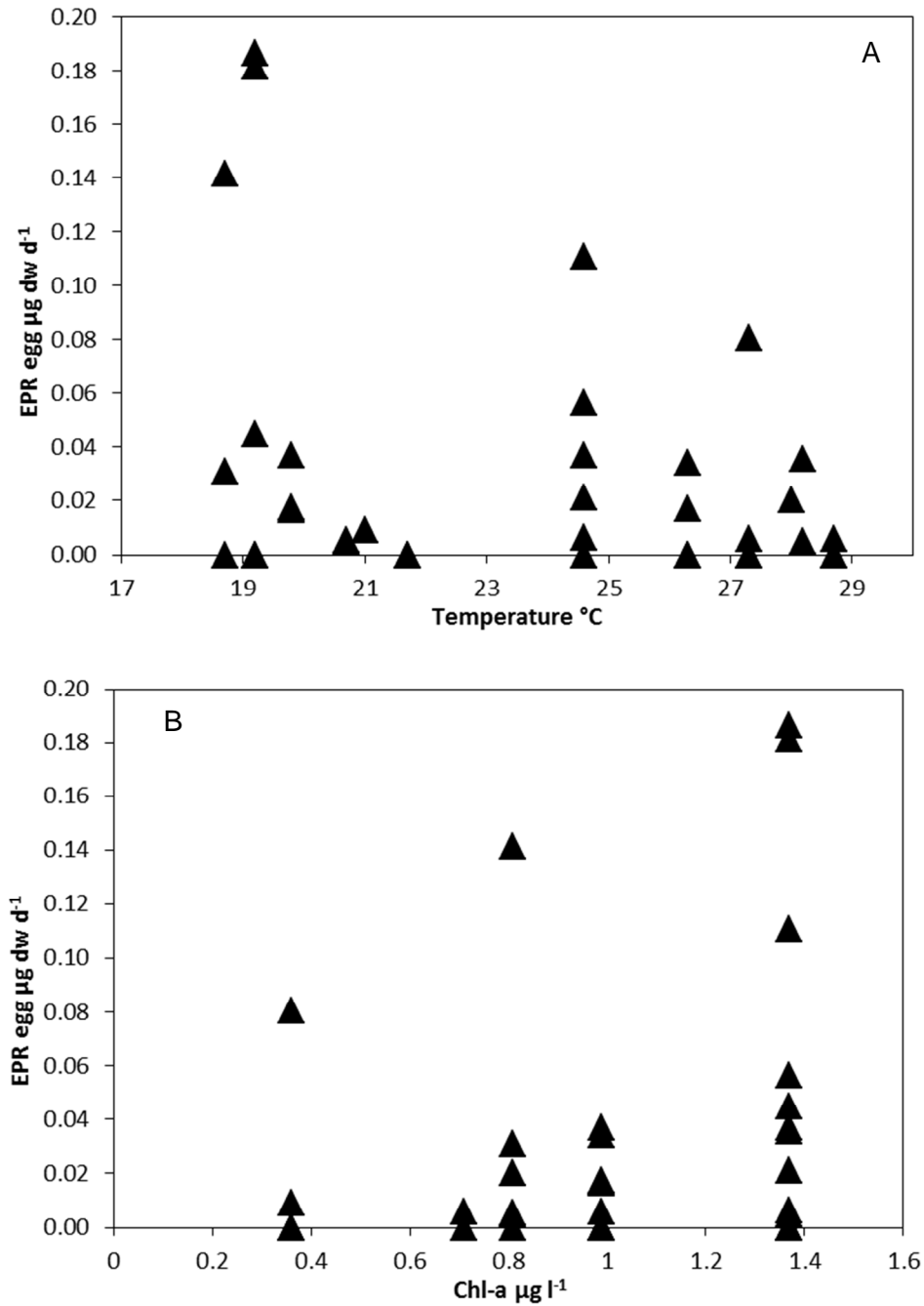


**Figure 5.12.** *Undinula vulgaris* egg production rates on AMT20. A) EPR vs. temperature ( $^{\circ}\text{C}$ ). B) EPR vs chlorophyll-a (Chl-a  $\mu\text{g L}^{-1}$ ). Rates are dry weight adjusted.

## 5.4 Discussion

The present investigation aimed to study the metabolic and reproductive response of a few selected species of copepods distributed across 6 (5 for respiration) Atlantic ecological domains (Marañón et al. 2001) during an Atlantic Meridional Transect. The data were compared to the existing literature and in addition, the assumptions of the Metabolic Theory of Ecology (Brown et al. 2004) to species-specific rates were tested and the sensitivity of low to mid- latitude Atlantic pelagic species to temperature variation was evaluated.

### 5.4.1 Species distribution

This study included mostly species found in warm water from tropical and subtropical systems and some from the temperate domains. SST varied from 11 to 29°C and chl-a concentration ranged from 0.3 to 2.1  $\mu\text{g L}^{-1}$ . The temperate region was defined as SST ranging between 11-17°C, the subtropical region was defined as the region where SST ranged between 17-24°C and the tropical where SST was between 24-30°C (Mauchline 1998, Ikeda 2001).

For the most re-occurring medium to large copepod species both EPR and respiration rates were measured, for *Clausocalanus sp.* only EPR was measured. *Undinula vulgaris* and *Pleuromamma gracilis* were the species with the broadest distributional ranges (both latitudinal and in terms of temperature range ~17-20°C). *Pleuromamma abdominalis*, *Nannocalanus minor* and *Euchirella sp.* (possibly *curticauda*) were abundantly found at a narrower range of latitudes and within a temperature range of ~10°C. The species were all identified as broadcast spawners and diel vertical migrators commonly distributed in the meso- and epipelagic zones (Razouls et al. 2012).

*Clausocalanus sp.* was the smallest copepod species considered in this study, adult female body length varied from 1.2 to 1.6 mm. This is a widely distributed species, mostly found in neritic habitats within the epipelagic zone (Razouls et al. 2012). During AMT20 this species was abundant in the temperate N domain between 11-17°C (SST).

*U. vulgaris* is an epi- (0 - ~150 m) and mesopelagic (~150 – 1000 m) species also found in neritic habitats and a cosmopolite in subtropical and tropical oceans (Razouls et al. 2012) where SST varies from ~17 to 30°C. *U. vulgaris* is considered one of the key species in its respective habitat (Park and Landry 1993 and references therein). During AMT20 the female adult body size ranged from ~2.5 to ~3 mm in length. The species was found in the Oligotrophic and Equatorial domains and in abundance in the Upwelling domain, from

21°N to 27°S where SST ranged from ~22 to 29°C and temperatures (in the surface 200 m) ranged from ~11°C to 29°C.

*P. gracilis* is an epi- and mesopelagic cosmopolite species and widely distributed throughout the world's oceans from Antarctic to tropical waters (excluding the arctic region) (Razouls et al. 2012), where SST varies from ~-2 to 30°C. The species was one of the smaller copepods considered in this study, adult female body size ranged from ~1.8 to ~2.6 mm in length. The species occurred most between 34°N to 16°N and 20°S to 42°S in the Temperate, Oligotrophic and Upwelling domains where SST ranged from ~13 to 27°C and temperatures (in the surface 200 m) ranged from ~7°C to 27°C.

*P. abdominalis* is a cosmopolite epi- meso- and bathypelagic species and a strong vertical migrator found in boreal, temperate, subtropical and tropical waters (Razouls et al. 2012) where SST varies from 3 to 30°C. *P. abdominalis* was the largest species considered in this study, the female adult body size ranged from ~3 to ~4 mm in length. The species was found in the northern and southern hemisphere between 34°N to 16°N and 20°S to 42°S in the Temperate, Oligotrophic Upwelling and Equatorial domains where SST ranged from ~23 to 27°C and depth integrated temperatures for the surface 200 m ranged from ~13°C to 27°C.

*N. minor* is a cosmopolite epi- and mesopelagic species found mainly in subtropical and tropical waters (Razouls et al. 2012) where SST varies from ~17 to 30°C. This species was one of the smaller considered here with adult female body size ranging from ~2 to ~2.5 mm in length. *N. minor* was found in the southern hemisphere between 20°S to 27°S in the Oligotrophic domain where SST ranged from ~22 to 24°C and temperatures (in the surface 200 m) ranged from ~16°C to 24°C.

Species belonging to the genus *Euchirella* are mainly epi- and mesopelagic subtropical and tropical species (Mulyadi 2001), though bathypelagic species also occur, where SST varies from ~17 to 30°C. During AMT20 the female adult body size of *Euchirella sp.* ranged from ~2.2 to ~2.5 mm. The species was found between 21°N to 10°N in the northern hemisphere and 4°S to 13°S in the southern hemisphere in the Oligotrophic, Upwelling and Equatorial domains. AMT20 *Euchirella sp.* appeared most abundant where SST ranged from ~24 to 29°C and temperatures through the depth profile ranged from ~13°C to 29°C.

#### 5.4.2 Egg production rates (EPR)

Data on oceanic and mesopelagic copepods EPR is scarce, with the exception of a study on the neritic/oceanic *U. vulgaris* in the Pacific Ocean (Hawaii) (Park and Landry 1993), or epipelagic population-level investigations (Calbet and Agustí 1999), open-ocean subtropical and tropical species have been poorly investigated, making these data all the more valuable for a better understanding of the ecology of these copepods.

The overall relationship between copepod reproduction and temperature on AMT20 was negative. The EPR of free-spawners appeared to increase with decreasing temperatures, with rates higher in the Temperate N domain. This was also due to the high fecundity of the neritic, temperate *Clausocalanus* sp. with  $>50$  egg individual<sup>-1</sup> day<sup>-1</sup> between 11-16°C. At the same time no distinct pattern between EPR and chl-a concentration (as a proxy of food quantity) was found. This is in contrast with a previous study carried out by Calbet and Agustí (1999) which showed an increase in EPR of epipelagic copepods with temperature and food quantity across an Atlantic latitudinal transect.

EPR should increase with temperature (diet depending) up to a limit fixed by the adaptation strategy of the organism, then decline again. Most of the species investigated were not day-time surface dwellers, suggesting that 24 hours exposure at constant temperatures (some as high as SST) could have been detrimental for some of them, affecting reproduction rates and/or egg development time. This is since the realised niche of mesopelagic migratory copepods resides in colder habitats (as cold as 4-7°C (AMT data at 1000 m) and although surface temperatures are still within their ecological niche, they are usually exposed to these higher temperatures only for a short time.

However the results also show that this relationship between EPR and chl-a, could be a methodological artefact since it was influenced by the effects of species-specific reproductive strategies. This is because mainly species with lower reproductive rates were incubated in the southern hemisphere and at locations with higher chl-a concentrations. In particular, all species belonging to the genus *Pleuromamma* produced few eggs throughout the investigation; *P. gracilis* had a maximum EPR of 4 eggs individual<sup>-1</sup> day<sup>-1</sup> and appeared not affected by temperature or chl-a concentration. This could be due to an overall reproductive strategy of some *Pleuromamma*; genus including many meso- and bathypelagic species showing low reproductive potential and longer egg development times (Mauchline 1998; Yamaguchi and Ikeda 2000; Mayzaud et al. 2002).

*Euchirella* sp. EPR was only measured between temperatures ranging from 21 to 28°C showing low fecundity with a maximum of 2 eggs individual<sup>-1</sup> day<sup>-1</sup>. Although some

mesopelagic free-spawning copepods have been shown to produce clutches of only a few eggs (Mauchline 1998; Yamaguchi and Ikeda 2000; Mayzaud et al. 2002) this narrow range of incubations precludes a general deduction regarding the fecundity of the species. The genus is a vertical migrator (Mulyadi 2001), suggesting that the optimal range of temperatures, where the species' fecundity is at its maximum, could lie at lower temperatures than the incubation temperatures selected in this study. Therefore these results may not be representative of the ecology of the species.

The EPR of *U. vulgaris* as shown in Figure 5.12 followed a more complex pattern, defined by a combination of temperature (negative) and food concentration (positive) effects. A maximum EPR of 35 eggs individual<sup>-1</sup> day<sup>-1</sup> occurred in the Upwelling domain at CM temperatures of ~19°C and chl-a concentrations of 1.4 µg L<sup>-1</sup> (Figure 5.12), compared to a maximum EPR of 53 eggs individual<sup>-1</sup> day<sup>-1</sup> at 26°C found by Park and Landry (1993) in coastal conditions (neritic, food replete). This suggests that fecundity was inhibited at high temperatures and particularly limited by low food quantity throughout the Atlantic transect.

#### 5.4.3 Species-specific carbon demand and respiration rates

The carbon demand of copepods ranging from 35 to 160 µg C in weight, and found at temperatures ranging from 4.7 to 30°C followed an exponential relationship with temperature where the maximum carbon demand of 47 µg C ind<sup>-1</sup> d<sup>-1</sup> was found for *P. abdominalis* at 27°C and a minimum 0.71 µg C ind<sup>-1</sup> d<sup>-1</sup> was measured for *P. gracilis* at 13°C. This varied from a maximum of 42% of body carbon to a minimum of 1.78% of body carbon. Generally the carbon demands for *U. vulgaris* and *Euchirella* sp. remained <25 µg C ind<sup>-1</sup> d<sup>-1</sup> corresponding to <35% and <32% of body C respectively (at maximum incubation temperatures). *N. minor* and *P. gracilis* carbon demands were low at <5 and 8 µg C ind<sup>-1</sup> d<sup>-1</sup> respectively, corresponding to <35% and <12% of body C. Overall this indicated that *P. abdominalis*, *U. vulgaris* and *Euchirella* sp. had a high individual carbon requirement (>10 µg C ind<sup>-1</sup> d<sup>-1</sup> Schukat et al. 2013). This was in agreement with Schukat et al. (2013), who found high individual carbon requirements for *Euchirella* sp. and *Pleuromamma* sp.

Overall the species-specific respiration rates measured in this study appeared to match those of Ikeda et al (2007) for some of the species (Ikeda et al. 2007, epipelagic copepods only. See supplementary material: Table 5.7). For instance, *U. vulgaris* respiration rates measured by Ikeda (1970) at 23.5°C and 27.6°C averaged 125 and 201 µL O<sub>2</sub> mg dw<sup>-1</sup> d<sup>-1</sup> respectively, comparing well with our estimates of 125 and 197 µL O<sub>2</sub> mg dw<sup>-1</sup> d<sup>-1</sup> at the same temperatures (estimated via regression analysis between dry weight adjusted respiration and temperature). *P. abdominalis* respiration rates also compared well with

45.8  $\mu\text{L O}_2 \text{ mg dw}^{-1} \text{ d}^{-1}$  (Ikeda 1970) to 40.6  $\mu\text{L O}_2 \text{ mg dw}^{-1} \text{ d}^{-1}$  (this study) at 13.6°C. Although these results are lower than Schukat et al.'s (2013) estimate of 75.6  $\mu\text{L O}_2 \text{ mg dw}^{-1} \text{ d}^{-1}$  at 14°C. Respiration data for *N. minor* were lower in this study with a calculated 42-46.1  $\mu\text{L O}_2 \text{ mg dw}^{-1} \text{ d}^{-1}$  (this study) compared to 55.3  $\mu\text{L O}_2 \text{ mg dw}^{-1} \text{ d}^{-1}$  measured by Schukat et al. (2013) at 17-18°C, albeit within the error limits  $\pm 21.6 \mu\text{L O}_2 \text{ mg dw}^{-1} \text{ d}^{-1}$  SD.

It is uncommon for other studies to report the absolute respiration rate of oceanic copepods incubated at *in situ* temperatures, preferring to interrogate datasets collected by few individuals (e.g. Ivleva 1980), discuss allometric relationships (e.g. Vidal and Whitley 1982), or focus on neritic species (e.g. Gauld and Raymond 1953; Raymond 1959). Therefore our ability to further compare our dataset with others is limited. However there are a number of caveats which could have affected the variability in the results. Raymond (1959) discuss potential sources of variability between estimates of respiration rates for the same species and concludes that the principal cause of this is differences in size. In our study for instance, the dry-weight of the animals was calculated using a general relationship (section 2.3.6) and therefore we could have introduced an estimation error for some of the species that may not fit accurately within the model shape.

Other factors besides size and temperature influence respiratory rates of zooplankton. Geographical and hydrological constraints may account for some of the differences. A comparison of the respiratory rates of marine copepods of the same species from different areas was undertaken by Raymond (1959) and Conover (1956). The neritic copepod *Acartia clausi* from the British coast was found to respire  $\sim 0.08 \mu\text{L O}_2 \text{ ind}^{-1} \text{ h}^{-1}$  at 17°C by Gauld and Raymond (1953). Conover (1956) obtained lower rates for specimens from North America (Long Island Sound) from 0.04 to 0.02  $\mu\text{L O}_2 \text{ ind}^{-1} \text{ h}^{-1}$  at 15°C. Factors such as size, degree of maturity, and generation were considered as the main causes of these respiratory differences, although size alone was not accountable for the difference. In addition, Conover (1959) and Marshall and Orr (1958) observed a possible seasonal adaptation to the changing temperature regime for certain species of copepods.

Another potential source of variation, when trying to estimate routine metabolic demand, is the effect of feeding on respiration. This could also contribute to the remaining 15-25% deviation of respiration rates from the MTE (Lin et al. 2013). For instance, copepods from the Benguela Upwelling system (Schukat et al. 2013) show higher respiration rates compared to Ikeda (2007). Although copepods were incubated in filtered seawater after starving them for a few hours, the respiration of *Pleuromamma xiphia* at 14°C (Schukat et al. 2013) is 66% higher compared to the measurement of Ikeda et al. (2007) at 12°C. This difference amounts to a much higher increase in respiration, with 2°C change, than

expected when assuming a  $Q_{10}$  of 2 (as suggested by both authors from Ikeda et al. (2001)). Our preliminary tests on the effects of chl-a concentration on respiration (temperature and mass adjusted) proved inconclusive, possibly due to the relatively constant low food concentration in the mostly oligotrophic transect, the large variation of other parameters and the limited range of copepod species analysed. The ability of some species to store lipid reserves may also have affected this relationship. This is since these organisms metabolism would not enter in “maintenance only” mode at the same time as those species unable to draw additional energy.

Since respiration rates are lower during periods of oligotrophy and higher when chl-a is abundant (Lampitt and Gamble 1982), it is possible that this respiratory increment observed in copepods from the Benguela system (Schukat et al. 2013) was affected by feeding history. Isla et al. (2004) and Huskin et al. (2001) measured ingestion rates of copepods during four different AMT cruises, crossing oligotrophic, temperate and upwelling regions of the Atlantic Ocean and found maximum ingestion rates in the upwelling regions and higher productivity areas. Thus, relating possible impacts of grazing rates on interspecific latitudinal variation of respiration rates. Schukat et al. (2013) data for instance, were collected in eutrophic upwelled waters whilst Ikeda’s data were collected in oligotrophic and mesotrophic environments. Likewise our data were collected mostly in oligotrophic waters, mesotrophic at times. In addition, as shown in chapter 3, food quality could also have an effect on copepod feeding history contributing to an increase or decrease in routine metabolic rates.

Methodological factors may well have contributed to the difference between the estimates observed in the 3 studies. Ikeda (1970) for instance, incubated some of his temperate and tropical species for 12 hours rather than 24 whilst Schukat et al. (2013) incubated the animals for an undisclosed amount of time, possibly 6 hours (Köster et al. 2008). It has been suggested that Initial respiratory rates are higher and that they level off after a few hours of incubation following the initial stress-induced rate increment potentially making 6-12 hours too short an incubation time (Conover 1959). Incubating animals for 24 hours also contributes to overcoming potential variation in diurnal rates (Pavlova 1994). It is known that the volume of the incubation bottle can also play a major role due to overcrowding and the so called “bottle effect” (Ikeda et al. 2000). Schukat et al. (2013) incubated the copepods in 12–13 ml vessels where the numbers of specimens per bottle varied between one individual for large species and ten individuals for small species. This suggests that in such a small incubation volume in Schukat et al. (2013) experiments, most copepod densities were within the levels affecting metabolic rates, hence the higher respiration rates (Ikeda et al., 2000).

#### 5.4.4 Allometric exponent

Variations in body mass and temperature accounted for between 85% and 75% of individual and mass-specific respiration rates respectively ( $p < 0.001$ ). Overall the measured respiration rates (Table 5.6 of supplementary material) compared well with assumed MTE values. Nevertheless the allometric coefficient  $b^{1.036}$  calculated for this dataset is significantly higher with the value of  $b^{3/4}$  suggested by the MTE (Gillooly et al. 2001; Brown et al. 2004). This should not be considered as the average of an entire population, albeit a  $b$  exponent of 1.036 represents copepods ranging from 0.09 to 0.4 mg dry weight (35-160  $\mu\text{g C}$ ) found at temperatures ranging from 4.7 to 30°C.

The mean value of 0.75 suggested by the MTE has been considered as the standard exponent for heterotrophic plankton with body sizes ranging from  $10^{-5}$  to  $10^5$   $\mu\text{g C}$  (Moloney and Field 1989). However, the universal  $3/4$  power scaling law has been heavily criticised and numerous intraspecific and interspecific variations in metabolic scalings have been identified (Clarke 2004; Glazier 2005, 2006 and 2010). Empirical evidence suggests that the allometric exponent  $b$  can vary from 0.4 to 1.4 (Ivleva 1980; Clarke 2004; Glazier 2006) between aquatic species, in response to ecological circumstances (Glazier 2006). A review of Ikeda's (2007) data on epipelagic copepods reveals that the allometric relationship varies depending on temperature and the range of sizes considered. For instance, his results show that the  $b$  exponent calculated for copepod respiration between -1.7 and 28.5 °C (1 to  $2 \times 10^3$   $\mu\text{g C}$ ) equals 0.76, close to the  $3/4$  scaling hypothesis, whilst for copepods occurring between 4.7 and 28.5 °C (temperatures matching this dataset) (1 to  $2 \times 10^3$   $\mu\text{g C}$  size),  $b$  equals 1.4 (Ikeda et al. 2007), even higher than a  $b$  of 1.036 (this study). Furthermore, Lopez-Urrutia et al. (2005) for instance, found an allometric exponent of  $0.87 \pm 0.005$  SE, for heterotrophs (including a wider range of sizes) across an average of 6 Atlantic Meridional transect cruises (mid-latitudes to tropical domains).

Although we weren't able to calculate species-specific allometric relationships, except for *P. abdominalis* (panel B Figures 5.5 to 5.9) an average exponent closer to 1 indicates a higher species-specific  $b$  for most of the species considered in this study. This is supported by the study of Vidal and Whitledge (1982) which showed that *U. vulgaris* had an allometric exponent of  $\sim 0.92$ , (Vidal and Whitledge 1982). Interestingly we found an allometric exponent  $> 2$  for *P. abdominalis*, this suggests that the species may respire a large amount of energy per unit body mass.

#### 5.4.5 Temperature dependent metabolic rates, $E_a$ and $Q_{10}$ coefficients

By measuring metabolic rates across a range of temperatures, it is possible to characterize the response to environmental variability from the species to the population level. Temperature effects can be evaluated by calculating activation energy  $E_a$  or/and the  $Q_{10}$  values, with higher values indicating higher sensitivity to increasing temperatures. The use of the  $Q_{10}$  quotient has the disadvantage of possible errors due to the large number of equations commonly used in its calculation. This can result in up-to 31% (Table 5.5) variability between values. Ikeda (1985) also found that the results depended significantly on the units by which the respiration rates were normalised (dry weight or allometric exponent).

In this study  $Q_{10}$  estimates were based on dry-weight normalised respiration rates and on the ranges between the 4 most commonly used equations as shown in section 5.2.2. Our critical evaluation of these estimates suggest that the use of the van't Hoff equation 5.4 can give rise to the highest discrepancy whilst formulae including a rate/temperature integrated approach (eq. 5.2, 5.3 and 5.5) agree with <10% difference. Overall the offset between estimates derived from equations 5.5, 5.3 and 5.2 varied resulting in an uncertainty of about 10%; yet neither of these was consistently higher or lower than the others. However equation 5.5 could provide a more accurate method for the estimation of  $Q_{10}$  coefficients since estimations calculated with equation 5.2 and 5.3 include a larger number of uncertainties caused by a larger number of assumptions such as the relationship with the  $E_a$  parameter.

Overall metabolic rates, normalised to per unit of copepod biomass, increased exponentially with increasing temperature (Figure 5.1). The estimated temperature coefficient for the dataset (Table 5.2) was  $E_a = 0.76$  eV, above the average predicted by the MTE (0.6–0.7eV), although within the range suggested by Gillooly et al. (2001) (0.2–1.2 eV). Using the dataset given in Ikeda et al. (2007) we estimated an average  $E_a$  of 0.59 eV for epipelagic copepods for temperatures between -1.7 and 28.5 °C. The general  $Q_{10}$  range of 2.75 to 2.82 (excluding equation 5.4) was higher than the  $Q_{10}$  of 2.1 estimated by Ikeda (1985) for copepods in the Pacific Ocean. However, it is within the range (between 2 to 3) derived from a global compilation of respiration data by Ivleva (1980), Ikeda (1985), and Ikeda et al. (2001) (Hernandez-Leon and Ikeda 2005). The higher values could have been influenced by the atmospheric phenomena of La Niña, affecting the hydrography of the Atlantic basin and causing an overall increase in habitat temperatures at the time of the investigation. However, no  $Q_{10}$  data for the species considered in this study are available for the years not affected by ENSO events. Overall

$E_a$  and  $Q_{10}$  are in agreement, suggesting a higher sensitivity to temperature increase than expected within the migrator copepods considered in this dataset. This suggests that the larger mesopelagic migratory copepods considered in this study are more sensitive to temperature changes and climatic variability than epipelagic species. This has also been suggested by Hernandez-Leon and Ikeda (2005), who calculated higher values of  $Q_{10}$  for mesopelagic copepods.

There have been relatively few investigations on the species-specific response of oceanic copepods to environmental variation therefore we have little comparable data. Species-specific  $E_a$  values (Table 5.4) were high for *P. abdominalis* (1.066 eV) whilst the parameters for *U. vulgaris* (0.69 eV) and *P. gracilis* (0.7 eV), were within the MTE expected range of 0.6 to 0.7 eV (Gillooly et al. 2001; Brown et al. 2004). The  $E_a$  coefficients for *Euchirella* sp. and *N. minor* were lower at 0.58 eV and 0.59 eV respectively. Higher and lower values were still within the range of variation (95% CI) proposed by Gillooly et al. (2001) of 0.2 to 1.2 eV. High  $E_a$  coefficients have been observed for the respiration of Arctic copepods, with values ranging from 1.05 eV to 1.68 eV (Alcaraz et al. 2013 and references therein). This suggests that species from different ecosystems can have similar sensitivities to changes in temperature (Tropical and Arctic habitats).

The calculated  $E_a$  values were in agreement with the species-specific  $Q_{10}$  values showing a stronger sensitivity to temperature changes of *P. abdominalis* with a  $Q_{10}$  ranging 3.68-4.07 (excluding estimate of eq. 5.4). The  $Q_{10}$  values for *U. vulgaris* were between 2.5 - 3.03 and for *P. gracilis* were between 2.57 and 2.59. The  $Q_{10}$  calculations suggest that *N. minor* had the lowest coefficient 2.07-2.2 compared to 2.14-2.46 for *Euchirella* sp.

Overall these results suggest that although these mesopelagic species may have similar latitudinal adaptation strategies (tropical and subtropical distribution), it can result in different metabolic sensitivities. These temperature-related tolerances and boundaries are dictated by the species-specific optimal range of physiological performance and ecological niche, with some species able to withstand larger habitat fluctuations than others. This is shaped through evolutionary mechanisms guiding the species' physiological adaptation to an "optimal range of temperatures" (Withers 1992). The larger species belonging to the genus *Pleuromamma*, for instance, are strong vertical migrators that inhabit the upper mesopelagic, lower epipelagic zones (also bathypelagic for *P. abdominalis*). They are not found at the surface during the day-time, indicating their preference for colder waters (<10°C at the base of the mesopelagic layer). This is supported by our data,

demonstrating the potential *P. abdominalis* sensitivity to change through high  $E_a$  and  $Q_{10}$  values.

Importantly, respiration is closely coupled with growth therefore production and metabolism are linked (Ikeda et al. 2001; Nobili et al. 2013). Little is known regarding the life cycle of *P. abdominalis* however other mesopelagic members of the same genus, such as *Pleuromamma robusta* and possibly *Pleuromamma scutellata*, can have fewer than ~3 generations per year (Yamaguchi and Ikeda 2000 and references therein). Females of *P. abdominalis* produced very few or no eggs during AMT20 (Table 5.8 supplementary material) possibly in agreement with mesopelagic reproductive strategies. This suggests that any negative effect on metabolic processes such as an increase in carbon demand due to increasing temperatures, could seriously affect the already low reproduction rates with feedbacks on the species gross growth efficiency and biomass.

As climate conditions continue to warm and ENSO events occur cyclically, copepods are subjected to shifts in temperature. Some species are able to compensate for large habitat changes while others have minimal adaptation potential. This could affect the copepod energy balance by inducing respiratory losses higher than energy intake (ingestion) (Vaquer-Sunyer et al. 2010) as well as increasing  $CO_2$  production. Ultimately, this is driving ecosystem change at the macro scale and leading to changes in the metabolic balance of the oceans (Vaquer-Sunyer et al. 2010). For instance, in a climate warming scenario an estimated SST increase of 1.5-2.6°C by 2100 is predicted (IPCC 2007). The response predicted for the copepods considered in this study (0.09 to 0.4 mg dry weight) suggests an average 31% increase in weight-specific respiration rates by the end of the century. These increased metabolic demands will limit the energy and substrate available for biosynthesis, leading to a reduction in the production to respiration ratio with increasing ocean warming (Vaquer Sunyer et al. 2010).

#### 5.4.6 Summary and Conclusions

Methodological artefacts affected the relationships between EPR, temperature and chl-a concentration. These comprised of a limited number of species selected, mostly migrators, low reproductive potential and high incidence of zero values for EPR. Therefore no general conclusions regarding the effects of temperature and food concentration on Atlantic copepods EPR can be suggested here. However, this study was able to provide valuable information on the ecology and reproductive potential of some medium-large sized migratory copepods as well as evidence for some species-specific responses to natural habitat variation. Except *U. vulgaris*, species belonging to the genus *Pleuromamma* and *Euchirella sp.* had generally very low reproductive responses at the

range of temperatures investigated. This suggests that some of these species, *Pleuromamma* for instance, may have low fecundity strategies producing few generations per year.

The neritic and oceanic tropical subtropical ubiquitous *U. vulgaris* showed a relatively high response to temperature changes with individual carbon requirements increasing with temperature; Its EPR also declined with temperature increases. The pelagic mid-latitude species *P. gracilis* was found across a wide latitudinal range. Similarly to *U. vulgaris* it had high  $Q_{10}$  and  $E_a$  values although with a low individual carbon requirement. The pelagic subtropical and tropical species *N. minor* displayed low  $E_a$  and  $Q_{10}$  coefficients in this study possibly indicating lower sensitivity to temperature changes and had low individual carbon requirements. *Euchirella sp.* was the least sensitive to temperature variation albeit with high individual carbon requirements within the range of temperatures measured during AMT20. The mesopelagic species *P. abdominalis* had high individual carbon requirements and was the most sensitive species to temperature increase, with an elevated  $Q_{10}$  and an  $E_a$  coefficient comparable to those found for Arctic copepods.

Our analysis suggests 75-85% of the variability in respiration can be explained by variations in body size and temperature. Overall the MTE can be used to quantitatively describe the variation in respiration rates of some copepods across an Atlantic latitudinal transect. However, the average and the species-specific scaling coefficients of temperature and body size, for copepods ranging from 0.09 to 0.4  $\mu\text{g}$  of dry-weight found between temperatures from 4.7 to 30°C, deviate from predictions. Within the range of temperatures measured during AMT20, estimates of the Arrhenius  $E_a$  and  $Q_{10}$  were generally in agreement with each other, suggesting a high sensitivity to temperature increase within the copepods considered in this dataset. Diet-specific effects of not only food quantity, but also food quality could be important factors affecting copepod metabolism and contributing to the remaining 15-25% variation in metabolic rates.

The life-strategies of these open-ocean mesopelagic copepods have been shown to have different basic tolerances and responses to changes in temperature and food availability (and quality). These species-specific life histories and adaptations determine their ability to withstand habitat fluctuations within their ecological niche. As we face climate-driven changes in the global ocean is of uppermost importance to investigate species-specific responses to habitat variability in a variety of different ecosystems. This since investigating variations in species interactions will help improve our estimations of metabolic demands and production in some of the less studied areas of the oceans and

improve predictions of long-term changes in the ecology and dynamics of these ecosystems and at a global scale.

## 5.5 Supplementary material

**Table 5.6.** Copepod respiration measured during AMT20. Station number (STN), incubation temperature, body volume ( $\text{mm}^3$ ) and weight (carbon and dry-weight  $\mu\text{g}$ ) and respiration rates.

Species	STN	Temp. °C	Incubation	Volume $\text{mm}^3$	C weight $\mu\text{g}$	Dry-weight mg	Respiration	
							$\mu\text{l O}_2 \text{ ind}^{-1} \text{ d}^{-1}$	$\mu\text{l O}_2 \text{ mg dw}^{-1} \text{ d}^{-1}$
<i>Pleuromamma</i>	71	4.7	acute	0.26	0.045	0.112	3.94	35.28
<i>gracilis</i>	71	4.7	acute	0.32	0.048	0.121	3.46	28.60
	71	5.6	acute	0.34	0.050	0.125	4.22	33.71
	71	10.6	in situ	0.27	0.045	0.112	3.09	27.54
	67	10.7	acute	0.17	0.038	0.094	4.32	45.82
	67	10.7	acute	0.17	0.038	0.095	5.97	62.89
	67	10.7	acute	0.22	0.041	0.103	4.18	40.52
	71	11.1	in situ	0.28	0.046	0.114	2.95	25.88
	67	11.9	acute	0.18	0.039	0.097	8.51	87.58
	67	11.9	acute	0.23	0.042	0.106	3.31	31.32
	67	11.9	acute	0.27	0.045	0.113	7.10	62.86
	67	11.9	acute	0.18	0.039	0.097	2.43	25.05
	60	12.8	in situ	0.15	0.037	0.092	3.59	39.02
	60	13	acute	0.16	0.038	0.094	2.25	23.97
	71	13.4	in situ	0.20	0.040	0.100	1.36	13.62
	71	13.4	in situ	0.41	0.055	0.138	10.65	76.99
	56	14	acute	0.15	0.036	0.091	2.75	30.15
	56	14	acute	0.15	0.037	0.091	2.23	24.37
	56	14.1	acute	0.15	0.037	0.091	4.28	46.79
	67	16	in situ	0.30	0.047	0.118	7.65	64.93
	67	16	in situ	0.30	0.047	0.118	13.71	116.22
	67	16	in situ	0.33	0.050	0.124	10.30	83.21
	60	19.7	in situ	0.15	0.037	0.092	7.76	84.19
	60	19.7	in situ	0.14	0.036	0.089	9.58	107.03
	60	19.8	in situ	0.58	0.067	0.167	15.52	92.88
	14	22.5	in situ	0.20	0.040	0.100	14.53	145.81
	14	22.5	in situ	0.22	0.041	0.103	13.42	130.03
	56	22.5	in situ	0.14	0.036	0.089	12.55	141.11
	56	22.6	in situ	0.14	0.036	0.089	13.08	146.52
	56	22.6	in situ	0.17	0.038	0.094	11.10	117.78
	30	27.3	in situ	0.15	0.036	0.091	16.82	184.97

Table 5.6. Cont' (1).

Species	STN	Temp. °C	Incubation	Volume mm <sup>3</sup>	C weight µg	Dry-weight mg	Respiration		
							µl O <sub>2</sub> ind <sup>-1</sup> d <sup>-1</sup>	µl O <sub>2</sub> mg dw <sup>-1</sup> d <sup>-1</sup>	
<i>Pleuromamma xiphia</i>	14	21.4	in situ	1.84	0.156	0.390	49.89	127.99	
	56	22.4	in situ	1.35	0.122	0.305	54.60	179.17	
	56	22.4	in situ	1.65	0.143	0.358	60.71	169.78	
	14	22.5	in situ	1.44	0.128	0.319	17.04	53.39	
	22	25.9	in situ	1.84	0.156	0.390	68.77	176.43	
<i>Pleuromamma abdominalis</i>	50	18.1	in situ	0.51	0.062	0.156	12.25	78.55	
	45	20.9	in situ	0.91	0.090	0.225	26.46	117.35	
	14	22.4	in situ	0.67	0.074	0.184	17.59	95.69	
	14	22.5	in situ	0.65	0.072	0.180	25.29	140.11	
	30	22.7	in situ	0.89	0.089	0.222	33.30	149.66	
	30	23.3	in situ	0.99	0.096	0.240	30.60	127.48	
	30	23.3	in situ	1.16	0.108	0.270	33.91	125.72	
	22	26.3	in situ	0.93	0.092	0.230	48.91	212.56	
	30	27.1	in situ	1.21	0.112	0.279	90.74	325.10	
	30	27.3	in situ	0.96	0.094	0.234	47.47	202.47	
	<i>Euchaeta acuta</i>	50	10.9	in situ	1.13	0.106	0.265	8.59	32.45
		50	17.9	in situ	1.25	0.114	0.285	13.20	46.24
50		18	in situ	1.90	0.161	0.402	16.48	41.04	
56		22.4	in situ	1.80	0.154	0.384	65.73	171.06	
<i>Nannocalanus minor</i>	50	23.6	in situ	2.21	0.182	0.456	44.96	98.69	
	60	12.8	acute	0.32	0.048	0.121	4.17	34.50	
	60	12.8	acute	0.32	0.049	0.122	3.31	27.08	
	56	13.8	in situ	0.31	0.048	0.119	4.24	35.52	
	56	14	acute	0.13	0.035	0.088	3.92	44.63	
	56	14	acute	0.18	0.038	0.096	2.92	30.31	
	60	19.7	in situ	0.33	0.049	0.123	4.73	38.44	
	60	21.8	in situ	0.42	0.056	0.140	5.96	42.67	
	60	21.8	in situ	0.32	0.049	0.122	8.56	70.07	
	56	22.4	in situ	0.22	0.042	0.104	9.73	93.36	
<i>Metridia gerlachei</i>	71	13.4	in situ	0.40	0.054	0.136	6.87	50.57	
	71	13.6	in situ	0.38	0.053	0.133	3.65	27.53	
	71	13.4	in situ	0.34	0.050	0.125	7.24	57.86	
<i>Calanus sp.</i>	34	19.6	in situ	0.77	0.081	0.201	14.69	72.92	
	34	19.3	in situ	0.73	0.078	0.195	12.49	64.18	
	34	24.5	in situ	0.72	0.077	0.192	25.47	132.66	
	26	28	in situ	0.80	0.083	0.207	44.19	213.24	
<i>Euchirella sp.</i>	34	19.6	in situ	0.81	0.083	0.209	33.46	160.43	
	45	20.8	in situ	0.70	0.076	0.189	15.73	83.14	
	45	20.8	in situ	0.79	0.082	0.204	14.06	68.89	
	50	24	in situ	0.58	0.067	0.168	37.91	225.85	
	26	28	in situ	0.60	0.068	0.171	38.53	225.90	
	45	28.5	in situ	0.77	0.080	0.201	41.78	207.68	
	34	29.3	in situ	0.82	0.084	0.210	45.12	215.20	
	34	29.3	in situ	0.69	0.075	0.188	47.62	253.66	
	34	29.3	in situ	0.70	0.076	0.189	45.49	240.65	

Table 5.6. Cont' (2).

Species	STN	Temp. °C	Incubati on	Volume mm <sup>3</sup>	C weight µg	Dry-weight mg	Respiration	
							µl O <sub>2</sub> ind <sup>-1</sup> d <sup>-1</sup>	µl O <sub>2</sub> mg dw <sup>-1</sup> d <sup>-1</sup>
<i>Undinula</i>	50	10.6	in situ	0.64	0.071	0.178	4.60	25.81
<i>vulgaris</i>	50	10.9	in situ	0.55	0.065	0.162	7.03	43.44
	50	17.9	in situ	0.73	0.078	0.194	11.01	56.79
	50	18.1	in situ	0.65	0.072	0.181	5.15	28.50
	45	18.7	in situ	0.67	0.073	0.183	13.50	73.73
	45	18.9	in situ	0.63	0.071	0.177	15.17	85.60
	45	18.9	in situ	0.65	0.072	0.179	11.93	66.50
	45	18.9	in situ	0.63	0.070	0.176	14.91	84.72
	34	19.3	in situ	0.67	0.074	0.184	11.98	65.05
	34	19.3	in situ	0.70	0.075	0.189	11.12	58.99
	34	19.6	in situ	0.80	0.083	0.207	18.76	90.47
	38	19.7	in situ	0.64	0.071	0.178	13.53	75.79
	38	19.7	in situ	0.63	0.071	0.177	19.15	108.08
	38	19.8	in situ	0.51	0.062	0.155	12.68	81.56
	45	20.8	in situ	0.57	0.066	0.166	13.39	80.63
	45	20.8	in situ	0.74	0.079	0.196	23.59	120.14
	45	21	in situ	0.57	0.066	0.166	15.38	92.63
	26	21.6	in situ	0.64	0.071	0.179	11.55	64.62
	26	21.6	in situ	0.66	0.073	0.182	13.66	75.24
	26	21.7	in situ	0.47	0.059	0.148	14.37	97.20
	56	22.4	in situ	0.32	0.048	0.121	17.33	143.24
	56	22.4	in situ	0.34	0.050	0.125	18.52	147.69
	50	23.9	in situ	0.72	0.077	0.193	43.37	225.07
	50	23.9	in situ	0.62	0.070	0.175	43.18	246.78
	50	24	in situ	0.73	0.077	0.193	44.34	229.27
	34	24.5	in situ	0.59	0.067	0.169	19.53	115.79
	34	24.5	in situ	0.49	0.061	0.151	21.61	142.66
	38	25.9	in situ	0.65	0.072	0.180	31.40	174.91
	38	26.1	in situ	0.57	0.067	0.167	35.90	215.55
	38	26.5	in situ	0.63	0.071	0.177	27.56	155.52
	26	27.8	in situ	0.58	0.067	0.168	35.42	210.91
	26	27.8	in situ	0.58	0.067	0.168	41.57	247.52
	26	27.8	in situ	0.67	0.074	0.184	49.77	270.08
	26	27.8	in situ	0.61	0.069	0.174	44.87	258.47
	26	27.8	in situ	0.55	0.065	0.162	40.47	250.53
	45	28.3	in situ	0.73	0.078	0.194	39.62	204.08
	45	28.3	in situ	0.74	0.079	0.196	37.47	190.86
	45	28.3	in situ	0.73	0.078	0.194	43.31	223.51
	38	28.6	in situ	0.65	0.072	0.180	25.49	141.99
	38	28.6	in situ	0.63	0.071	0.177	30.97	174.92
	38	28.8	in situ	0.74	0.078	0.196	70.28	359.38
	38	28.8	in situ	0.96	0.094	0.234	26.88	114.80
	34	29	in situ	0.71	0.076	0.190	37.52	197.08
	34	29	in situ	0.80	0.083	0.207	39.97	192.76
	34	29	in situ	0.71	0.076	0.191	34.21	179.33
	45	29.5	in situ	0.74	0.078	0.195	38.15	195.49

**Table 5.7.** Egg Production Rates measured on AMT20. Egg production after 24 hours at a range of in situ and other temperatures (see table 5.6 for details). Station number (STN), temperature of incubation (°C), Number of eggs per female (egg f<sup>-1</sup> d<sup>-1</sup>) number of nauplii found after 24 hours, carbon and dry weight of the females (µg) and egg diameter ± SD.

<i>Species</i>	STN	°C	Eggs number	Nauplii	C weight µg	Dry-weight µg	Egg size µm ± SD
<i>Nannocalanus minor</i>	60	19.7	0		47.13	117.82	
	60	19.7	0		48.58	121.45	
	60	19.7	0		44.80	111.99	
	60	19.7	0		48.63	121.56	
	60	19.7	0		48.63	121.56	
<i>Pleuromamma gracilis</i>	71	10.5	0		47.68	119.21	
	71	10.5	0		47.95	119.88	
	71	10.5	3		54.93	137.33	108 ± 6.9
	71	10.5	1	1	51.20	128.00	
	67	11.5	0		39.73	99.33	
	67	11.5	1		42.19	105.48	116 ± NA
	67	11.5	1		44.72	111.81	110 ± NA
	67	11.5	0		42.39	105.98	
	71	13.3	0		50.65	126.62	
	71	13.3	0		47.68	119.21	
	71	13.3	0		47.25	118.11	
	71	13.3	0		50.76	126.90	
	71	13.4	0		51.37	128.42	
	71	13.4	4		54.97	137.43	116 ± 4.0
	67	16	0		45.92	114.81	
	67	16	0		44.75	111.88	
		14	23.3	0		36.05	90.11
14		23.3	0		40.06	100.15	
14		23.3	0		39.79	99.47	
<i>Euchaeta acuta</i>	60	19.7	1		185.68	464.19	140 ± NA
	26	27.3	0		127.90	319.76	
<i>Pleuromamma xiphia</i>	14	23	2		139.82	349.55	
	18	25.3	1		149.13	372.83	200 ± NA

Table 5.7. Cont' (1).

<b>Species</b>	<b>STN</b>	<b>°C</b>	<b>Eggs number</b>	<b>Nauplii</b>	<b>C weight µg</b>	<b>Dry-weight µg</b>	<b>Egg size µm ± SD</b>
<i>Undinula vulgaris</i>	45	18.7	0		78.24	195.59	
	45	18.7	28		79.19	197.96	139 ± 2
	45	18.7	6		78.03	195.06	140 ± NA
	34	19.2	35		77.08	192.69	
	34	19.2	0		66.55	166.37	
	34	19.2	8		71.26	178.15	143 ± 5.8
	34	19.2	0		83.09	207.72	
	34	19.2	33		70.83	177.08	143 ± 4.6
	38	19.8	3		72.06	180.15	121 ± 9.0
	38	19.8	7		76.10	190.25	120 ± NA
	38	19.8	3	1	69.55	173.87	135 ± 7.1
	45	20.7	1		78.92	197.29	140 ± NA
	45	20.7	1		77.02	192.55	136 ± NA
	26	21	1		44.90	112.25	100 ± NA
	26	21.7	0		56.60	141.51	
	26	21.7	0		56.41	141.03	
	34	24.6	11	1	78.03	195.06	
	34	24.6	7	1	75.90	189.74	140 ± NA
	34	24.6	21	4	75.90	189.74	137 ± 5.8
	34	24.6	0		65.16	162.90	
	34	24.6	1		65.16	162.90	120 ± NA
	34	24.6	4		75.55	188.88	120 ± NA
	38	26.3	0		77.53	193.81	
	38	26.3	3		71.53	178.82	
	38	26.3	0		50.45	126.12	
	38	26.3	6		69.92	174.80	137 ± 5.8
	26	27.3	13	1	64.42	161.05	120 ± NA
	26	27.3	0		52.79	131.98	
	30	27.3	1		71.32	178.30	160 ± NA
	30	27.3	0		78.50	196.25	
	45	28	4		78.98	197.46	
	34	28.2	6	2	67.52	168.81	160 ± NA
	34	28.2	1		78.97	197.44	152 ± NA
	38	28.7	1		71.29	178.22	
	38	28.7	0		76.13	190.32	
	38	28.7	0		71.32	178.30	

Table 5.7. Cont' (2).

<i>Species</i>	STN	°C	Eggs number	Nauplii	C weight µg	Dry-weight µg	Egg size µm ± SD
<i>Pleuromamma borealis</i>	71	10.5	0		57.97	144.93	
<i>Clausocalanus sp.</i>	4	11	31		35.02	87.55	
	4	11	17		34.70	86.75	
	4	11	9		31.18	77.96	
	8	11.4	53		31.12	77.81	
	8	11.4	15		34.85	87.13	73 ± 5.8
	4	16	3		29.29	73.22	
	4	16	25		35.27	88.19	
	4	16	2		35.76	89.39	68 ±
	4	16	51		33.89	84.73	60 ± NA
	4	16	51		31.01	77.51	
	4	16	2		33.97	84.93	50 ± NA
	8	16.7	2		31.86	79.65	
	4	20	0		35.76	89.39	
	4	20	0		34.01	85.02	
	4	20	3		35.08	87.69	
<i>Pleuromamma abdominalis</i>	8	21.2	0		30.44	76.09	
	12	20.8	2		70.12	175.30	
	12	20.8	1		77.55	193.89	
	30	22.7	0		64.28	160.71	
	30	22.7	0		74.46	186.14	
	14	23.3	4		82.33	205.82	
	14	23.3	0		68.33	170.82	
	14	23.3	2		69.36	173.41	140 ± NA
	34	24.6	0		67.96	169.91	
	18	25.3	0		80.04	200.11	
	22	26	0		85.48	213.71	
	38	26.3	0		67.24	168.10	
	38	26.3	0		61.78	154.46	
	26	27.3	0		67.47	168.68	
	30	27.3	0		66.97	167.42	
30	27.3	0		58.65	146.64		
<i>Euchirella sp.</i>	45	20.7	2		73.46	183.65	
	26	21	0		57.63	144.06	
	26	21.7	2		61.11	152.78	260 ± NA
	26	21.7	0		58.64	146.61	
	26	21.7	2		66.03	165.07	270 ± 14
	26	27.3	1		49.06	122.65	272 ± NA
	26	27.3	1		61.11	152.78	
45	27.8	0		76.57	191.44		

**Table 5.8.** Copepod respiration from Ikeda et al. (2007). Copepod stage/sex (M: male, F: female), respiration rate, body mass (mg), incubation temperature and depth of occurrence.

Copepod Species	Stage	Depth m	Temp. °C	Dry-weight mg	Respiration	
					$\mu\text{l O}_2 \text{ ind}^{-1} \text{ d}^{-1}$	$\mu\text{l O}_2 \text{ mg dw}^{-1} \text{ d}^{-1}$
<i>Rhincalanus gigas</i>		50	-1.7	1.08	10.49	9.71
<i>Metridia gerlachei</i>		2	-1.4	0.2654	7.67	28.89
<i>Calanus propinquus</i>		2	-1	1.0425	28.29	27.14
<i>Calanoides acutus</i>	C4.5	2	-0.6	0.266	3.90	14.66
<i>Calanus hyperboreus</i>	C5	50	-0.3	2.677	25.30	9.45
<i>Calanoides acutus</i>	C5	2	-0.2	0.3936	5.06	12.85
<i>Calanus finmarchicus</i>	C6F	2	0.1	0.3865	7.87	20.36
<i>Metridia longa</i>	C6F	50	0.1	0.353	9.74	27.59
<i>Calanus hyperboreus</i>	C5	50	0.9	1.943	24.66	12.69
<i>Calanus hyperboreus</i>	C6F	50	1.3	3.95	35.64	9.02
<i>Calanus glacialis</i>	C6F	21.2	1.9	0.4736	14.78	31.21
	C6F	100	3	0.3588	8.06	22.47
	C6F	100	3	0.4343	6.54	15.05
<i>Metridia pacifica</i>	C6F	135	4.7	0.2032	9.54	46.95
<i>Candacia columbiae</i>	C6F	100	4.7	0.5589	18.25	32.65
<i>Neocalanus cristatus</i>	C5	25	5	1.72	24.00	13.95
<i>Neocalanus plumchrus</i>	C4	2	5.6	0.2633	6.72	25.52
<i>Neocalanus plumchrus</i>	C5	75	5.8	0.244	6.02	24.69
	C6F	75	5.8	0.183	6.66	36.39
	C6F	75	5.8	0.4025	10.15	25.22
<i>Eucalanus bungii</i>		2	6	1.01	19.08	18.89
<i>Pleuromamma scutullata</i>	C6F	75	6	0.3223	10.40	32.28
<i>Gaetanus simplex</i>	C6F	75	6	0.4508	8.72	19.35
<i>Neocalanus cristatus</i>	C5	2	6.3	1.5873	40.08	25.25
<i>Tortanus discaudatus</i>		2	7	0.0569	2.88	50.62
<i>Neocalanus plumchrus</i>	C5	2	7.3	0.7852	16.32	20.78
<i>Calanus marshallae</i>	C5	15	8	0.4211	9.19	21.82
	C5	15	8	0.9278	15.55	16.76
<i>Metridia pacifica</i>		2	8.2	0.1476	9.17	62.15
<i>Pseudocalanus elongatus</i>		2	8.6	0.0116	0.95	82.14
<i>Acartia longiremis</i>		2	9.6	0.0081	0.67	82.96
<i>Euchaeta marina</i>	C6F	100	11.3	0.415	14.47	34.86

Table 5.8. Con't.

Copepod Species	Stage	Depth m	Temp. °C	Dry-weight mg	Respiration	
					$\mu\text{l O}_2 \text{ ind}^{-1} \text{ d}^{-1}$	$\mu\text{l O}_2 \text{ mg dw}^{-1} \text{ d}^{-1}$
<i>Candacia bipinnata</i>	C6F	100	11.3	0.3325	17.01	51.16
<i>Pleuromamma xiphias</i>	C6F	100	12	0.3873	13.17	34.01
<i>Metridia pacifica</i>	2	13		0.094	6.57	69.88
	C6F	100	13	0.1636	9.70	59.28
<i>Pleuromamma abdominalis</i>	C6F	100	13.6	0.3585	16.40	45.76
<i>Paracalanus parvus</i>		2	13.9	0.0038	0.74	195.79
<i>Pseudodiaptomus marinus</i>		2	14.3	0.0142	1.35	95.15
<i>Acartia clausi</i>		2	14.8	0.0085	0.73	86.12
<i>Neocalanus plumchrus</i>		2	15.1	0.294	13.32	45.31
<i>Mesocalanus tenuicornis</i>		2	15.8	0.0313	5.28	168.69
<i>Centropages abdominalis</i>		2	15.9	0.0167	2.05	122.87
	C6F	100	16	0.335	21.69	64.74
<i>Centropages brachiatus</i>		2	17.3	0.0198	2.76	139.39
<i>Neocalanus gracilis</i>		2	19.7	0.5	39.36	78.72
	C6F	100	20	0.23	21.80	94.80
	C6F	15	20.2	0.18	17.83	99.07
	C6F	15	20.3	0.1017	11.43	112.40
<i>Acartia tonsa</i>		2	22	0.0072	1.35	188.00
<i>Mesocalanus tenuicornis</i>	C6F	15	22	0.265	14.38	54.28
<i>Undinula vulgaris</i>		2	23.5	0.1854	23.19	125.09
<i>Euchaeta marina</i>		2	24	0.2905	32.10	110.50
<i>Eucalanus subcrassus</i>		2	24	0.1037	15.72	151.59
<i>Labidocera acuta</i>		2	24	0.2334	45.36	194.34
<i>Acartia australis</i>		2	25	0.0091	1.33	145.85
<i>Acartia pacifica</i>		2	26	0.0078	1.11	142.77
<i>Calanopia elliptica</i>		2	26	0.0563	6.73	119.49
<i>Tortanus gracilis</i>		2	26	0.0235	3.44	146.35
<i>Labidocera nerii</i>		2	26.4	0.221	36.36	164.52
<i>Pontella danae</i>		2	26.4	0.7	82.32	117.60
<i>Nannocalanus minor</i>		2	26.9	0.0401	5.04	125.69
<i>Eucalanus attenuatus</i>		2	27.4	0.1374	21.72	158.08
<i>Undinula vulgaris</i>		2	27.6	0.1673	33.57	200.68
<i>Labidocera acuta</i>		2	28.5	0.2315	49.68	214.60

## **CHAPTER 6**

## 6. Summary, general discussion and conclusions

### 6.1 Thesis summary

In chapter 3 we describe a laboratory study to determine the effect of phytoplankton quality on feeding, respiration, reproduction and the resulting carbon budget of the neritic copepod *Temora longicornis*. Cultures of *Rhodomonas salina* were provided as food and the quality was determined from the % content of 4 classes of fatty acids (PUFA, MUFA, SAFA and n-3/n-6) and the stoichiometry of organic nutrients (N:P, C:N and C:P ratios).

We aimed to test the following hypotheses:

1. Maximum metabolic and growth rates occur when copepods are fed on phytoplankton which has an optimal food quality.
2. The effects of seston N:P ratio on copepod biomass can be seen in the field.
3. A balanced diet for all copepods corresponds to an elemental ratio of 16N:1P (molar) (Redfield ratio).

An important finding was the marked biphasic response of copepod physiology to a Threshold Nutrient Ratio (TNR) of 16:1 N:P, therefore defining it as the optimum diet for *T. longicornis*. Hence, maximum respiration (R), egg production rate (EPR), assimilation efficiency (AE), gross growth efficiency (GGE) and metabolic increment (MI) occurred when *T. longicornis* was fed on phytoplankton with an N:P ratio of ~16:1. EPR, MI, GGE and AE decreased with decreasing C:N ratio, EPR also decreased with decreasing n-3/n-6 ratio and PUFA (weak trend). Respiration decreased with increasing MUFA. The data showed that copepod rates varied proportionally to the quality of food ingested, proving hypothesis 1.

Importantly, we found that GGE was negatively affected at dietary ratios above and below 16N:1P, which in the natural environment could lead to a decline in species biomass with detrimental consequences for trophic transfer of energy and carbon export. Time-series data from the North Sea (Redfield system) and NPSG (P stressed system) showed that seston organic N:P ratios varied on a range of timescales and that this was an important factor affecting copepod abundance. This shows that hypothesis 2 was consistent with the observations, but due to co-variations with other environmental variables (e.g. temperature and time of year) hypothesis 2 could not be definitively proven.

The zooplankton size-fractionated biomass data from HOT suggested that copepod GGE (and therefore biomass) was sensitive to changes in the N:P ratio of their diet. However

the biomass of different zooplankton size fractions did not all peak at 16:1 as seen for *T. longicornis*, suggesting possible species-specific TNR. Moreover, for each zooplankton size-fraction, the N:P ratio of the zooplankton was ~9.5 lower than the N:P of the food, therefore disproving hypothesis 3.

In chapter 3 we acknowledged that the lack of temporal and spatial data on seston particulate C:N:P ratios currently limits an investigation of the contribution of food quality to zooplankton dynamics in the field. Therefore in chapter 4 we describe an analysis of food quantity (particulate organic nutrient concentrations) and quality (stoichiometry and fatty acid concentrations) at the chlorophyll maximum (CM) within six ecological domains of the Atlantic Ocean.

We tested the following hypotheses:

4. Food quality, in terms of stoichiometric ratios and fatty acid concentrations, is lower in oligotrophic domains and higher in upwelling and temperate regions of the Atlantic Ocean.
5. Particulate organic nutrient concentrations can be predicted from environmental parameters measured by sensors deployed on the CTD rosette.
6. Empirical relationships between particulate organic nutrient concentrations and environmental factors allow the determination and the prediction of food quality when *in situ* data is not available.
7. Food quality has decreased over time in the Atlantic basin.

Our definition of nutritious food included seston with lower C:N ratios, N:P ratios close to Redfield values and a higher proportion of autotroph-derived PUFA, essential fatty acids (FA) such as 20:5(*n*-3) and 22:6(*n*-3), high (*n*-3):(n-6) ratios and lower proportions of SAFA.

Marked latitudinal and temporal variations in food quantity and quality occurred at the CM in the Atlantic Ocean. The oligotrophic regions in the subtropical and tropical Atlantic Ocean were characterised by warm and well-stratified waters which contained poor quality food with high C:N ratios and high SAFA concentrations. These oligotrophic gyres were separated by the equatorial upwelling, a region of increased production containing consistently higher quality and quantities of food. At the poleward extremities of these oligotrophic domains the temperate regions of the North and South Atlantic were

characterised by waters with seasonally-driven higher quality seston. Thus food quality is lower in oligotrophic domains which confirms hypothesis 4.

Organic nutrient concentrations on previous cruises were predicted from inorganic nutrient concentrations and CTD measured environmental parameters, proving hypothesis 5. However, due to the uncertainties caused by variations in chlorophyll-a estimations between cruises, we were not able to accurately predict variations in seston stoichiometry, disproving hypothesis 6.

Time-series data from AMT transects between 2003 and 2010 showed that food quantity and quality declined over time in the temperate region of the North Atlantic. POC and PON concentrations increased in the South Atlantic temperate region, although no significant changes in seston stoichiometry (C:N ratio) over time were detected at this location. This proved that at present hypothesis 4, can only be verified in the northern hemisphere. In addition, a correlation between some organic nutrient concentrations and the MEI index was found suggesting that climatic trends affect the availability and the quality of the food in the Atlantic Ocean.

Chapter 5 describes a field study to determine the effects of temperature and body size on copepod physiology across a latitudinal variation in temperature and food quantity (chl-a concentration). The following hypotheses were tested:

8. The variations in respiration rates, carbon demand and egg production rates of different mesopelagic species of copepod respond differently to latitudinal variations in temperature.
9. Body size and temperature are not the only factors affecting copepod metabolism across a latitudinal transect in the Atlantic Ocean.
10. Mesopelagic copepods have higher sensitivities to temperature increase than epipelagic species.

Some of the most widespread oceanic mesopelagic species were selected for the determination of egg production (EPR) and routine respiration rates. EPR was also measured for the neritic epipelagic species *Clausocalanus sp.* The EPR of the most fecund species, *Clausocalanus sp.* and *Undinula vulgaris*, had a negative relationship with temperature and a positive relationship with food quantity. While the EPR of species of the genus *Pleuromamma* did not have a relationship with environmental variables and was constantly low; this was possibly the result of the reproductive strategy of this genus. This confirms hypothesis 8 showing that mesopelagic species from similar latitudes can show

different physiological responses to similar variation in environmental factors, including different adaptation strategies of their reproductive cycle.

Our results indicated that on AMT20 75-85% of the variability in basal and routine respiration rates was explained by variations in body size and temperature. However our tests on the effects of stoichiometry and chl-a concentration on respiration proved inconclusive. Based on our findings in chapter 3, the remaining unaccounted 15-25% of variation in metabolic rates could be due to the effects of food quantity and quality; although other factors such as swimming activity and age could also play a role. Therefore further investigation into the role of food quality and quantity on routine metabolic rates is needed to prove or disprove hypothesis 9.

Within the range of temperatures measured during AMT20, estimates of  $E_a$  and  $Q_{10}$  suggested the migratory mesopelagic copepods considered in this dataset were highly sensitive to changes in temperature, with  $Q_{10}$  values of  $\sim 2.8$  compared to a  $Q_{10}$  of  $\sim 2$  for their epipelagic counterparts (Ikeda 2001), confirming hypothesis 10.

## 6.2 Discussion

Copepods play a significant role in trophic interactions and in all marine biogeochemical cycles (Buitenhuis et al. 2006; Ikeda et al. 2007), therefore estimating how their physiological rates are affected by changing environmental parameters is of particular relevance in quantitatively and qualitatively understanding their dynamics and their effects on the ecosystems (Hernandez-Leon and Ikeda 2005; Buitenhuis et al. 2006; Ikeda et al. 2007; Moloney et al. 2011).

The focus of this thesis was to assess copepod physiological responses to variations in the quality of their diet and habitat temperature. Therefore, through laboratory, field studies and time-series data collation, we aimed to evaluate these interactions between copepods and their environment and extrapolate these findings to assess their possible ecological implications.

This study has contributed to addressing important questions such as:

- How does food quality affect copepod metabolism?
- What is a balanced diet for copepods?
- Is the organic N:P ratio of the food a good indicator of food quality?
- Does food quality vary with latitude? Does it vary over a range of time scales?

- How do temperature variations affect the physiology of migratory mesopelagic copepods?

Further questions arise from this:

- What are the ecological implications and the effects of nutritional imbalance in copepods on biogeochemical cycles and trophic transfer of energy?
- What effect will ocean warming have on copepod physiology?
- Can copepod respiration, under different ecological constraints, be used as an indicator to define the species response to environmental change?

### 6.2.1 Food Quality

A variety of stoichiometric and biochemical parameters can be used as food quality indicators, however the majority of published studies have focused on carbon containing mineral ratios and compounds, such as C:N (e.g. Anderson et al. 2005) and C:P ratios (Urabe and Watanabe 1992) or fatty acids (e.g. Mayor 2009a). Data described in chapters 3 and 4, show that biogeochemistry and the carbon stoichiometry of the food is tightly interlinked; PUFA, SAFA and n-3/n-6 all co-varied with the mineral C:N ratio, indicating that these parameters are affected by similar environmental variables, hence can affect copepod physiology in analogous ways. The current study was one of the first to test the effect of the N:P ratio of the food on copepod physiology. Our results suggest that focussing on the effect of carbon based indicators limits the representation of the effects of food quality by overlooking the effects of the mineral N:P ratio. One of the key discoveries in this study is a biphasic response of copepod physiology to mineral N:P ratio, which enabled us to define a  $TNR_{N:P}$  of copepod growth, either side of which AE and GGE are N or P-limited. Therefore chapter 3 shows that mineral N:P, in field and laboratory stoichiometric analyses, adds complexity to the representation of the effects of food quality on copepod physiological processes, providing significant information on trophic-mediated biochemical dynamics as well as an additional perspective to the C:X ratio and biochemistry in some ecological interactions.

This finding has further ecological implications, one aspect of which suggests that the classic linear or kinetic curves (e.g. Anderson et al. 2005) can be inadequate as models to describe some physiological processes and their links with nutrition. These results also support the suggestions made in previous studies that nutritional deficiency negatively affects copepod production (Pond et al. 1996; Anderson and Pond 2000; Jónasdóttir et al.

2002; Vargas et al. 2006), and metabolism (Thor 2002). Even relatively small changes in seston N:P ratios are shown to have a large impact on the metabolism, assimilation and growth of copepods; for instance, based on the empirical relationships discussed in chapter 3, a change in food quality ratio of ~1 N:P, from 16.5:1 to 15.5:1 N:P, leads to a dramatic decline in AE, and < 48% decrease in the GGE of *T. longicornis*.

Furthermore, chapter 3 shows possible links between zooplankton biomass and seston N:P ratio in the field. However, in contrast to *T. longicornis*' biomass in the North Sea, not all zooplankton size fractions in the NPSG peak at an elemental ratio of 16N:1P and interestingly each of the different size fractions show a consistent biomass peak in the years when the seston N:P ratio is ~9.5N:1P lower than their average body ratio. These preferences for different diets between taxa and ecosystems, and this constant consumer–resource composition offset are a product of homeostasis and species-specific dietary requirements. This is caused by evolutionary and adaptation processes shaped through trophic mutualistic exchanges, an organism's interactions with abiotic conditions (Kay et al. 2005; Olff et al. 2009) and through speciation processes driven by resource competition within an ecological niche (Kay et al. 2005). Such differences in the elemental ratios between zooplankton and their food and always in the same direction (zooplankton ratio < seston ratio), have been found in a variety of studies e.g. Urabe and Watanabe (1992), Pertola et al. (2002), Kay et al. (2005). This suggests that marine copepods concentrate P relative to N in their bodies (Urabe and Watanabe 1992), causing higher daily N requirements on female adults. For instance, the cost of egg production (CoE) in *T. longicornis*, with a body N:P ratio of 8-12:1 (Pertola et al. 2002) and maximum GGE at ~16:1, decreased with increasing N. This element is a particularly important component in proteins and EPR making up to 55% of the egg mass (Kiorboe et al. 1985), suggesting that the daily N requirements in this species are indeed high and possibly due to continuous proteic cost of reproduction.

Since the seminal paper by Redfield (1934) the role of stoichiometric interactions between trophic levels and their environment as regulators of biogeochemical cycles and ecosystem structure has been recognised. Food quality therefore could influence the efficiency of zooplankton physiological processes, affecting not only the health of copepods but also having knock on effects on ocean biogeochemical cycles and food web dynamics. Figure 6.1 shows the predicted consequences of altered physiological performance on biogeochemical cycles and trophic energy transfer in a decreased food quality scenario. The general assumptions of this model are that temperature and food quantity are neither limiting nor inhibiting these processes.

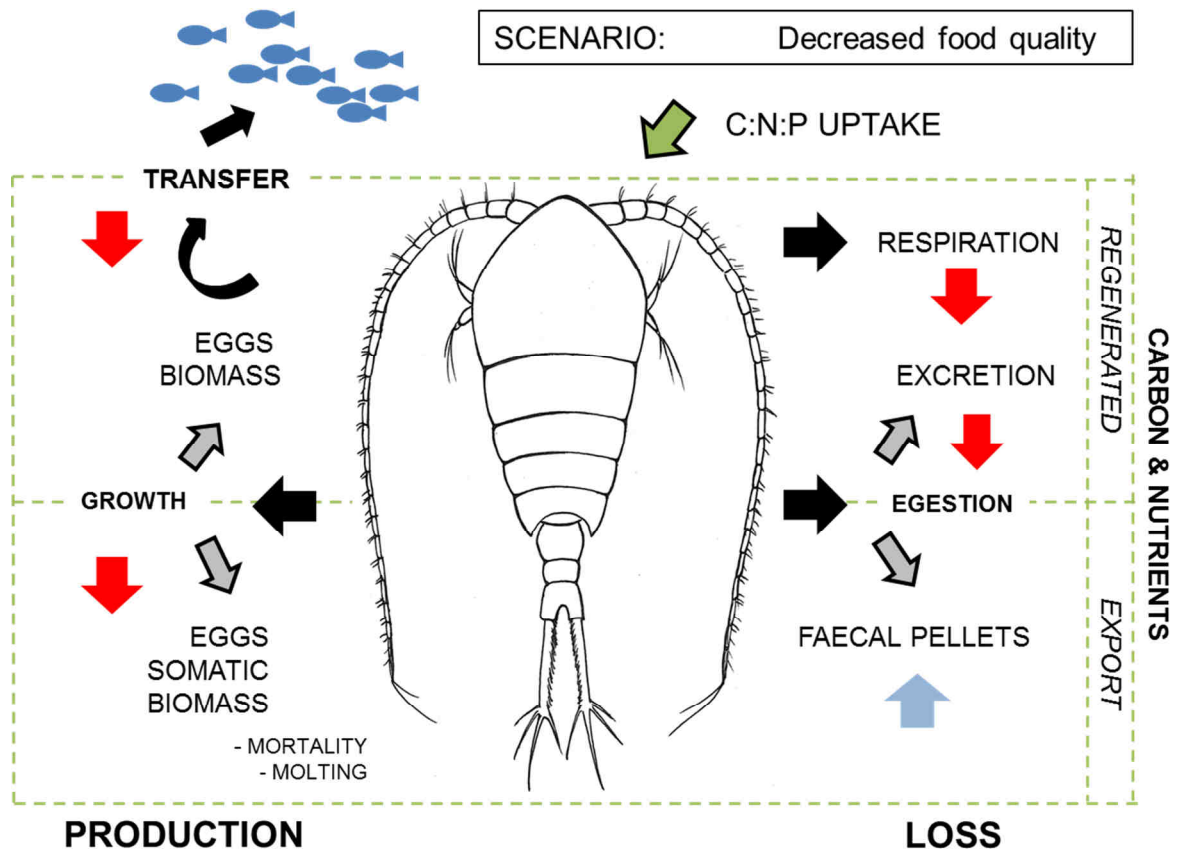


**Figure 6.1.** General mechanistic model of copepod physiological pathways in a decreased food quality scenario. The arrows indicate where the fluxes of carbon and nutrients are predicted to decrease (red arrow) or increase (blue arrow).

Figure 6.1 shows that with decreasing food quality metabolic rates and assimilation efficiency decrease affecting metabolism (respiration,  $\text{CO}_2$  production and excretion) and growth (GGE), overall decreasing nutrient, carbon transfer and regeneration processes. This scenario also suggests that faecal pellet production would increase (Tirelli and Mayzaud 2005) leading to an increase in carbon export per individual. Therefore biogeochemical cycles and food web dynamics are constrained by the efficiencies with which macronutrients are assimilated, allocated and transferred within the organism. Each feeding interaction, from primary producers to fish stocks is affected by stoichiometry (Sterner and Elser 2002; Moloney et al. 2011).

However, as discussed in chapters 3 and 4, changes in food quality are usually coupled with changes in other environmental variables such as prey size, temperature and food quantity. Therefore, this shift in food quality scenario will possibly be affected by a shift in mesozooplankton community composition at the same time. Beaugrand and Reid (2003)

already noted long-term changes in zooplankton communities in the North Atlantic coinciding with an increase in smaller copepod species, Landry et al. (2001) and Hannides et al. (2009) found a similar pattern in the NPSG.

Data collation and analysis in chapters 3 and 4 show that food quality (stoichiometry and biochemistry) is not always balanced throughout the world's oceans, with seston stoichiometry mostly following a non-Redfield ratio distribution and varying with latitude. Our study also suggests that current climate trends can contribute to alterations in food quality over time (chapter 4); therefore showing that food stoichiometry and biochemistry can vary on temporal and spatial scales in the ocean.

This could ultimately affect the magnitude and the efficiency of the biological carbon pump since smaller, lighter faecal material is more easily retained and remineralised in the euphotic zone (Svensen et al. 2012), reducing the supply of nutrients and carbon to the benthos, meso- and bathypelagic nekton and also affecting nutrient cycles below. These cascade effects would also affect trophic transfer of energy since a decline in larger, more nutritious copepod biomass has already been shown to affect cod and salmon recruitment rates in the North Atlantic (Beaugrand et al. 2003; Beaugrand and Reid 2003).

### 6.2.2 Temperature

Chapter 4 discusses temperature variability in the Atlantic Ocean and chapter 5 investigates how temperature affects copepod metabolism and growth. Reproduction rates in the Atlantic Ocean were affected at higher temperatures, inducing generally a lower number of eggs produced per individual (chapter 5). Calbet and Augusti (1999) suggested that phytoplankton biomass (chlorophyll-a concentration) and temperature together can explain up to 70% of the carbon specific egg production rates. One of the limitations of our study is that the higher temperatures were found in oligotrophic regions of the Atlantic Ocean, where food concentrations were generally low (chapter 4) making it difficult to determine the relative importance of low food concentration (or quality) and separate it from the effect of temperature.

Respiration rates of different mesopelagic copepod species were affected by the vertical and latitudinal distribution of temperature. High  $Q_{10}$  values  $\sim 2.8$ , compared to  $\sim 2$  for epipelagic species (Ikeda 2001), show that medium to large migratory mesopelagic copepod species are very sensitive to temperature increases. Therefore, even a small rise in SST could increase their respiration considerably. Poikilotherm species do have quite well defined thermal ranges which largely determine their geographical and seasonal distribution. However, many species possess some degree of physiological plasticity and

are able to compensate for moderate habitat changes while others have minimal adaptation potential. Although many species are remarkably tolerant of short-term variation in habitat temperature (acclimation), future estimation of temperature rise with climate change implies the need for long-term adaptation (Clarke 1987). In addition, since the amount of energy and material allocated to growth and reproduction is proportionally smaller at higher temperatures (growth efficiencies) (Clarke 1987), the potential increase in metabolic demands with climate change (IPCC report 2007) will possibly reduce growth therefore decreasing trophic transfer of energy.

### 6.2.3 Respiration

In chapter 3 we discuss the effects of food quality on fed and unfed respiration rates whilst in chapter 5 we measure routine respiration in some copepod species on an Atlantic Meridional Transect.

Although usually only basal respiration rates are considered in copepod energy budgets, in the natural world copepod metabolic demands are affected daily by environmental variability, their nutritional condition and by the level of physiological activity. Chapter 3, for instance, shows that measuring respiration under different environmental conditions provides information on the energetic cost of growth and biosynthesis as well as the health state of the organism. Therefore by estimating copepod respiration under a variety of activities (such as feeding) and ecological drivers (such as food quality) we can gain information and a better understanding of the mechanisms behind the impact of their physiological processes on biochemical and food web dynamics. This means that by measuring respiration under different conditions we can improve the estimates of the growth potential of an organism and its level of adaptation to the habitat it occupies.

This concept was proposed by Clarke (1987), who suggested that the total oxygen demand of an organism is given by the sum of different respiratory components (eq. 6.1):

$$\sum R = R_b + R_s + R_g + R_a \quad (6.1)$$

Where,  $R_b$  is basal respiration (maintenance),  $R_s$  is the respiratory cost of synthesis (anabolic process, including SDA),  $R_g$  is the respiratory cost of growth (catabolic process) and  $R_a$  is the respiratory cost of locomotor activity (Clarke 1987).  $R_s$  and  $R_g$  are dependent on the substrate assimilated and metabolised by the organism and can be difficult to measure separately. The overall efficiency of assimilation and synthesis is dependent on the stoichiometry and biochemical composition of the food ingested (food quality) as suggested in chapter 3.

Our data agree with Clarke's (1987) study; we found that calculating the metabolic increment (MI) between feeding and unfed copepods provided a direct estimate of assimilation efficiency and therefore an estimate of the magnitude of the metabolic demand linked to the growth potential of the organism under the conditions the copepod was exposed to. Although routine respiration rates do not include the effects of  $R_s$  and  $R_g$  and therefore the effects of the substrate metabolised, it includes the demand for minimal energy required for survival which are dictated by the organism's habitat, its level of adaptation and its nutritional requirements based on their specific TNR (Threshold Nutrient Ratio). The MI, which included the effects of  $R_s$  and  $R_g$  together, showed an 8.6-fold increase above the basal rates (maintenance) of *T. longicornis* (at the  $TNR_{N:P}$ ) (chapter 3).

The determination of MI has a variety of potential applications in the field of ecology. Constructing metabolic budgets based on respiratory responses that take into account the substrate metabolised as well as the abiotic conditions, can provide quantitative information on the sensitivity and adaptation capabilities of a species or a population to environmental change. This could also improve estimates of the metabolic balance of the oceans since basal metabolism is not representative of the normal functioning of an organism, thus underestimating the scale of  $CO_2$  production processes in the ocean. For instance, a diet corresponding to an average GGE of 26%, matching the global average estimate for copepods proposed by Straile (1997), is equivalent to a 15.5N:1P in *T. longicornis*. Therefore, assuming this as the global average quality of the food ingested by copepods, would suggest a 7.5-fold increase on the current global depth integrated estimate of mesozooplankton respiration. However copepod feed discontinuously, according to diel rhythms of activity; since estimations of diel periodicity are contradictory, hindering generalisation (Mauchline 1998), we suggest a convenient approximation of 12 hours feeding per day to account for continuous night time feeding. With these assumptions in place the current global respiration assessment of  $13 \pm 4.2 \text{ Gt C year}^{-1}$  (Hernandez-Leon and Ikeda 2005b), increases 3.75-fold to  $48.75 \text{ Gt C year}^{-1}$ . However, further data are necessary to validate this estimate by assessing other species-specific responses of MI to food quality and account for factors such as diel temperature and variations in copepod swimming activity (such as routine versus active rates).

### 6.3 Conclusions

The most important contribution of this study to contemporary research centres on aspects of copepod respiration rates and the applicability of MI determination under different ecological constraints, the effects of food quality on copepod physiology and

carbon budget, and the effects of temperature on key mesopelagic copepod respiration and reproduction in the Atlantic Ocean.

Our results show that food quantity, stoichiometric ratio, fatty acid content and temperature co-vary. This suggests that previous work which interpreted variations in the physiological rates of copepods in terms of variations of food quantity and temperature only, have overlooked the effects of food quality, and that routine measurement of nutrient stoichiometry (C:N:P) and biochemistry is needed to separate how these three environmental parameters drive population dynamics and production of copepods in the field. We suggest that current changes in temperature, food availability and stoichiometry in the oceans could be having a negative impact on primary (chapter 4) and secondary (chapter 3) producers. For instance, a decrease in food quality and an increase in temperature would limit copepod production due to a decrease in energy allocation to growth, therefore potentially affecting the ecosystem on many levels, such as altering oceanic nutrient cycles, the quality and rate of organic matter export, and zooplankton metabolism and productivity. This could potentially have knock on effects on trophic dynamics. Furthermore, if the relationships between food quality and copepod abundance observed in the field apply globally, these results suggest that food quality, together with food quantity, predation, mortality and temperature, could also contribute to the limitation of zooplankton biomass in the Atlantic; particularly in the food quality (and quantity) poor waters in the oligotrophic domains where decreased zooplankton biomass has been found (Gallienne et al. 2001; Huskin et al. 2001).

We set out to identify and understand both general patterns in the ocean as well as specific instances of deviations from those patterns to predict the consequences of local and global change (Moloney et al. 2011). For instance, the discovery of a specific  $TNR_{N:P}$  linked to a North Sea species of copepod in chapter 3 lead to the identification of defined optimal metabolic and growth demands. This specific physiological response to mineral N:P ratio and its effects on MI and GGE helped us identify the species range of nutrient repletion and limitation, linked to its tolerance limits marked by a sharp decline in MI. This process highlighted the mechanisms behind the effects of food quality on physiology of a single species, giving us the ability to interrogate the responses of other zooplankton communities to natural food quality variation on a larger scale. In the NPSG zooplankton size fractionated biomass appeared affected by different N:P ratios revealing the existence of groups or possible species-specific TNR linked to the habitat they occupy. This contributes to our understanding of the regulatory processes occurring in the environment. The estimation of these stoichiometric relationships can also provide quantitative data on the rate of utilization of organic matter processed through the

copepod trophic level and estimate the efficiency of the energy transfer through the food web.

Chapter 4 showed how the identification of temporal and spatial patterns in seston organic nutrients and stoichiometry can help provide a more complete picture on the magnitude of current ecosystem changes and help estimate the potential effects on trophic structure. In chapter 5, the deviation of mesopelagic species from known epipelagic species patterns and the variety of responses between species found within similar environmental conditions, showed how ecological parameterisations would benefit from investigating single species-specific responses to changes within their ecological niche. This is because the sum of the different functional responses of single species will influence the overall population dynamic and ecosystem structure.

#### **6.4 Future work**

Recent developments in research on spatial and temporal variations in environmental variables and climate change have increased the need to understand the processes that regulate zooplankton dynamics and their feedback on the ecosystems. We need to improve our understanding of ecological interactions as well as predict and prevent detrimental long-term changes in ecosystem structures. Many studies (including the present thesis), looking into all aspects of copepods' relationships with their environment show how their physiological responses can actively vary depending on the state of the ecosystem. This ability to physiologically respond to habitat variations makes them potentially very sensitive to changes in climate; this could result in negative feedbacks on ocean biogeochemical cycles and trophic transfer of energy.

In terms of future work the main question is: What additional information is required to understand and predict changes in mesozooplankton physiological interactions with biogeochemical cycles and food web dynamics? The results presented here suggest a number of topics for further research:

- 1) An important problem in the field of ecosystem dynamics research is the extent to which elemental stoichiometry alters trophic webs and complex biogeochemical cycles (such as recycling of nutrients, export and remineralisation). Therefore further research is required to assess how much of the change in zooplankton physiological activity can be attributed to changes in food quality and temperature co-variance. Laboratory experiments, combining phytoplankton cultures at different N:P ratios grown at different temperatures, would help determine the combined effects of food quality and temperature on copepod physiology. The choice of temperature ranges should take into account the

species-specific optimal temperature ranges and moreover investigate 2100 (IPCC 2007) increased temperature scenarios.

2) In addition, measuring zooplankton body C:N:P ratio at the same time as MI and GGE responses to food stoichiometry, could help improve our understanding behind the intraspecific and interspecific mechanisms of the theory of homeostasis. Further research could investigate possible  $TNR_{N:P}$  variations between ontogenic stages of the same species, known to have a different diet to the adults (Paffenhofer 1988), to identify potential differences in nutritional demands. Since P is an important component of skeletal material and RNA it could mean that juvenile stages, undergoing moulting, have a higher daily requirement for P (Urabe and Sterner 2001) and therefore a different  $TNR_{N:P}$ .

3) Changes in phytoplankton community structure and grazers and the balance between limiting nutrients and temperature may influence biogeochemical cycles and transfer of energy up the food web. Further effort should be made to compare optimal TNR (threshold nutrient ratios) between copepod species. The diversity of copepod taxa means that there are potentially many variations in optimal TNR affected by their feeding behaviour. For instance, some studies suggest that in oligotrophic areas the existence of a very tight and efficient coupling between primary production and grazers (possibly higher than in productive areas) indicates a delicate balance between trophic links (Calbet 2001; Huskin et al. 2001; Gasol et al. 1997). This top-down versus bottom-up control determines the efficiency of the energy and nutrient flow through the system and gross growth efficiencies. Food quality has a direct influence on copepod physiology therefore it is important to assess these effects in different regions of the world's ocean. An investigation should be carried out in order to better understand species' sensitivities to change, adaptive strategies, food web dynamics and the potential effects of climatic and habitat shifts on a species-specific basis. A selection of key species, such as *Calanus finmarchicus* and species from different productivity and nutrient limitation systems, such as upwelling regimes and the P-limited Mediterranean Sea or the NPSG, could contribute to an understanding of the relative importance of different environments on copepod nutritional demands and their feedbacks on the ecosystems.

4) We are a long way from a full assessment of the metabolic balance of the oceans. The current global assessment of mesozooplankton respiration in the ocean carried out by Hernández-León and Ikeda (2005b) has estimated their total respiration as  $1.1 \text{ Pmol C a}^{-1}$ , amounting to 17-32% of primary production in the ocean (Hernández-León and Ikeda 2005). However, this assessment is based on some broad generalisations and most of all on a dataset where respiration rates are calculated as maintenance rates only (basal

respiration). An effort should be made to measure ecologically relevant respiration rates of animals exposed to naturally variable *in situ* conditions and during a variety of physiological activities such as during feeding. This is because measuring copepod respiration under natural conditions could only improve our parameterisation of carbon fluxes and improve current estimates of metabolic budgets in the ocean. In particular, since the determination of all other physiological rates such as egg production, ingestion and egestion by default take the metabolic substrate into consideration; respiration should also be measured in the same way. The advantage of this is that respiration has a much faster response time than reproduction since eggs reflect the food ingested many hours before. In addition, since for all living organisms there is a cost to merely staying alive, empirically estimating how an organism divides incoming energy between growth and maintenance could clarify the process behind the trade-off between mere survival and species success.

5) Our attempt to work on the PlankTOM10 global ecosystem model proved unfruitful due to the current limitation of the model algorithms when facing variable stoichiometry in the field. We advocate the inclusion of variable C:N:P stoichiometry in all global ecosystem models such as PlankTOM10, which could also contribute to improved agreement with observations on ecosystem variability as suggested by Moloney (2012) and help us address questions regarding the effects of food quality on a global scale. Therefore, more observations and analyses of stoichiometric variability of organic and inorganic fractions are needed for tropical regions where data are scarce, as well as temperate, subpolar and polar regions.

6) The current lack of time-series data in many regions of the ocean and the added lack of data on particulate organic phosphorus from most of the existing programmes, limited the course of the investigation as suggested in chapter 3. Monitoring temporal variations in food quality could help us identify the long term effects of climate change on oceanic ecosystems. Renewed interest in spatial variability of nutrient concentration and stoichiometry (e.g. Martiny et al. 2013) suggest that this investigation should be extended to temporal variability in a range of biomes. However, present nutrient data are often limited to the dissolved inorganic fraction, possibly under the false assumption that inorganic nutrient ratios would reflect organic ratios. Biologically relevant data include the macronutrients POC, PON and POP. Although POC and PON data are increasingly available in current datasets, we encourage the inclusion of POP analysis in all baseline data.

## **APPENDICES A and B**

## 7. Methodological appendices A and B

### 7.1 Appendix A O<sub>2</sub> analysis and determination – Winkler technique

Zooplankton respiration measurements were determined by whole bottle Winkler titrations (Winkler, 1888; Carpenter, 1965; Dickson, 1996). The basis of the principle is that O<sub>2</sub> reacts with Mn(II) under alkaline conditions forming MnO(OH)<sub>2</sub>, which is a brown/yellow precipitate. Before titration, acid is added so that MnO(OH)<sub>2</sub> dissolves and is reduced by I<sup>-</sup> to Mn<sup>2+</sup>. The liberated iodine is then titrated to iodide with sodium thiosulphate (Williams and Jenkinson 1981). Dissolved O<sub>2</sub> concentration was determined by automated Winkler titration (Methrom titrator) using photometric end-point detection as described in Williams and Jenkinson (1981) and the method of Robinson et al. (2002).

#### 7.1.1 Chemicals

Chemicals needed (Carpenter 1965; Strickland and Parsons 1972):

- Manganese (II) sulphate MnSO<sub>4</sub> (rather than MnCl<sub>2</sub> (Carpenter 1965))
- Sodium Iodide (NaI)
- Sodium Hydroxide NaOH
- Sulphuric Acid (H<sub>2</sub>SO<sub>4</sub>) gr. 1.84
- Sodium Thiosulphate (Na<sub>2</sub>S<sub>2</sub>O<sub>3</sub>)
- Potassium Iodate (KIO<sub>3</sub>)

Potassium Iodate (0.1N KIO<sub>3</sub>): this is oven dried at 110 °C for 2-4 h before weighing out 3.567g. This is diluted to 1 litre with milliQ water, giving a 0.1N solution

Manganese Sulphate (3M MnSO<sub>4</sub>): Dissolve 450 g MnSO<sub>4</sub> in milliQ water. After complete dissolution, make the solution up to a final volume of 1 litre.

NaI+NaOH solution: Sodium Iodide (NaI 4M: reagent grade) and Sodium Hydroxide (NaOH 8M: reagent grade). Dissolve 600 g of NaI in 600 mL of milliQ water. NOTE: This is an exothermic reaction, it will generate heat. Cool the solution in an ice bath While cooling the mixture, add 320 g of NaOH to the solution, and make up the volume to 1 litre with milliQ water. The solution is then stored in an amber glass bottle.

Sulphuric Acid (10M H<sub>2</sub>SO<sub>4</sub>): To 720 mL of milliQ water carefully add 280 mL of H<sub>2</sub>SO<sub>4</sub>. NOTE: This is an exothermic reaction, it will generate heat Cool the solution in an ice.

Sodium thiosulphate ( $\text{Na}_2\text{S}_2\text{O}_3$ ): Molecular Weight  $\text{Na}_2\text{S}_2\text{O}_3 + 5\text{H}_2\text{O} = 248.21$  g/mol. Dissolve the required amount (Concentration = Molecular weight x Normality of choice) in milliQ water. After complete dissolution, make the solution up to a final volume of 1 litre.

### 7.1.2 Calibrating thiosulphate with iodate standard

$\text{Na}_2\text{S}_2\text{O}_3$  should be calibrated every ~2 days with gravimetrically prepared 0.1N  $\text{KIO}_3$  standard (Carrit and Carpenter 1966).

Fill 10 x 125 mL calibrated glass bottles 75% full with milliQ water

Add 1 mL of  $\text{H}_2\text{SO}_4$  and then 1 mL of  $\text{NaI} + \text{NaOH}$  to each bottle. Add 0.95 mL of 0.1N  $\text{KIO}_3$  to each bottle (note down exact  $\text{KIO}_3$  addition to each bottle).

Top the bottles up with MilliQ water and place in the dark for 20 minutes.

Titrate the bottles using  $\text{Na}_2\text{S}_2\text{O}_3$  as described in section 8.1.4 without adding  $\text{H}_2\text{SO}_4$ .

Calculate  $\text{Na}_2\text{S}_2\text{O}_3$  normality = volume of  $\text{KIO}_3$  (mL) x normality of  $\text{KIO}_3$  / volume of  $\text{Na}_2\text{S}_2\text{O}_3$  (mL).

The accuracy of the calibration had a replicates average of  $\text{SD} \pm 0.0001$ .

### 7.1.3 Procedure for collection and fixing of oxygen samples

Rinse the calibrated and numbered oxygen bottles with sample water.

Fill bottles carefully with silicon tubing avoiding bubbles, overflowing the bottle volume by about 4 times. Add the zooplankton to the bottles.

Carefully add the stopper without entrapping bubbles. Store underwater until ready to be fixed.

Remove bottle stoppers and place either in box or in a stopper tray to allow the same stopper to be replaced into the same bottle.

Take from the CTD or measure and record the salinity of the water used.

For each bottle to be fixed measure the temperature as quickly as possible using what and to what precision. Add  $\text{MnSO}_4$  to each bottle with a calibrated repetitive pipette (1 mL to 150 mL bottles, 0.5 mL to 60 mL bottles). Add  $\text{NaI} + \text{NaOH}$  to each bottle with a calibrated repetitive pipette (1 mL to 150 mL bottles, 0.5 mL to 60 mL). Table 8.1 shows the accuracy of the calibrated pipettes.

**Table 7.1.** Pipettes calibration and accuracy.

<b>Pipette Model</b>	<b>Serial</b>	<b>Accuracy</b>
BCL8000 Stepper	330002A	-0.16%
BCL8000 Stepper	33000B	0.34%
BCL8000 Stepper	13004	0.15%

Carefully re-stopper the bottles without entrapping bubbles. Note down if bubbles are formed.

Mix each bottle thoroughly and immediately. The solution must be uniform. Place underwater until ready for analysis once the precipitate settles (usually takes 1-2h).

#### 7.1.4 Analysing oxygen samples

Take 1-3 bottles at a time from underwater storage, remove stopper and carefully add H<sub>2</sub>SO<sub>4</sub> down the side of the bottle and beneath the precipitate (1 mL to 150 mL bottles, 0.5 mL to 60 mL bottles). Don't acidify more than 3 bottles at once as the iodine concentration may decrease due to evaporation and light degradation while waiting to be analysed.

Titrate with calibrated Na<sub>2</sub>S<sub>2</sub>O<sub>3</sub> and once the titration has finished note the end-point titre addition.

Keep checking that there are no bubbles in any tubing, syringes and bottles.

#### 7.1.5 Dissolved oxygen calculation

The concentration of dissolved oxygen is directly proportional to the titration of iodine with a thiosulfate solution and can then be calculated from the relationship: 1 mole O<sub>2</sub> = 4 moles Na<sub>2</sub>S<sub>2</sub>O<sub>3</sub>.

The calculation of dissolved oxygen concentration (μmol L<sup>-1</sup>) is based on the principles proposed by Carpenter (1965):

$$O_2 (\mu\text{mol L}^{-1}) = [(V_{\text{Thio}} \times N_{\text{Thio}}) \left(\frac{1000}{4}\right) \left(\frac{1000}{V_b - V_{\text{ch}}}\right) \times \gamma] \left(\frac{\rho_i}{\rho_{\text{S25}}}\right) \quad (8.1)$$

Where; thiosulfate normality  $N_{\text{Thio}}$  is calculated as per equation (8.2):

$$N_{\text{Thio}} = \frac{V_{\text{KIO}_3} \times N_{\text{KIO}_3}}{V_{\text{Thio}}} \quad (8.2)$$

$V_{\text{KIO}_3}$  is the volume of  $\text{KIO}_3$  added to the calibration samples  $N_{\text{KIO}_3}$  is the Normality of  $\text{KIO}_3$  and  $V_{\text{Thio}}$  is the volume of Thiosulfate needed to titrate the sample. Whilst the glass expansion correction  $\gamma$  is calculated as per equation (8.3):

$$\gamma = \frac{\rho_{s25}}{\{\rho_{\text{fix}} [1+10^{-5}(t-25)]\}} \quad (8.3)$$

Where;  $t$  is the fixing temperature ( $^{\circ}\text{C}$ ) of the sample and  $25^{\circ}\text{C}$  is the standard laboratory temperature the bottles were calibrated at and  $\rho_{s25}$  is the density of seawater ( $\text{kg m}^{-3}$ ) at *in situ* salinity and  $25^{\circ}\text{C}$ ,  $\rho_{\text{fix}}$  is the density of the sea water ( $\text{kg m}^{-3}$ ) at fixing temperature and salinity while  $\rho_i$  (in equation (8.1)) is the density of the seawater ( $\text{kg m}^{-3}$ ) at *in situ* temperature and salinity calculated according to Dickson (1996) and references therein.

The percentage of dissolved oxygen saturation was calculated as the percentage of dissolved  $\text{O}_2$  concentration relative to that when completely saturated at the temperature of the measurement. The percentage of dissolved oxygen 100% saturated ( $\text{InC}^*$ ) was calculated from the equation (8.4) of Garcia and Gordon (1992) using the equilibrium constants of Benson and Krause (1984) as shown in Table 8.1.

$$\text{InC}_o^* = A_0 + A_1 T_S + A_2 T_S^2 + A_3 T_S^2 + A_3 T_S^3 + A_4 T_S^4 + A_5 T_S^5 + S(B_0 + B_1 T_S + B_2 T_S^2 + B_3 T_S^3) + C_0 S^2 \quad (8.4)$$

$\text{InC}_o^*$  represents the solubility of  $\text{O}_2$  ( $o$ ) per mass or volume of seawater at the temperature of equilibrium ( $*$ ) at 1 atm.  $S$  is the *in situ* salinity,  $T_S$  is the *in situ* temperature (Kelvin) calculated using equation (8.5) and  $A$  and  $B$  are the Benson and Krause (1984) constant coefficients as shown in Table 8.2.

$$T_S = \ln[(298.15 - t)(273.15 + t) - 1] \quad (8.5)$$

**Table 7.2.** Benson and Krause (1984) solubility constants. Constants in equilibrium at 1 atm total pressure, in pure water and seawater.

Constant	$\mu\text{mol/kg}$
A <sub>0</sub>	5.80871
A <sub>1</sub>	3.20291
A <sub>2</sub>	4.17887
A <sub>3</sub>	5.10006
A <sub>4</sub>	-0.0986643
A <sub>5</sub>	3.80369
B <sub>0</sub>	-0.00701577
B <sub>1</sub>	-0.00770028
B <sub>2</sub>	-0.0113864
B <sub>3</sub>	-0.00951519
C <sub>0</sub>	2.75915E-07

## 7.2 Appendix B Particulate Organic Phosphorus method (POP)

### 7.2.1 Digestion protocol from Suzumura (2008)

Reagent Required:

- Potassium Persulfate solution 3% [ $\text{K}_2\text{S}_2\text{O}_8$ ]

Prepare 3% Persulfate solution to the amount required.

Prepare 50 mL glass autoclavable pressure bottle/tubes washed in 10% HCl or 10% Decon 90 and add the dried 25mm GF/F filters samples, blanks and standard stock solution prepared according to Strickland and Parson (1972) to the required concentration. Dispense 18 mL of the 3% Persulfate solution into the pressure bottles and seal.

Autoclave for 30 minutes at 120°C. Let cool. Add 18 mL Milli-Q water to the samples to reduce the Persulfate solution  $\leq 2\%$  and increase the pH to  $>1.5$ .

Add the mixed reagent according to Strickland and Parson (1972), section 7.2.2.

### 7.2.2 Colorimetric method (Strickland and Parson 1972)

Reagents required:

- Ammonium paramolybdate [ $(\text{NH}_4)_6\text{Mo}_7\text{O}_{24} \cdot 4\text{H}_2\text{O}$ ]

- Sulphuric acid [H<sub>2</sub>SO<sub>4</sub>]
- Ascorbic acid [C<sub>6</sub>H<sub>8</sub>O<sub>6</sub>]
- Potassium antimonyl-tartrate [C<sub>4</sub>H<sub>4</sub>KO<sub>7</sub>Sb.0.5H<sub>2</sub>O]
- Anhydrous potassium dihydrogen phosphate [KH<sub>2</sub>PO<sub>4</sub>]

Reagent preparation:

Ammonium molybdate solution: Dissolve 15 gr of ammonium paramolybdate in 500 mL of milliQ water. Store in dark plastic bottle. The solution is stable.

Sulphuric acid solution: Add 140 mL of concentrated sulphuric acid to 900 mL of distilled water. Allow solution to cool and store it in a glass bottle. The solution is stable indefinitely.

Ascorbic acid solution: Dissolve 27 gr of ascorbic acid in 500 mL of distilled water. Store in freezer in plastic bottle so that solution is frozen. Thaw for use and refreeze at once. The solution is stable for several months. (Note: should not be kept for more than a week at room temperature)

Potassium antimonyl-tartrate solution: Dissolve 0.34 gr of potassium antimonyl-tartrate in 250 mL of distilled water. Store in glass or plastic bottle. The solution is stable for several months

Mixed Reagent: Mix together in a dark glass bottle, 100 mL ammonium molybdate, 250 mL sulphuric acid, 100 mL ascorbic acid, and 50 mL potassium antimonyl-tartrate solution. This solution will be stable for up to six hours after preparation. These volumes are suitable for 50 samples.

Potassium dihydrogen phosphate (standard): Dissolve 1.361 gr of anhydrous potassium dihydrogen phosphate in milliQ water and make up to 1 L. The solution is stable for several months.

Colorimetric determination procedure:

Dilute the stock solution of potassium dihydrogen phosphate directly in 3% Persulfate to make solutions of known concentrations to be used to create a calibration curve.

Digest the samples according to Suzumura (2008) (8.2.1).

Prepare mixed reagent and make a 10:1 mixture of sample:mixed reagent. Make sure samples are at room temperature before adding mixed reagent

Wait at least 10 minutes, measure absorbance at 885nm (Absorbance measurements should be made within 2 hours after the addition of the mixed reagent)

## **APPENDIX C**

## 8. Appendix C: O<sub>2</sub> evolution in *Emiliania huxleyi* cultures measured by electrodes and optode

Garcia-Martin E.E.<sup>a</sup>, Nobili R.<sup>b</sup>, Heinle M.<sup>b</sup>, Serret P.<sup>a</sup>, Buitenhuis E.T.<sup>b</sup>, Robinson C.<sup>b</sup>

<sup>a</sup> Dept. Ecología y Biología animal, Facultad de Ciencias del Mar, Universidad de Vigo, CP 36210 Vigo (Pontevedra) Spain

<sup>b</sup> School of Environmental Science, University of East Anglia, Norwich, UK

### 8.1 Abstract

Over the past few decades, sensor technology has developed a great variety of new devices for determining dissolved oxygen in water. In this article we evaluate the use of three commercially available oxygen sensors (two electrodes and one optode) while measuring primary production and respiration of Coccolithophoridae cultures at different light irradiances and short incubation times. Small fast changes were detected by the three devices, indicating their good capacity to apply them to the study of short time plankton dynamics. However differences in their precision, inner calibration and external interferences should be considered for optimal results depending on the type of experiments to be performed.

Keyword: oxygen sensors, electrodes, optode, primary production, community respiration.

### 8.2 Introduction

Measuring changes in dissolved oxygen in the water has been one of the most frequently used methods to study plankton metabolism, primary production and community respiration. This is because oxygen plays a major role in these processes and its concentration may be measured with enough precision to detect the small differences caused by these processes. Soon after 1888 when Winkler (Winkler 1888) proposed a way to chemically determine *in vitro* the oxygen concentration in a water sample, the light/dark incubation method was established (Marshall and Orr 1927) and became the standard approach. Despite being a widely accepted technique, the light/dark incubation method is subject to continual criticism because assumptions related to its procedure may introduce several biases. Examples are the need for long incubation times, the enclosure of the incubated water sample inside a bottle, the assumption of linearity in the consumption of oxygen, and the assumption of similar respiration rates in the light and darkness (Robinson and Williams 2005). Moreover, this method cannot be applied to

study the dynamics of photosynthesis or respiration at short time scales and low rates, as the technique is not sensitive enough to detect small changes in O<sub>2</sub> concentration (< 0.1 μmol L<sup>-1</sup>) during short incubation times. Time scale is one of the biggest problems when trying to study a natural plankton community, as the different components of the communities (small metazoans, auto and heterotrophic protists and bacteria) have different response times. This implies that different incubation times and techniques would be required to characterise their metabolic rates. To some extent, standard techniques cover this scale range (~ 2 hours for bacterial production, typically 6–12 hours for <sup>14</sup>C primary production, and 24h for Δ O<sub>2</sub> community respiration), but they use different principles and units, so that comparison of results requires conversions that rely on factors and assumptions that are not easy to test.

Over the past few decades, sensor technology has evolved considerably and a variety of new devices have been developed for the determination of *in vivo* dissolved oxygen in water. The development of new systems circumvents many of the biases and restrictions caused by the older techniques. In particular, the 1980's saw the rise of a new technique to estimate oxygen changes in marine systems (Revsbech et al. 1980), based on a modification of the electrochemical sensor developed by Clark (Clark 1959). Furthermore, in 1995, Klimant and colleagues (Klimant et al. 1985) applied an optode in aquatic science, based on the dynamic fluorescence quenching principle that is able to measure the oxygen molecules dissolved in the water. Since then, a number of papers have been published where these technologies have been used to try to analyse short time scale processes (Glud et al. 1992; Briand et al. 2004; Pringault et al. 2009; Schapira et al. 2009; Garcia-Martin et al. 2011). Both techniques have also been successfully applied *in situ*: monitoring the oxygen concentration from buoys and floats (Glud et al. 1999; Körtzinger et al. 2005; Tengberg et al. 2006; Martini et al. 2007; Uchida et al. 2008), determining the oxygen concentration, production and consumption in benthic mats (Glud et al. 1999; Glud et al. 2005; Fischer and Wenzhöfer 2010), calculating the net community production using gliders (Nicholson et al. 2008), and determining plankton community and bacterial respiration (Briand et al. 2004; Pringault et al. 2009; Schapira et al. 2009; Garcia-Martin et al. 2011; Fischer and Wenzhöfer 2010; Warkentin et al. 2007).

The advantages and disadvantages of both devices are well-known: both techniques have a fast response time with a high accuracy and resolution (Körtzinger et al. 2005; Klimant et al. 1996; Glud et al. 2000 and references therein). Optode sensors do not consume oxygen, so they can be deployed for months-years as they have long-term stability and a constant calibration is not needed, although they are sensitive to excitation light (Klimant

et al 1996). Meanwhile, the electrode sensors consume small quantities of oxygen and need to be recalibrated constantly if used for a long period of time (Glud et al. 2000; Gundersen et al. 1998). Sensitivity to temperature is important, as electrode readings can be subject to temperature effects. New optodes can include a coupled temperature sensor that allows for internal temperature correction of the oxygen readings. These differences in sensitivity and performance imply that each system may have different requirements, scope and application.

In this article we evaluate three commercially available oxygen sensors, two electrodes (Hansatech planar sensor, Unisense microsensor) and one optode (Ocean Optics Neofox optode) by comparing their measurements of production/respiration ratios at short time scale in Cocolithophoridae cultures incubated under different light intensities. Despite both systems having shown their efficiency, a direct intercalibration to compare their stability, precision and sensitivity is necessary in order to select the appropriate device depending on the environment, experimental set-up, the variable to measure and the organisms to study.

### **8.3 Material and methods**

#### **8.3.1 System set up and sensor calibrations**

Oxygen concentration was measured inside two 5 ml Oxygraph jacketed chambers using three different sensors: Clark-type microelectrode probe (Unisense S.A), Clark-type electrode disc (Oxygraph, Hansatech instruments) and a needle-supported optode probe with a silicone overcoat (FOXY-AF-MG, NeoFox, Ocean Optics sensors). The optode was placed inside the Oxygraph chamber 1, and the Unisense microelectrode was placed within the Oxygraph chamber 2 (see Figure 8.1).

Our experimental setup did not allow us to put all the sensors in the same sample, as the optode and the Unisense microelectrode did not fit together in the Oxygraph chamber. So the measurements could only be compared between two sensors at once (optode vs Oxygraph 1 and Unisense microelectrode vs Oxygraph 2). Water samples were continuously stirred in all the experiments, and the two sensors in each chamber were placed as close as possible to each other. Thus the effect of any gradient in oxygen was thought to be minimal.

Temperature was kept stable in the sample (mean SD 0.02 °C) by a continuous flow of water between the Oxygraph chamber jackets and a water bath cooling system. The temperature was recorded continuously with a temperature data logger.

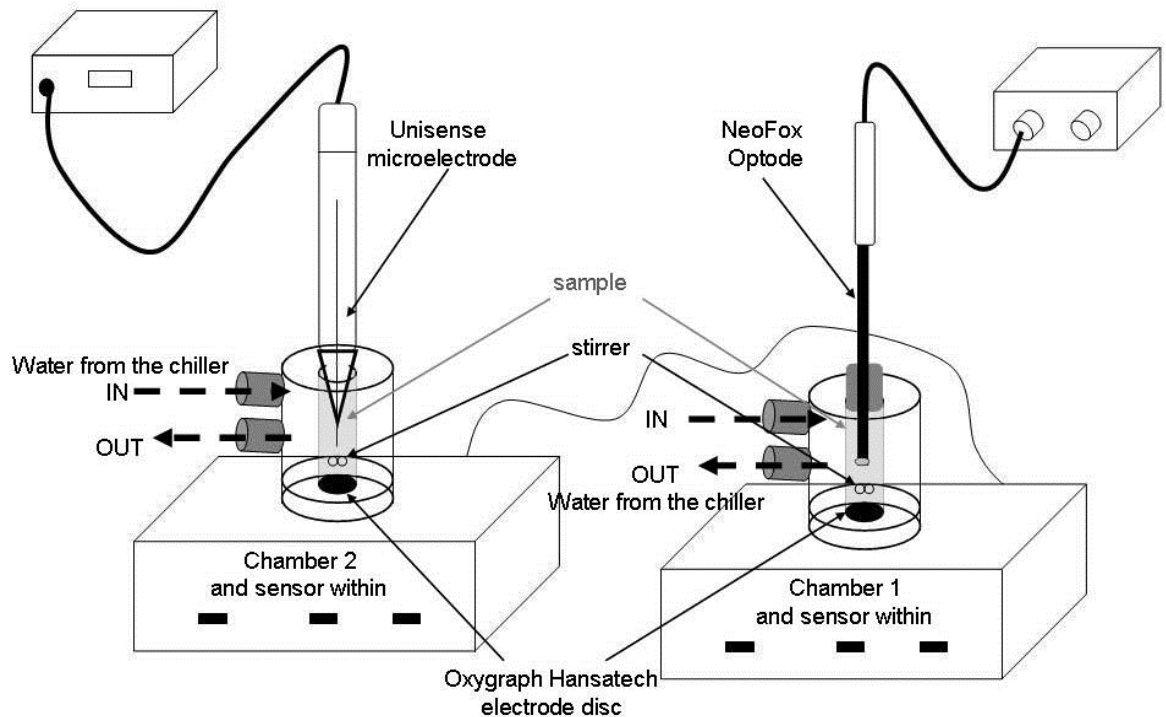


**Figure 8.1.** Schematic of the experimental setup with the three sensors: Unisense microelectrode, NeoFox optode and two Oxygraph Hansatech electrodes.

Optode sensors experience some drift as they use an LED to excite the fluorescence in the oxygen sensitive coating. The calculated drift for our experiments was 0.003% for the precision test and 0.05% for the comparison tests (see below). The electrodes are known to consume oxygen, but this has been previously reported to be negligible with these Clark-type microsensors (Briand et al. 2004; Garcia-Martin et al. 2011; Glud et al. 2000).

Prior to each experiment, all the sensors were calibrated simultaneously using a two point procedure with water samples at 0% and 100% oxygen saturation. To obtain the 0% oxygen concentration a small quantity of instant reducing agent in the form of sodium dithionite salt was dissolved into deionized water. The 100% saturated water was achieved by vigorously bubbling water with air. For the precision test (described below) autoclaved deionized water was used and for the comparison test filtered culture medium was employed.

Although the two point calibration was the same for the three sensors, the working principle of each device means the calibrations differ. The calibration procedure of the electrodes is based on the association of the voltage readings to a known oxygen concentration sample while the optode uses the relationship between LED excitation and

photodiode detection to the oxygen partial pressure of the sample. Although the 0 mmol O<sub>2</sub> m<sup>-3</sup> oxygen concentration may be accurately obtained from the 0% saturation sample, the O<sub>2</sub> concentration at the 100% saturation sample is calculated with the oxygen solubility equation utilised by each system. The Unisense and the Neofox Viewer software use the equation by Benson and Krause (1984), as proposed by Garcia and Gordon (1992), which takes into account the temperature and salinity to calculate the solubility of oxygen, whilst the Oxygraph uses the equation proposed by Truesdale and Downing (1954), which only takes into account the temperature and partial pressure. This implies that the O<sub>2</sub> concentration estimated from the 100% oxygen saturation sample by the Oxygraph will be greater than the one derived by the Unisense microelectrode and Neofox optode from the same sample. As both probes (Unisense microelectrode and Neofox optode) and Oxygraph share the 0% calibration, then the linear adjustment of the calibration values will be different. Moreover, the Oxygraph's output data only include the time, a calibration factor and the oxygen concentration, but not all the values of the calibration equation and the voltage readings, so the equation or the calibration cannot be modified.

A salinity correction was applied to the Oxygraph data during postprocessing using a correction factor to try to minimise the error associated with the salinity effect on the oxygen concentration. The salinity correction factor was calculated from the Benson and Krause (1984) equation for the determination of the solubility of oxygen depending on salinity and temperature. Each final O<sub>2</sub> concentration measurement was obtained by multiplying each O<sub>2</sub> output value from the Oxygraph by the term of the Benson and Krause (1984) equation where salinity is included: correction factor =  $(\exp)^{-S(0.017674 - 10.754/T + 2,140.7/T^2)}$  where S is the salinity and T is the Temperature in Kelvin.

Both the Oxygraph and Unisense electrodes logged the variations continuously while the optode worked semicontinuously with cycles of the LED on and off (10 seconds on every 30 seconds or 1 second on every 3 seconds) to avoid sensor drift.

### 8.3.2 Precision test

Before comparing the performance of the sensors measuring plankton metabolism, a precision test was performed, where we studied the degree to which repeated measurements of each system under constant conditions showed the same O<sub>2</sub> concentration results. The temperature was kept stable at 16.99 °C, SD 0.02.

Once the sensors were calibrated, the oxygen concentration was recorded during 8-10 minutes at four different concentrations obtained by combining different proportions of air

bubbled (O<sub>2</sub> saturated) deionized water and N<sub>2</sub> bubbled (O<sub>2</sub> sub saturated) deionized water. Oxygen concentration was measured first in the O<sub>2</sub> saturated deionized water sample and after the measuring time, a small volume of water was substituted with N<sub>2</sub> bubbled water. In order to allow the addition of the N<sub>2</sub> bubbled water, the Unisense microelectrode and the Neofox optode were removed from their chambers each time the water sample was added. These were then replaced, and the samples were sealed again. The sensors and samples were allowed to stabilize to the new oxygen concentration for 3-5 minutes before measurements were resumed.

### 8.3.3 Comparison test

Thirteen experiments were performed to study the variation in the oxygen concentration with changing light intensity in an *Emiliana huxleyi* culture (strain RCC1229) with a cell concentration ranging from 3.7 to 29 x10<sup>6</sup> cells ml<sup>-1</sup> in exponential growth phase.

For each experiment, 5 ml of *Emiliana huxleyi* culture was incubated for 1.7-2.5 hours at 8-9 increasing light intensities (0, 2, 25, 65, 135, 315, 600, 1300, 2000 μE m<sup>-2</sup> s<sup>-1</sup>). Light was supplied from two white lamps (Deltech GU10-1HP3W LED's), one for each chamber, and attenuated by layers of neutral density screening in front of the chambers. Every ten minutes the screen filters were changed to obtain the next higher light intensity. The culture response and sensor's signal reached stability within 2 minutes from the start of the incubations however the first five minutes at each light intensity were considered to be an adjustment period and not taken into account for the measurements.

Cells were counted at the beginning of the experiments to confirm that the cell density in the two chambers was similar. Temperature was kept stable and the average of the standard deviations of the thirteen experiments was 0.02 °C.

### 8.3.4 Data processing

All statistical analyses were performed using the SPSS software. Coefficients of variations in the precision test were corrected for time effects.

## 8.4 Results

### 8.4.1 Precision test

Figure 8.2 shows the oxygen concentration recorded in the two chambers by the three electrodes and the optode in deionised water. The oxygen concentration recorded in chamber 1 with the Oxygraph and the Neofox optode (Figure 8.2A) showed a slight decrease and a minor increase of the oxygen concentration in the first and second set of

measurements. Both devices recorded the increment although its validity is not confirmed. It could be related to a poor sealing of the incubation chambers, although special care was taken. The fairly constant difference of the oxygen concentration measured in this chamber by the optode and electrode could be related to the calibration discrepancy of the two sensors. Chamber 2 where the Oxygraph and Unisense electrodes were put together showed very similar measurements by the two sensors and negligible drift (Figure 8.2B).

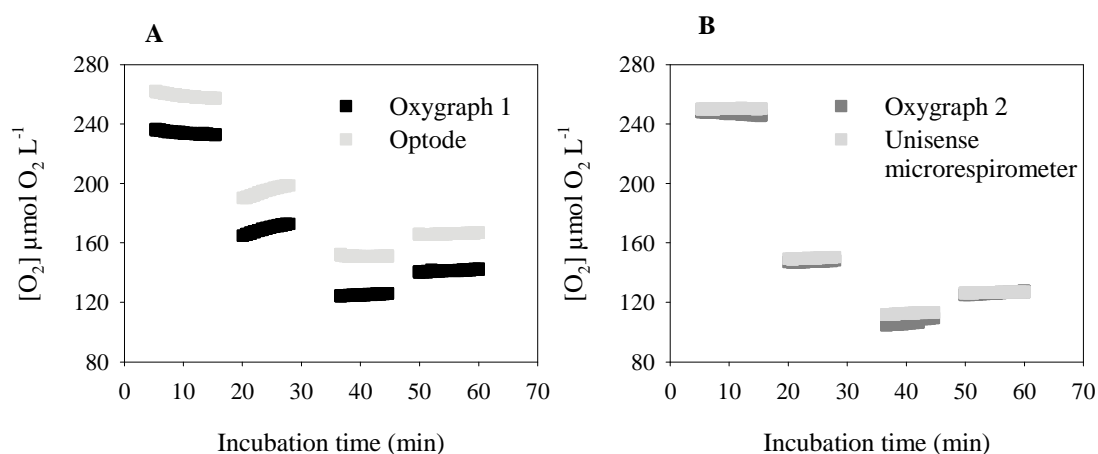


**Figure 8.2.** Oxygen concentration ( $\mu\text{mol O}_2 \text{ L}^{-1}$ ) in deionised water at 16.99 °C as a function of time (min) measured by the different sensors in the two chambers. A) chamber 1 with an Oxygraph electrode disc and the Neofox optode, and B) chamber 2 with an Oxygraph electrode disc and the Unisense microrespirometer.

The lowest standard deviation and the coefficient of variation, so the highest precision, was acquired by the Unisense microelectrode in all the samples (Table 8.1). Furthermore, the CV achieved by the Unisense system was low and constant at the four different concentrations. Notice that the slight increase and decrease mentioned above are reflected in a higher SD and CV in the sensor measurements of chamber 1 for sample 1 and 2. Considering only samples 3 and 4, the precision of the Neofox optode and the Unisense microelectrode were similar, and slightly lower than that of the Oxygraph.

#### 8.4.2 Respiration/Production experiments

Figure 3 shows the oxygen changes in the thirteen experiments with the *Emiliania huxleyi* cultures at different light intensities. Each set of data corresponds to the same light intensity, starting always at the lowest,  $0 \mu\text{E m}^{-2} \text{ s}^{-1}$ , and incrementing progressively up to

2000  $\mu\text{E m}^{-2} \text{s}^{-1}$ . We may expect an initial decrease in the  $\text{O}_2$  concentration due to the prevalence of respiratory consumption, then an increase when photosynthesis gains relative importance at higher light intensities.

All sensors had a fast response time, which allowed the recording of respiration rates of 0.9 (Figure 8.3.8) to 1.6 (Figure 8.3.6)  $\mu\text{mol O}_2 \text{L}^{-1} \text{min}^{-1}$  during the first 5 minutes in darkness.

Although the sensors were calibrated under the same conditions, the dissolved oxygen concentration measurements were not always in agreement. Given the small differences that could exist in the internal calibrations, we will focus on the trends of the measurements rather than the actual concentration measured by each sensor. Analysis of the parameters from the photosynthesis light response curve will be presented elsewhere (Heinle et al. unpublished).

The sensors in the same chambers always produced the same trend, even in those cases where a shift was observed (e.g., Figure 8.3.3 and 8.3.4). We attribute these shifts to physiological changes of the culture cells and not to problems associated with the devices.

There was a significant relationship between the readings of the two sensors in the same chamber (Unisense-Oxygraph and Neofox-Oxygraph) in all the experiments (Table 8.2,  $p < 0.001$ ). Although the regressions of the two chambers were significant, and the slopes close to 1, all the regression slopes (Neofox vs Oxygraph and Unisense vs Oxygraph) were significantly different to 1 at the 95% level (Clarke test,  $p < 0.036$ ). This difference was more relevant in the Neofox-Oxygraph relationship where a systematic trend was observed that implied a shift from underestimation to overestimation.

In all Neofox optode-Oxygraph comparison tests, the ratio of measurements decreased with increasing irradiance of the incubation, suggesting that higher irradiances produced a decreased in the optical signal of the optode (Table 8.3). However the decrease in the Neofox-Oxygraph ratio varied between 4 and 20 % and not always occurring at the same light intensity. The oxygen membrane of the Neofox optode faced away from the light, so we are left to speculate that scattered light could have caused the variability. In contrast, the ratio Unisense microelectrode/Oxygraph electrode was stable in 9 out of the 13 cases. In two experiments (B and M) the ratio decreased over the first four irradiances, and in two experiments (J and L) it increased at 65  $\mu\text{E m}^{-2}\text{s}^{-1}$ .

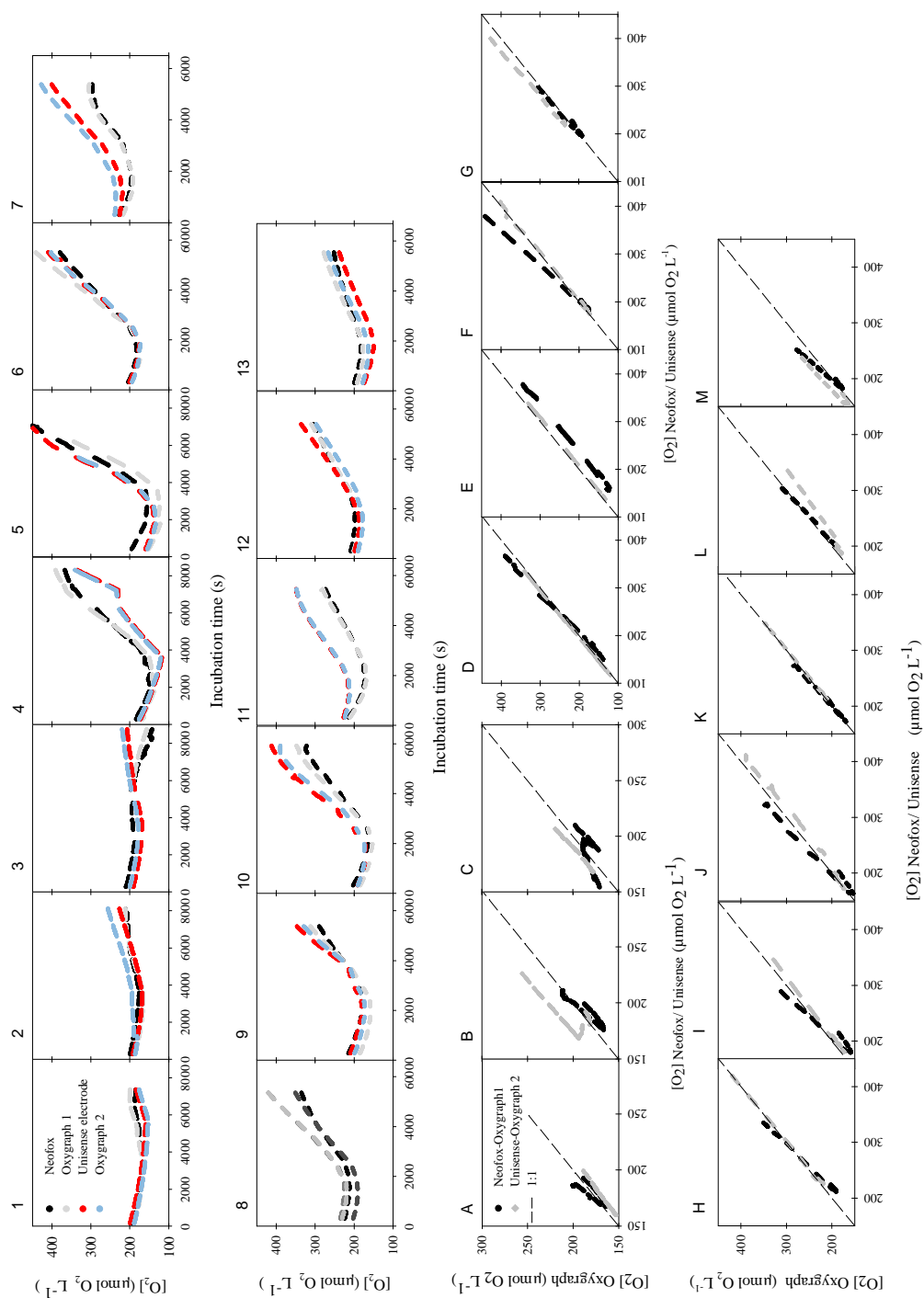


**Figure 8.3.** Oxygen concentration changes in the thirteen experiments carried out with the three different devices in the two chambers (numbers 1-13). The darker colours are data from the devices of chamber 1 (optode, Oxygraph 1), and the brighter colours those from chamber 2 ( $\mu$ electrode, Oxygraph 2). Relationships between the  $O_2$  concentrations measured by the two sensors in the same chamber (A-M) during the thirteen experiments. Oxygraphs measurements are represented in the vertical axis while the optode and the Unisense microelectrode data are in the horizontal axis. The dotted line represents the 1:1 relationship. Numerical and alphabetic graphs are related (1-A, 2-B...).

**Table 8.1.** Mean oxygen concentration and standard deviation measured by the four sensors at 4 sample intervals in the precision test.

		Sample 1				Sample 2				Sample 3				Sample 4			
		Mean [O <sub>2</sub> ]	SD	CV	n data	Mean [O <sub>2</sub> ]	SD	CV	n data	Mean [O <sub>2</sub> ]	SD	CV	n data	Mean [O <sub>2</sub> ]	SD	CV	n data
		$\mu\text{mol O}_2 \text{ L}^{-1}$		%		$\mu\text{mol O}_2 \text{ L}^{-1}$		%		$\mu\text{mol O}_2 \text{ L}^{-1}$		%		$\mu\text{mol O}_2 \text{ L}^{-1}$		%	
<b>Chamber 1</b>	<b>Oxygraph 1</b>	234,15	1,04	0,14		169,5	2,29	0,22		125,18	0,5	0,16		141,41	0,55	0,15	
	<b>Neofox optode</b>	259,06	1,39	0,12		194,88	2,65	0,20		151,17	0,31	0,16		166,14	0,35	0,06	
<b>Chamber 2</b>	<b>Oxygraph 2</b>	247,13	0,79	0,09	160	147,62	0,34	0,11	113	106,79	1,7	0,82	126	126,24	0,68	0,16	160
	<b>Unisense microelectrode</b>	250,32	0,19	0,07		149,74	0,31	0,08		112,63	0,49	0,05		126,76	0,22	0,04	

**Table 8.2.** Regression parameters of the two sensors from the same chamber. \*\*\* means  $p < 0.001$ .

		Sample 1				Sample 2				Sample 3				Sample 4			
		Mean [O <sub>2</sub> ]	SD	CV	n data	Mean [O <sub>2</sub> ]	SD	CV	n data	Mean [O <sub>2</sub> ]	SD	CV	n data	Mean [O <sub>2</sub> ]	SD	CV	n data
		$\mu\text{mol O}_2 \text{ L}^{-1}$		%		$\mu\text{mol O}_2 \text{ L}^{-1}$		%		$\mu\text{mol O}_2 \text{ L}^{-1}$		%		$\mu\text{mol O}_2 \text{ L}^{-1}$		%	
<b>Chamber 1</b>	<b>Oxygraph 1</b>	234,15	1,04	0,14		169,5	2,29	0,22		125,18	0,5	0,16		141,41	0,55	0,15	
	<b>Neofox optode</b>	259,06	1,39	0,12		194,88	2,65	0,20		151,17	0,31	0,16		166,14	0,35	0,06	
<b>Chamber 2</b>	<b>Oxygraph 2</b>	247,13	0,79	0,09	160	147,62	0,34	0,11	113	106,79	1,7	0,82	126	126,24	0,68	0,16	160
	<b>Unisense microelectrode</b>	250,32	0,19	0,07		149,74	0,31	0,08		112,63	0,49	0,05		126,76	0,22	0,04	

**Table 8.3.** Mean of the ratios of the oxygen concentrations measured by the two sensors inside the same chamber at the different light intensities: A) optode/ Oxygraph ratio, B) Unisense/ Oxygraph ratio. The mark (\*) indicates a lack of value as the Oxygraph stopped working, the empty space indicates that no measurements were made. The SD for all the ratios was smaller than 0.03 (data not shown).

A

Light $\mu\text{E m}^{-2} \text{ s}^{-1}$	Experiment													
	A	B	C	D	E	F	G	H	I	J	K	L	M	
0	1,03	1,07	1,07	1,08	1,30	1,04	1,04	1,11	1,16	1,10	1,02	1,04	1,04	
2	1,04	1,08	1,09	1,08	1,32	1,06	1,03	1,12	1,17	1,09	1,02	1,06	1,04	
25	1,04	1,08	1,09	1,07	1,26	1,05	1,02	1,11	1,15	1,07	1,02	1,06	1,03	
65	1,03	1,06	1,07	1,07	1,24	1,02	1,00	1,08	1,13	1,02	1,02	1,05	1,00	
150	0,99	1,05	1,05	1,03	1,22	0,96	0,99	1,04	1,07	0,99	1,00	1,02	0,98	
315		1,02	1,02	1,01	1,16	0,94	0,97	1,02	1,03	0,96	0,99	1,03	0,95	
600	0,97	1,00	0,98	0,96	*	0,91	0,98	1,00	1,00	0,93	0,99	1,01	0,94	
1300	0,96	0,98	0,92	0,94	*	0,88	0,98	0,98	0,96	0,94	0,98	1,00	0,92	
2000	0,93	0,99	0,90	0,94	*	0,86	0,97	0,96	0,93	0,94	0,98	0,99	0,91	
<b>Abundance (<math>10^6</math> cells <math>\text{mL}^{-1}</math>)</b>	5,6	4,4	3,7	8,5	11	9,9	6	29	2,8	13,2	5,7	9,1	6,2	

B

Light $\mu\text{E m}^{-2} \text{ s}^{-1}$	Experiment													
	A	B	C	D	E	F	G	H	I	J	K	L	M	
0	1,06	1,03	0,95	0,98	1,04	1,03	0,95	1,02	1,06	1,00	1,01	1,04	0,98	
2	1,05	0,95	0,95	0,98	1,04	1,02	0,93	1,03	1,06	0,99	1,01	1,04	0,95	
25	1,05	0,90	0,95	0,98	1,03	1,01	0,93	1,03	1,05	0,99	1,01	1,05	0,92	
65	1,05	0,87	0,94	0,98	1,03	1,01	0,92	0,99	1,04	1,04	1,01	1,07	0,90	
150	1,05	0,87	0,95	0,97	1,03	1,01	0,93	1,01	1,05	1,07	1,01	1,12	0,90	
315		0,87	0,95	0,98	1,03	1,01	0,94	1,01	1,03	1,07	1,01	1,12	0,89	
600	1,05	0,88	0,95	0,98	*	1,01	0,93	1,00	1,04	1,05	1,00	1,12	0,89	
1300	1,05	0,88	0,94	0,98	*	1,00	0,93	1,00	1,05	1,04	1,00	1,13	0,89	
2000	1,04	0,88	0,94	0,98	*	1,01	0,93	1,00	1,05	1,05	1,00	1,13	0,89	
<b>Abundance (<math>10^6</math> cells <math>\text{mL}^{-1}</math>)</b>	5,6	4,1	4,9	10,4	11	9,9	5,7	25	27	9,5	6	6,3	6,2	

## 8.5 Discussion

The application of the three sensors utilized here has been individually demonstrated in several reports, but there are few papers where measurements were concurrently performed using more than one sensor (Glazer et al. 2004; Truesdale and Downing 1954). Despite the different working principle, data from our experiments indicate that the three oxygen sensors achieve comparable and reliable results. The lack of Winkler measurements in our experiments, because of the small volume of culture media, do not allow us to test for the accuracy of the three methods, although the precision of all the sensors (see coefficients of variation in Table 8.1) was similar to the typical coefficients of variation reported for O<sub>2</sub> concentration changes measured with the light/dark incubation method (Robinson and Williams 2005). Though previously published reports indicate that electrodes consume oxygen and hence are affected by stirring sensitivity (Glud et al. 2000; Revsbech et al. 1989; Lassen et al 1998), we have not noticed these effects as the Unisense microelectrode achieved a systematically lower SD in the precision test compared to the other devices. Moreover, in most sample intervals of the precision test, the variability of the oxygen concentration for the three devices was similar to those previously reported (Briand et al. 2004 and references therein; Warkentin et al. 2007).

This correspondence between sensors validates the salinity correction applied in post processing to the Oxygraph data, which has minimized the disagreement between the dissolved oxygen concentration calculated with the salinity effect (Unisense microelectrode and Neofox optode) and without it (Oxygraph electrodes). However, it would be preferable that this salinity correction would have been included in the calibration equation provided by the manufacturer for calculating the 100% saturated oxygen. Further comparison with Winkler measurements is necessary to test for the accuracy of this post processing.

The data of the comparison test clearly confirmed that all the devices were suitable for measuring cultured plankton photosynthesis and respiration, although several discordances were found. The good agreement in the ratio Unisense/Oxygraph measured in the same chamber was maintained over a broad range of light intensities and oxygen concentrations. However, it is intriguing why this ratio changed from higher to lower than one between experiments. The salinity correction of the electrode output data and not in the calibration equation could not be the cause of this discrepancy, because whether there was an effect, it should always be the same (overestimation of the Oxygraph measurements at high [O<sub>2</sub>]).

By contrast, the relationships between the electrode and the optode inside chamber 1 were weaker, as shown by the shifts in the ratio Neofox/Oxygraph. These shifts were not dependent on the cell concentration of the sample, as each experiment varied in the number of cells, neither on the  $[O_2]$ . Some studies have reported a higher signal of the optode compared to electrode at  $O_2$  concentrations below 75% (Truesdale and Downing 1954; Glazer et al. 2004; Markfort and Hondzo 2009), which could explain our observations of lower Neofox optode signal at higher  $[O_2]$ . However, in our experiments the percentage of oxygen saturation when the shift occurred was not consistent between tests. Moreover, due to the nature of the experiment, in some cases the same concentration was achieved twice during the same experiment and only one Neofox/Oxygraph ratio shift occurred. The growth light acclimation may also not explain these variations since the same culture showed different shifts (Figure 8.3A, D, I and M belong to the same acclimation light intensity but sampled on different days). One possible reason could be related to an interference of the experimental light on the excitement of the fluorophore of the optode, although, as far as we know, there are no reports about this effect and the fluorescence lifetime signal is expected to be independent of the light (Glud et al. 2000). Furthermore, our optode probe had a silicone external coating to exclude ambient light and reduce refractive index effects. This silicone jacket seals the sensor from ambient light but is porous to the oxygen that penetrates into the probe easily, which causes a slower response but with the same precision.

In order to know which sensor is better for a specific experiment, further tests should be undertaken assessing the precision and accuracy of measurements of photosynthesis and respiration of different species and natural communities, lowering the metabolic rates, and therefore approaching values normally found in the ocean. Moreover, longer (at least up to the standard 24 h) incubation time tests are required in order to compare the measurements made with the three sensors to data derived from Winkler titrations.

### 8.5.1 Conclusion and recommendations

Our results indicate that the three devices used (Neofox optode, Oxygraph electrode and Unisense microelectrode) are practical to study photosynthesis and respiration at short time scales due to the ability to measure oxygen concentration changes at short incubation times (minimum rates of  $0.06 \mu\text{mol } O_2 \text{ L}^{-1}\text{min}^{-1}$ ). This capacity for a laboratory intercomparison will make it easier to intercalibrate techniques and variables for field studies that require different incubation times and establish whether any conversion factors will be needed to make them directly comparable, and thus help in the study of short time and space scale dynamics of plankton photosynthesis and respiration.

However, the advantages and disadvantages of each sensor (Table 8.4) should be considered depending on the environment, the studied organism and the expected rates of production and respiration.

Further research should deal with the possible interference of the external light, and other types of external coatings that could improve the optode measurements.

**Table 8.4.** Advantages and disadvantages of the sensors used in the present article.

Device	Advantages	Disadvantages
<b>Oxygraph electrode disc</b>	Faster response (ms)	Software:
	Continuous measurements	Calibration
<b>Unisense microelectrode</b>	Multiple array chambers	no salinity correction possible
	Chambers with an outer water bath jacket (higher T stability)	no data of the mV measured for the calibration
<b>NeoFox Optode FOXY-AF-MG</b>		Measurements:
		no salinity adjustment
		Not flexible like probes
		Possible stirring effect and O <sub>2</sub> consumption
<b>Unisense microelectrode</b>	Faster response (ms)	Long time needed for prepolarization
	Continuous measurements	Multiple calibrations required if the T is not stable ( $\Delta T > 0,2 \text{ }^{\circ}\text{C}$ )
<b>NeoFox Optode FOXY-AF-MG</b>	Software:	High Temperature sensitivity
	easy manipulation	Possible stirring effect and O <sub>2</sub> consumption
<b>NeoFox Optode FOXY-AF-MG</b>	easy postcalculations	
	Salinity corrected in the calibration equations	
<b>NeoFox Optode FOXY-AF-MG</b>	Stability	
	Probe: flexible and adaptable to any sample, volume or chamber	
<b>NeoFox Optode FOXY-AF-MG</b>	Multiple array probes	
	No stirring effects or O <sub>2</sub> consumption	
<b>NeoFox Optode FOXY-AF-MG</b>	Easy set up	Sensitive to temperature (if temperature compensation is not included)
	Salinity corrected in the calibration equations	Possible sensitive to light
<b>NeoFox Optode FOXY-AF-MG</b>	Probe: flexible and adaptable to any sample, volume or chamber	Semicontinuous logging (duty cycles on and off)
	Multiple array probes	Low response time (min)
<b>NeoFox Optode FOXY-AF-MG</b>	No stirring effects or O <sub>2</sub> consumption	Culture cells adhere to the surface of the coating

### Acknowledgements

We gratefully acknowledge Ocean Optics for their advice and recommendations. E.EG-M was funded by FPU MEC fellowship and MICINN project CTM2009-08069-E/MAR, R. N was funded by NERC in conjunction with SAHFOS ([www.sahfos.ac.uk](http://www.sahfos.ac.uk)) awarded to CR, EB, Claudia Castellani (SAHFOS) and M. H.

## 8.6 References

Benson B.B., Krause D.Jr., 1984. The concentration and isotopic fractionation of oxygen dissolved in freshwater and seawater in equilibrium with the atmosphere. *Limnology and Oceanography* 29, pp. 620–632.

Briand E., Pringault O., Jacquet S., Torréton J.P., 2004. The use of oxygen microprobes to measure bacterial respiration for determining bacterioplankton growth efficiency. *Limnology and Oceanography: Methods* 2, pp. 406–416.

Clark L.C.Jr., 1959. Electrochemical device for chemical analysis, US Patent no. 2,913,386.

Fischer J.P., Wenzhöfer F., 2010. A novel planar optode setup for concurrent oxygen and light field imaging: Application to a benthic phototrophic community. *Limnology and oceanography: Methods* 8, pp. 254-268.

Garcia H.E., Gordon L.I., 1992. Oxygen solubility in seawater: better fitting equations. *Limnology and Oceanography* 37, pp. 1307-1312.

Garcia-Martin E.E., Serret P., Pérez-Lorenzo M., 2011. Testing potential bias in marine plankton respiration rates by dark bottle incubations in the NW Iberian Shelf: incubation time and bottle volume. *Continental Shelf Research* 31, pp. 496-506.

Glazer B.T., March A.G., Stierhoff K., Luther G.W., 2004. The dynamic response of optical oxygen sensors and voltammetric electrodes to temporal changes in dissolved oxygen concentrations. *Analytica Chimica Acta* 518, pp. 93-100.

Glud R.N., Gundersen J.K., Ramsing N.B., 2000. Electrochemical and optical oxygen microsensors for in situ measurements. In: Buffle J., Horvai G. (Eds.), *In Situ Monitoring of Aquatic Systems: Chemical Analysis and Speciation*, pp. 19-73.

Glud R.N., Klimant I., Holst G., Kohls O., Meyer V., Kühl M., Gundersen J.K., 1999. Adaptation, test and in situ measurements with O<sub>2</sub> microoptodes on benthic landers. *Deep-Sea Research I* 46, pp. 171-183.

Glud R.N., Kühl M., Kohls O., Ramsing N.B., 1999. Heterogeneity of oxygen production and consumption in a photosynthetic microbial mat as studied by planar optodes. *Journal of Phycology* 35, pp. 270-279.

Glud R.N., Ramsing N.B., Revsbech N.P., 1992. Photosynthesis and photosynthesis-coupled respiration in natural biofilms quantified with oxygen microsensors. *Journal of Phycology* 28, pp. 51-60.

Glud R.N., Wenzhofer F., Tengberg A., Middelboe M., Oguri K., Kitazato H., 2005. Benthic oxygen distribution in central Sagami Bay, Japan: in situ measurements by microelectrodes and planar optodes. *Deep Sea Research I* 52, pp. 1974-1987.

Gundersen J.K., Ramsing N.B., Glud R.N., 1998. Predicting the signal of O<sub>2</sub> microsensors from physical dimensions, salinity and O<sub>2</sub> concentration. *Limnology and Oceanography* 43, pp. 1932-1940.

Klimant I., Kühl M., Glud R.N., Holst G., 1996. Optical measurement of oxygen and temperature in microscale: strategies and biological applications. *Sensors and Actuators B* 38-39, pp. 29-37

Klimant I., Meyer V., Kohls M., 1995. Fibre-optic oxygen microsensors, a new tool in aquatic biology. *Limnology and Oceanography* 40, pp. 1159-1165.

Körtzinger A., Schimanski J., Send U., 2005. High-quality oxygen measurements from profiling floats: A promising new technique. *Journal of Atmospheric and Oceanic Technology* 22, pp. 302-308.

Lassen C., Glud R.N., Ramsing N.B., Revsbech N.P., 1998. A method to improve the spatial resolution of photosynthetic rates obtained by oxygen microsensors. *Journal of Phycology* 34, pp. 89-93.

Markfort C.D., Hondzo M., 2009. Dissolved oxygen measurements in aquatic environments: the effects of changing temperature and pressure on three sensor technologies. *Journal of Environmental Quality* 38, 1766–1774.

Marshall S.M, Orr A.P., 1927. The relation of the plankton to some chemical and physical factors of the Clyde Sea area. *Journal of Marine Biology Association of the United Kingdom* 14, pp. 837-868.

Martini M., Butman B., Mickelson M., 2007. Long-term performance of Aanderaa optodes and Sea-Bird SBE-43 dissolved-oxygen sensors bottom mounted at 32 m in Massachusetts Bay. *Journal of Atmospheric and Oceanic Technology* 24, pp. 1924-1935.

Nicholson D., Emerson S., Eriksen C.C., 2008. Net community production in the deep euphotic zone of the subtropical North Pacific gyre from glider surveys. *Limnology and Oceanography* 53, pp.2226–2236.

Pringault O., Tesson S., and Rochelle-Newall E., 2009. Respiration in the light and bacterio-phytoplankton coupling in a coastal environment. *Microbial Ecology* 57, pp. 321-334.

Revsbech N.P., 1989. An oxygen microelectrode with a guard cathode. *Limnology and Oceanography* 34, pp. 474-478.

Revsbech N.P., Sørensen J., Blackburn T.H., Lomholt J.P., 1980. Distribution of oxygen in marine sediments measured with microelectrodes. *Limnology and Oceanography* 25, pp. 403.

Robinson C., Williams P., 2005. Respiration and its measurement in the surface waters. In: P.A. del Giorgio, P.J.LeB. Williams (Eds.). *Respiration in Aquatic Ecosystems*, Oxford University Press, New York, pp. 147–180.

Schapira M., Pollet T., Mitchell J.G., Seuront I., 2009. Respiration rates in marine heterotrophic bacteria relate to the cytometric characteristics of bacterioplankton communities. *Journal of Marine Biology Association of the United Kingdom* 89 (6), pp. 1161-1169.

Tengberg A., Hovdenes J., Andersson J.H., Brocandel O., Diaz R., Hebert D., Arnerich T., Huber C., Körtzinger A., Khrpounoff A., Rey F., Rønning C., Schimanski J., Sommer S., Stangelmayer A., 2006. Evaluation of a life time based optode to measure oxygen in aquatic systems. *Limnology and Oceanography: Methods* 4, pp. 7-17.

Truesdale G.A., Downing A.L., 1954. Solubility of oxygen in water. *Nature* 173, pp. 1236.

Uchida H., Kawano T., Kaneko I., Fukasawa M., 2008. In-situ calibration of optode-based oxygen sensors. *Journal of Atmospheric and Oceanic Technology* 25, pp. 2271-2281.

Warkentin M., Freese H.M., Karsten U., Schumann R., 2007. New and fast method to quantify respiration rates of bacteria and plankton communities in freshwater ecosystems by using optical oxygen sensor spots. *Applied and Environmental Microbiology* 73 (21), pp. 6722–6729.

Winkler L.W., 1888. Die Bestimmung des in Wasser Gelösten Sauerstoffes. *Berichte der Deutschen Chemischen Gesellschaft* 21 pp. 2843–2855.

## **REFERENCES**

## 9. References

- Abou Debs, C., 1984. Carbon and nitrogen budget of the calanoid copepod *Temora stylifera*: effect of concentration and composition of food. *Marine Ecology Progress Series*, 15, pp.213–223.
- Acheampong, E., Nielsen, M., Mitra, A., St. John, M., 2012. Towards an adaptive model for simulating growth of marine mesozooplankton: a macromolecular perspective. *Ecological Modelling*, 225, pp.1–18.
- Ackman R., Tocher C., 1968. Marine phytoplankter fatty acids. *Journal of the Fisheries Research Board of Canada* 25, pp.1603-1620.
- Ahlgren, G., Lundstedt, L., Brett, M., Forsberg, C., 1990. Lipid composition and food quality of some freshwater phytoplankton for cladoceran zooplankters. *Journal of Plankton Research*, 12(4), pp.809–818.
- Aiken, J., Pradhan, Y., Barlow, R., Lavender, S., Poulton, A., Holligan, P., and Hardman-Mountford, N. 2009. Phytoplankton pigments and functional types in the Atlantic Ocean: a decadal assessment, 1995–2005. *Deep Sea Research Part II: Topical Studies in Oceanography*, 56(15), pp. 899–917.
- Alcaraz, M., Saiz, E., Calbet, A., Trepas, I., Broglio, E., 2003. Estimating zooplankton biomass through image analysis. *Marine Biology*, 143(2), pp.307–315.
- Alcaraz, M., Almeda, R., Calbet, A., Saiz, E., Duarte, C., Lasternas, S., 2010. The role of arctic zooplankton in biogeochemical cycles: respiration and excretion of ammonia and phosphate during summer. *Polar Biology*, 33(12), pp.1719–1731.
- Alcaraz, M., Almeda, R., Saiz, E., Calbet, A., Duarte, C., Agustí, S., Santiago, R., Alonso, A., 2013. Effects of temperature on the metabolic stoichiometry of Arctic zooplankton. *Biogeosciences*, 10(2), pp.689–697.
- Ambler, J., 1986. Effect of food quantity and quality on egg production of *Acartia tonsa* Dana from East Lagoon, Galveston, Texas. *Estuarine, Coastal and Shelf Science*, 23(2), pp. 183–196.
- Andersen, R., 2005. *Algal culturing techniques*. Phycological Society of America. Elsevier Academic Press, Ch.18.

- Andersen, T., Færøvig, P., Hessen, D., 2007. Growth rate versus biomass accumulation: different roles of food quality and quantity for consumers. *Limnology and Oceanography*, 52, pp. 2128–2134.
- Anderson, T., 1992. Modelling the influence of food C:N ratio, and respiration on growth and nitrogen excretion in marine zooplankton and bacteria. *Journal of Plankton Research*, 14(12), pp.1645–1671.
- Anderson, L., 1995. On the hydrogen and oxygen content of marine phytoplankton. *Deep Sea Research Part I: Oceanographic Research Papers*, 42(9), pp.1675–1680.
- Anderson, L., Sarmiento, J., 1994. Redfield ratio of remineralization determined by nutrient data analysis. *Global Biogeochemical Cycles*, 8(1), pp.65–80.
- Anderson, T., Hessen, D., 1995. Carbon or nitrogen limitation in marine copepods? *Journal of Plankton Research*, 17(2), pp.317–331.
- Anderson, T., Pond, D., 2000. Stoichiometric theory extended to micronutrients: comparison of the roles of essential fatty acids, carbon, and nitrogen in the nutrition of marine copepods. *Limnology and Oceanography*, 45(5), pp.1162–1167.
- Anderson, T., Hessen, D., Elser, J., Urabe, J., 2005. Metabolic stoichiometry and the fate of excess carbon and nutrients in consumers. *The American Naturalist*, 165(1), pp.1–15.
- Arendt, K., Jónasdóttir, S., Hansen, P., Gartner, S., 2005. Effects of dietary fatty acids on the reproductive success of the calanoid copepod *Temora longicornis*. *Marine Biology*, 146(3), pp.513–530.
- Arrigo, K., 2005. Marine microorganisms and global nutrient cycles. *Nature*, 437, pp. 349–55.
- Arrigo, K., 1999. Phytoplankton community structure and the drawdown of nutrients and CO<sub>2</sub> in the Southern Ocean. *Science*, 283(5400), pp.365–367.
- Atlantic meridional transect programme. AMT20 information. Available at: <http://www.amt-uk.org/>. [Accessed October 2012].
- Bamstedt, U., Gifford, D., Atkinson, A, Roman, M., 2000. Feeding. In Harris, R. et al. (eds), *ICES Zooplankton Methodology Manual*. Academic Press, San Diego, CA, USA, pp. 297–399.

- Bamstedt U., 1986. Chemical composition and energy content. Pages 1-58 in: The Biological Chemistry of Marine Copepods, edited by E. Corner and S. O'Hara. Oxford University Press, Oxford.
- Banase, K., 1974. On the Interpretation of data for the carbon-to-nitrogen ratio of phytoplankton. *Limnology and Oceanography*, 19(4), pp.695–699.
- Beaugrand, G., Brander, K., Lindley, J., Souissi, S., Reid, P., 2003. Plankton effect on cod recruitment in the North Sea. *Nature*, 426, pp.661–664.
- Beaugrand, G., Reid, P., 2003. Long-term changes in phytoplankton, zooplankton and salmon related to climate. *Global Change Biology*, 9, pp. 801–817.
- Behrenfeld, M., O'Malley, R., Siegel, D., McClain, C., Sarmiento, J., Feldman, G., Milligan A., Falkowski, P., Letelier, R., Boss, E., 2006. Climate-driven trends in contemporary ocean productivity. *Nature* 444, pp.752-755.
- Benson, B., Krause, D., 1984. The concentration and isotopic fractionation of oxygen dissolved in fresh- water and seawater in equilibrium with the atmosphere. *Limnology and Oceanography* 29, pp. 620-632.
- Berg, J., Tymoczko, J., Stryer, I., 2007. *Biochemistry*. Sixth ed. W.H. Freeman and Company. New York. Ch. 12.
- Berges, J., Franklin, D., Harrison, P. 2001. Evolution of an artificial seawater medium: improvements in Enriched Seawater, Artificial Water over the last two decades. *Journal of Phycology*, 37(6), pp. 1138–1145.
- Bonnet, D., Carlotti, F., 2001. Development and egg production in *Centropages typicus* (Copepoda: Calanoida) fed different food types: a laboratory study. *Marine Ecology Progress Series*, 224(1993), pp.133–148
- Bonnet, D., Harris, R., Richardson, A., Hirst, A., Beaugrand, G., Edwards, M., Ceballos, S., Diekman, R., Valdes, L., Lopez-Urrutia, A., Molinero, J., Weikert, H., Greve, W., Lucic, D., Albaina, A., Yahia, N., Umani, S., Miranda, A., Cook, K., Robinson, S., Luz, M., Puellas, F., 2005. An overview of *Calanus helgolandicus* ecology in European waters. *Progress in Oceanography*, 65, pp.1–53.
- Boyd, C., 1976. Selection of particle sizes by filter feeding copepods: a plea for reason. *Limnology and Oceanography* 21, pp. 175-179.

- Brand, L., 1981. Genetic variability in reproduction rates in marine phytoplankton populations. *Evolution*, 35 pp.1117– 27.
- Brewer, P., Riley, J., 1965. The automatic determination of nitrate in seawater. *Deep Sea Research*, 12, pp. 765-772
- British Oceanographic Data Centre (BODC). AMT20 data. Available at: <http://www.bodc.ac.uk/>. [Accessed October 2012].
- Broglio, E., Jónasdóttir, S., Calbet, A., Jakobsen, H., Saiz, E., 2003. Effect of heterotrophic versus autotrophic food on feeding and reproduction of the calanoid copepod *Acartia tonsa*: relationship with prey fatty acid composition. *Aquatic Microbial Ecology*, 31, pp. 267–278.
- Brown, J., Gillooly, F., Allen, A., Savage, V., West, G., 2004. Toward a metabolic theory of ecology. *Ecology* 85(7), pp.1771–1789.
- Brown, M., Jeffrey, S., Volkman, J., Dunstan, G., 1997. Nutritional properties of microalgae for mariculture. *Aquaculture* 151, pp.315–331.
- Buitenhuis, E., Le Quéré, C., Aumont, O, Beaugrand, G., Bunker, A., Hirst, A., Ikeda, T., O'Brien, T., Piontkovski, S. and Straile, D., 2006. Biogeochemical fluxes through mesozooplankton. *Global Biogeochemical Cycles*, 20, pp. 1–18.
- Cahoon, L., 1981. Reproductive response of *Acartia tonsa* to variations in food ration and quality. *Deep Sea Research Part I*, 28(10), pp.1215–1221.
- Calbet, A., Agustí, S., 1999. Latitudinal changes of copepod egg production rates in Atlantic waters: temperature and food availability as the main driving factors. *Marine Ecology Progress Series*, 181, pp.155–162.
- Calbet, A., 2001. Mesozooplankton grazing effect on primary production: A global comparative analysis in marine ecosystems. *Limnology and Oceanography* 46, pp. 1824-1830.
- Carpenter, J., 1965. The Accuracy of the Winkler Method for Dissolved Oxygen Analysis. *Limnology and Oceanography*, 10(1), pp. 135-140.
- Carrillo, P., Villar-argaiz, M., Medina-Sanchez, J., 2001. Relationship Between N:P Ratio and Growth Rate During the Life Cycle of Calanoid Copepods: An in situ Measurement. *Journal of Plankton Research*, 23(5), pp. 537–547.

- Carrit, D., Carpenter, J., 1966. Recommendation procedure for Winkler analyses of sea water for dissolved oxygen. *Journal of Marine Research*, 24, pp. 313-318.
- Castellani, C., Altunbaş, Y., 2006. Factors controlling the temporal dynamics of egg production in the copepod *Temora longicornis*. *Marine Ecology Progress Series*, 308, pp. 143–153.
- Castellani, C., Altunbaş Y., 2013. Seasonal changes in the respiration rate of *Temora longicornis* (Müller) at in situ conditions, *Marine Ecology Progress Series*, (submitted).
- Cavender-Bares, K., Karl, D., Chisholm, S., 2001. Nutrient gradients in the western North Atlantic Ocean: Relationship to microbial community structure and comparison to patterns in the Pacific Ocean. *Deep Sea Research Part I: Oceanographic Research Papers*, 48(11), pp.2373–2395.
- Ceballos, S., Alvarez-Marques, F., 2006. Reproductive activity and physiological status of the calanoid copepods *Calanus helgolandicus* and *Calanoides carinatus* under food-limiting conditions. *Journal of Experimental Marine Biology and Ecology*, 339, pp.189–203.
- Checkley, M., 1980. The egg production of a marine planktonic copepod in relation to its food supply: laboratory studies. *Deep Sea Research Part B. Oceanographic Literature Review*, 25(3), pp. 430–446.
- Christie, W., 1989. *Gas chromatography and lipids: a practical guide*. The oily Press UK.
- Chuecas L., Riley J., 1969. Component fatty acids of the total lipids of marine phytoplankton. *Journal of the Marine Biological Association of the United Kingdom*, 49, pp. 97-116.
- Clark L., 1959. Electrochemical device for chemical analysis, US Patent no. 2, 913, 386.
- Clarke, A., 1987. Temperature, latitude and reproductive effort. *Marine Ecology Progress Series*, 38, pp.89–99.
- Clarke, A., 2004. Is there a universal temperature dependence of metabolism? *Functional Ecology*, 18(2), pp.252–256.
- Codispoti, L., 1989. Phosphorus vs. nitrogen limitation of new and export production. In: Berger, W.H. et al. (Eds.), *Productivity of the ocean: Present and past*. Wiley, New York, pp. 377–394.

- Conover, R., 1956. Oceanography of Long Island Sound, 1952-1954. VI. Biology of *Acartia clausi* and *A. tonsa*. Bulletin of the Bingham Oceanographic Collection, 15, pp. 156-233.
- Conover, R., 1959. Regional and seasonal variation in the respiratory rate of marine copepods. Limnology and Oceanography, 4(3), pp. 259-268.
- Copin-montegut, C., Copin-montegut, G., 1983. Stoichiometry of carbon, nitrogen, and phosphorus in marine particulate matter. Deep Sea Research, 30(1), pp.31-46.
- Corner E., O'Hara S., 1986. Ch. 1. In: The biological chemistry of marine copepods, edited by E. Corner and S. O'Hara. Oxford University Press, Oxford.
- Cotconnect, G., Brunet, C., Sautour, B., Thoumelin, G., 2001. Nutritive value and selection of food particles by copepods during a spring bloom of *Phaeocystis sp.* in the English Channel, as determined by pigment and fatty acid analyses. Journal of Plankton Research, 23(7), pp.693-703.
- Cowles, T., Strickler, J., 1983. Characterization of feeding activity patterns in the planktonic copepod *Centropages typicus* (Kroyer) under various food conditions. Limnology and Oceanography, 28(1), pp.106-115.
- Cowles, T., Olson, R., Chisholm, S., 1988. Food selection by copepods: discrimination on the basis of food quality. Marine Biology, 49(100), pp.41-49.
- Crawford, K., Raven, J., Wheeler, G., Baxter, E., Joint, I., 2011. The Response of *Thalassiosira pseudonana* to long-term exposure to increased CO<sub>2</sub> and decreased pH. Browman H., ed. PLoS ONE, 6(10), p.e26695.
- Cullen, J., 1982. The deep chlorophyll maximum: comparing vertical profiles of chlorophyll a. Canadian Journal of Fisheries and Aquatic Sciences, 39, pp.791-803.
- Dahms, H., 1995. Dormancy in the copepoda? An overview. Hydrobiologia, 306(3), pp.199-211.
- Dam, H., Lopes, R., 2003. Omnivory in the calanoid copepod *Temora longicornis*: feeding, egg production and egg hatching rates. Journal of Experimental Marine Biology and Ecology, 292(2), pp.119-137.
- Davis, A., Weatherby, T., Hartline, D., Lenz, P., 1999. Myelin-like sheaths in copepod axons. Nature 398, pp. 571.

- De Baar, H., 1994. von Liebig's law of the minimum and plankton ecology (1899–1991). *Progress in Oceanography*, 33(4), pp.347–386.
- DeMott, W., 1989. Optimal foraging theory as a predictor of chemically mediated food selection by suspension-feeding copepods. *Limnology and Oceanography*, 34(1), pp.140–154.
- Deutsch, C., Weber, T., 2012. Nutrient Ratios as a tracer and driver of ocean biogeochemistry. *Annual Review of Marine Sciences*, 4, pp.113–141.
- Dickson, A., Sabine, C., Christian, J., 2007. Guide to best practices for ocean CO<sub>2</sub> measurements. PICES Special Publication 3, pp. 191.
- Dunne, J., Sarmiento, J., Gnanadesikan, A., 2007. A synthesis of global particle export from the surface ocean and cycling through the ocean interior and on the seafloor. *Global Biogeochemical Cycles*, 21(4), pp.1–16.
- Dunstan, G., Volkman, K., Jeffrey, S., Barrett, S., 1992. Biochemical composition of microalgae from the green algal classes Chlorophyceae and Prasinophyceae . 2 . Lipid classes and fatty acids. *Journal of Experimental Marine Biology and Ecology*, 161, pp.115–134.
- Dutz, J., Koski, M., Jónasdóttir, S., 2008. Copepod reproduction is unaffected by diatom aldehydes or lipid composition. *Limnology and Oceanography*, 53(1), pp. 225–235.
- Edwards, M., Richardson, A., 2004. Impact of climate change on marine pelagic phenology and trophic mismatch. *Nature*, 430(7002), pp. 881–4.
- El-Sabaawi, R., Sastri, A., Dower, J., Mazumder, A., 2010. Deciphering the seasonal cycle of copepod trophic dynamics in the strait of Georgia, Canada, using stable isotopes and fatty acids. *Estuaries and Coasts*, 33(3), pp. 738–752.
- Elser, J., Acharya, K., Kyle, M., Cotner, J., Makino, W., Markow, T., Watts, T., Hobbie, S., Fagan, W., Schade, J., Hood J., and Sterner, R., 2003. Growth rate-stoichiometry couplings in diverse biota. *Ecology Letters*, 6, pp. 936-943.
- Elser, J., Bracken, M., Cleland, E., Gruner, D., Harpole, S., Hillebrand, H., Ngai, J., Seabloom, E., Shurin, J., Smith, J., 2007. Global analysis of nitrogen and phosphorus limitation of primary producers in freshwater, marine and terrestrial ecosystems. *Ecology Letters* 10, pp. 1135–1142.

- Evjemo, J., Tokle, N., Vadstein, O., Olsen, Y., 2008. Effect of essential dietary fatty acids on egg production and hatching success of the marine copepod *Temora longicornis*. *Journal of Experimental Marine Biology and Ecology*, 365(1), pp. 31–37.
- Falkowski, P., Davis, C.S., 2004. Natural proportions. Redfield ratios: the uniformity of elemental ratios in the oceans and the life they contain underpins our understanding of marine biogeochemistry. *Nature*, 431(7005), pp.131.
- Falkowski, P., 1997. Evolution of the nitrogen cycle and its influence on the biological sequestration of CO<sub>2</sub> in the ocean. *Nature* 387, pp. 272-275.
- Folch, J., Lees, N., Sloan-Stanley G., 1957. A simple method for the isolation and purification of total lipid. *The Journal of Biological Chemistry*, 226, pp. 497–509.
- Fraser, A., Sargent, J., Gamble, J., 1989. Lipid class and fatty acid composition of *Calanus finmarchicus* (Gunnerus), *Pseudocalanus sp.* and *Temora longicornis* Muller from a nutrient-enriched seawater enclosure. *Journal of Experimental Marine Biology and Ecology*, 130(1), pp. 81–92.
- Frigstad, H., Andersen, T., Hessen, D., Naustvoll, L., Johnsen, T., Bellerby, R., 2011. Seasonal variation in marine C:N:P stoichiometry: can the composition of seston explain stable Redfield ratios? *Biogeosciences*, 8(10), pp. 2917–2933.
- Frigstad, H., Andersen, T., Hessen, D., Naustvoll, L., Johnsen, T., and Bellerby, R., 2011. Seasonal variation in marine C:N:P stoichiometry: can the composition of seston explain stable Redfield ratios? *Biogeosciences*, 8(10), pp. 2917–2933.
- Frost, B., 1972. Effects of size and concentration of food particles on the feeding behavior of the marine planktonic copepod *Calanus pacificus*. *Limnology and Oceanography*, 17(6), pp. 805–815.
- Fuller, J., 1937. Feeding rate of *Calanus finmarchicus* in relation to environmental conditions. *The Biological Bulletin*, 72(2), pp. 233–246.
- Gallienne, C., Robins, D., Woodd-walker, R., 2001. Abundance, distribution and size structure of zooplankton along a 20° west meridional transect of the northeast. *Deep-Sea Research II*, 48, pp. 925–949.
- Garcia, H., Gordon, L., 1992. Oxygen solubility in seawater: Better fitting equations. *Limnology and Oceanography*, 37(6), pp. 1307–1312.

- Garcia, V., Garcia, C., Mata, M., Pollery, R., Piola, A., Signorini, S., McClain, C., Iglesias-Rodriguez, M., 2008. Environmental factors controlling the phytoplankton blooms at the Patagonia shelf-break in spring. *Deep Sea Research Part I: Oceanographic Research Papers*, 55(9), pp. 1150–1166.
- Gasol, J., del Giorgio, P., Duarte, C., 1997. Biomass distribution in marine planktonic communities. *Limnology and Oceanography* 42, pp. 1353-1363.
- Gatten, R., Sargent, J., Forsberg, T., O'Hara, S., Corner, E., 1980. On the nutrition and metabolism of zooplankton XIV. Utilization of lipid by *Calanus helgolandicus* during maturation and reproduction. *Journal of the Marine Biological Association of the United Kingdom*, 60, pp. 391–399.
- Gauld, D., Raymont, J., 1953. The respiration of some planktonic copepods. II. The effect of temperature. *Journal of the Marine Biological Association of the United Kingdom*, 31, pp. 447-460.
- Geider, R., La Roche, J., 2002. Redfield revisited: variability of C:N:P in marine microalgae and its biochemical basis. *European Journal of Phycology*, 37(1), pp. 1–17.
- Gentsch, E., Kreibich, T., Hagen, W., Niehoff, B., 2008. Dietary shifts in the copepod *Temora longicornis* during spring: evidence from stable isotope signatures, fatty acid biomarkers and feeding experiments. *Journal of Plankton Research*, 31(1), pp. 45–60.
- Gillooly, J., Brown, J., West, G., Savage, V., Charnov, E., 2001. Effects of size and temperature on metabolic rate. *Science* 293, pp. 2248–2251.
- Gist, N., Serret, P., Woodward, E., Chamberlain, K., Robinson, C., 2009. Seasonal and spatial variability in plankton production and respiration in the Subtropical Gyres of the Atlantic Ocean. *Deep Sea Research Part II: Topical Studies in Oceanography*, 56(15), pp. 931–940.
- Glazier, D., 2005. Beyond the “3/4-power law”: variation in the intra- and interspecific scaling of metabolic rate in animals. *Biological reviews of the Cambridge Philosophical Society*, 80(4), pp.611–62.
- Glazier, D., 2006. The 3/4-power law is not universal: evolution of isometric, ontogenetic metabolic scaling in pelagic animals. *BioScience*, 56(4), pp. 325.
- Glazier, D., 2010. A unifying explanation for diverse metabolic scaling in animals and plants. *Biological reviews of the Cambridge Philosophical Society*, 85(1), pp. 111–38.

- Glibert, P., Kana T., Brown K., 2012. From limitation to excess: the consequences of substrate excess and stoichiometry for phytoplankton physiology, trophodynamics and biogeochemistry, and the implications for modelling. *Journal of Marine Systems* (in press).
- Glover, D., Brewer, P., 1988. Estimates of wintertime mixed layer nutrient concentrations in the North Atlantic. *Deep Sea Research Part II* 35, pp. 1525–1546.
- Glud R., Gundersen J., Ramsing N., 2000. Electrochemical and optical oxygen microsensors for in situ measurements, in: J. Buffle, G. Horvai (Eds.), *In situ monitoring of aquatic systems: chemical analysis and speciation*, 2000, pp. 19-73.
- Gnaiger, E., Bitterlich, G., 1984. Proximate biochemical composition and caloric content calculated from elemental CHN analysis: a stoichiometric concept. *Oecologia*, 62, pp. 289–298.
- Goebel, N., Turk, K., Achilles M., Paerl. R, Hewson, I., Morrison A., Montoya J., Edwards C., Zehr, J., 2010. Abundance and distribution of major groups of diazotrophic cyanobacteria and their potential contribution to N<sub>2</sub> fixation in the tropical Atlantic Ocean. *Environmental Microbiology*, 12 (12), pp.3272-89.
- Goldman, J., McCarthy, J. and Peavey, D., 1979. Growth rate influence on the chemical composition of phytoplankton in oceanic waters. *Nature*, 279, pp. 210–215.
- Gordon D., 1969. Examination of methods in particulate organic carbon analysis. *Deep Sea Research Part I: Oceanographic Research Papers*, 16, pp. 661-665.
- Graeve, M., Kattner, G., Hagen, W., 1994. Diet-induced changes in the fatty acid composition of Arctic herbivorous copepods: Experimental evidence of trophic markers. *Journal of Experimental Marine Biology and Ecology*, 182(1), pp. 97–110.
- Grasshoff, K., 1976. *Methods of sea-water analysis*, Verlag Chemie, Weinheim: pp.317.
- Graziano, L., Geider, R., Li, W., Olaizola, M., 1996. Nitrogen limitation of North Atlantic phytoplankton: Analysis of physiological condition in nutrient enrichment experiments. *Aquatic Microbial Ecology* 11, pp. 53-64.
- Grob, C., Ostrowski, M., Holland, R., Heldal, M., Norland, S., Erichsen, E., Blindauer, C., Martin, A., Zubkov, M., Scanlan, D., 2013. Elemental composition of natural populations of key microbial groups in Atlantic waters. *Environmental Microbiology*, p.n/a–n/a doi: 10.1111/1462-2920.12145.

- Grodsky, S., Carton, J., Mc Clain, C., 2008. Variability of upwelling and chlorophyll in the equatorial Atlantic. *Geophysical Research Letters*, 35(3), pp.1–6.
- Guisande, C., 2006. Biochemical fingerprints in zooplankton. *Limnetica*, 25(1-2), pp. 369–376.
- Guisande, C., Harris, R., 1995. Effect of total organic content of eggs on hatching success and naupliar survival in the copepod *Calanus helgolandicus*. *Limnology and Oceanography*, 40(3), pp. 476–482.
- Guisande, C., Maniero, I., Riveiro, I., 1999. Homeostasis in the essential amino acid composition of the marine copepod *Euterpina acutifrons*. *Limnology and Oceanography*, 44(3), pp.691–696.
- Guisande, C., Riveiro, I., Maneiro, I., 2000. Comparisons among the amino acid composition of females, eggs and food to determine the relative importance of food quantity and food quality to copepod reproduction. *Marine Ecology Progress Series*, 202, pp.135–142.
- Hirston, N., Munns, W., 1984. The timing of copepod diapause as an evolutionarily stable strategy. *The American Naturalist*, 123(6), pp. 733–751.
- Hannides, C., Landry, M., Benitez-nelson, C., Styles, R., Montoya, J. and Karl, D., 2009. Export stoichiometry and migrant-mediated flux of phosphorus in the North Pacific Subtropical Gyre. *Deep Sea Research Part I: Oceanographic Research Papers*, 56(1), pp. 73–88.
- Harris R., Wiebe P., Lenz J., Skjoldal H., Huntley M., 2006. ICES Zooplankton methodology manual. Elsevier Academic Press.
- Harris, R., 1988. Interactions between diel vertical migratory behavior of marine zooplankton and the subsurface chlorophyll maximum. *Bulletin of Marine Sciences* 43(3), pp. 663-674.
- Hays, G., Richardson, A. and Robinson, C., 2005. Climate change and marine plankton. *Trends in Ecology and Evolution*, 20(6), pp. 337–344.
- Hazzard, S., Kleppel, G., 2003. Egg production of the copepod *Acartia tonsa* in Florida Bay: role of fatty acids in the nutritional composition of the food environment. *Marine Ecology Progress Series*, 252, pp.199–206.

- Hecky, R., Kilham, P., 1988. Nutrient limitation of phytoplankton in freshwater and marine environments: a review of recent evidence on the effects of enrichment. *Limnology and Oceanography*, 33(4), pp. 796–822.
- Hedges, J., Baldock, J., Gelin, Y., Lee, C, Peterson, M., Wakeham, S., 2002. The biochemical and elemental compositions of marine plankton: A NMR perspective. *Marine Chemistry*, 78(1), pp. 47–63.
- Hernandez-leon, S., Gomez, M., 1996. Factors affecting the respiration / ETS ratio in marine zooplankton. *Journal of Plankton Research*, 18(2), pp. 239–255.
- Hernandez-leon, S., Ikeda, T., 2005a. Zooplankton respiration. In: *Respiration in Aquatic Ecosystems*. Del Giorgio P., and Williams P. Oxford University Press 2005. Ch.5.
- Hernandez-leon, S., Ikeda, T., 2005b. A global assessment of mesozooplankton respiration in the ocean. *Journal of Plankton Research*, 27(2), pp.153–158.
- Hessen, D., Anderson, T., 2008. Excess carbon in aquatic organisms and ecosystems : Physiological, ecological, and evolutionary implications. *Limnology and Oceanography*, 53(4), pp.1685–1696.
- Hessen, D., Lyche A., 1991. Inter- and intraspecific variations in zooplankton element composition. *Archiv fur Hydrobiologie* 121, pp. 343–353.
- Hessen, D., 1992. Nutrient element limitation of zooplankton production. *American Naturalist*, 140(5), pp. 799–814.
- Hinder, S., Hays, G., Edwards, M., Roberts, E., Walne, A., Gravenor, M., 2012. Changes in marine dinoflagellate and diatom abundance under climate change. *Nature Climate Change*, 2(4), pp. 271–275.
- Hirche, J., Meyer, U. and Niehoff, B., 1997. Egg production of *Calanus finmarchicus*: effect of temperature, food and season. *Marine Biology*, 127, pp. 609–620.
- Hitchcock, G., 1982. A comparative study of the size-dependent organic composition of marine diatoms and dinoflagellates. *Journal of Plankton Research*, 4(2), pp. 363–377.
- Hooker, S., Rees, N., Aiken, J., 2000. An objective methodology for identifying oceanic provinces. *Progress in Oceanography*, 45, pp. 313–338.
- HOT time-series data 1990-2010. Available online at: <http://hahana.soest.hawaii.edu/hot/> (Accessed: November 2012).

- Howarth, R., 1988. Nutrient limitation of net primary production in marine ecosystems. *Annual Review of Ecology*, 19, pp. 89–110.
- Huntley, M., Lopez, M., 1992. Temperature-dependent production of marine copepods: a global synthesis. *The American naturalist*, 140(2), pp. 201–242.
- Huntley, M., 1988. Feeding biology of *Calanus*: a new perspective. *Hydrobiologia*, 167-168(1), pp. 83–99.
- Huskin, I., Anadon, R., Woodd-walker, R., Harris, R., 2001. Basin-scale latitudinal patterns of copepod grazing in the Atlantic Ocean. *Journal of Plankton Research*, 23(12), pp.1361–1371.
- Hutchings, L., Pitcher G., Probyn T., Bailey G., 1995. The chemical and biological consequences of coastal upwelling. In: Summerhayes C. P., Emeis K.-C., Angel M. V., Smith R. L., and Zeitzchel B., editors. *Upwelling in the oceans: modern processes and ancient records*. John Wiley and Sons, New York, New York, USA pp. 65–81.
- Ianora, A., Poulet, S., 1993. Egg viability in the copepod *Temora stylifera*, *Limnology and Oceanography*, 38(8), pp. 1615–1626.
- Ikeda, T., Skjoldal H., 1980. In: Harris R., P., Wiebe P., h., Lenz J., Skjoldal H., R., Huntley M. 2006. *ICES Zooplankton methodology manual*. Elsevier Academic Press. Ch. 10.
- Ikeda, T., 1970. Relationship between respiration and body size in marine plankton animals as a function of the temperature of habitat. *Bulletin of the Faculty of Fisheries, Hokkaido University (Japan)* 21, pp. 91-112.
- Ikeda, T., 1985. Metabolic rates of epipelagic marine zooplankton as a function of body mass and temperature. *Marine Biology*, 85, pp.1–11.
- Ikeda, T., Torres, J., Hernández-León, S., Geiger, S., 2000. Metabolism. In: Harris, R., Wiebe, P.H., Lenz, J., Skojoldal, H.R., Hintley, M. (Eds.), *ICES Zooplankton Methodology Manual*. Academic Press, London, pp. 455–532.
- Ikeda, T., Kanno, Y., Ozaki, K., Shinada, A., 2001. Metabolic rates of epipelagic marine copepods as a function of body mass and temperature. *Marine Biology*, 139, pp.587–596.
- Ikeda, T., Sano, F., Yamaguchi, A., Matsuishi, T., 2006. Metabolism of mesopelagic and bathypelagic copepods in the western North Pacific Ocean. *Marine Ecology Progress Series*, 322, pp.199–211.

- Ikeda, T., Sano, F. and Yamaguchi, A., 2007. Respiration in marine pelagic copepods: a global-bathymetric model. *Marine Ecology Progress Series*, 339, pp. 215–219.
- IPCC AR4 WG2., 2007. In Parry, M., Canziani, O., Palutikof, J., van der Linden, P., Hanson, C., *Climate Change 2007: Impacts, adaptation and vulnerability, contribution of working group ii to the fourth assessment report of the intergovernmental panel on climate change*. Cambridge University Press.
- Irigoiien, X., 1998. Gut clearance rate constant, temperature and initial gut contents: a review. *Journal of Plankton Research*, 20(5), pp. 997–1003.
- Isla, J., Llope, M., Anadon, R., 2004. Size-fractionated mesozooplankton biomass, metabolism and grazing along a 50°N to 30°S transect of the Atlantic Ocean. *Journal of Plankton Research*, 26(11), pp. 1301–1313.
- Ivleva, I., 1980. The dependence of crustacean respiration rate on body mass and habitat temperature. *Internationale Revue der gesamten Hydrobiologie und Hydrographie*, 65(1), pp. 1–47.
- Jónasdóttir, S., 1994. Effects of food quality on the reproductive success of *Acartia tonsa* and *Acartia hudsonica*: laboratory observations. *Marine Biology*, 121(1), pp. 67–81.
- Jónasdóttir, S., Fields, D., Pantoja, S., 1995. Copepod egg production in Long Island Sound, USA, as a function of the chemical composition of seston. *Marine Ecology Progress Series*, 119, pp. 87–98.
- Jónasdóttir, S., Kiorboe, T., 1996. Copepod recruitment and food composition: do diatoms affect hatching success? *Marine Biology*, 125(4), pp. 743–750.
- Jónasdóttir, S., Gudfinnsson H., Gislason A., Astthorsson O., 2002. Diet composition and quality for *Calanus finmarchicus* egg production and hatching success off south-west Iceland. *Marine Biology*, 140, pp. 1195–1206.
- Jónasdóttir, S., 2005. Egg production and hatching success in the calanoid copepods *Calanus helgolandicus* and *Calanus finmarchicus* in the North Sea from March to September 2001. *Journal of Plankton Research*, 27(12), pp.1239–1259.
- Jónasdóttir, S., Richardson, K., Heath, M., Ingvarsdottir, A., Christoffersen, A., 2008. Spring production of *Calanus finmarchicus* at the Iceland–Scotland Ridge. *Deep Sea Research Part I: Oceanographic Research Papers*, 55(4), pp. 471–489.

- Jónasdóttir, S., Visser, A., Jespersen, C., 2009. Assessing the role of food quality in the production and hatching of *Temora longicornis* eggs. *Marine Ecology Progress Series*, 382, pp. 139–150.
- Jones, R., Flynn, K. and Anderson, T., 2002. Effect of food quality on carbon and nitrogen growth efficiency in the copepod *Acartia tonsa*. *Marine Ecology Progress Series*, 235, pp. 147–156.
- Kana, T., Glibert, P., 1987. Effect of irradiances up to 2000 mE m<sup>-2</sup> s<sup>-1</sup> on marine *Synechococcus* WH7803. I. Growth, pigmentation, and cell composition. *Deep-Sea Research Part I. Oceanographic Research Papers* 34, pp. 479–95.
- Karl, D., Yanagi, K., 1997. Partial characterization of the dissolved organic phosphorus pool in the oligotrophic North Pacific Ocean. *Limnology and Oceanography* 42, pp. 1398–1405.
- Karl, D., Bidigare, R., Letelier, R., 2001. Long-term changes in plankton community structure and productivity in the North Pacific Subtropical Gyre: The domain shift hypothesis, *Deep Sea Research Part II*, 48, pp. 1449–1470.
- Kattner G., Gercken G., Eberlein K., 1983. Development of lipids during a spring plankton bloom in the northern North Sea. I. Particulate fatty acids. *Marine Chemistry* 14, pp. 149–162.
- Kattner, G., Hagen, W., Lee, R., Campbell, R., Deibel, D., Falk Petersen, S., Graeve, M., Hansen, B., Hirche, H., Jónasdóttir, S., Madsen, M., Mayzaud, P., Müller-Navarra, D., Nichols, P., Paffenhofer, G., Pond, D., Saito, H., Stübing, D., Virtue, P., 2007. Perspectives on marine zooplankton lipids. *Canadian Journal of Fisheries and Aquatic Sciences*, 64(11), pp.1628–1639.
- Kay, A., Ashton, I., Gorokhova, E., Kerkhoff, A., Liess, A., Litchman, E., 2005. Toward a stoichiometric framework for evolutionary biology. *Oikos*, 109, pp. 6–17.
- King, F., Devol, A., Packard, T., 1978. Plankton metabolic activity in the eastern tropical North Pacific. *Deep-Sea Research*, 25, pp. 689–704.
- Kiorboe T., 2008. *A Mechanistic Approach to Plankton Ecology*. Princeton University Press. Ch. 6.
- Kiorboe, T., Nielsen, T., 1994. Regulation of zooplankton biomass and production in a temperate, coastal ecosystem I. *Limnology and Oceanography*, 39(3), pp.493–507.

- Kiorboe, T., 1989. Phytoplankton growth rate and nitrogen content: implications for feeding and fecundity in a herbivorous copepod. *Marine Ecology Progress Series*, 55, pp. 229–234.
- Kiorboe, T., Mohlenberg, F., Hamburger, K., 1985. Bioenergetics of the planktonic copepod *Acartia tonsa*: relation between feeding, egg production and respiration, and composition of specific dynamic action. *Marine Ecology Progress Series*, 26, pp. 85–97.
- Kirkwood, D., 1989. Simultaneous determination of selected nutrients in sea-water, ICES CM 1989/C:29.
- Klausmeier, C., Litchman, E., Daufresne, T., Levin, S., 2004a. Optimal nitrogen-to-phosphorus stoichiometry of phytoplankton. *Letters to Nature*, 429(May), pp. 171–174.
- Klausmeier, C., Litchman, E., Levin, S., 2004b. Phytoplankton growth and stoichiometry under multiple nutrient limitation. *Limnology and Oceanography*, 49 (4 part 2), pp. 1463–1470.
- Kleiber, M., 1947. Body size and metabolic rate. *Physiological Reviews*, 27, pp. 511–541.
- Klein Breteler, W., Gonzalez, S., 1982. Influence of cultivation and food concentration on body length of calanoid copepods. *Marine Biology*, 71, pp. 157–161.
- Kleppel, G., Burkart, C., 1995. Egg production and the nutritional environment of *Acartia tonsa*: the role of food quality in copepod nutrition. *ICES Journal of Marine Science*, 52, pp. 297–304.
- Kleppel, G., 1993. On the diets of calanoid copepods. *Marine Ecology Progress Series*, 99, pp.183–195.
- Kleppel, G., Burkart, C., Houchin, L., 1998. Nutrition and the regulation of egg production in the calanoid copepod *Acartia tonsa*. *Limnology and Oceanography*, 43(5), pp.1000–1007.
- Kortzinger, A., Koeve, W., Kahler, P., Mintrop, L., 2001. C : N ratios in the mixed layer during the productive season in the northeast Atlantic Ocean. *Deep Sea Research Part I*, 48, pp. 661–688.
- Koski, M., Klein Breteler, W., Schogt, N., 1998. Effect of food quality on rate of growth and development of the pelagic copepod *Pseudocalanus elongatus* (Copepoda, Calanoida). *Marine Ecology Progress Series*, 170, pp. 169–187.

- Koski, M., Dutz J., Klein Breteler W., Rampen S., Noordeloos, A. 2010. Seasonal changes in food quantity and quality of the common North Sea copepods *Temora longicornis* and *Pseudocalanus elongatus*: a bioassay approach. Marine Ecology Progress Series, 399, pp. 141–155.
- Köster, M., Krause, C., Paffenhöfer, G., 2008. Time-series measurements of oxygen consumption of copepod nauplii. Marine Ecology Progress Series, 353(1943), pp. 157–164.
- Krom, M., Herut, B., Mantoura, R., 2004. Nutrient budget for the Eastern Mediterranean : Implications for phosphorus limitation. Limnology and Oceanography, 49(5), pp.1582–1592.
- Lacoste, A., Poulet, S., Cueff, A., Kattner, G., Ianora, A., Laabir, M., 2001. New evidence of the copepod maternal food effects on reproduction. Journal of experimental marine biology and ecology, 259(1), pp. 85–107.
- Lagus, A., 2004. Species-specific differences in phytoplankton responses to N and P enrichments and the N:P ratio in the Archipelago Sea, northern Baltic Sea. Journal of Plankton Research, 26(7), pp. 779–798.
- Lampitt, R., Gamble, J., 1982. Diet and respiration of the small planktonic marine copepod *Oithona nana*. Mar Biol 66, pp. 185–190.
- Landry, M., Hassett, R., 1982. Estimating the grazing impact of marine micro-zooplankton. Marine Biology, 67(3), pp. 283–288.
- Landry, M., Al-Mutairi, H., Selph, K., Christensen, S., Nunnery S., 2001. Seasonal patterns of mesozooplankton abundance and biomass at Station ALOHA. Deep Sea Research Part II: Topical Studies in Oceanography, 48(8-9), pp. 2037–2061.
- Lenz, P., 2012. The biogeography and ecology of myelin in marine copepods. Journal of Plankton Research 34, pp. 575–589.
- Lenz, P., Hartline, D., Davis, A., 2000. The need for speed. I. Fast reactions and myelinated axons in copepods. Journal of Comparative Physiology A, 186, pp. 337–345.
- Leonardos, N., Geider, R., 2004. Responses of elemental and biochemical composition of *Chaetoceros muelleri* to growth under varying light and nitrate:phosphate supply ratios and their influence on critical N : P. Limnology and Oceanography, 49(6), pp. 2105–2114.

- Leterme, S., Seuront, L. and Edwards, M., 2006. Differential contribution of diatoms and dinoflagellates to phytoplankton biomass in the NE Atlantic Ocean and the North Sea. *Marine Ecology Progress Series*, 312, pp. 57–65.
- Lin, K., Sastri, A., Gong, G., Hsieh, C., 2013. Copepod community growth rates in relation to body size, temperature, and food availability in the East China Sea: a test of metabolic theory of ecology. *Biogeosciences*, 10(3), pp. 1877–1892.
- Loftus, M., Carpenter, J., 1971. A fluorimetric method for determining chlorophylls a, b and c. *Journal of Marine Research*, 29, pp. 319-338.
- Longhurst, A., 1985. The structure and evolution of plankton communities. *Progress In Oceanography*, 15(1), pp. 1–35.
- Longhurst, A., 1995. Seasonal cycles of pelagic production and consumption. *Progress in Oceanography*, 36, pp. 77–167.
- Longhurst, A., Sathyendranath, S., Platt, T., Caverhill, C., 1995. An estimate of global primary production in the ocean from satellite radiometer data. *Journal of Plankton Research*, 17(6), pp. 1245–1271.
- Longhurst, A., Harrison, W., 1989. The biological pump: profiles of plankton production and consumption in the upper ocean. *Progress in Oceanography*, 22, pp. 47–123.
- Lopez-Urrutia, A., San Martin, E., Harris, R., Irigoien, X., 2006. Scaling the metabolic balance of the oceans. *Proceedings of the National Academy of Sciences of the United States of America*, 103(23), pp. 8739–44.
- Lourenco, S., Barbarino E., Lanfer Marquez U., Adar E., 1998. Distribution of intracellular nitrogen in marine microalgae: basis for the calculation of specific nitrogen-to-protein conversion factors. *Journal of Phycology*, 34, pp. 798–811.
- Main, T., Dobberfuhl, D., Elser, J., 1997. N:P Stoichiometry and ontogeny of crustacean zooplankton: a test of the growth rate hypothesis. *Limnology and Oceanography*, 42(6), pp.1474–1478.
- Malzahn, A., Boersma, M. 2012. Effects of poor food quality on copepod growth are dose dependent and non-reversible. *Oikos*, 121(9), pp.1408–1416.
- Marañón, E., Holligan, P., Barciela R., González, N., Mouriño, B., Pazó, M., 2001. Patterns of phytoplankton size structure and productivity in contrasting open-ocean environments. *Marine Ecology Progress Series*, 216, pp. 43–56.

- Marañón, E., Holligan, P., Varela, M., Mourino, B., Bale, A., 2000. Basin-scale variability of phytoplankton biomass, production and growth in the Atlantic Ocean. *Deep Sea Research Part B. Oceanographic Literature Review*, 47, pp. 825–857.
- Marshall S., M., Nicholls A., Orr, P., 1935. In: Harris R., Wiebe P., Lenz J., Skjoldal H., Huntley M., 2006. ICES Zooplankton methodology manual. Elsevier Academic Press. Ch. 10.
- Marshall S., Orr P., 1958. On the biology of *Calanus Finmarchicus*. X. Seasonal changes in oxygen consumption. *Journal of the Marine Biological Association of the United Kingdom*, 37, pp. 459-472.
- Marshall S., Orr P., 1972. The biology of a marine copepod. Reprint. Springer, Berlin: I-VII, pp. 1-195.
- Martin, R., Quigg, A., Podkovyrov, V., 2008. Marine biodiversification in response to evolving phytoplankton stoichiometry. *Palaeogeography, Palaeoclimatology, Palaeoecology*, 258, pp. 277–291.
- Martinez-Vicente, V., Dall’Olmo, G., Tarran, G., Boss, E., Sathyendranath, S., 2013. Optical backscattering is correlated with phytoplankton carbon across the Atlantic Ocean, *Geophysical Research Letters*, 40, pp. 1154–1158.
- Martiny, A., Pham, C., Primeau, F., Vrugt, J., Moore, J., Levin, S., and Lomas, M., 2013. Strong latitudinal patterns in the elemental ratios of marine plankton and organic matter. *Nature Geoscience*, 6(4), pp. 279–283.
- Mather, R., Reynolds, S., Wolff, G., Williams, R., Torres-Valdes, S., Woodward, E., Landolfi, A., Pan, X., Sanders, R., Achterberg, E., 2008. Phosphorus cycling in the North and South Atlantic Ocean subtropical gyres. *Nature Geoscience*, 1(7), pp.439–443.
- Mauchline, J., 1998. The biology of calanoid copepods. *Advances in Marine Biology*. Vol.33. Academic Press.
- Mayor, D., Anderson, T., Pond, D., Irigoien, X., 2009a. Limitation of egg production in *Calanus finmarchicus* in the field: a stoichiometric analysis. *Journal of Marine Systems*, 78(4), pp. 511–517
- Mayor, D., Anderson, T., Pond, D., Irigoien, X. 2009b. Egg production and associated losses of carbon, nitrogen and fatty acids from maternal biomass in *Calanus finmarchicus* before the spring bloom. *Journal of Marine Systems*, 78(4), pp. 505–510.

- Mayzaud, P., Chanut, J.P. and Ackman, R., 1989. Seasonal changes of the biochemical composition of marine particulate matter with special reference to fatty acids and sterols. *Marine Ecology Progress Series*, 56, pp. 189–204.
- Mayzaud, P., Tirelli, V., Bernard, J., Roche-Mayzaud, O., 1998. The influence of food quality on the nutritional acclimation of the copepod *Acartia clausi*. *Journal of Marine Systems*, 15(1-4), pp. 483–493.
- Mayzaud, P., Razouls, S., Errhif, A., Tirelli, V., Labat, J., 2002. Feeding, respiration and egg production rates of copepods during austral spring in the Indian sector of the Antarctic Ocean: role of the zooplankton community in carbon transformation. *Deep Sea Research Part I: Oceanographic Research Papers*, 49(6), pp.1027–1048.
- McClain, C., Signorini S., Christian J., 2004. Subtropical gyre variability observed by ocean-colour satellites, *Deep Sea Res., Part II*, 51, pp. 281–301.
- Miller, C., Johnson, J., Heinle, D., 1977. Growth rules in the marine copepod genus *Acartia*. *Limnology and Oceanography*, 22(2), pp. 326–335.
- Mills, M., Ridame, C., Davey, M., La Roche, J., Geider R., 2004. Iron and phosphorus co-limit nitrogen fixation in the eastern tropical North Atlantic. *Nature*, 429, pp. 292-294.
- Mitra, A., Flynn, K., 2005. Predator-prey interactions: is “ecological stoichiometry” sufficient when good food goes bad? *Journal of Plankton Research*, 27(5), pp. 393–399.
- Moloney, C., Field, J., 1989. General allometric equations for rates of nutrient uptake, ingestion, and respiration in plankton organisms. *Limnology and Oceanography*, 34(7), pp. 1290–1299.
- Moloney, C., St John, M., Denman, K., Karl, D., Köster, F., Sundby, S., Wilson, R., 2011. Weaving marine food webs from end to end under global change. *Journal of Marine Systems*, 84(3-4), pp. 106–116.
- Monteiro, F., Follows, M., 2012. On nitrogen fixation and preferential remineralization of phosphorus. *Geophysical Research Letters*, 39, pp. 1–5.
- Moore C., Mills C., Achterberg, M., Geider E., La Roche R., Lucas J., McDonagh E., Pan X., Poulton A., Rijkenberg M., Suggett D., Ussher S., Woodward M., 2009. Large-scale distribution of Atlantic nitrogen fixation controlled by iron availability. *Nature Geoscience*, 2(12), pp. 867–871.

- Moore, C., Mills, M., Langlois, R., Milne, A., Achterberg, E., La Roche, J., Geider, R., 2008. Relative influence of nitrogen and phosphorus availability on phytoplankton physiology and productivity in the oligotrophic sub-tropical North Atlantic Ocean. *Limnology and Oceanography*, 53(1), pp. 291–305.
- Moore, J., Doney, S., Lindsay, K., 2004. Upper ocean ecosystem dynamics and iron cycling in a global three-dimensional model. *Global Biogeochemical Cycles*, 18(4), pp. 1–21.
- Morel, A., 1988. Optical modeling of the upper ocean in relation to its biogenous matter content (case I waters), *J. Geophys. Res.* 93, pp. 10749-10768.
- Moriarty, R., O'Brien, T., 2013. Distribution of mesozooplankton biomass in the global ocean. *Earth System Science Data*, 5(1), pp. 45–55.
- Mulyadi., 2001. Calanoid copepods of the genus *Euchirella* Giesbrecht, 1888 from the Flores Sea, Indonesia. *Crustaceana*, 74(9), pp. 809-824.
- Navarro, G., Caballero, I., Prieto, L., Vázquez, A., Flecha, S., Huertas, I., Ruiz, J., 2012. Seasonal-to-interannual variability of chlorophyll-a bloom timing associated with physical forcing in the Gulf of Cádiz. *Advances in Space Research*, 50(8), pp. 1164–1172.
- NOAA climate prediction centre. La Niña event 2010. Available at: <http://www.cpc.ncep.noaa.gov>. [Accessed October 2012].
- Nobili R., Robinson C., Buitenhuis E., Castellani C., 2013. Food quality regulates the metabolism and reproduction of *Temora longicornis*. *Biogeosciences*. Submitted.
- O'Connors, H., Biggs, D., Ninivaggi, D., 1980. Particle-size-dependent maximum grazing rates for *Temora longicornis* fed natural particle assemblages. *Marine Biology*, 56, pp. 65–70.
- Ocean Optics. NeoFox installation and operation manual for optode – Ocean Optics 2011. Available at: [www.oceanoptics.com/technical/neofox.pdf](http://www.oceanoptics.com/technical/neofox.pdf). [Accessed October 2011].
- Ohman, M., 1987. Energy sources for recruitment of the subantarctic copepod *Neocalanus tonsus*. *Limnology and Oceanography*, 32(6), pp.1317–1330.
- Olf, H., Alonso, D., Berg, M., Eriksson, B., Loreau, M., Piersma, T., Rooney, N., 2009. Parallel ecological networks in ecosystems. *Philosophical transactions of the Royal Society of London. Series B, Biological sciences*, 364(1524), pp.1755–79.

- Omori M., Ikeda T., 1992. Methods in marine zooplankton ecology. Krieger Publishing Company.
- Oreslandl, V., Ward, P., 1993. Summer and winter diet of four carnivorous copepod species around South Georgia. Marine Ecology Progress Series, 98, pp.73–78.
- Osterroht, C., Thomas, H., 2000. New production enhanced by nutrient supply from non-Redfield remineralisation of freshly produced organic material. Journal of Marine Systems, 25(1), pp.33–46.
- Paffenhofer, G., Van Sant, K., 1985. The feeding response of a marine planktonic copepod to quantity and quality of particles. Marine Ecology Progress Series, 27, pp. 55–65.
- Paffenhofer, G., Bundy, M., Lewis, K., Metz, C., 1995. Rates of ingestion and their variability between individual calanoid copepods: direct observations. Journal of Plankton Research, 17(7), pp. 1573–1585.
- Paffenhofer, G., 1988. Feeding rates and behavior of zooplankton. Bulletin of Marine Sciences, 43(3), pp. 430–445.
- Park C., Landry, M., 1993. Egg production by the subtropical copepod *Undinula vulgaris*. Marine Biology, 421, pp. 415–421.
- Pavlova, Z., 1994. Diel changes in copepod respiration rates. Hydrobiologia, 292/293, pp. 333–339.
- Pertola, S., Koski, M., Viitasalo, M., 2002. Stoichiometry of mesozooplankton in N- and P-limited areas of the Baltic Sea. Marine Biology, 140(2), pp. 425–434.
- Peters, J., Dutz, J., Hagen, W., 2013. Trophodynamics and life-cycle strategies of the copepods *Temora longicornis* and *Acartia longiremis* in the Central Baltic Sea. Journal of Plankton Research, 35(3), pp. 595–609
- Piontkovski, S., Castellani, C., 2009. Long-term declining trend of zooplankton biomass in the Tropical Atlantic. Hydrobiologia, 632(1), pp. 365–370.
- Plath, K., Boersma, M., 2001. Mineral Limitation of Zooplankton: Stoichiometric Constraints and Optimal Foraging. Ecology, 82(5), pp. 1260.

- Pond, D., Bell, M., Harris, R., Sargent, J., 1998. Microplanktonic polyunsaturated fatty acids markers: a mesocosmos trial. *Estuarine, Coastal and Shelf Science*, 46 (supplement A0), pp. 61–67.
- Pond, D., Harris, R., Head, R., Harbour, D., 1996. Environmental and nutritional factors determining seasonal variability in the fecundity and egg viability of *Calanus helgolandicus* in coastal waters off Plymouth, UK. *Marine Ecology Progress Series*, 143, pp. 45–63.
- Postel, L., Fock, H., Hagen, W., 2000. Biomass and abundance. In *ICES Zooplankton Methodology Manual*, pp. 83e192. Ed. by R. Harris, P. Wiebe, J. Lens, H. R. Skjoldal, and M. Huntley. Academic Press, San Diego.
- Poulet, S., Marsot, P., 1978. Chemosensory grazing by marine calanoid copepods (Arthropoda : Crustacea ). *Nature*, 200, pp.1403–1405.
- Poulet, S., 1978. Comparison between five coexisting species of marine copepods feeding on naturally occurring particulate matter. *Limnology and Oceanography*, 23(6), pp.1126–1143.
- Quigg, A., Finkel, Z., Irwin, A., Rosenthal, Y., Ho, T., Reinfelder, J., Schofield, O., 2003. The evolutionary inheritance of elemental stoichiometry in marine phytoplankton. *Nature*, 425, pp. 291–294.
- Raymont, J., 1959. The respiration of some planktonic copepoda. III. The oxygen requirements of some American species. *Limnology and Oceanography*, 4, pp.479-491.
- Razouls C., de Bovée F., Kouwenberg J. et Desreumaux N., 2005-2012. - Diversity and geographic distribution of marine planktonic copepods. Available at <http://copepodes.obs-banyuls.fr/en> [Accessed April, 2013].
- Redfield, A., 1934. On the proportions of organic derivatives in sea water and their relation to the composition of plankton. In *James Johnstone Memorial Volume*. (Ed. Daniel R). (Liverpool University Press). pp. 177–92.
- Redfield, A., 1958. The biological control of chemical factors in the environment, *American Scientist*.
- Rhee, G., 1978. Effects of N:P atomic ratios and nitrate limitation on algal growth, cell composition, and nitrate uptake. *Limnology and Oceanography*, 23 (January).
- Rhee, G., Gotham, I., 1980. Optimum N:P ratios and the coexistence of planktonic algae. *Journal of Phycology*, 16, pp.486–9.

- Rhee, G., Gotham, I., 1981. The Effect of environmental factors on phytoplankton growth : light and the interactions of light with nitrate limitation. *Limnology and Oceanography*, 26(4), pp.649–659.
- Ryther, J., 1954. Inhibitory effects of phytoplankton on the feeding of *Daphnia magna* with reference to growth, reproduction and survival. *Ecology*, 35, pp. 522-533.
- Robinson, C., Serret, P., Tilstone, G., Teira, E., Zubkov, M., Rees, A., Woodward, E., 2002. Plankton respiration in the Eastern Atlantic Ocean. *Deep Sea Research Part I*, 49(5), pp.787–813.
- Robinson, C., Serret, P., Tilstone, G., Teira, E., Zubkov, M., Rees, A. and Woodward, E. 2002. Plankton respiration in the Eastern Atlantic Ocean. *Deep Sea Research Part I*, 49(5), pp. 787–813.
- Roman, M., 1991. Pathways of carbon incorporation in marine copepods: Effects of developmental stage and food quantity. *Limnology and Oceanography*, 36(4), pp. 796–807.
- Romero, S., Piola, A., Charo, M., Garcia, C., 2006. Chlorophyll- a variability off Patagonia based on SeaWiFS data. *Journal of Geophysical Research*, 111(C5), pp. 1–11.
- Saiz, E., A. Calbet, 2007. Scaling of feeding in marine calanoid copepods. *Limnology and Oceanography* 52, pp. 668–675.
- Saiz, E., Calbet, A, 2011. Copepod feeding in the ocean: scaling patterns, composition of their diet and the bias of estimates due to microzooplankton grazing during incubations. *Hydrobiologia*. 666, pp. 181-196.
- Sargent J., Henderson R., 1986. In: *The biological chemistry of marine copepods*. Edited by Corner E., D., S., O'Hara S., C., M. Oxford University Press, Oxford. Ch.2.
- Sargent, J., Falk-Petersen, S., 1988. The lipid biochemistry of calanoid copepods. *Hydrobiologia*, 167-168(1), pp.101–114.
- Sarmiento, J., 2004. Response of ocean ecosystems to climate warming. *Global Biogeochemical Cycles*, 18(3), pp. 6–7.
- Sarmiento, J., Gruber, N., 2006. *Ocean Biogeochemical Dyamics*. Princeton, New Jersey, USA, Princeton University Press.

- Schmoker, C., Hernandez-leon, S., 2003. The effect of food on the respiration rates of *Daphnia magna* using a flow-through system. *Scientia Marina*, 67(3), pp. 361–365.
- Schneider, B., Schlitzer, R., 2003. Depth-dependent elemental compositions of particulate organic matter (POM) in the ocean. *Global Biogeochemical Cycles*, 17(2), pp. 1–15.
- Schoo, K., Aberle, N., Malzahn, A., Boersma, M., 2012. Food quality affects secondary consumers even at low quantities: an experimental test with larval European lobster. *PloS one*, 7(3), e33550.
- Schukat, A., Teuber, L., Hagen, W., Wasmund, N., Auel H., 2013. Energetics and carbon budgets of dominant calanoid copepods in the northern Bengueal upwelling system. *Journal of Experimental Marine Biology and Ecology*. 442, pp. 1-9.
- Secor, S., 2008. Specific dynamic action: a review of the postprandial metabolic response. *Journal of comparative physiology B, Biochemical, systemic, and environmental physiology*, 179(1), pp. 1–56.
- Starmiski, D., Reynolds, R., Mitchell, B., 1998. Relationship between the backscattering coefficient, beam attenuation coefficient and particulate organic matter concentrations in the Ross Sea. *Ocean Optics XIV*, pp. 1-10.
- Sterner, R., 1990. The Ratio of nitrogen to phosphorus resupplied by herbivores: zooplankton and the algal competitive arena. *The American Naturalist*, 136(2), pp.209–229.
- Sterner, R., Elser, J., 2002. *Ecological Stoichiometry: The Biology of Elements from Molecules to the Biosphere*. Princeton University Press.
- Sterner, R., Hessen, D., 1994. Algal nutrient limitation and the nutrition of aquatic herbivores. *Annual Review of Ecology and Systematics*, 25(1), pp. 1–29.
- Sterner, R., Schulz, K., 1998. Zooplankton nutrition: recent progress and a reality check. *Aquatic Ecology*, 32, pp. 261–279.
- Sterner, R., Andersen, T., Elser, J., Hessen, D., Hood, J., Mccauley, E., Urabe, J., 2008. Scale-dependent carbon:nitrogen:phosphorus seston stoichiometry in marine and freshwaters. *Limnology and Oceanography*, 53, pp. 1169–118.
- Stoecker, D., Egloff, D., 1987 Predation by *Acartia tonsa* Dana on planktonic ciliates and rotifers. *Journal of Experimental Marine Biology and Ecology*, 110, pp. 53–68.

- Straile, D., 1997. Gross growth efficiencies of protozoan and metazoan zooplankton and their dependence on food concentration, predator-prey weight ratio, and taxonomic group, *Limnology and Oceanography*, 42(6), pp. 1375–1385.
- Stramma, L., 2001. Current systems in the Atlantic Ocean. *Encyclopaedia of Ocean Sciences*. Academic Press, London Vol. 1, pp. 589–598.
- Strickland, J., Parsons, T., 1972. A manual of seawater analysis: Canada Fisheries Research Board. Bulletin 167 (Second Edition). Ch. II.2.
- Suzumura, M., 2008. Persulfate chemical wet oxidation method for the determination of particulate phosphorus in comparison with a high-temperature dry combustion method. *Limnology and Oceanography: Methods*, 6, pp. 619–629.
- Svensen, C., Wexels Riser, C., Reigstad, M., Seuthe, L., 2012. Degradation of copepod faecal pellets in the upper layer: role of microbial community and *Calanus finmarchicus*. *Marine Ecology Progress Series*, 462(2007), pp. 39–49.
- Tackx, M., Bakker, C., Francke, J., Vink, M., 1989. Size and phytoplankton selection by oosterschelde zooplankton. *Netherlands Journal of Sea Research*, 23(1), pp. 35–43.
- Tang, K., Dam, H., 1999. Limitation of zooplankton production: beyond stoichiometry. *Oikos*. 84 (3), pp. 537-542.
- Terry, K., Laws E., Burns D., 1985. Growth rate variation in the N:P requirement ratio of phytoplankton. *Journal of Phycology* 21, pp. 323–329.
- Tester, P., Turner, J., 1990. How long does it take copepods to make eggs? *Journal of Experimental Marine Biology and Ecology*, 141(2-3), pp.169–182.
- Tezuka, Y., 1989. The C:N:P ratio of phytoplankton determines the relative amounts of dissolved inorganic nitrogen and phosphorus released during aerobic decomposition. *Hydrobiologia*, 173(1), pp. 55–62.
- Thor, P., 2000. Relationship between specific dynamic action and protein deposition in calanoid copepods. *Journal of experimental marine biology and ecology*, 245(2), pp. 171–182.
- Thor, P., 2002. Influence of two different green algal diets on specific dynamic action and incorporation of carbon into biochemical fractions in the copepod *Acartia tonsa*. *Journal of Plankton Research*, 24(4), pp. 293–300.

- Thor, P., 2003. Elevated respiration rates of the neritic copepod *Acartia tonsa* during recovery from starvation. *Journal of Experimental Marine Biology and Ecology*, 283(1-2), pp.133–143.
- Tilstone, G., Smyth, T., Poulton, A., Hutson, R., 2009. Measured and remotely sensed estimates of primary production in the Atlantic Ocean from 1998 to 2005. *Deep Sea Research Part II: Topical Studies in Oceanography*, 56(15), pp. 918–930.
- Tirelli, V., Mayzaud, P., 2005. Relationship between functional response and gut transit time in the calanoid copepod *Acartia clausi*: role of food quantity and quality. *Journal of Plankton Research*, 27(6), pp. 557–568.
- Tiselius P., Hansen B., Jonsson P., Kiørboe T., Nielsen T., Piontkovski S., Saiz E., 1995. Can we use laboratory-reared copepods for experiments? A comparison of feeding behaviour and reproduction between a field and a laboratory population of *Acartia tonsa*. *ICES Journal of Marine Sciences*, 52, pp. 369–376.
- Touratier, F., Legendre, L., Vezina, A., 1999. Model of copepod growth influenced by the food carbon:nitrogen ratio and concentration, under the hypothesis of strict homeostasis. *Journal of Plankton Research*, 21(6), pp. 1111–1132.
- Turner, J., 2002. Zooplankton faecal pellets, marine snow and sinking phytoplankton blooms. *Aquatic Microbial Ecology*, 27, pp. 57–102.
- Tyrrell, T., 1999. The relative influences of nitrogen and phosphorus on oceanic primary production. *Nature*, 400, pp. 525–531.
- Urabe, J., Watanabe, Y., 1992. Possibility of N or P limitation for planktonic cladocerans: an experimental test. *Limnology and Oceanography*, 37(2), pp. 244–251.
- Urabe, J., Sterner R., 2001. Contrasting effects of different types of resource depletion on life-history traits in *Daphnia*. *Functional Ecology* 15, pp. 165-174.
- Vaquer-Sunyer, R., Duarte, C., Santiago, R., Wassmann, P., Reigstad, M., 2010. Experimental evaluation of planktonic respiration response to warming in the European Arctic Sector, *Polar Biol.*, 33, pp. 1661–1671.
- Vargas, C., Escribano, R., Poulet, S., 2006. Phytoplankton food quality determines time windows for successful zooplankton reproductive pulses. *Ecology*, 87(12), pp. 2992–2999.
- Vidal, J., Whitedge, T., 1982. Rates of metabolism of planktonic crustaceans as related to body weight and temperature of habitat. *Journal of Plankton Research*, 4(1), pp. 77–84.

- Vidal, J., 1980. Physio-ecology of zooplankton. III. Effects of phytoplankton concentration, temperature and body size on the metabolic rate of *Calanus pacificus*. *Marine Biology*, 56, pp. 195–202.
- Volkman, J., Jeffrey S., Nichols P., Rogers G., Garland C., 1989 Fatty-acid and lipid-composition of 10 species of microalgae used in mariculture. *Journal of Experimental Marine Biology and Ecology*, 128, pp. 219-240.
- Vrede, T., Dobberfuhl, D. R., Kooijman, S., Elser J., 2004. Fundamental connections among organism C:N:P stoichiometry, macromolecular composition and growth. *Ecology* 85, pp. 1217–1229.
- Walve, J., Larsson, U., 2010. Seasonal changes in Baltic Sea seston stoichiometry: the influence of diazotrophic cyano- bacteria. *Marine Ecology Progress Series*, 407, pp. 13 – 25.
- Weber, T., Deutsch, C., 2010. Ocean nutrient ratios governed by plankton biogeography. *Nature*, 467(7315), pp. 550–554.
- Weisstein, Eric W., "Prolate Spheroid" From MathWorld - a wolfram web resource. <http://mathworld.wolfram.com/ProlateSpheroid.html>. [Accessed October 2011].
- Whiteley, N., Robertson, R., Meagor, J., El Haj, A., Taylor, E., 2001. Protein synthesis and specific dynamic action in crustaceans: effects of temperature. *Comparative biochemistry and physiology Part A, Molecular and integrative physiology*, 128(3), pp. 595–606.
- Williams, P., del Giorgio, P., 2005. Respiration in aquatic ecosystems: history and background. In: *Respiration in Aquatic Ecosystems*. Del Giorgio P., Williams P. Oxford University Press 2005. Ch.1.
- Wilson, S., Steinberg, D., Chu, F., Bishop, J., 2010. Feeding ecology of mesopelagic zooplankton of the subtropical and subarctic North Pacific Ocean determined with fatty acid biomarkers. *Deep Sea Research Part I: Oceanographic Research Papers*, 57(10), pp. 1278–1294.
- Winkler, L., 1888. Die Bestimmung des in Wasser Gelösten Sauerstoffes, *Berichte der Deutschen Chemischen Gesellschaft* 2, pp. 2843–2855.
- Withers, P., 1992. *Comparative animal physiology*. Saunders College Publishing HBJ.

WMO: World Meteorological Organisation (online). La Niña event 2010. Available at: [http://www.wmo.int/pages/mediacentre/press\\_releases/pr\\_904\\_en.html](http://www.wmo.int/pages/mediacentre/press_releases/pr_904_en.html). [Accessed October 2012].

Wolff, G., Billett, D., Bett, B., Holtvoeth, J., FitzGeorge-Balfour, T., Fisher, E., Cross, I., Shannon, R., Salter, I., Boorman, B., King, N., Jamieson, A., Chaillan, F., 2011. The effects of natural iron fertilisation on deep-sea ecology: the Crozet Plateau, Southern Indian Ocean. *PloS one*, 6(6), p.e20697.

Wu, J., Sunda W., Boyle E., Karl, D., 2000. Phosphate depletion in the western North Atlantic Ocean. *Science* 289, pp. 759–762.

Wynne, D., Rhee, G., 1986. Effects of light intensity and quality on the relative N and P requirement (the optimum N:P ratio) of marine planktonic algae. *Journal of Plankton Research*, 8(1), pp. 91–103.

Yamaguchi, A., Ikeda, T., 2000. Vertical distribution, life cycle and body allometry of two oceanic calanoid copepods (*Pleuromamma scutullata* and *Heterorhabdus tanneri*) in the Oyashio region, western North Pacific Ocean. *Journal of Plankton Research*, 22(1), pp. 29–46.

Yvon-Durocher, G., Caffrey, J., Cescatti, A., Dossena, M., del Giorgio, P., Gasol, J., Montoya, J., Pumpanen, J., Staehr, P., Trimmer, M., Woodward, G., Allen, A., 2012. Reconciling the temperature dependence of respiration across timescales and ecosystem types. *Nature*, 487(7408), pp. 472–6.

Zhai L., Platt, T., Tang, C., Sathyendranath, S., Walne, A., 2013. The responses of phytoplankton to climate variability associated with the North Atlantic Oscillation. *Deep Sea Research Part II: Tropical Studies in Oceanography* (in press).

Zhukova, N., Aizdaicher, N., 1995. Fatty acid composition of 15 species of marine microalgae. *Phytochemistry*, 39(2), pp. 351-356.

---

**FINE.**